TITLE OF THESIS:

METHODS AND TOOLS FOR THE ASSESSMENT OF DAYLIGHT TRANSMITTANCE THROUGH EXPANDED METAL MESHES

A Dissertation Presented

by

JOSÉ MIGUEL RICO MARTÍNEZ

Submitted to the *Doctoral Subcommittee* of the

University of the Basque Country in partial fulfilment

of the requirements for the degree of

DOCTOR OF PHILOSOPHY

(or DOCTOR OF EDUCATION)

March 2015

Doctoral program: Idea, forma y materia en arquitectura

University of the Basque Country

Universidad del País Vasco Euskal Herriko Unibertsitatea

DEDICATION

To Erika and Martxel

ACKNOWLEDGMENTS

AITOR LECETA MURGUZUR, IÑIGO CANTERO LOINAZ and IBAI LAMARCA SOTO

for their collaboration and essential support

ANGEL LANCHAS HERVALEJO and JOSEBA ESCRIBANO VILLÁN

for their support

IMANOL MOZO CAROLLO

for support on mathematical bases

TERREL MONTGOMERY

for language review

TECNALIA RESEARCH AND INNOVATION

for equipment and financing support

for manufacture knowledge and sample supply

UPV/EHU, ARCHITECTURE DEPARTMENT

for administrative and financial support

ABSTRACT

Daylight performance of building envelopes is a key issue in sustainable architecture. This work develops and tests tools and methods for a better assessment of daylight transmittance of expanded metal, a widely used industrial product in façade design that has not been accurately analyzed.

JOSÉ MIGUEL RICO MARTÍNEZ, UNIVERSITY OF THE BASQUE COUNTRY

Directed by: Lauren Etxepare Igiñiz

TABLE OF CONTENTS

1.1 Building envelope and solar control in architecture

If we are able to define *design* as a consolidated answer to a group of conditions, we are able to understand *architecture* as the design that answers to the questions of a space and its users.

The building skin is the reason for the creation of all architecture because architecture itself is born as a consequence of the capacity of man to manipulate materials and change the factors affecting comfort: temperature, humidity, daylight, intimacy, security, noise, exterior-interior visual relation, etc. That skin is also one of the elements that more greatly affect the identity of collective spaces colonized by people.

The main evolution trends in contemporary architecture often focus on the envelope and we can emphasize two distinct conditions that coincide in its crystallization:

1. The search of continuity and uniformity in the outer skin as a composition resource: what we could define as: a *neutral* skin.

2. The endeavour to obtain better control of the energy flow through the envelope: an *efficient* skin.

1.1.1 The neutral skin

One of the bases for some historical and vernacular buildings such as Berber tents or Gothic churches is the dissociation between bearing capacity and envelope. This theme was picked up again by the beginning of the 20th century's avant-garde architects as one of their main means for separating the building image from the structural tectonics. Later, technological development in construction has allowed for the exploitation of much more expressive and phenomenological envelopes, which - added to new design and graphic tools- are the basic means of contemporary architectural trends.

Hans Ibelings described the status of that development at the end of the 20th century:

Abstraction arises in radical contrast to[1] *the extravagance and deconstructivist complexity that have constituted the aesthetic frame of reference for the past two decades. This simplicity is not primarily a reaction to the aesthetic of visual excess, although that aspect certainly plays a role. In essence the new abstraction is an expression of a fundamentally different attitude to architecture which it sees less and less as significant and filled with symbolic meaning, and more and more as a neutral object.*(Ibelings 2002)

Fig. 1.1. New Museum of Contemporary Art in New York

The New Museum of Contemporary Art in New York clearly illustrates this idea. Designed as a set of boxes placed on top of each other, the off-centre arrangement of the boxes generates a dynamic but self-controlled effect as well as a series of terraces and skylights. The continuous skin is sparingly marked with windows offering views of the city, which does not detract from the clear, vivid and abstract image of the building. The skin is made of a silver-plated aluminum expanded metal mesh which is able to respond to changes in

[1] Own translation

artificial light and daylight to generate varying images and moods within and around the building (Fig 1.1).

Being abstract or not, rejecting or not considerations about form and its meaning, many architectural works have emphasized the virtues of transparency and translucency and their identity is not necessarily bound to what they contain but to their material nature and meticulous details, giving priority to the sensorial experience.

1.1.2 The efficient skin

Beyond the relationship that postmodern, high-tech or *supermodern* architecture has had with technology and above any stylistic consideration; architecture must now lead a more sustainable path in construction, if not actually a de-growth path (Degrowth 2014). Neutral and efficient facades can significantly enhance the credentials of a building, improve energy efficiency by regulating the flow of energy through the envelope, reduce energy consumption and avoid seasonal fluctuations in temperature.

When it comes to preventing heat-gain through translucent facade elements, we talk about solar control. Traditional architecture has had comfort as a primary objective by protection from and exploitation of atmospheric conditions. Therefore, the relationship between a building and the sun has always been an unavoidable issue. In fact the word climate comes from the Greek *klima*, which means “sun inclination”.

Architecture that concerns itself with climate has been defined as *bioclimatic* but we find that the most important knowledge from this point of view comes from the natural logic of vernacular architecture. The effect of the last century’s progress towards bioclimatic efficiency will be l even if it is covered with a technological halo.

The best contemporary contribution is the objective of passivity by means of energy auto sufficiency and a high control of energy flow through the envelope. This requires progress

in assessing and simulating the performance of insulating, ventilating, solar control and daylight control materials and devices.

In the field of solar or daylight control we can observe many frequent inconsistencies such as - for instance- the excessive use of glass surfaces in envelopes designed by self called *sustainable architects* or the use of the same kind of glass in all the facades of a building. We need simple design tools to quantify the performance of systems for practical, logical and widespread application.

Nowadays, daylight simulation software for building designers is quite common. Computer simulation of daylight performance can, with a minimum effort, offer considerable value to the design process, but finding reliable models of non-standard materials is still a problem for designers. Modeling techniques are underdeveloped and require expert knowledge. Current building design needs development of the latest parametric trend design in order to facilitate modeling (Reinhart 2011).

1.2 Translucent metal screens

There is a range of solutions that are appropriate for the previously described requirements for a neutral and efficient facade. These are defined as *translucent metal screens* which are based on woven metal fabrics, perforated metal sheets or expanded metal meshes. Their translucency allows them to be used as a solar control layer and allows one to see through the building skin. Placing them outside the glazed and opaque parts of the skin homogenizes the exterior image of the building, blurring the differences between hollow and solid.

They can also function as a rain screen if they are designed as the outer layer of a ventilated facade. Their lightweight helps avoiding heavy loads and thick peripheral structures; they are easily prefabricated, can be recycled and their manufacturing processes include a range of variables that allows obtaining products with a variety of appearances and qualities.

These variations can be related to the type of metal or its finish but mainly to geometrical parameters such as the thickness of wire or the cutting and perforating patterns that will involve changes in the image, texture, mechanical and energetic performance of the skin.

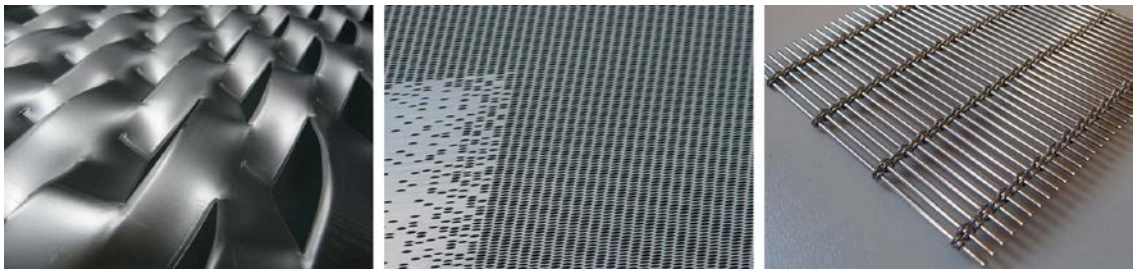

Fig. 1.2. Translucent metal screen products

Perforated sheets and expanded meshes are produced from metal coils subjected to cutting operations in press-machines. In the case of expanded metal we also add deforming operations that increase the mechanical inertia (stiffness) of the section and reduce waste materials.

Translucent metal screens are widely used in contemporary architectural envelopes but often not accurately characterized. As a facade component they have to be assessed from many points of view and should follow the evolution paths of Light Facades, included Daylight performance. This research is focused on the performance of Expanded Metal meshes as daylight control devices. From now on we will refer to expanded metal as E.M.

1.2.1 Translucent metal screens in the context of light facades

The term *Light Facade* has been considered as the one covering two facade solutions that answer many of the construction challenges of nowadays: the ventilated facade and the curtain wall.

We can distinguish between the traditional ventilated facade with an external layer of brickwork supported by the slabs and lintels (or the British cavity wall) that has been extensively constructed during the last century and the ventilated facade with an external

layer of light panels fixed to the internal wall. The actual tendency leans towards the second one due to its higher precision, security and quality of the finish, the huge range of materials and services that can be incorporated and the total freedom in the sizing of the openings of the facade, essential to establish the relationship between the building and its surroundings.

The technical characterization of the new constructive solutions of ventilated facades that are emerging in the panorama of contemporary building is an indispensable step for its approval and certification, with the aim of offering guaranties in its application in design.

The innovation in ventilated facade solutions is affected by a knowledge fragmentation because very diverse elements participate in its composition, such as the unlimited materials of the external layer, the different fixing solutions, substructures, intermediate layers and internal wall.

Nowadays, designers introduce new materials for the external layer in the design of facades without knowing how they affect the air movements in the camera, the general acoustic behavior of the closure, the air tightness, etc. In the same way, improvements in the blind parts of the facade mean new problems in their joining with the openings. It is clear that it is necessary to maintain a global vision when trying to innovate any component of facades.

There is a need to produce valuable knowledge for the integration of translucent metal screens in ventilated facades without losing sight of the global functioning of the envelope, which is so difficult to summarize given the huge amount of requirements that must be satisfied. For architects and engineers to design secure facade solutions, it is essential to persevere in the study and research of the envelope's behavior and the clear classification of its variations.

All this should lead to the documentation of specifications that will protect the use of the ventilated facade. Taking into account the speed in which changes happen in construction practices nowadays, the publication of technical models of reference is especially necessary.

With the objective of architectural integration of translucent metal screens in ventilated and light facades, the following issues should be assessed:

- **Parts of the outside layer:** the different characteristics regarding malleability, corrosion, finish options, alloys, etc. that can influence the performance of the facade. The installation options of the outside layers in the facade, the diversity of formats and the solution of the joints must also be taken into account.
- **Fixings:** one of the most important aspects in the design of the outside layer is the manner of fixing that allows for the correct straightening and fitting of the joints. What initially was done by simple moorings in the field of stone cladding, later evolved to three-dimensionally adjustable fixing systems supported by battens or connected to peripheral structures that nowadays can be applied to any material. Each material has different determinants in their connection with those structures and fixings.
- **Control of water filtration (rain screen concept):** The external layer of the facade must be the first barrier to water infiltration, preventing it from reaching the outside face of the inner wall. However, the external layer must border the ventilated camera, which allows the evaporation of the condensation coming from the inside of the building and avoids the capillarity problems of traditional facades. Therefore, the external layer is not necessarily watertight and allows for a relatively free air flux along the camera, the joints, between pieces, or the drillings in its mass.
- **Mechanical resistance of the external layer:** in ventilated facades we can distinguish the heaviest external layers, such as those made of natural or artificial stone from those lighter external layers composed by materials with a low specific weight and large thickness or high specific weight and very small thickness. Translucent metal screens belong to the latter group, where geometry and design should provide sufficient resistance to wind pressure and impact.

Sometimes, lightness and resistance are achieved thanks to the combination of several materials. The great properties of the metals in flexion or traction make them a good partner for other materials, where they can be introduced as a reinforcing element. Another way of improving mechanic resistance is the use of geometry to provide the appropriate inertia to the pieces.

- **Visual filter and other services:** certain sun protection elements, such as curtains, venetian blinds or louvers, offer a double advantage: besides providing shade from sun radiation, they allow nuanced views and control the privacy of the inner space. Translucent metal screens offer a higher security from intrusion, apart from the mentioned visual and luminance control.

1.3 Daylight performance in the context of Complex Fenestration Systems

Window and facade technologies have developed multi-layered systems sometimes called Complex Fenestration Systems (CFS) which can include several types of glass, louvers, curtains, exterior screens or shading devices, translucent and transparent insulation, etc. These systems must be characterized to control energy transfer and indoor comfort of buildings.

Sun radiation is the main outside source of energy that a building envelope has to address. Sunlight is a portion of the electromagnetic radiation emitted by the Sun including infrared, visible and ultraviolet light, each with different wavelengths ranges. The Infrared range, from 780 to 10^6 nm, is related to heat transfer and thermal comfort. The visible range or light spans 380 to 780 nm and is obviously visible by human naked eye.

Assessing transmission of radiation through a CFS is quite different for thermal and visible radiation. The main difference lies in the fact that transmitted thermal radiation is influenced by the ability of the shading device to absorb heat and re-irradiate it again. This absorption and re-irradiation depends on the color and type of material, its shape and

surrounding ventilation. Analyzing the effect of ventilation is very complex and requires the use of powerful computer calculations. This is why, for some research purposes, it is assumed that the space between device and glass is not ventilated.

The visible range of sun radiation produces *Daylight*, a combination of direct and indirect sunlight including: direct sunlight, diffuse sky radiation and light reflected by earth and objects. Its transmission through a CFS can be simulated considering geometry, color and reflectance of the surfaces.

Scientists, engineers and architects invented and used the concept of Daylight factor to asses the ability of a building to control Daylight (see section 3.2.2). The Daylight factor makes a comparison between the light received on a horizontal surface outside the building (normally measured on the roof) and the light arriving to a horizontal surface inside a room of the building. This is a quite easily measureable factor that provides the characteristics of a point of a horizontal plane of a room. It is thought to assess illumination on work surfaces (i.e. a desk).

The development of rendering software run parallel to the illumination assessment software and demonstrated that more complex concepts than Daylight factor were necessary. Daylight factor does not provide any information about the direction of incident light and its distribution after crossing the facade. A much more complex surface characterization was necessary and provided by Bidirectional Scattering Distribution Functions (BSDF 2014), designed to describe the behavior of light when reaching a surface, collecting information for several angles of incidence of light on that surface and several angles of that light reflected from or transmitted through that surface; i.e. scattered light (see section 6.6.1.1). As for each angle of incidence we can assess several transmission and reflection angles, we obtain a large amount of data to characterize the surface. This information can be calculated by simulation software (e.g. *radiance* of *tracepro*) or measured by specific tools as the so called goniophotometers (Andersen and de Boer 2006).

Once we obtain the BSDF of a material or product we can use it with other software designed for the characterization of CFS (e.g. *Window*. (Window Optics n.d.)) that considers the interaction of several layers, products and materials and provides overall characteristics of CFS.

1.4 Tools, methods and parameters to assess daylight performance of expanded metal

The shape of expanded metal meshes involves a complex behavior of light because of reflection on its 3D bended surfaces as happens with louvers. When it comes to louvers any assessment method analyzes just one vertical section because its geometry can be understood as the result of a direct extrusion and the section's results can later be applied to the louver's width but expanded metal's geometry is more complex and we cannot analyze just one section alone.

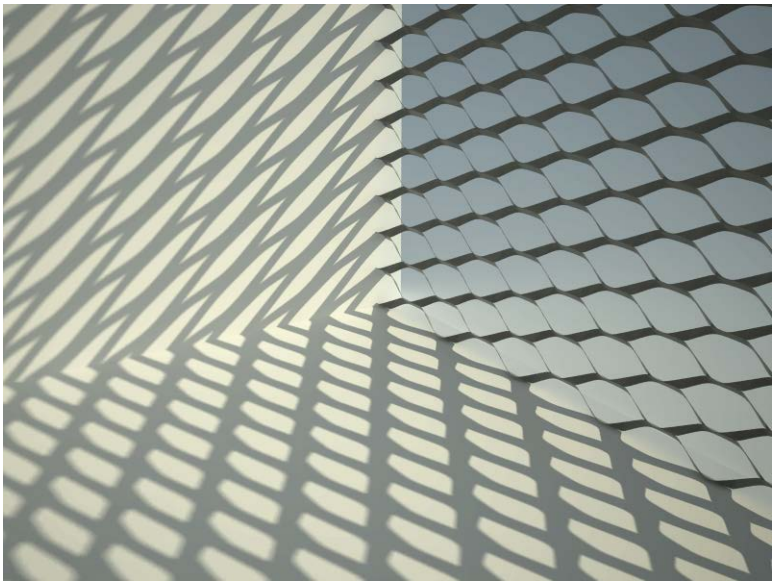

Fig. 1.3. Shading by expanded metal

We distinguish three groups of methods to assess the daylight transmittance of expanded metal: Computer aided assessment, Laboratory assessment and Measurement of real daylight transmittance.

The objective is to quantify the luminous transmittance of expanded metal meshes and, as it changes very much depending on the incidence angle of the radiation, we should offer data for a representative range of angles of incidence and transmittance, repeating the process for different samples (varying geometrical and coating parameters). The most precise way to do this is the use of BTDF and Goniophotometry but beyond these complex methods we have developed some other simple procedures in order to achieve an intuitive understanding of the whole.

Testing several samples can provide useful information about the parameters that affect the performance of an expanded metal mesh as a daylight control device and which combinations of parameters allow for a better luminous transmittance. Working with different colors of the meshes coatings can offer information about the influence of the portion of light transmitted after interior reflections in the mesh.

We intend to clarify the methodology in order to be able to obtain information about the light transmittance performance of EM. For instance we could need to assess the influence of the size of the holes and its relation with the thickness of the sheet in an expanded metal mesh. With very small holes, the thickness's influence might become important. Other issues that may be considered in a study of daylight transmittance through EM are: the nature of metal that constitutes the mesh (especially if it is not lacquered), the influence of each of the geometrical parameters of EM or the position of the mesh (upwards-downwards / backwards-forwards).

Anyway it has not been our aim to cover all the variables that affect transmittance but to research the different ways to assess them. Results of the different assessment methods will be compared in order to analyze the percentage and causes of deviation or error of each one.

1.4.1 Laboratory assessment

There are some laboratory sets that can fulfill the requirements of this assessment.

Nowadays, the most advanced hardware to carry out a reflectance and transmittance assessment of sheet-material are goniophotometers, which are able to obtain BSDF data from layer samples. A goniophotometer is a system where the light source and the measuring device rotate around the sample monitoring all the outgoing light flux for every incoming light source direction. These devices are quite expensive and beyond our possibilities.

Another lab device to obtain accurate daylight transmittance data is the spectrophotometer. This hardware is usually built for small samples, for approximate areas of 10cm x 10cm. They are commonly used to assess glass samples, where the entire sample has a uniform mass. In the case of the Expanded Metal meshes, an area of 10cm x 10cm is usually not representative of the whole mesh, as the area of the hollows in many meshes is larger than the mentioned measurable area. An assessment device capable to assess larger samples was necessary considering our objectives. Even so, EM meshes with the smallest holes were analyzed in a spectrophotometer (see section 5.5) in order to validate other methods.

Thus, we built a specular transmittance assessment lab device (see section 5.2). As a handmade device, it has some accuracy limitations. The calculations of light transmittance are made only in the direction of specular transmission, comparing the measurements without EM sample with the ones with EM sample. This set has a fixed light source and a fixed measuring device. Between them we placed a rotary sample holder for samples of 70cm x 70cm, allowing for the obtainment of specular transmittance for different incident radiation angles. All the obtained data was registered in a computer.

Only a limited amount of some specific EM meshes could be assessed in that device due to the manual process to obtain data for each mesh and to sample supplying limitations. Besides, there is a huge range of EM meshes, whose overall assessment is unattainable due to

the enormous variety of possible forms and dimensions. Even so, we assessed EM meshes with different geometrical parameters and colors.

1.4.2 Computer simulation

Another approach to the problem is reached by means of computer simulation programs and parametric design software.

We first need to make a geometrical analysis of the manufacturing process of the product to understand its specificity and emulate it by means of parametric design modeling. Then we can use existing radiation simulation programs on the created 3D models.

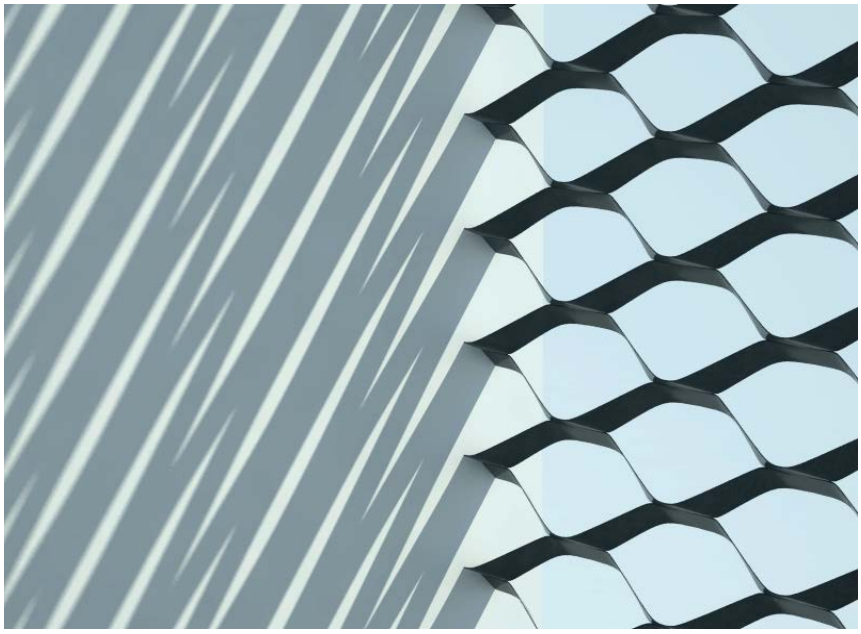

Fig. 1.4. Grasshopper modeled mesh rendered with Radiance

The parametric design software enables us to create 3D models of the expanded metal meshes starting from a given number of geometrical data. This software can make it easier to choose the type of expanded metal mesh that a designer wants for a project because we are able to see it before production.

As we will explain, the definition of the shape of expanded metal depends on seven geometrical parameters and, therefore, from the vast amount of possible combinations of

different values of these parameters (considering several limitations for the value of each parameter and for the relations between them) we can consequently obtain an enormous variety of expanded metal meshes.

In section 2.2 we'll explain the genesis of the shape and then in section 6.2 the way of modeling it.

1.4.3 Measurement of real daylight transmittance

Laboratory assessment and computer simulation have been chosen because of their advantages to control the parameters affecting the phenomena (light availability, light type, direction and intensity, etc) but it is obvious that another possibility is to place EM meshes exposed to real sun radiation and assess transmittance. This last kind of assessment implies a precise control of the time and the consequent deduction of the direction of radiation by means of solar position calculations. The continuous change of sun illuminance due to atmosphere conditions implies that every register of transmission must be accompanied by a register of the incident radiation on the outer side of the mesh.

Finally, we also developed a rough geometrical analysis of light transmittance through EM (described in chapter 4) which will complement the other methods.

Fig. 1.5. Daylit EM mesh

References

Andersen, Marilyne, and Jan de Boer
2006 Goniophotometry and Assessment of Bidirectional Photometric Properties of Complex Fenestration Systems. Energy and Buildings 38(7): 836–848.

BSDF
2014 Wikipedia, the Free Encyclopedia. http://en.wikipedia.org/w/index.php?title=Bidirectional_scattering_distribution_function&oldid=612813141, accessed July 2, 2014.

Degrowth
2014 Wikipedia, the Free Encyclopedia. http://en.wikipedia.org/w/index.php?title=Degrowth&oldid=628134842, accessed November 30, 2014.

Espectro electromagnético
2014 Wikipedia, la enciclopedia libre. http://es.wikipedia.org/w/index.php?title=Espectro_electromagn%C3%A9tico&oldid=78292378, accessed December 3, 2014.

Ibelings, Hans
2002 Supermodernism: Architecture in the Age of Globalization. Nai Publishers.

Reinhart, Christoph F.
2011 Simulation-based Daylight Performance Predictions. *In* Building Performance Simulation for Design and Operation. London ; New York: Routledge.

Window Optics
N.d. http://windowoptics.lbl.gov/, accessed November 23, 2014.

Expanded metal is a metal product made by shearing and stretching a metal sheet in a press, leaving voids surrounded by the stretched strands of the metal.

The term used for expanded metal in other languages is: *métal déployé* in French, *metal expandido* in Spanish (colloquial: déployé), *lamiere stirate* or *rete stirate* in Italian and *streckmetall* in German. Sometimes it is also referred as *corrugated metal* in English.

EM manufacture has traditionally been used to produce grilles and offers some advantages compared with other techniques: it is formed from a single piece of metal; no welding or weaving is involved, neither joints nor welded knots are created and therefore there is less risk for ruptures. Besides, as there are no woven threads EM does not unravel (as an advantage in comparison with other kind of grilles). In heavy formats EM is difficult to breach without gross cutting equipment or explosives.

Compared with other translucent metal screens as perforated metal or woven metal fabrics, expanded metal can offer greater flexural stiffness because the manufactured mesh has a larger overall thickness and therefore a better moment of inertia than the initial metal sheet. In perforation we do not increase the product's thickness because there is no bending operation involved. Woven metal fabrics are obviously not very stiff and need to be installed using pulling tensions to maintain flatness. This feature of EM makes it very appropriate to install in facades, which are all subjected to wind pressure.

2.1 History

The procedure and machines for the manufacture of EM were patented by Mr. John French Golding, Chicago. He registered what he called a machine for making *slashed metallic screening* (Golding 1885). The first procedures consisted of first cutting some slits in a metal sheet to then open the cuts thus formed by bending the strands in a direction at right angles to the plane of the sheet. Those first procedures didn't cause any elongation of the metal strands.

Later procedures took advantage of the ability of the metal to stretch and bend and simplified the process.

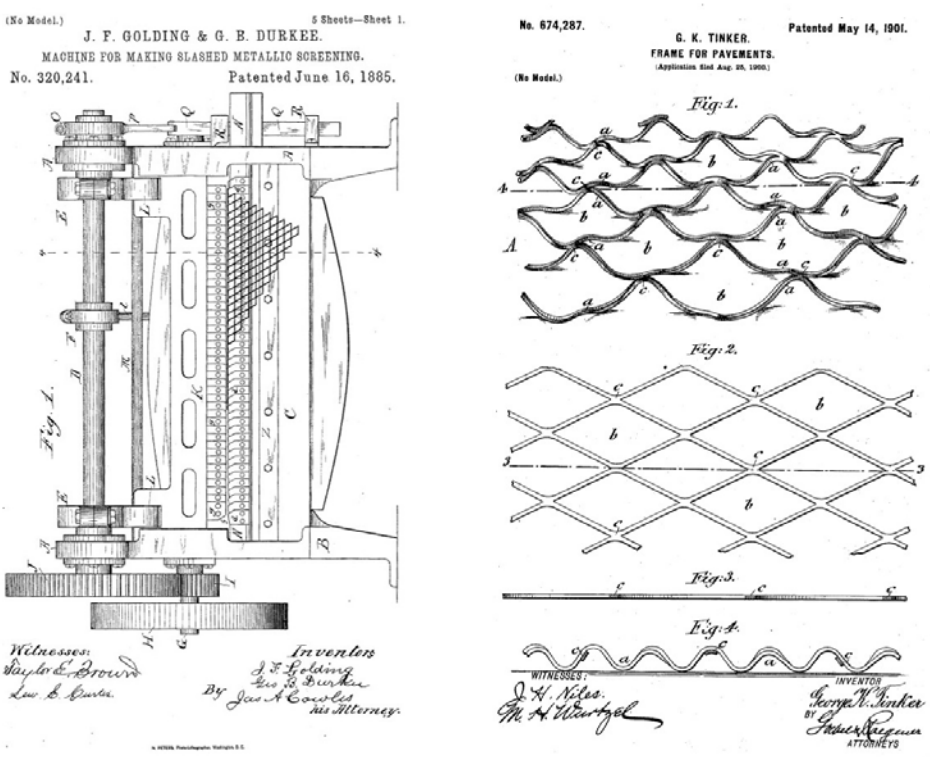

Fig. 2.1. Left: Golding's machine(Golding 1885). Right: EM application as frame for pavements (reinforcing cement or asphalt) (Tinker 1900)

At the end of the XIX century the EM meshes were used worldwide as a product for construction, fences, doors, windows, baskets, etc. The main use in buildings was for ceilings, walls and partitions with cement, plaster and lime mortar but also as structural elements for reinforced concrete floor slabs (de Tejada, Sonier, and Maluquer 1900). By that time there were 10 American companies and some others in Europe producing EM.

A huge amount of patents have been developed about other ways of manufacture, transformations and applications of EM. *Google patents* search engine shows 565000 results related with EM. The most common transformation of an EM mesh is to flatten it in order to get a smoother surface of the mesh, suitable for several applications as filters.

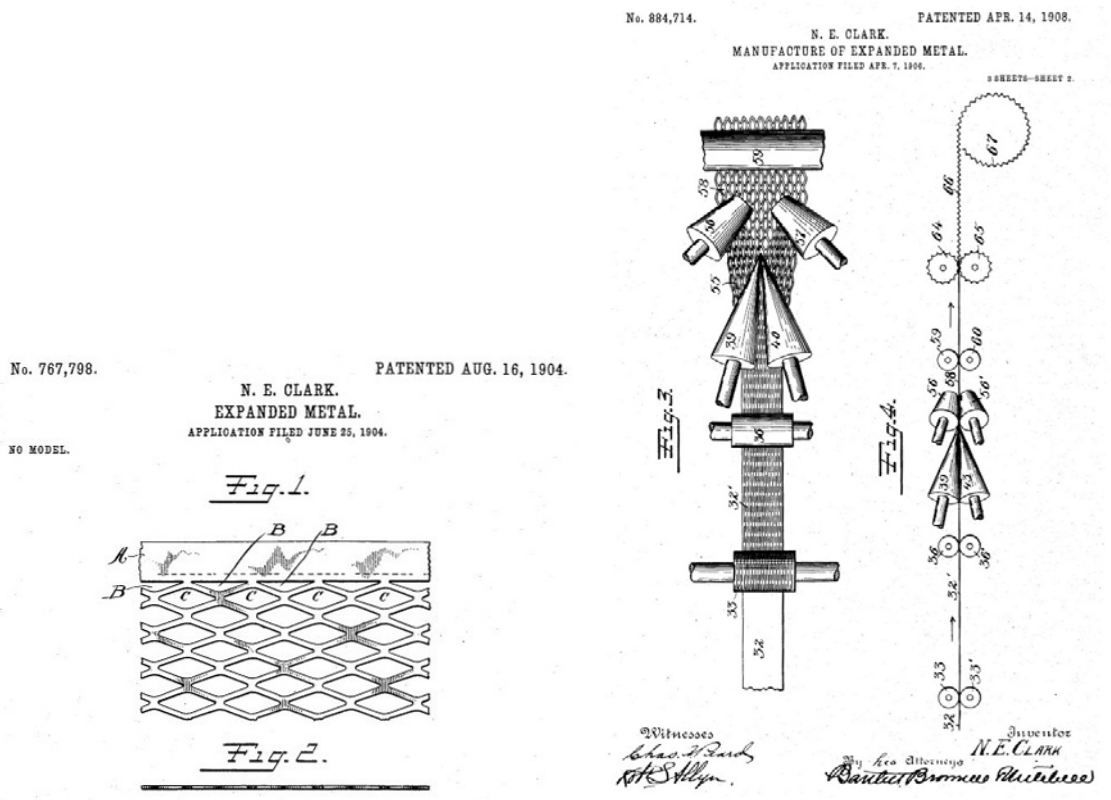

Fig. 2.2. Left: Image from flattened EM patent (Clark 1904). Right: Image from EM manufacture process patent (Clark 1908)

Nowadays EM is present in every built environment as part of many types of products like filters for fans, grates, street benches and bins, fences, catwalks, lathing, plastering, furniture, fences, heating floors, etc. It is also widely used as architectural surface for walls, floors and suspended ceilings. The expanding procedure is used also in different ways to obtain design products as furniture.

Fig. 2.3. Left: Window fence. Amsterdam. Right: Loll Lounge table. Pulpo products. Design: e27, Berlin. **http://www.e27.com/produkte/loll-lounger/kategorie/produkt_loll_lounger.html**

Fig. 2.4. Catalano bench by Lluís Clotet and Oscar Tusquets, 1974

Fig. 2.5. Subway station entrance in Amsterdam. Frank Mandersloot, 2009

The use as the outside layer in building facades has been more and more common during the last decades and designers often choose meshes with bigger nerves and holes than in other applications. Many manufacturing companies have a range of products under the name of architectural or decorative, including a wider variety of colors and sizes.

Fig. 2.6. Jahrhunderthalle in Bochum (Germany), façade refurbishment of industrial building transformed in concert-hall. Petzinka Pink Architekten, 2003

Fig. 2.7. Carina store. Tokyo 2012. SANAA architects 2009.
https://www.flickr.com/photos/kirabelle9/ https://creativecommons.org/licenses/by-nc-nd/2.0/

2.2 Manufacture process

For an adequate understanding of the geometry of EM that will help to create the parametrical design software to build EM meshes models, we needed an in-depth analysis of

its shape, and therefore its manufacturing process. One of the strong points of this product is its simple manufacture and use versatility.

In industrial manufacturing we need to get over the creep-resistance of the material so as to be able to change its shape. Compression stresses are usual but in this case cutting and bending stresses are applied. Therefore, we need a low creep resistance and high ductility of the material, these properties being very well met by metals (Groover 2012). Other well known properties of metals are a high thermal and electrical conductivity, opacity and reflectivity. Expanded metal can be produced in aluminum, mild steel, galvanized steel, stainless steel, copper, brass, nickel, titanium, platinum, zinc, silver and gold, but between 80 to 90 % of production is made in steel.

The process consists in metal coils subjected to shearing and expanding operations in press-machines. This is almost the only mechanical operation of the process (except for leveling and flattening); afterwards we can coat the resulting mesh. Metal coils are previously produced by lamination. Press operations are usually cold-processes except when we need to apply large distortions or we have great thickness of the sheets, both conditions being avoided in expanding metal. Thickness usually goes from 0.4 to 6 mm.

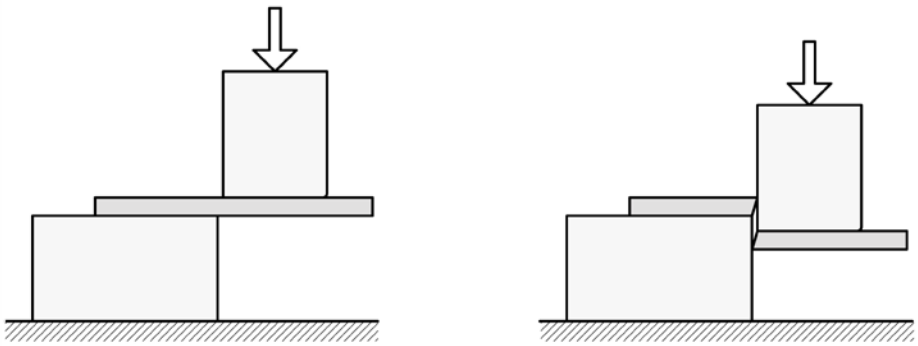

Fig. 2.8. Cutting in a press-machine

Generally speaking, shearing refers to the operation of cutting a metal sheet along a straight line. The blade is usually oblique, this way reducing the required cutting force because

the whole cut is not made simultaneously (in any case the whole energy required for the total cut is the same).

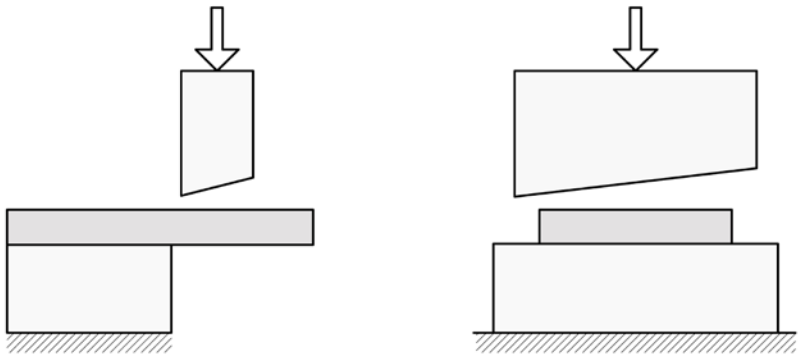

Fig. 2.9. Oblique blade for shearing, lateral and front view

Besides shearing, we need an operation of expanding or deploying which is a combination of cutting and bending or cutting and forming in one step to partially separate the metal from the sheets plane. The following figure shows several ways of expanding.

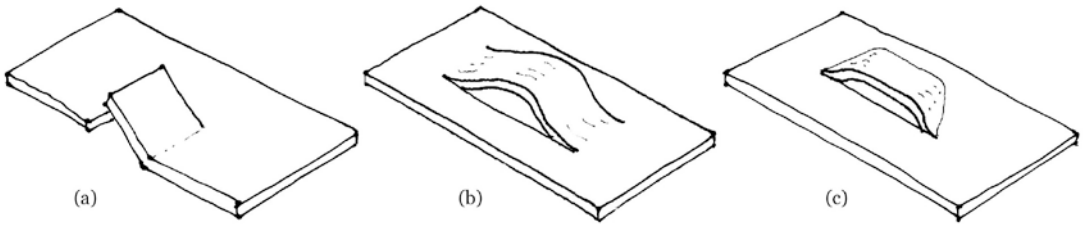

Fig. 2.10. (a): cutting and bending. (b) and (c): two types of cutting and forming

Most usual expanded metal meshes have equal holes spread in a uniform pattern. The manufacturing process consists in making consecutive cutting and forming operations in discontinuous segments of straight lines by means of a serrated blade (a saw shaped blade).

Fig. 2.11. Saw shaped blades

The following figure shows a sketch of the described mechanical operation. The metal sheet advances on a conveyor belt towards the press. A vertical movement of the blade (move 1) makes a row of cuts perpendicular to the advancing movement of the sheet (move 3) and simultaneously distorts the part of the sheet that has advanced beyond the cutting-line, pushing it downwards.

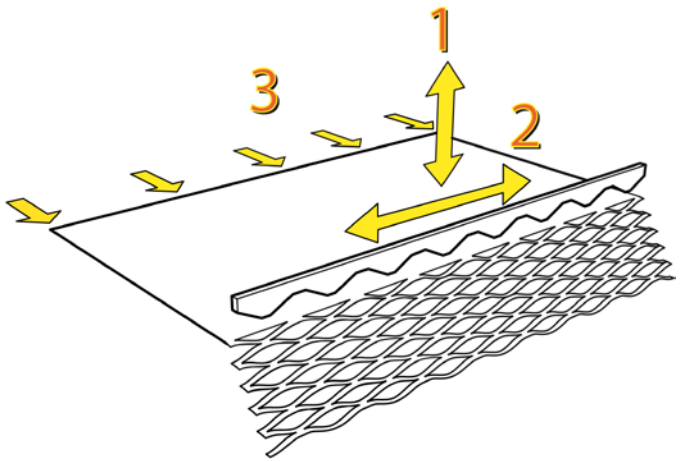

Fig. 2.12. The 3 manufacture movements

After this first cut-and-pushing operation, the blade rises and moves a certain horizontal distance (move 2) perpendicular to the advancing movement of the sheet. This distance is equal to the half-distance between two cut-segments in the same row of cuts. Then the sheet advances again a certain distance in the conveyor belt (move 3) and the blade

repeats the cutting-and-forming vertical movement (move 1). This way, two rows of cuts end up displaced one from each other in a zigzag pattern.

The saw-shape of the blade allows reducing the power needed for shearing as explained before because of the oblique cutting. The pushing force is exerted by the peaks of the blade and by its oblique sides which cut and push at the same time. The peaks are beveled to lightly increase the pushing surface at the beginning of the cutting, avoiding punching. This way the resulting metal strips draw some kind of zigzags or sinusoid lines. The part of the sheet that has been pushed downwards has the same profile as the blade itself, obviously.

The following link shows a video of the described manufacture process:

http://youtu.be/6M8N6sR0QKw

Most of the meshes are leveled after having been expanded to get a flat surface because expanding produces a slight curvature to the whole. Another available mechanical procedure is the flattening of the mesh to obtain a minimum overall thickness and eliminate any relief.

In this process starting from a flat sheet we obtain a three-dimensional section without wasting materials.

There are several kinds of expanded metal depending on the form and magnitude of the movements of the blade and the consequent shape of the holes (see section 2.4). The simplest and most common type has rhomboid holes, it's usually known as *rhombus-shaped* or *diamond-shaped* and this will be the object of our research.

Different types of EM can be produced changing the previously explained manufacture rules. For instance, when the horizontal movement of the blade is not equal to the half-distance between two of its peaks, we obtain a mesh like the one in the following figure.

Fig. 2.13. EM mesh obtained when: blade's horizontal movement < LW/2.

2.3 Geometrical parameters of Expanded Metal

The geometry of a rhombus-shaped expanded metal mesh can be described by means of the parts and parameters of the mesh and press-machine listed in the following two sections.

2.3.1 Parts of an Expanded Metal mesh

We call *strands* to the elongated metal strips that form the mesh.

We call *knuckle* or *bond* to the joining area of 4 strands

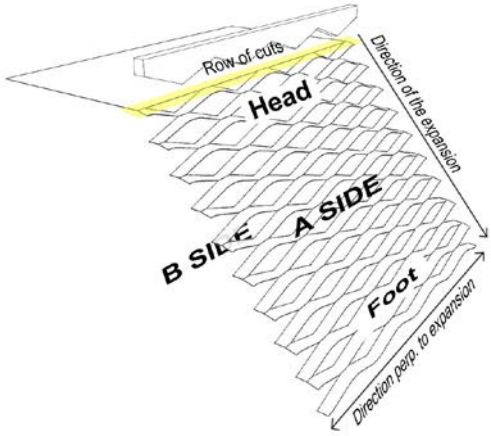

Fig. 2.14. References for positions and sides, related to manufacture procedure

2.3.2 Parameters of an Expanded Metal mesh

The following table exposes the name and explanation of each geometrical parameter suitable to define a rhombus shaped EM mesh. Those parameters are dimensions of the mesh itself or of the blade used for manufacture. Each parameter is also identified with a letter or abbreviation. Some manufacturers use different names and abbreviations but we tried to choose the most common and intuitive.

length of sheet	***L***	Dimension of the mesh measured in the direction of expansion. See fig. 2.14
width of sheet	***W***	Dimension of the mesh measured in the direction perpendicular to expansion. See fig 2.14
overall thickness	***T***	The finished thickness of the mesh which often determines the selection of framing members.
long way of mesh	***LW***	Aka *long way of diamond*, *length of mesh* or *pitch* by some manufacturers, it is the length of the cut plus the distance between consecutive cuts in one same row or the distance between two equal points of two consecutive cuts in the same row (for instance: distance between the centre of two cuts in the same row or between the centre of two knuckles in the same row). See fig. 2.16 and 2.17
short way of mesh	***SW***	Aka *width of mesh*. Distance between two equal consecutive points of the mesh in the direction of expansion, after the expansion. This dimension is useful for production because it can be easily and quite precisely measured when making the manufacture tests to adjust the press-machine's movements. See fig. 2.16 and 2.17
strand thickness	***e***	It is similar to the thickness of the original metal sheet except for the deformation due to Poisson effect after expansion. See fig. 2.16

strand width	***w***	We could also call it *advance* because it's the distance that the sheet advances between two cutting movements. We can also define it as the distance between the cuts in two rows, before expansion. Strictly the advance-move of the press machine and the width of the finished product's strips are not identical. The light difference between them is due to the fact that the width of the strand varies noticeably from one point to another in meshes with a high value of the ratio *e*/*w*, because of different deformations (e.g. bending of strands and Poisson effect due to elongating). In meshes with thin and wide strands, that is with a low value of the ratio *e*/*w*, the strands can easily bend in transversal direction creating concavity-convexity effects in the surface. In fact the strand thickness becomes also variable after the stretching. Anyway all these differences can be neglected for most purposes. See fig. 2.16 and 2.17
intercut	***i***	We could also call it *knuckle width*. EM suppliers usually do not mention intercut in their product specification, they only provide this data: long way (*LW*), short way (*SW*), strand thickness (*e*) and strand width (*w*). Many resulting different meshes are possible with those equal 4 parameters and it is not possible to define the precise geometry of a mesh if we don't provide at least 7 parameters. For commercial purposes providing more than those 4 dimensions would make it too complicated for non-specialized costumers. See fig. 2.16 and 2.17
cut width	***c***	Aka *long way of opening*, it is the width of the mesh's holes or the width of the blade at a height from its bottom equal to the blade descent (*d*). The *cut width* is the difference between *long way of mesh* and *intercut*. See fig. 2.16 and 2.17
blade bevel width	***b***	Width of the chamfer created at each spike of the saw shaped blade. See fig. 2.16 and 2.17
blade thickness	***t***	Thickness of the blade, it can sometimes be noticed because of a groove in the middle of the knuckle (when $t<w$). See fig. 2.16 and 2.17
blade descent	***d***	Distance that the blade descents with each of its vertical movements. It's one of the legs of a right triangle witch other leg is the *width of the strand* (*w*) and the hypotenuse is half of *short way of mesh* (*SW*). See fig. 2.17
blade tooth's height	***h***	It's the height of the triangles that the blade would have if its spikes were not chamfered. See fig. 2.17
bevel's height	h_b	The height of the triangle that disappears when chamfering the blade's spikes. See fig. 2.17

blade's slope	α	The slope of the sides of the blades teeth. As the expansion of the metal sheet is obtained pushing it by the blade, the profile of the down-edges of one rhombus shaped hole is exactly the same of the blade's edge. See fig. 2.17

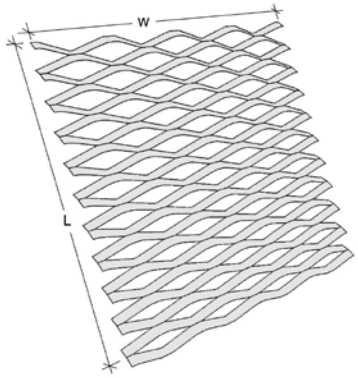

Fig. 2.15. Parameters of an EM mesh. Length of sheet (*L*), width of sheet (*W*)

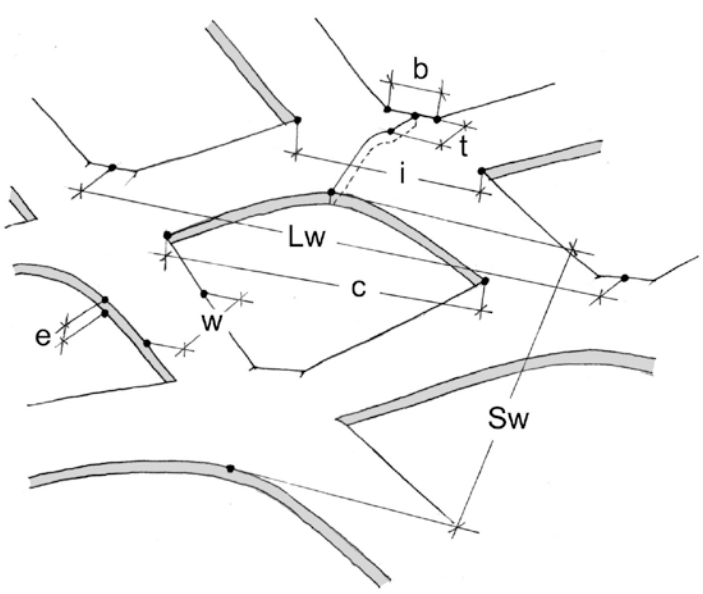

Fig. 2.16. Parameters of an EM mesh. Long way of mesh (*LW*), short way of mesh (*SW*), strand thickness (*e*), strand width (*w*), intercut (*i*), cut width (*c*), blade bevel width (*b*), blade thickness (*t*)

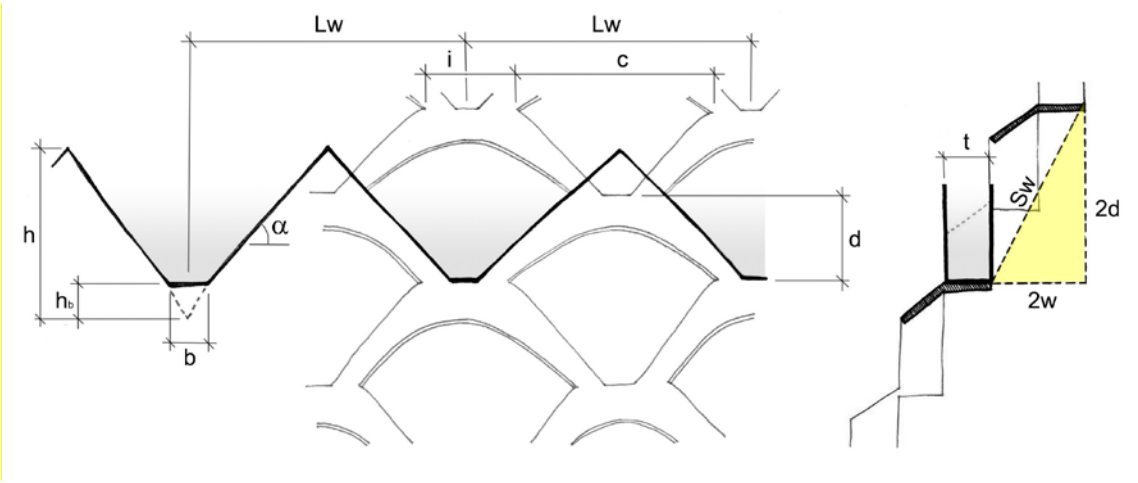

Fig. 2.17. Parameters of an EM mesh. Long way of mesh (*LW*), short way of mesh (*SW*), intercut (*i*), cut width (*c*), blade bevel width (*b*), blade thickness (*t*), blade descent (*d*), blade tooth's height (*h*), bevel's height (h_b), blade's slope (α)

We don't need each and every one of the previously mentioned parameters to define the geometry of an EM mesh.

We can define a blade by means of:

(***LW, α, b, t***)
or
(***LW, h, b, t***)

To obtain a mesh from that blade, besides the previous four values, we need to give a value to the following 3 parameters (thickness and advance of the sheet and descent of the blade):

(***e, d, w***)

Consequently an EM mesh can be defined by means of the following combination of parameters (where *h* can replace α):

(***LW, α, b, t, e, d, w***)

But it might be more intuitive to use this combination (where *c* can replace *i*):

(***LW, SW, b, t, e, w, i***)

Obviously there are some limitations for the values of the described parameters. We divide them into manufacture conditions, geometrical necessary conditions and design conditions:

Manufacture conditions	
***LW* ≤ 300 mm**	The maximum horizontal movement of the blade is limited by the press-machine characteristics. For instance this limitation can be 150 mm. Thus a typical limitation for *LW* is 300 mm.
b<c	As bevel width gets closer to cut width, the mesh passes from having rhombus shaped holes to hexagonal shaped holes. In the limit, with *b*=*c* the blade would have vertical teeth (α=90^o) and we would obtain rectangular shaped holes.
d<h-h$_b$	This is a condition to avoid complete cut of the sheet at each vertical movement of the blade. It can be also be expressed like this: $d<\{(LW-b)/2\}\ tg\alpha$
w>e	This is an approximate condition. It seems difficult to cut a metal sheet in slices whose width is much smaller than its thickness without having undesired deformations or breaking.

Geometrical necessary conditions	
w≤SW/2	Condition necessary for the expansion. Those meshes with a wider strand than half the short way of mesh do not expand.

Design conditions	
b≤i	Intercut use to be equal or larger than bevel width (for rhomboidal, hexagonal and most usual meshes). If we want to get a more robust or square knuckle the relation between *b* and *i* should be close to: *2b≤i*. When *b>i* we obtain meshes with holes similar the one shown in the following figure.

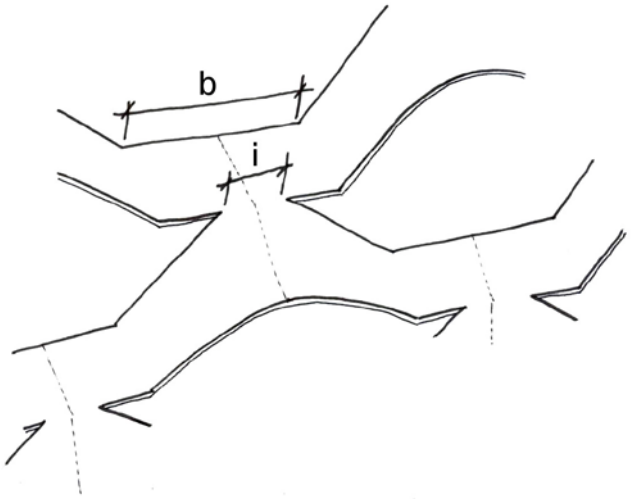

Fig. 2.18. Type of mesh obtained when *b>i*

Besides the conditions mentioned we can find the following arithmetical and trigonometric relations between groups of parameters:

SW, d and ***w***:	$(SW/2)^2=d^2+w^2$
c, d, α and ***b***:	$LW=c+i$
i, c and ***LW***:	$c=(2d/tg\alpha)+b$
a, h and ***LW***:	$tg\alpha = h / (LW/2)$
a, h_c and ***b***:	$tg\alpha = h_b / (b/2)$

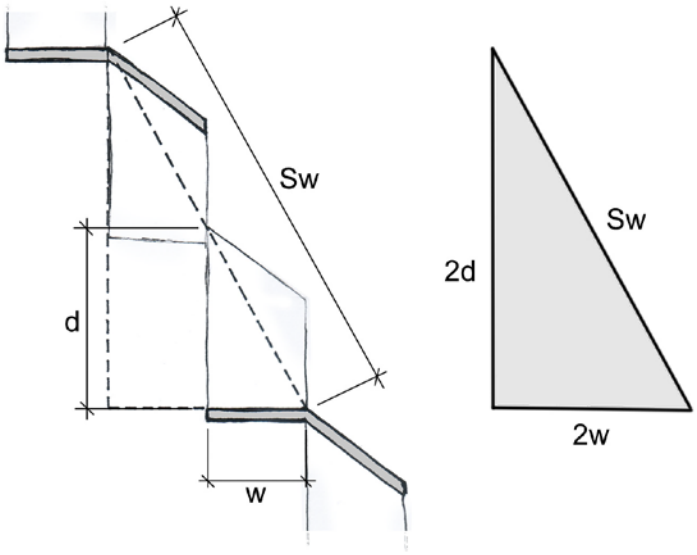

Fig. 2.19. Triangle formed by *descent*, *short way of mesh* and *strand width*

When describing an EM mesh manufacturers refer to two additional features: *percentage of open-area* and *expansion ratio* of the mesh.

The **percentage of open area (aka opening)** is related to the free area viewed from a direction perpendicular to the plane of the mesh. This is the area through which fluids, light rays, etc. can cross the mesh without being interfered by the metal. Some manufacturers provide an approximate (±10%) way of calculating the % of open area of a mesh from some of its manufacture parameters (*LW, SW, w* and *e*).

The **expansion ratio** is the relationship between the lengths of the original metal sheet and the subsequent expanded metal mesh. The length of the mesh is always larger than that of the initial sheet, due to the expansion. A 25% expansion ratio means that a sheet 1 meter long will become a mesh 1.25 meter long. It can be calculated with the following formula:

$$\textbf{Expansion ratio:} \quad \frac{L_f}{L_i} = \frac{SW}{2w} \cdot 100$$

Where L_f = final mesh length

L_i = original sheet length

Based on the expansion ratio of an EM product, any manufacturer can calculate the length of metal coil needed to produce a desired amount of that product, taking into consideration the waste due to changing coils, tests and possible mistakes.

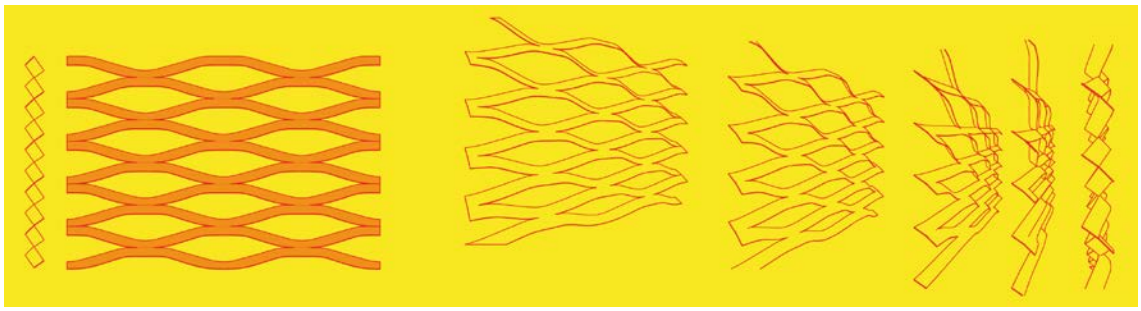

Fig. 2.20. Front and side views of an EM mesh

All mentioned characteristics and parameters are referred to meshes manufactured with rectilinear blades. This type of blade is the most common, but not the only one. Blades with different shapes can be used to manufacture meshes with specific geometries and forms.

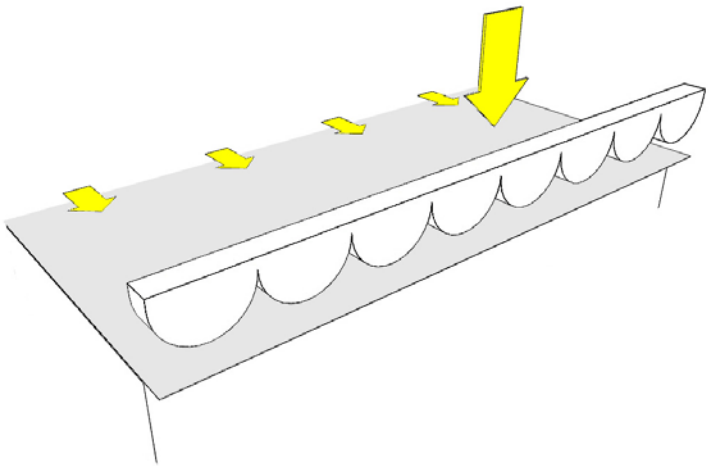

Fig. 2.21. Curved blade

As we said before, our aim is to model the mesh by means of parametric modeling software. In section 6.1 we introduce parametric modeling.

2.4 Types of Expanded Metal

Taking into consideration the available geometrical parameters and materials, we can get an uncountable amount of different types of EM that are possible to manufacture.

As mentioned in regards to material, most malleable materials can be expanded, but mild steel, aluminum and stainless steel are the most common. Each material has its own special characteristics: aluminum provides lightness and longevity; steel provides strength, copper ages beautifully, etc.

Depending on the manufacturing process, we can obtain very different shapes. The form of the blade and its movements are the conditions that define the shape and patterns of an EM mesh. Manufacturers usually refer to the different types with names such as rhombus

shaped (also called diamond), hexagonal, square and round, the most typical pattern being the rhombus shaped one. Another classification criterion used by manufacturers is the applications of the meshes: grating, catwalk grating, architectural or decorative, stair treads, etc. (EMMA 557-12 Standards for Expanded Metal 2012).

Standard or regular EM meshes are those that don't undergo any additional manufacturing process, they are used just as they come out from the expanding press. These meshes have uniform sized and regular openings. The openings can have diverse sizes, from large openings to precise and miniature versions from the same manufacturing process.

Other special varieties of EM meshes result from altering the parameters along one same mesh. For instance, we can vary the magnitude of the manufacturing movements and obtain a mesh whose strand width (varying advance) or short way (varying descent) changes along the mesh obtaining a non regular pattern. If we design a special blade with non equal peaks we can get a mesh with varying expansions or opening forms and dimensions in each cutting row of the mesh.

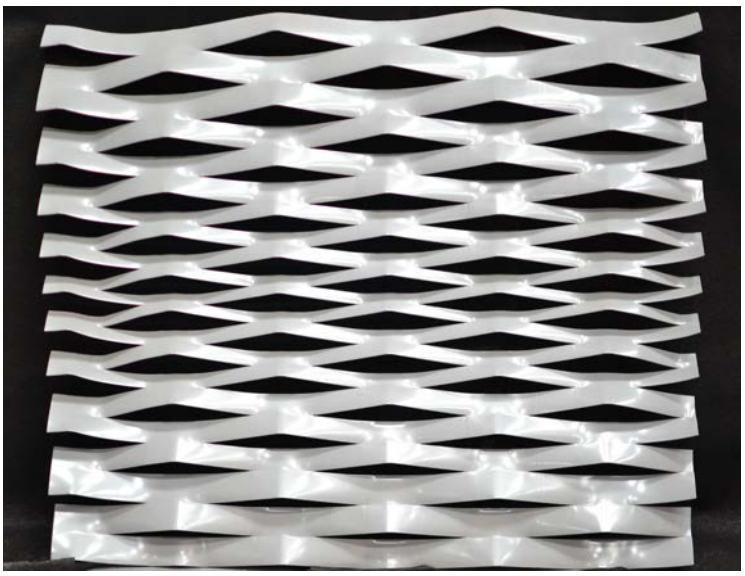

Fig. 2.22. EM mesh with varying strand width. Manufactured by IMAR (2014).

This kind of product seems to be the inspiration for Herzog&deMeuron architects in the design of Basel Exhibition Center (2013).

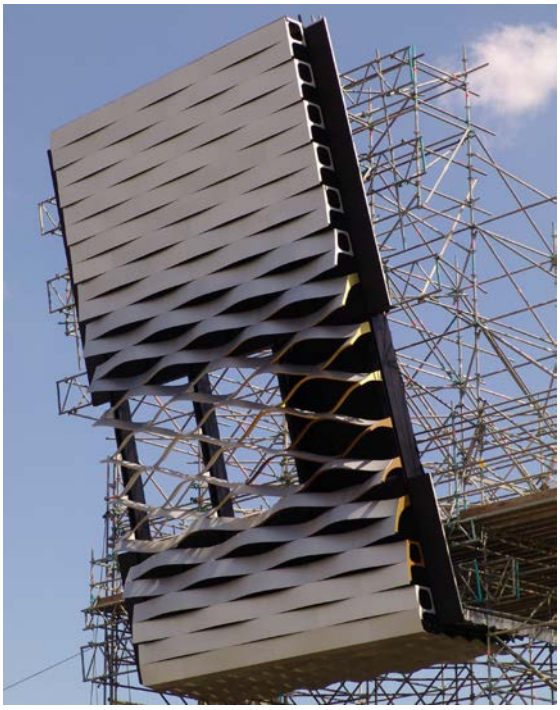

Fig. 2.23. Basel Exhibition Hall. Cladding Mock-Up. 2009. Architects: Herzog&deMeuron
https://www.flickr.com/photos/detlefschobert/ https://creativecommons.org/licenses/by-nd/2.0/

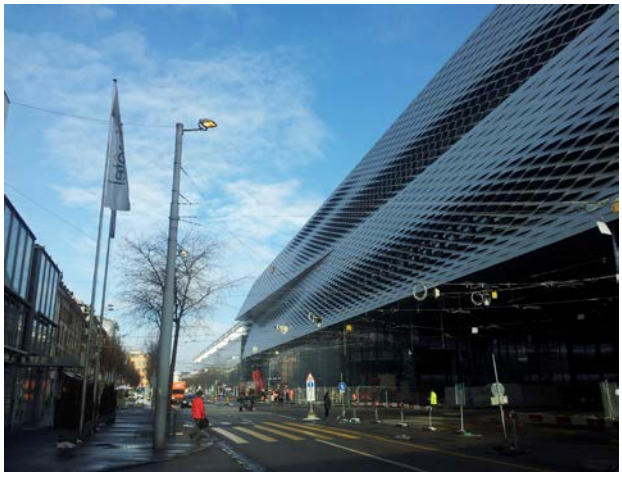

Fig. 2.24. Messe Basel. Exhibition Hall. 2013. Architects: Herzog & de Meuron.
https://www.flickr.com/photos/patsch/ https://creativecommons.org/licenses/by/2.0/

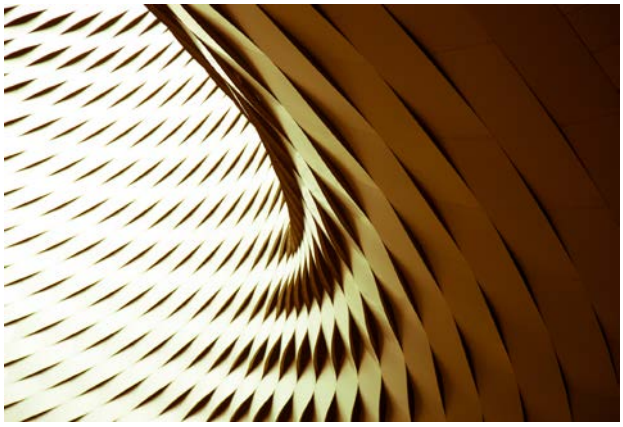

Fig. 2.25. Messe Basel. Exhibition Hall. 2013. Architects: Herzog & de Meuron.
https://www.flickr.com/photos/85189931@N00/ https://creativecommons.org/licenses/by/2.0/

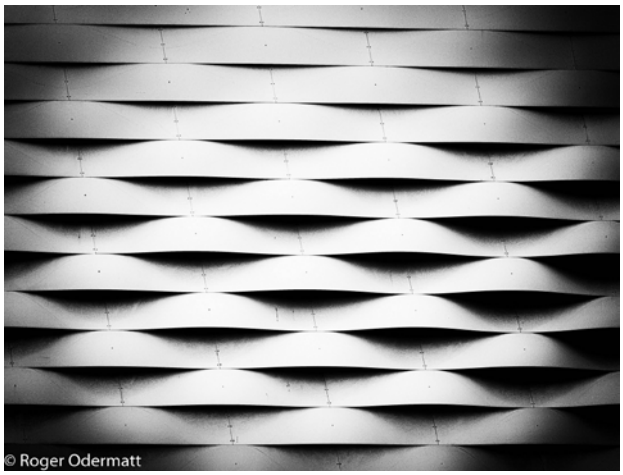

Fig. 2.26. Messe Basel. Exhibition Hall. 2014. Architects: Herzog & de Meuron.
https://www.flickr.com/photos/rogerodermatt/ https://creativecommons.org/licenses/by-nc-nd/2.0/

Starting from standard meshes and combining them with other manufacturing processes, we can obtain some other special products. Flattened EM meshes are quite common; they are cold rolled after expansion providing a smooth, flat and level sheet(EMMA 557-12 Standards for Expanded Metal 2012).

They can be bended or manipulated in any other way. For instance they can be transformed by embossing, to obtain an EM mesh with an irregular surface. Herzog&deMeuron designed a special embossed expanded metal mesh to create a cladding for the *Caixa Forum* building in Madrid.

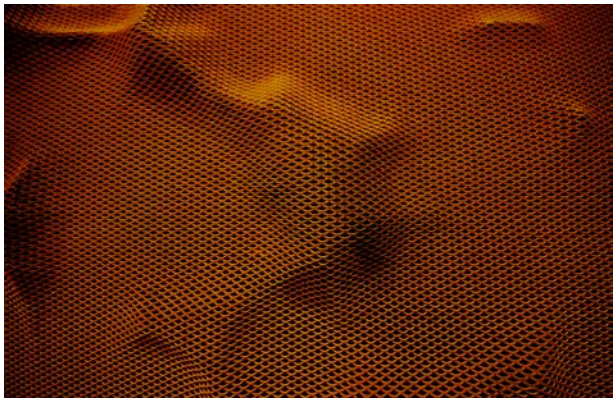

Fig. 2.27. Embossed EM mesh. Caixa Forum basement auditorium. 2011. Herzog&deMeuron architects. Manufacturer: IMAR.
https://www.flickr.com/photos/achejandro/ https://creativecommons.org/licenses/by-nc-nd/2.0/

Fig. 2.28. Embossed EM mesh cladding. Caixa Forum basement auditorium. 2011. Herzog&deMeuron architects. Manufacturer: IMAR.

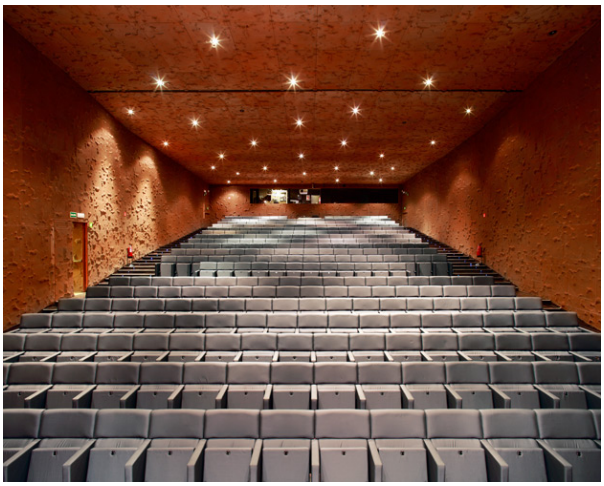

Fig. 2.29. Caixa Forum basement auditorium. 2011. Herzog&deMeuron architects.
https://www.flickr.com/photos/markbentleyphoto/ https://creativecommons.org/licenses/by-nc-nd/2.0/

In some other cases, metal sheets are subjected to a manufacturing process prior to the expansion, such as drilling, in order to obtain perforated EM meshes.

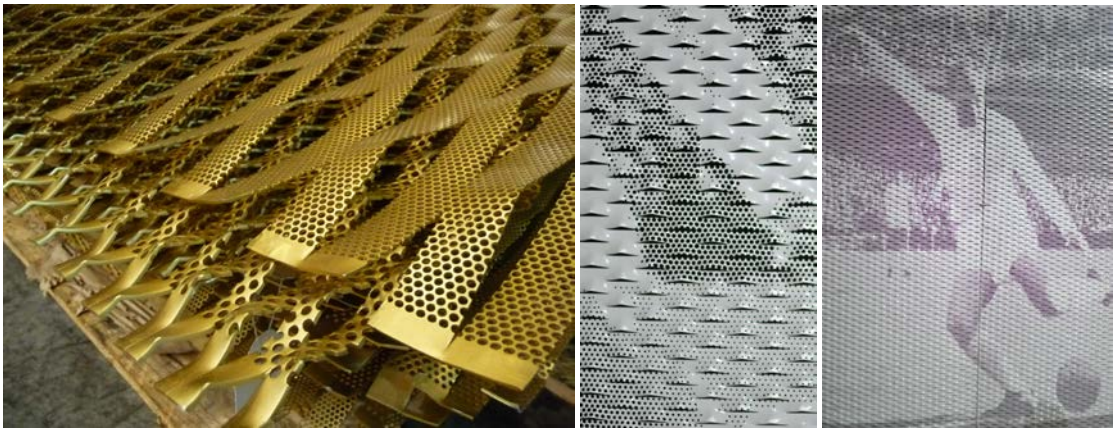

Fig. 2.30. EM meshes produced from previously perforated sheets. Manufactured by IMAR (2009 and 2014). The perforation pattern can be adjusted to reproduce an image.

Expanded metal mesh can be coated in a range of finishes to offer material protection and aesthetic value. Depending on the material of the EM mesh and the finish we want to accomplish, different processes can be carried out: hot-dip galvanizing, pre-galvanizing, anodizing, enameling, power coating, painting, plastic coating, etc.

2.5 Expanded metal facades

Expanded metal facades can help to build a more energy efficient environment thanks to their manufacture process and to their function as outer skin of a building.

The manufacturing process produces virtually no waste; the materials used to make EM meshes have a high amount of recycled material content (as aluminum, steel or copper); there are manufacturing plants in many different places, so that it is very likely to have regional producers, and it is a recyclable material. One of the disadvantages is that, being based on metal coils, EM implies using a great amount of energy in the recycling processes of the metals and in the production of the coils.

As well as other materials or products, EM can be used as a sun control device in facades. If it is properly designed, EM meshes may allow natural light to pass through whenever necessary as well as reducing cooling costs if used as sun shade.

The EM meshes can be installed in the same way as any other building product made of metal sheets. It can be installed as the outside sheet of a ventilated façade. This outside sheet can be placed on different self-supporting structures: directly fixed to the inner wall, on a precise fixing spaced out from the wall or on a totally independent structure from the rest of the building.

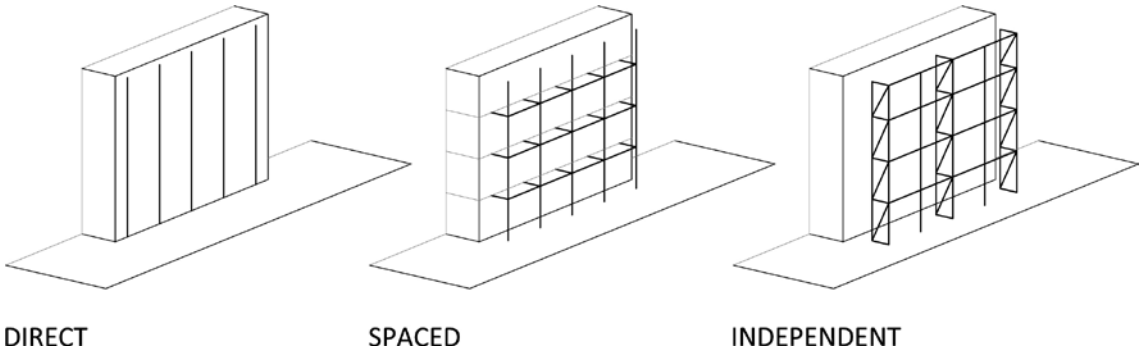

Fig. 2.31. Self-supporting structures for outside sheet of a facade

The EM sheets can be placed on those structures directly (bolted, welded, clipped…) or by means of a frame. In any case, these fixing systems are the common ones in metal ventilated facade systems. The joints between different EM mesh units can be visible or hidden by the frames or any other element. They can also be overlapped to achieve a continuous surface (producing a raised edge) or welded one to another.

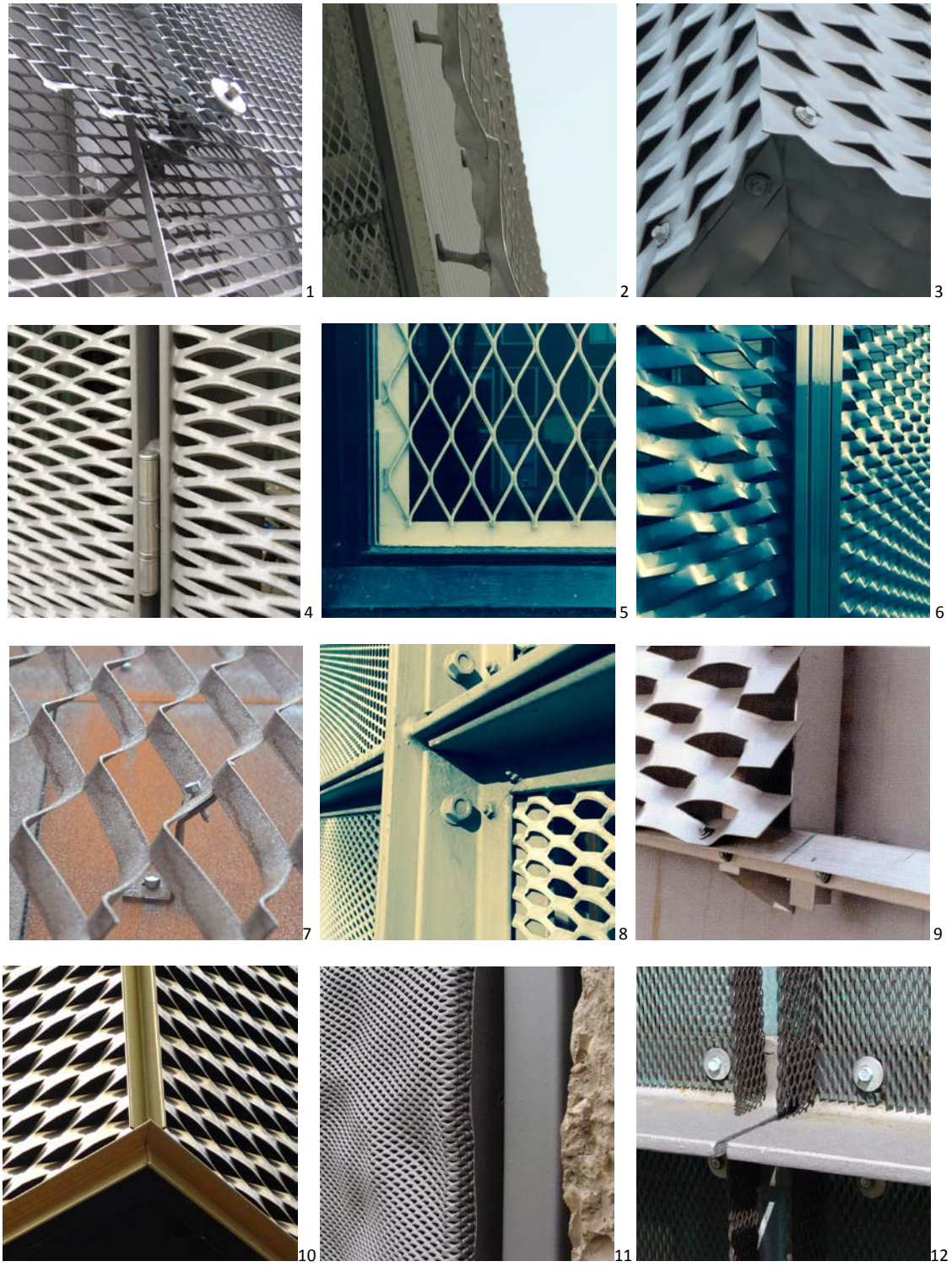

Fig. 2.32. Facade EM fixing solutions.

Picture 9 by Jesus Granada, first published in Tectonica n.22. Pictures 10,11,12:
https://www.flickr.com/photos/detlefschobert/ https://creativecommons.org/licenses/by-nd/2.0/

References

Clark, Norris Elmore
1904 Expanded Metal. Application. Plainville, Connecticut.
1908 Manufacture of Expanded Metal.

EMMA 557-12 Standards for Expanded Metal
2012. Expanded Metal Manufacturers Association division of National Association of Architectural Metal Manufacturers.
http://www.naamm.org/emma/emma_technical_literature.aspx.

Golding, J. P.
1885 Peters. Google Patents. http://www.google.com/patents/US320241.

Groover, Mikell P.
2012 Fundamentals of Modern Manufacturing: Materials, Processes, and Systems. Edición: Revised. Hoboken, NJ: John Wiley & Sons.

De Tejada, Leonardo, Antonio Sonier, and Manuel Maluquer
1900 El metal deployé en España. Revista de Obras Públicas. Fundada y sostenida por el cuerpo nacional de Ingenieros de Caminos, Canales y Puertos, March 15: 93–97.

Tinker, George K
1900 Frame for Pavements.

3.1 Daylight metrics

Light is an electromagnetic radiation with a wavelength from 380 to 780 nm. The electromagnetic spectrum is divided into radio waves, microwaves, infrared radiation, visible light, ultraviolet radiation, X-rays and gamma rays.

Daylight is the light received from the sun and the sky, which varies throughout the day, as modified by the seasons and the weather. It is therefore composed by skylight (received from the whole vault of the sky) and sunlight (received directly from the sun). Blinds, louvers, solar control glass and other devices can help to avoid excessive sunlight and solar gain (heat derived from the sun) in buildings.

3.1.1 Metrics

The main metrics of light are **luminous intensity**, **luminous flux**, **luminance** and **illuminance**.

Luminous intensity, *I* (unit: candela, cd) describes the power of a light source to emit light in a given direction or solid angle (a three dimensional angle).

Luminous flux, *F* (unit: lumen, lm) measures the power of light. 1 lm = 1 cd sr. Luminous flux is the total light emitted by a source while luminous intensity is the portion related to a specific direction.

Luminance, *L* (unit: cd/m^2) is the luminous intensity of a surface in a specific direction, divided by the projected area as viewed from that direction. The light emitted or reflected from a surface in a particular direction is a result of the illumination level and the reflectance.

Illuminance, *E* (unit: Lux = lm/m^2) is the luminous flux received per unit area of a surface. In USA Foot Candle is used, meaning 1 lm/square foot or 10,76 lux.

If we were to deal with electromagnetic radiation instead of just light, we talk about *radiance* and *irradiance* instead of *luminance* and *illuminance*.

To characterize materials in reference to light we use **reflectance**, **transmittance** and **absorption**. All of them are expressed as percentages.

Reflectance (ρ) is the ratio of light reflected from a surface to the light falling upon it; as affected by the lightness or darkness of the surface and whether it's shiny or matt.

Transmittance (τ) is the ratio of incident light falling upon a surface to the portion of that light that goes through the material. It can be determined using two illuminance meters in front and behind the surface.

Absorption indicates the portion of incident light on a material that is neither reflected nor transmitted.

With transmittance and reflectance we get an overall amount of light going through or being reflected from the material but those magnitudes do not tell us anything about light distribution after transmission or reflection. The following figure shows different types of reflections for different surfaces but possibilities are as uncountable as surface types.

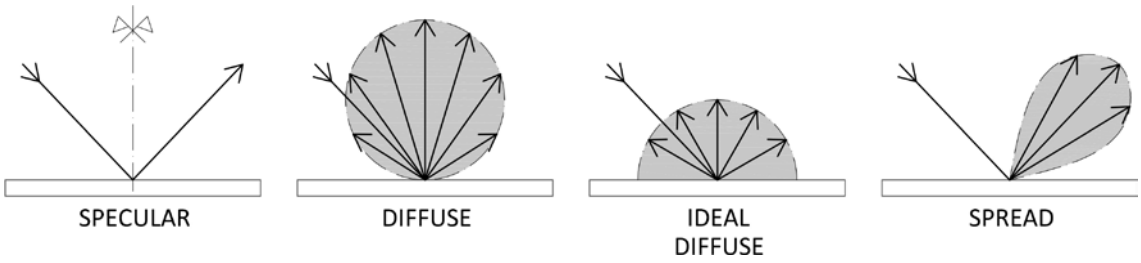

Fig. 3.1. Different types of reflections

Bidirectional Scattering Distribution Functions (BSDF) are mathematical functions describing that distribution. We can differentiate Bidirectional Transmittance Distribution Function (BTDF) and Bidirectional Reflectance Distribution Function (BRDF).

Reflectance, transmittance, absorption and BSDF are features that describe an even surface but they are also applicable to any discontinuous one-dimensional product that includes holes or void spaces. That is the case of many layers of complex fenestration systems as louvers, meshes, fabrics, etc.

When it comes to describing surfaces, we use the previously presented metrics but there are other parameters that were created to describe the daylight performance of a space taking into account its location, orientation, fenestration systems, shape and surface-materials. The most common is the Daylight factor, explained below (section 3.2.2).

3.2 Computer aid simulation of Daylight in buildings

Even if the use of computer simulation is growing in building design both at schematic level and later in development processes, it should definitely be a more extended practice to add to experience, rule of thumb and design guidelines (Galasiu and Reinhart 2008).

3.2.1 Modeling for simulation

In a recent publication, Christoph F. Reinhart (Reinhart 2011) listed a number of elements that must be taken into account for daylight performance simulation of a building: the scene, a sky model, an area of interest, a simulation algorithm and a dynamic simulation.

When a 3D model of the scene is constructed for daylight simulation, the accuracy and complexity of the model should be developed according to the design phase of the building and the calculations needed. Something important when constructing this kind of models is the construction of the ground plane, neighboring buildings and surrounding objects. All of them are essential elements during the simulation because they define shades and reflections which change the behavior of the light reaching the building. The optical properties of surface materials should be also defined.

Sky conditions are ever changing and depend on weather and sun position. For daylight simulations, sky models are used, that is, mathematical models created for that purpose. There are sky models that only describe diffuse daylight (sunlight scattered in the atmosphere). Other models also work with direct sunlight (incident straight from the position

of the sun), so they create direct lighting and shading. The most commonly used sky models are: *CIE* (Commission Internationale de l'Éclairage) *clear*, *overcast* and *standard general* skies, and the *Perez* sky. They attempt to include intermediate and cloudy skies between the defined overcast and clear skies. (Kittler, Perez, and Darula 1997) (Kittler, Perez, and Darula 1998) (Reinhart 2011). As for the scene, the sky model we choose should be suitable to the aim of the simulation.

The next step is to define an area of interest. This can be for instance a viewpoint, or any set of sensor points to register illumination in order to obtain representative graphs. The modeler should choose the area depending on the purpose of the simulation, e.g. the illuminance on a horizontal plane (such as the floor or the working area of a table) can be represented according to the distance from a window, and then, compare different results (testing different fenestration systems) in a diagram.

When running a simulation, it is important to know which simulation engine is used by a certain program, i.e. the simulation algorithm. The results can vary substantially depending on this. Different software work with different algorithms, and can show unexpected results if the modeler does not know how they operate. In addition, certain studies have shown that the differences related to the reliability of the results between a simulation expert and a novice are quite large (Ibarra and Reinhart 2009).

Dynamic simulations have been developed to study changing conditions of light, similar to real life behavior in order to obtain more realistic results. They consider changing daylight level values for a certain time step (e.g. every hour or every minute) for the whole year, based on regional climate information.

Such simulations are usually combined with thermal calculations to run an energetic simulation of a building.

Repeating a static simulation multiple times for varying sky conditions would need enormous simulation times. To avoid this problem, most researchers nowadays use a daylight

coefficient based approach. This method, originally proposed by Tregenza and Waters (Tregenza and Waters 1983), subdivides sky and ground hemisphere into patches or surface segments. Each patch represents a light-source (reflected light when referring to the ground). Then the luminance contribution of each patch to the illuminance of a point in a specific surface must be calculated. The contribution of each patch depends on the relative position between the model and the light-source, the optical properties of the model indoor surfaces, and the optical behavior of the fenestration system through which light reaches the measured space. If the mentioned parameters are invariable during the simulation period, the Daylight Coefficient can be calculated just once for each light-source.

$$DC_{\alpha}(x) = \frac{E_{\alpha}(x)}{L_{\alpha}\Delta S_{\alpha}}$$

Where,

$DC_{\alpha}(x)$ = Daylight Coefficient related to a certain light-source patch (S_{α}) and measured point(x)

$E_{\alpha}(x)$ = Illuminance at measured point (x) due to certain light-source patch (S_{α})

L_{α} = Luminance of a certain light-source (S_{α})

ΔS_{α} = Solid angle of a certain light-source (S_{α})

Therefore, given any change in sky luminance during the simulation period, the consequent illuminance in measured point can be calculated as follows:

$$E(x) = \sum_{\alpha=1}^{n} DC_{\alpha}(x) L_{\alpha} \Delta S_{\alpha}$$

3.2.2 Performance metrics

Once the simulation is ended, there are various parameters or indicators of the performance of a space or building. Reinhart refers to illuminance based metrics (e.g. daylight factor) and luminance-based metrics (e.g. glare indices).

Daylight factor is one of the most used indicators and responds to the ratio between the light received at a point within a building and that available outside the building, expressed as a percentage:

DF = Inside Illuminance/Outside Illuminance x 100

Since daylight varies continually, the amount of light from a given DF is not a finite figure but gives a good indication of the level of daylight available. This factor is defined under a CIE overcast sky and it is independent of surrounding elements, environment or local conditions, anyway, it is not related to absolute values but to a ratio between illuminance levels. The accuracy of a simulation can be improved, using CIE clear or standard sky models and direct sunlight. It is also possible to run a series of simulations under determined conditions, to model a space at different hours and days (e.g. 9 a.m., noon and 3 p.m., on solstice and equinox days). The next step would be to carry out the aforementioned dynamic simulations using annual illuminance profiles, and optimize calculations using occupancy models for each space type.

Besides illuminance-based parameters, other indicators are more related to excessive solar transmittance or glare. Glare is a human sensation, an unwanted “shine that is much too bright and feels as if it is hurting the eyes” (Cambridge Academic Content Dictionary 2008). Glare is measured with glare index, an arithmetical assessment of high dynamic range images based on research about human sense.

There are different glare indices: unified glare rating (UGR) (Sørensen 1996), daylight glare index (DGI) (Hopkinson 1973), and more recent, daylight glare probability (DGP) (Wienold and Christoffersen 2006).

3.2.3 Complementary simulations

When studying light behavior in buildings or spaces, it is also very useful to construct physical models and assess them under artificial sky or under natural outside sky conditions.

The results obtained in this kind of simulation, should be combined with those obtained with computer assistance.

Another type of simulation that is often combined with that of natural daylight is electric light simulation, which is simpler thanks to the constancy of the light emitted. There are many programs available to simulate illumination with commercial luminaries whose photometric behavior is described by IES files, easily obtained from manufacturers. Both are usually combined with thermal simulations to improve the energy efficiency of buildings and the implementing of Building Energy Management Systems, BEMS, which provide computer control of lighting systems within a building. (Phillips 2004)

3.3 Glass, louvers, translucent metal screens.

Detailed information about the daylight performance or transmittance of fenestration layers is needed for the previously described building simulation and assessment methods. Glass is the omnipresent element in fenestration but many other products are added to contemporary complex fenestration systems. Research about solar control devices has been mainly focused on solar factor values of glass and traditional devices as louvers. Solar factor is associated to heat-gain and its assessment implies considering reflection, absorption, re-irradiation and ventilation phenomena. As glass is transparent, glass layer technology has reached interesting results reducing the infrared radiation transmittance, i.e. heat transmittance, and maintaining good daylight transmittance by means of the so called selective glass (thus allowing a better transmission of light than heat, by differentiating the wavelengths of those radiations).

Some methods for calculating the solar factor of glazing does not take into consideration the influence of the direction of incident radiation; they assess just the case of radiation perpendicular to the glass pane. This kind of simplification is inadmissible when we assess daylight transmittance of surfaces with holes and three-dimensional parts. As the

direction of incident radiation depends on the position of sun and the location, orientation and inclination of the building skin, any incident direction is possible on a fenestration layer and very different transmittances must be considered. Standards for this kind of light redirecting materials are beginning to appear but there is much to do.

The transmittance assessment for louvers has been researched in depth and even though it is more complex than the one for glazing, it can be assessed taking just one section of the device because their shape results from extruding that section all along a straight line. Translucent metal screens have usually more complex shapes and require a 3D approach. Among translucent metal screens, perforated metal is seemingly the simplest to assess. Its transmittance is equal to the percentage of perforation when radiation is perpendicular to the sheet, but decreases when incidence angle changes. Thickness of the sheet becomes important when holes are small, because of reflection in the edges of the sheet's holes. Woven metal fabrics are very variable and it seems complicated to use a common assessment method for all of them. The case of expanded metal requires a particular assessment due to its shape, composed by bended strands, but most expanded metals are produced following the same basic process. By changing the dimensions of the elements, movements and deformations involved in manufacture we obtain different expanded metal meshes. Starting from the common manufacturing steps of regular expanded metal, some tool to ease daylight transmittance assessment would seem possible and useful. The 3D EM modeler presented in section 6.2 provides a fast tool to obtain different EM models to perform comparative assessments and that can be introduced in a building daylight simulation model to assess its influence as a façade layer. Ray tracing simulation software, as *Radiance*(Radiance WWW Server n.d.)) is able to calculate BSDF of those EM models that can then be introduced in software such as *Window* (Window Optics n.d.) to define the properties of complex fenestration systems (CFS) composed by several coplanar layers (Ward et al. 2011). The CFS's properties can be introduced back to simulation programs.

Window software's database contains BSDF data for some common shading systems. Feeding that database with different EM BSDF could be a task to develop. The European homologue program for CFS analysis is WIS (Advanced Window Information System). (WIS n.d.).

References

Cambridge Academic Content Dictionary
2008. New York: Cambridge University Press.

Galasiu, Anca D., and Christoph F. Reinhart
2008 Current Daylighting Design Practice: A Survey. Building Research & Information 36(2): 159–174.

Hopkinson, R. G.
1973 Glare from Daylighting in Buildings. Applied Ergonomics 3(4): 206–15.

Ibarra, Diego I., and Christoph F. Reinhart
2009 Daylight Factor Simulations - How Close Do Simulation Beginners "Really" Get? Proceedings of Building Simulation: 196–203.

Kittler, R., R. Perez, and S. Darula
1997 A New Generation of Sky Standards. *In* . Amsterdam.
1998 A Set of Standard Skies Characterizing Daylight Conditions for Computer and Energy Conscious Design. *In* .

Phillips, Derek
2004 Daylighting: Natural Light in Architecture. 1 edition. Architectural Press.

Radiance WWW Server
N.d. http://radsite.lbl.gov/radiance/, accessed November 23, 2014.

Reinhart, Christoph F.
2011 Simulation-based Daylight Performance Predictions. *In* Building Performance Simulation for Design and Operation. London ; New York: Routledge.

Sørensen, Kai
1996 Proposal for a General UGR Formula. Delta Lys & Optik.

Tregenza, P. R., and I. M. Waters
1983 Daylight Coefficients. Lighting Research and Technology 15(2): 65–71.

Ward, G., R. Mistrick, E. S. Lee, A. McNeil, and J. Jonsson
2011 Simulating the Daylight Performance of Complex Fenestration Systems Using Bidirectional Scattering Distribution Functions within Radiance. LEUKOS 7(4): 241–261.

Wienold, Jan, and Jens Christoffersen
2006 Evaluation Methods and Development of a New Glare Prediction Model for Daylight Environments with the Use of CCD Cameras. Energy and Buildings 38(7). Special Issue on Daylighting Buildings: 743–757.

Window Optics
N.d. http://windowoptics.lbl.gov/, accessed November 23, 2014.

WIS
N.d. http://www.windat.org/wis/html/index.html, accessed November 23, 2014.

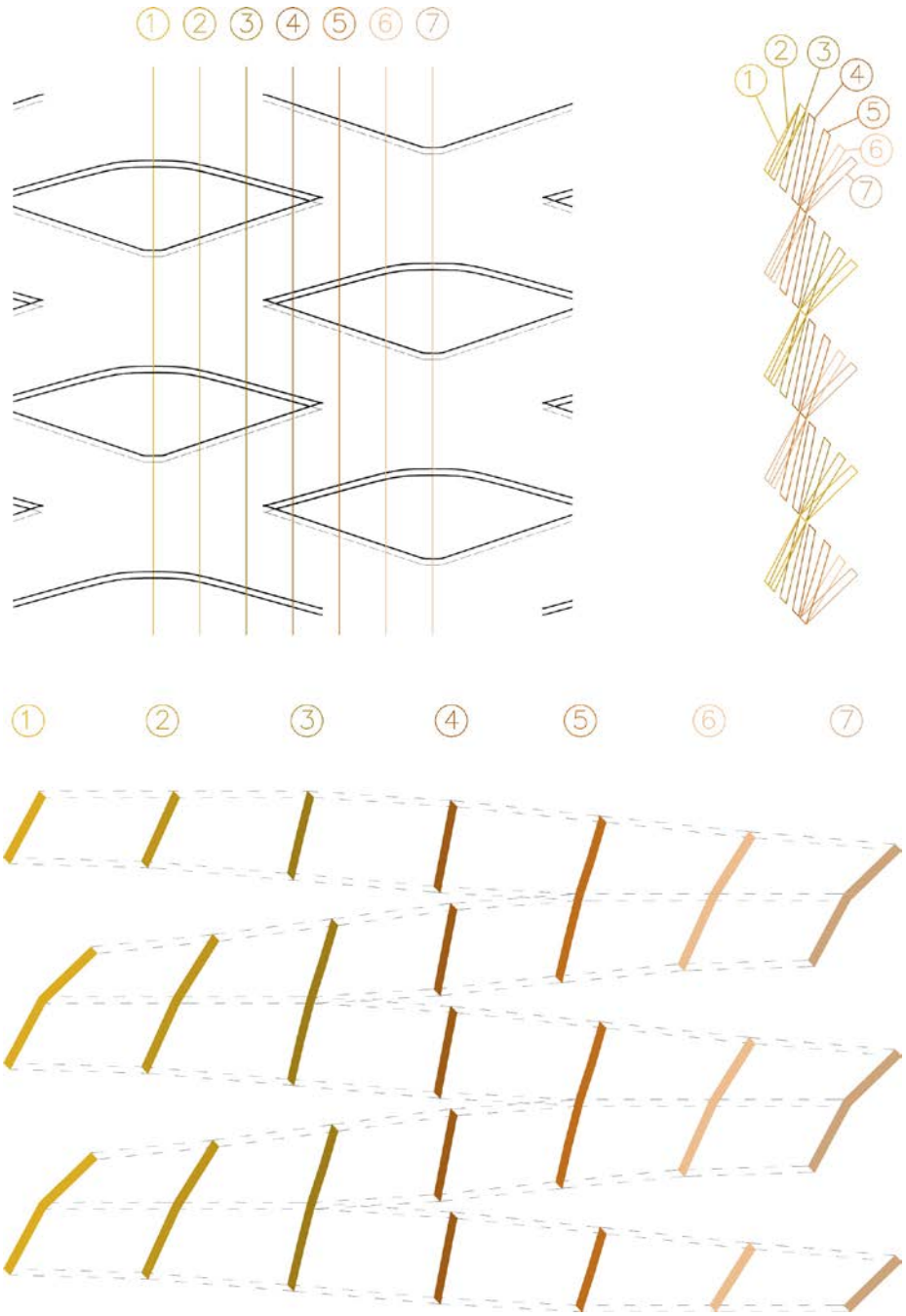

Fig. 4.1. Different vertical sections of an EM mesh (mesh number 03, defined in section 5.3)

As aforementioned, EM meshes do not have a continuous vertical section like louvers, whose analysis can be made on just one section in any assessment method. The geometry of the expanded metal is more complex. The transformation that the material undergoes during the manufacturing process not only changes the proportion between solid and hollow spaces that we find through different vertical sections of a mesh, but also varies the slope of the strands. In other words, the slope of the strands changes along the mesh.

The simplest daylight performance assessment methods usually analyze just one section of the fenestration system, simplifying the method itself. As shown in the previous figure, some of the vertical sections of an EM mesh are almost opaque while some others have spacious openings and a lower slope of the strands. That is why we find many different sections on an expanded metal mesh behaving in many different ways when facing incident radiation. For these reasons, to assess daylight performance of an EM mesh we cannot simply analyze one section; we need a more complex approach to reach a more precise analysis.

4.1 Mesh main section and geometrical features

With the objective of providing a first approach to an analysis of transmittance through EM meshes, we decided to make a rough geometrical analysis of transmittance through the main section of the mesh. We will take *EM mesh main section* as the one that crosses through the middle points of the straight lines defined by the parameters intercut (*i*), cut width (*c*) and blade bevel width (*b*); cutting off the mesh by the centre of the knuckles where the strands join and by the centre of the gaps in the meshes. That is to say that the main section of an expanded metal mesh is the one extracted from the cut by any vertical plane of symmetry of a virtually infinite EM mesh (in the previous image the sections named 1 and 7 are both main sections of the mesh).

The shape of an EM *main section* can be defined by its following parameters:

- Short way of mesh (*SW*): distance between two equal consecutive points in the main section.
- Strand width (*w*): distance that the sheet advances between two cutting movements in manufacture.
- Blade descent (*d*): Distance the blade descends with each of its vertical movements

- The sheet's thickness (*e*), which can be considered as null to simplify this analysis. The conclusions will not be valid for meshes with a high value of the ratio *e*/*w* (values higher than 1/5 could be considered as high)

As mentioned in section 2.3.2, the first three parameters form a right triangle (from now on *ABC* triangle) where the hypotenuse is the short way of mesh (*SW*) and the legs are twice the strand width (2*w*) and twice the blade descent (2*d*). So, the first relationship that can be extracted from these parameters is the following:

$$\left(SW/2\right)^2 = d^2 + w^2$$

Therefore, taking into account the relationship between the parameters, it is sufficient to know two in order to define the *ABC* triangle and -accordingly- the main section. Among these three parameters, short way of mesh and strand width are the most likely provided by manufacturers to customers, while blade descent is a parameter used just in manufacture. So *SW* and *w* will be the parameters of preference used in this analysis.

Considering the whole mesh of expanded metal as a plane, the direction defining this plan is the direction of *SW*. That is to say that the reference position of an EM mesh is the one where *SW* is vertical.

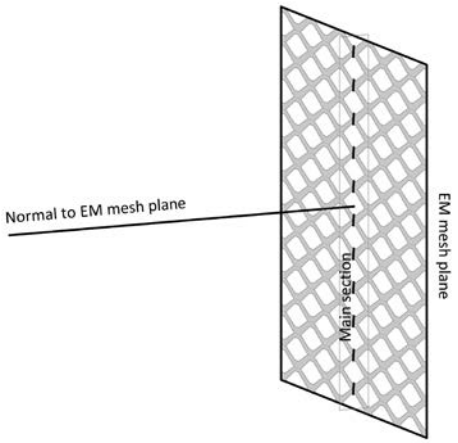

Fig. 4.2. EM mesh plane, normal to it and main section

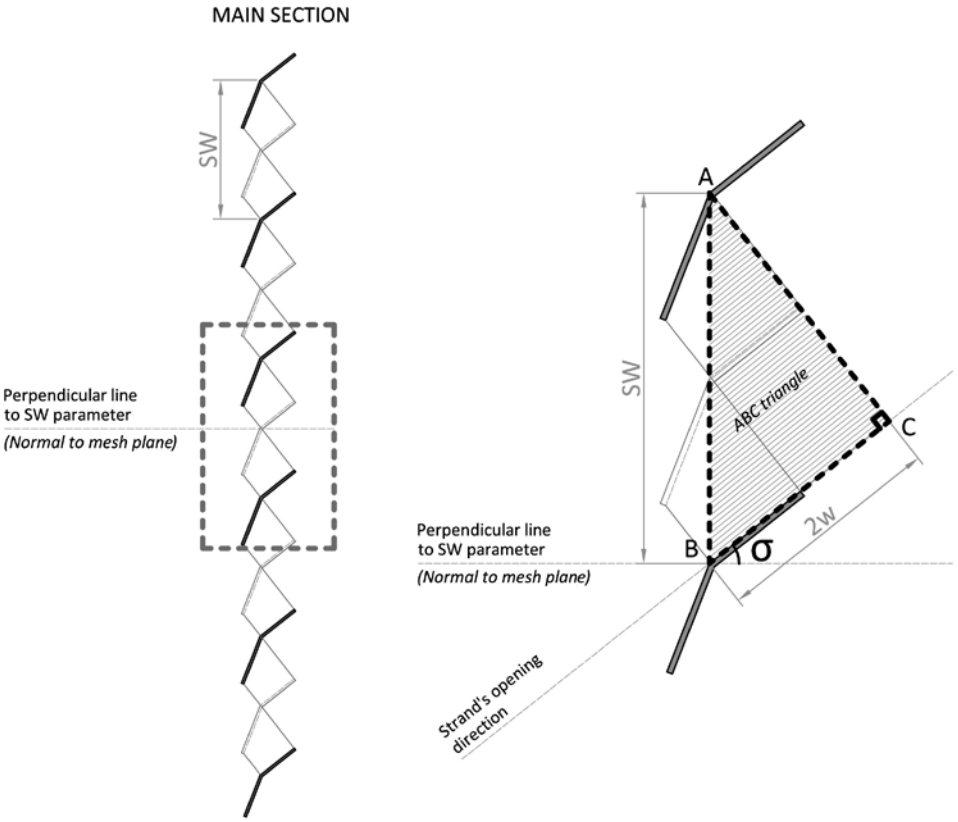

Fig. 4.3. EM mesh main section, opening angle of the strand (σ) and ABC triangle

That is why the *ABC* right triangle is defined by the parameters *SW* and *w*, knowing that these parameters are the hypotenuse and one of the legs of this triangle respectively and that *SW* parameter is positioned vertically.

Based on this reference position of the *ABC* triangle and the main section, an opening angle of the strands is defined, expressing the opening of the mesh depending on the inclination of the strands in the main section. This opening angle will be expressed by the letter σ, the angle formed by the normal to the plan of the mesh and the direction of the strands in the main section.

If the direction of the strands in the main section coincides with the direction of *w* in the triangle and the triangle is positioned in such a way that *SW* is vertical, σ can be expressed also as the angle between a perpendicular line to *SW* and *w*.

The relation between *SW* and *w* changes this σ angle, so it is possible to predict how *opened* or *closed* the mesh is from these two parameters.

4.2 Prediction of the direction of incident radiation with highest transmittance

At least initially, we could expect that the incident radiation with highest transmittance will be the one that finds less surface of the mesh obstructing direct transmission. That is the reason why the transmission through the EM mesh main section is expected to have an important influence in the overall transmittance of the mesh as that section has wider openings and less strand slope, offering less obstruction to incident radiation. We presume that transmission through the main section makes up an important part of the total transmittance.

In spite of this and depending on the material and color of the finish of the metal (i.e. it's reflectance), the reflections that occur in the mesh can gain more or less importance in transmittance. Anyway, it is difficult to find an EM mesh finish with such a specular reflectance that increases significantly total transmission through a mesh. Specular reflection occurs when a single incoming radiation direction is reflected on a surface symmetrically in a single outgoing direction (see Fig. 3.1). Both incoming and outgoing direction make a same angle with respect to the normal surface. It can be also understood as a mirror-like reflection (Specular Reflection 2014)

4.2.1 Geometric directional analysis of direct and reflected transmittance through the EM mesh main section

With the aim of visualizing and quantifying the transmission through an expanded metal mesh with different incidence radiation angles, a geometric analysis has been done

where, having as reference the main section of a case study[1] EM mesh, the light transmission has been studied as far as direct transmission and theoretical specular reflection is concerned. This study has been done in intervals of 15º angles, completing 360º.

Therefore we have drawn the light incident in one gap of the main section of an EM mesh, the specular reflections resulting when this radiation finds an obstacle and the specular transmitted light (light transmitted without obstacle and no change of direction). It is obvious that metals used for EM do not have a specular reflectance of 100%, but in order to facilitate the analysis we assumed that simplification including light transmitted after one or two reflections on the mesh surfaces as if it had no loss, i.e. as if specular reflectance was 100%. Depending on the real specular reflectance of the material of the mesh, those reflections would have more or less influence in total transmittance, but of course, directly transmitted radiation (aka *specular transmission*) will always be the main part of total transmittance.

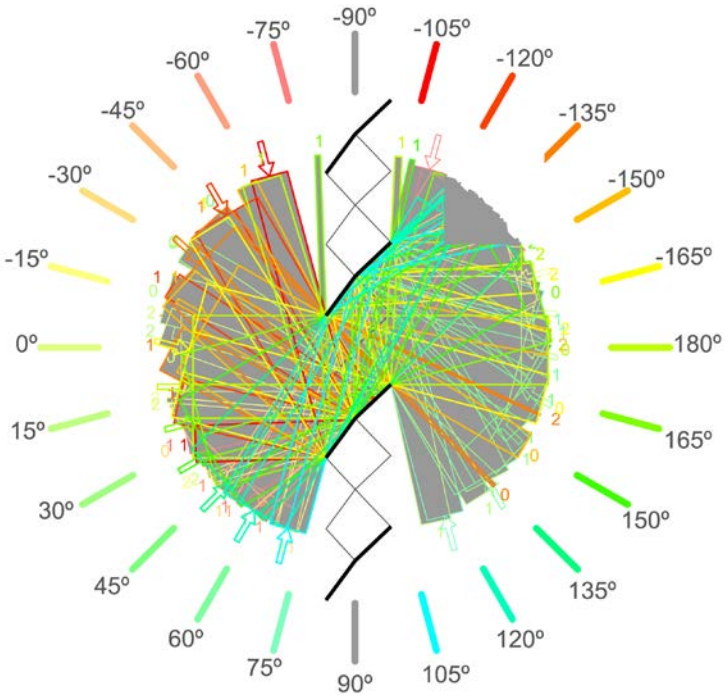

Fig. 4.4. Analyzed incident radiation direction angles (all directions superimposed on one graph)

[1] Mesh with the following parameters: *LW*= 62,5; *SW*= 23; *w*= 8; *e*= 1; *b*= 2; *i*= 25
(This mesh has been named as 03 in laboratory assessment; see section 5.3)

The directions of incident light are indicated by an arrow, while the transmitted radiations are indicated by a number. These numbers denote the amount of reflections that have been necessary to achieve transmission.

Afterwards, in order to quantify transmittance, the percentage that represents transmitted to incident radiation has been calculated by differentiating ranges by number of necessary reflections (considering only transmission after 1 or 2 reflections).

As we can observe in the following images and as expected, the closer the incident radiation angle to the strand's opening angle, the higher the percentage of directly transmitted radiation.

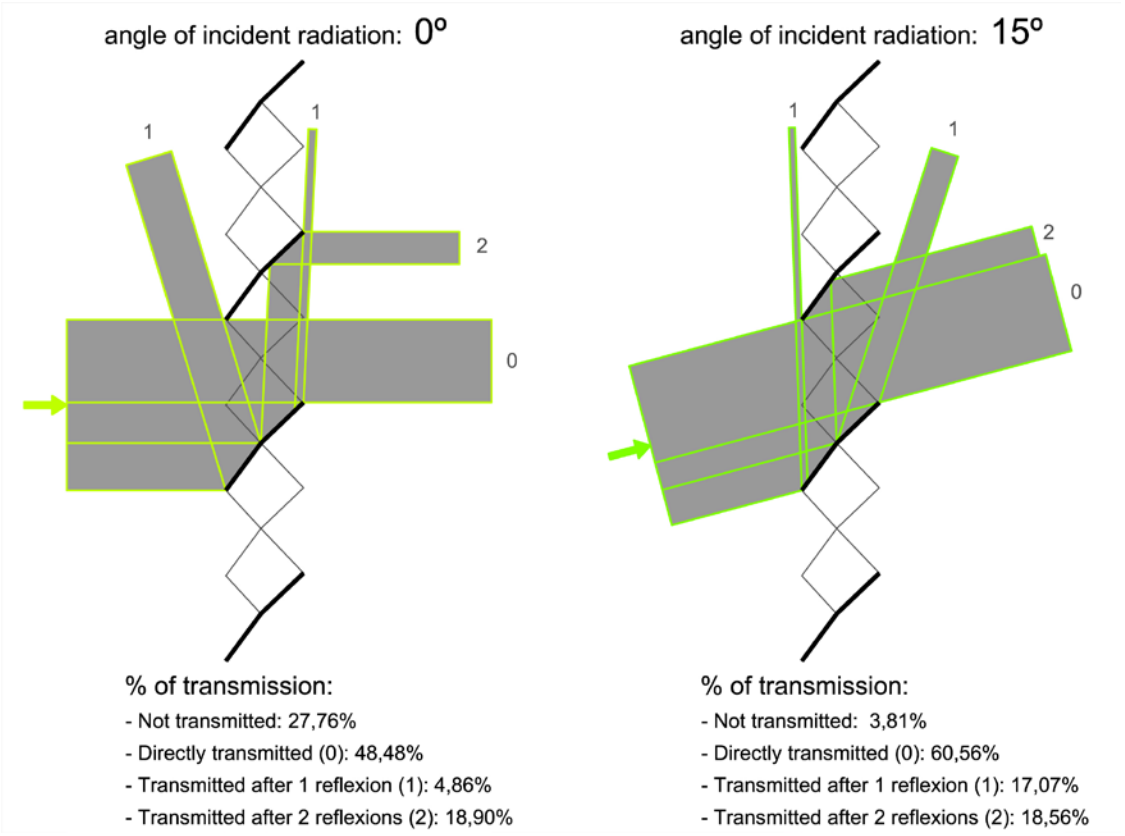

angle of incident radiation: 30º

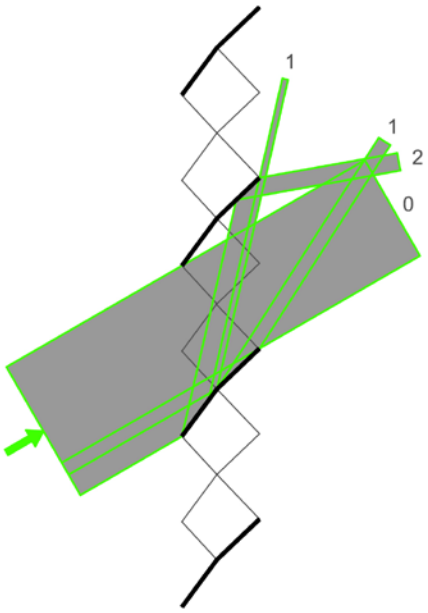

% of transmission:
- Not transmitted: 0%
- Directly transmitted (0): 74,75%
- Transmitted after 1 reflexion (1): 13,30%
- Transmitted after 2 reflexions (2): 11,95%

angle of incident radiation: 45º

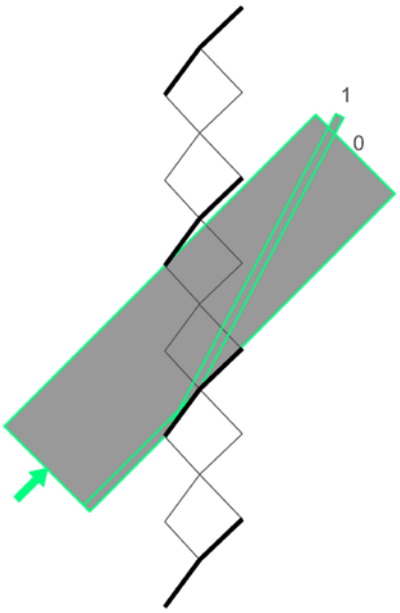

% of transmission:
- Not transmitted: 0%
- Directly transmitted (0): 92,75%
- Transmitted after 1 reflexion (1):7,25%
- Transmitted after 2 reflexions (2): 0%

angle of incident radiation: 60º

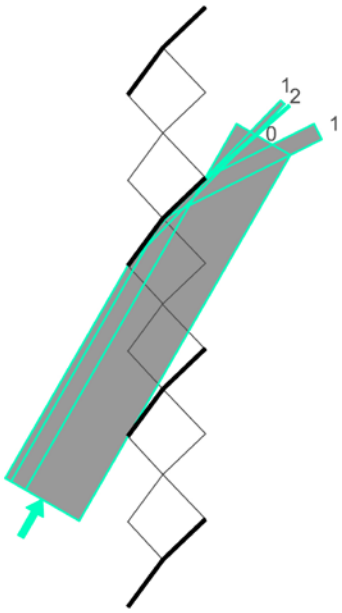

% of transmission:
- Not transmitted: 0%
- Directly transmitted (0): 72,04%
- Transmitted after 1 reflexion (1): 25,85%
- Transmitted after 2 reflexions (2):2,11%

angle of incident radiation: 75º

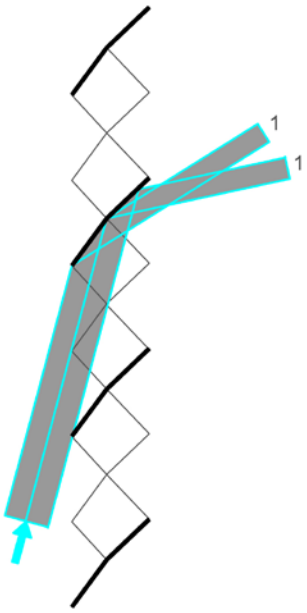

% of transmission:
- Not transmitted: 0%
- Directly transmitted (0): 0%
- Transmitted after 1 reflexion (1): 100%
- Transmitted after 2 reflexions (2): 0%

angle of incident radiation: 105º

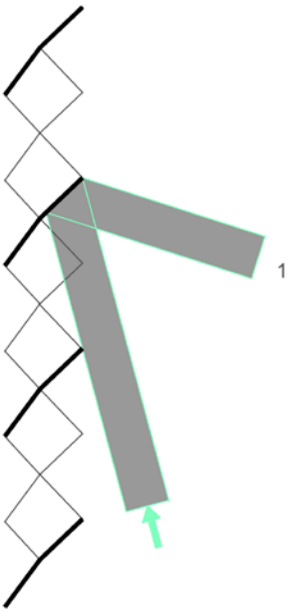

% of transmission:
- Not transmitted: 100%
- Directly transmitted (0): 0%
- Transmitted after 1 reflexion (1): 0%
- Transmitted after 2 reflexions (2): 0%

angle of incident radiation: 120º

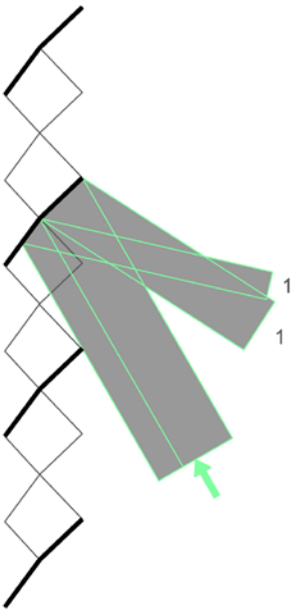

% of transmission:
- Not transmitted: 100%
- Directly transmitted (0): 0%
- Transmitted after 1 reflexion (1): 0%
- Transmitted after 2 reflexions (2): 0%

angle of incident radiation: 135º

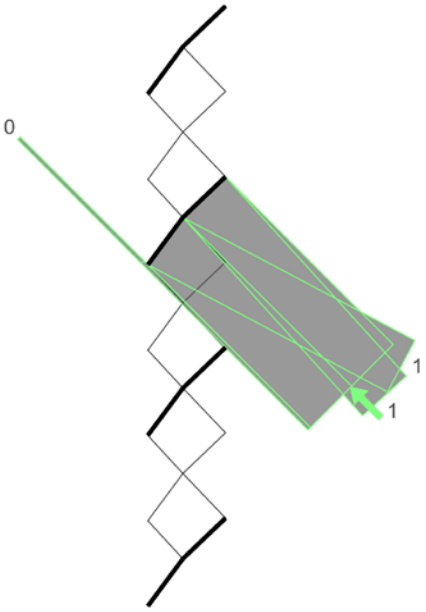

% of transmission:
- Not transmitted: 96,98%
- Directly transmitted (0): 3,02%
- Transmitted after 1 reflexion (1): 0%
- Transmitted after 2 reflexions (2): 0%

angle of incident radiation: 150º

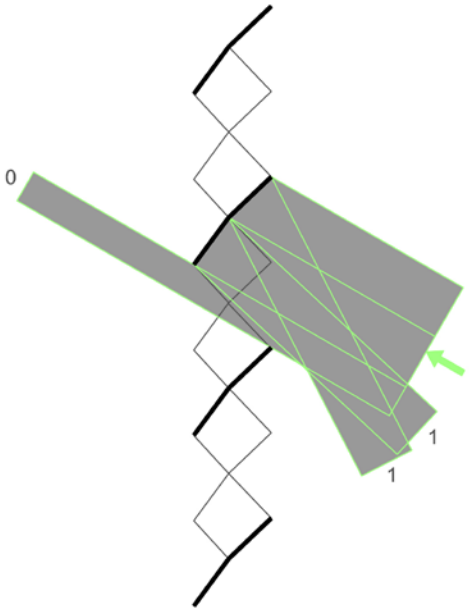

% of transmission:
- Not transmitted: 77,78%
- Directly transmitted (0): 22,22%
- Transmitted after 1 reflexion (1): 0%
- Transmitted after 2 reflexions (2): 0%

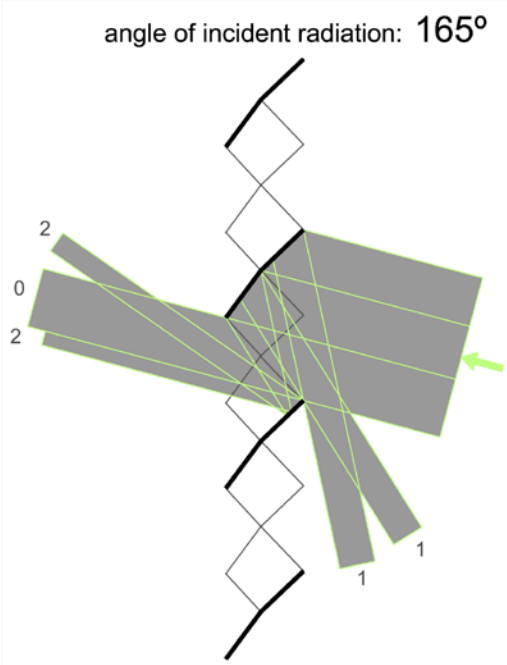

% of transmission:
- Not transmitted: 41,91%
- Directly transmitted (0): 36,31%
- Transmitted after 1 reflexion (1): 0%
- Transmitted after 2 reflexions (2): 21,78%

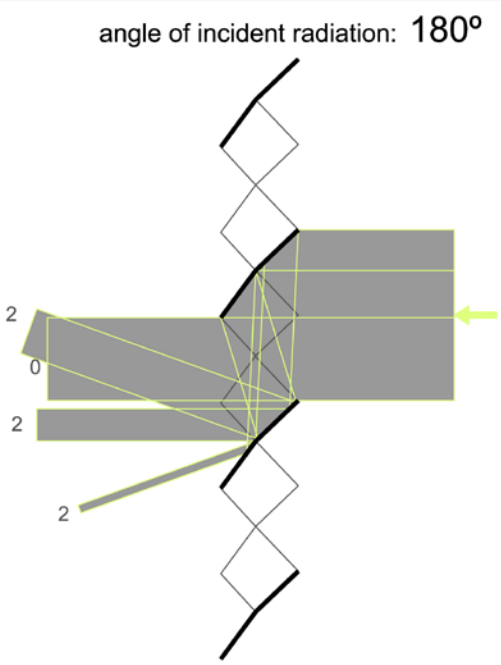

% of transmission:
- Not transmitted: 0%
- Directly transmitted (0): 64,47%
- Transmitted after 1 reflexion (1): 0%
- Transmitted after 2 reflexions (2): 51,48%

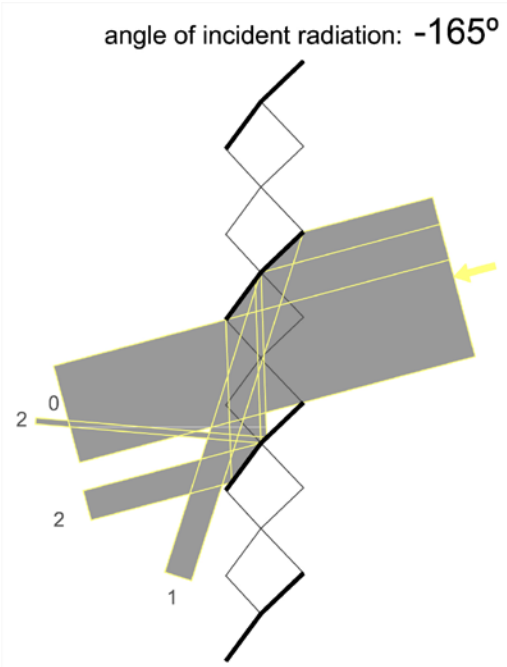

% of transmission:
- Not transmitted: 0%
- Directly transmitted (0): 60,68%
- Transmitted after 1 reflexion (1): 17,08%
- Transmitted after 2 reflexions (2):22,24%

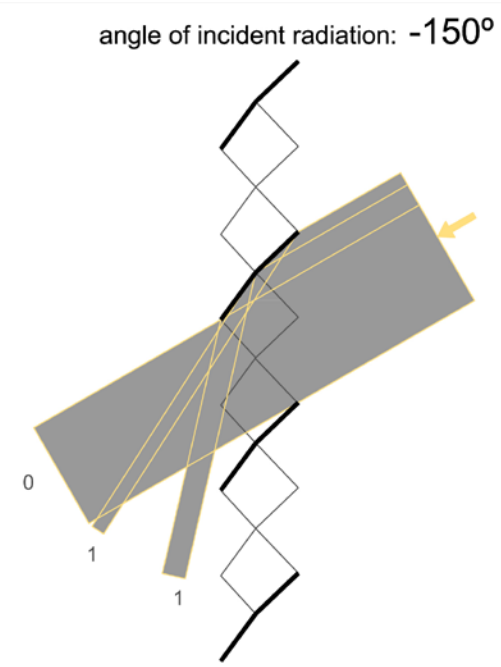

% of transmission:
- Not transmitted: 0%
- Directly transmitted (0): 74,75%
- Transmitted after 1 reflexion (1): 25,25%
- Transmitted after 2 reflexions (2): 0%

angle of incident radiation: -135º

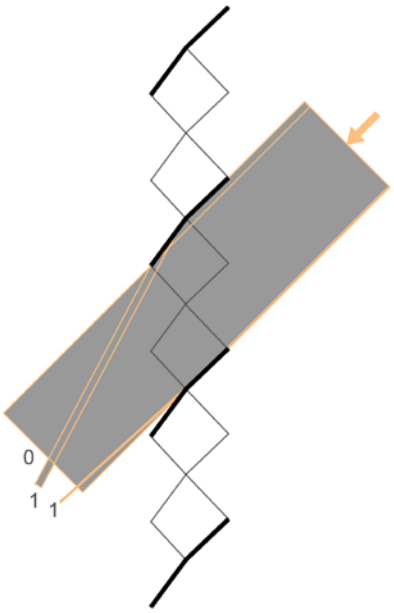

% of transmission:
- Not transmitted: 0%
- Directly transmitted (0): 93,23%
- Transmitted after 1 reflexion (1): 6,77%
- Transmitted after 2 reflexions (2): 0%

angle of incident radiation: -120º

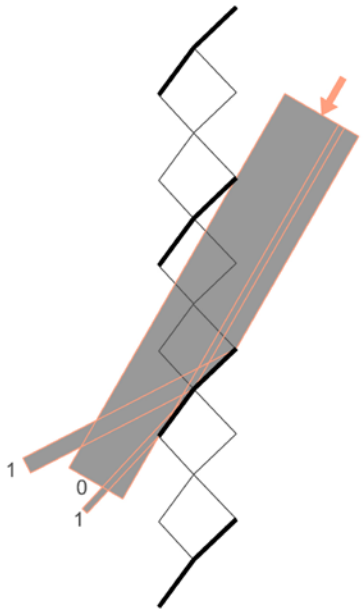

% of transmission:
- Not transmitted: 0%
- Directly transmitted (0): 72,76%
- Transmitted after 1 reflexion (1): 27,24%
- Transmitted after 2 reflexions (2): 0%

angle of incident radiation: -105º

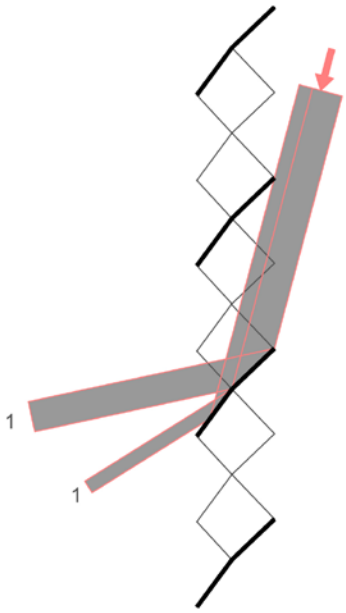

% of transmission:
- Not transmitted: 0%
- Directly transmitted (0): 0%
- Transmitted after 1 reflexion (1): 100%
- Transmitted after 2 reflexions (2): 0%

angle of incident radiation: -75º

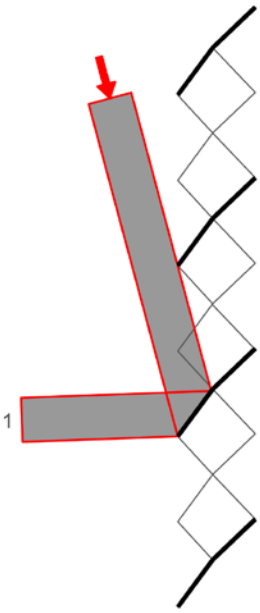

% of transmission:
- Not transmitted: 100%
- Directly transmitted (0): 0%
- Transmitted after 1 reflexion (1): 0%
- Transmitted after 2 reflexions (2): 0%

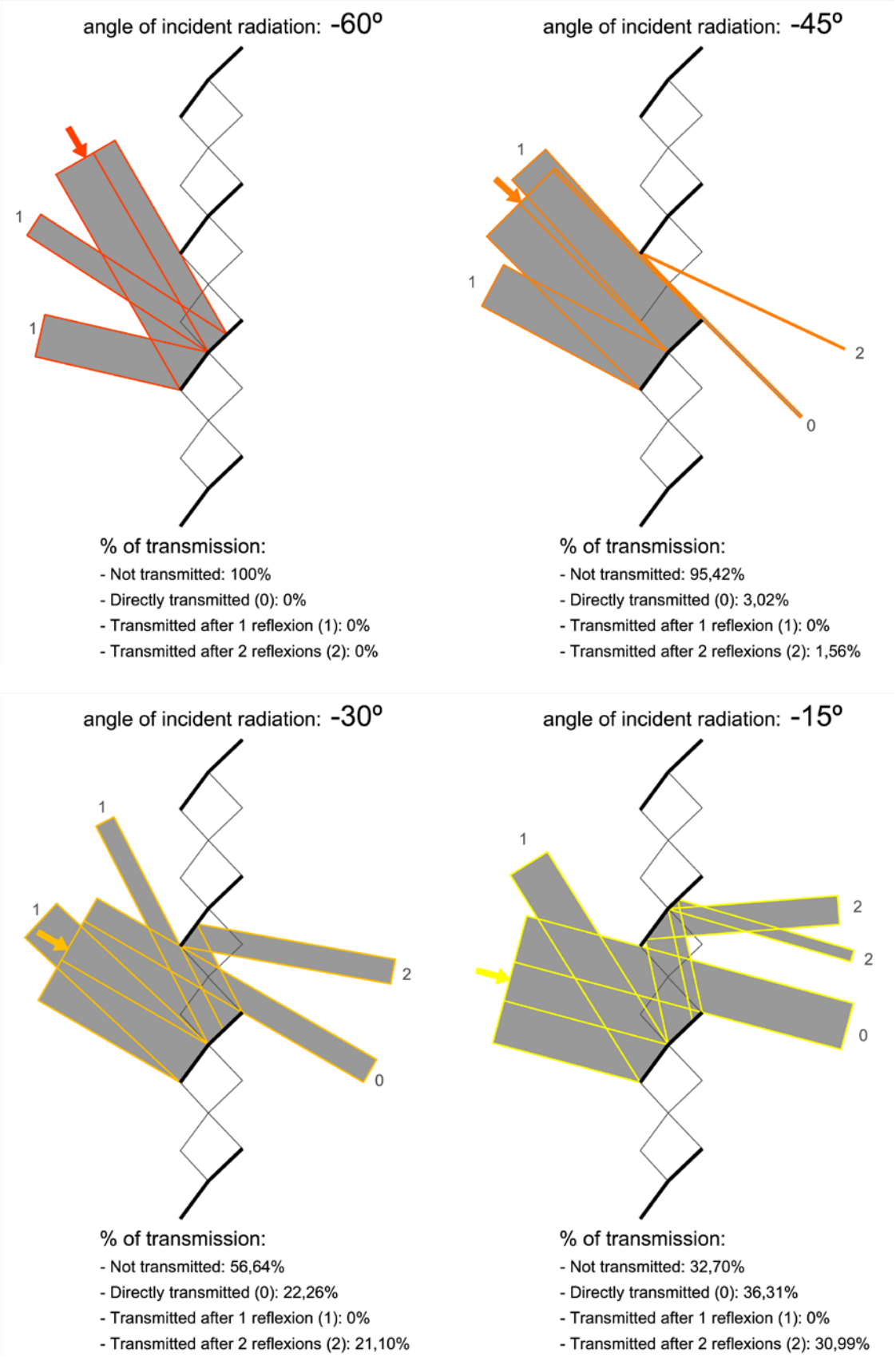

Fig. 4.5. Directly transmitted radiation and radiation transmitted after 1 or 2 reflections through an EM mesh gap (mesh number 03. *LW*= 62,5; *SW*= 23; *w*= 8; *e*= 1; *b*= 2; *i*= 25)

4.2.2 Calculation of the direction of incident radiation with highest transmittance

The angle of incident radiation with highest transmittance will coincide with the opening angle of the strands in the main section (σ), because radiation in that direction finds less surface of the mesh obstructing transmission.

Therefore, it is possible to get a first approximation to that direction by knowing the values of the parameters *SW* and *w* (usually provided by manufacturers) and based on the mentioned right triangle defined by *SW* and 2*w*:

$$\sigma = \arcsin\left({}^{2w}\!/_{SW}\right)$$

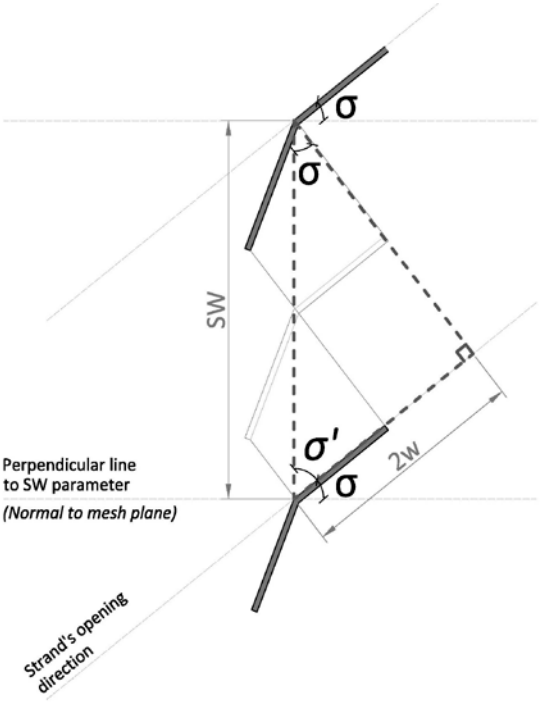

Fig. 4.6. EM mesh main section and relation between strand's opening angle, *ABC* triangle and parameters *SW* and *w*

In any case, as can be observed in the sections drawn up to now, and not mentioned, one of the ends of a strand in the main section descends from the opening direction of the strands, varying from this direction an angle named β. This descent is a consequence of pulling the strand when the blade cuts and pushes down the EM mesh in manufacture.

The descent made by the point at the edge of the strand is expressed by the letter *f*. This parameter *f* can be roughly considered equal to a fixed value (K_f) multiplied by blade descent (*d*) and strand width (*w*) and divided by cut width (*c*):

$$f = K_f \frac{d \cdot w}{c} \qquad ; \qquad K_f = 1,444$$

(K_f is an average value obtained from several assessed meshes)

This relationship between parameters will be explained later, in section 6.2.2.

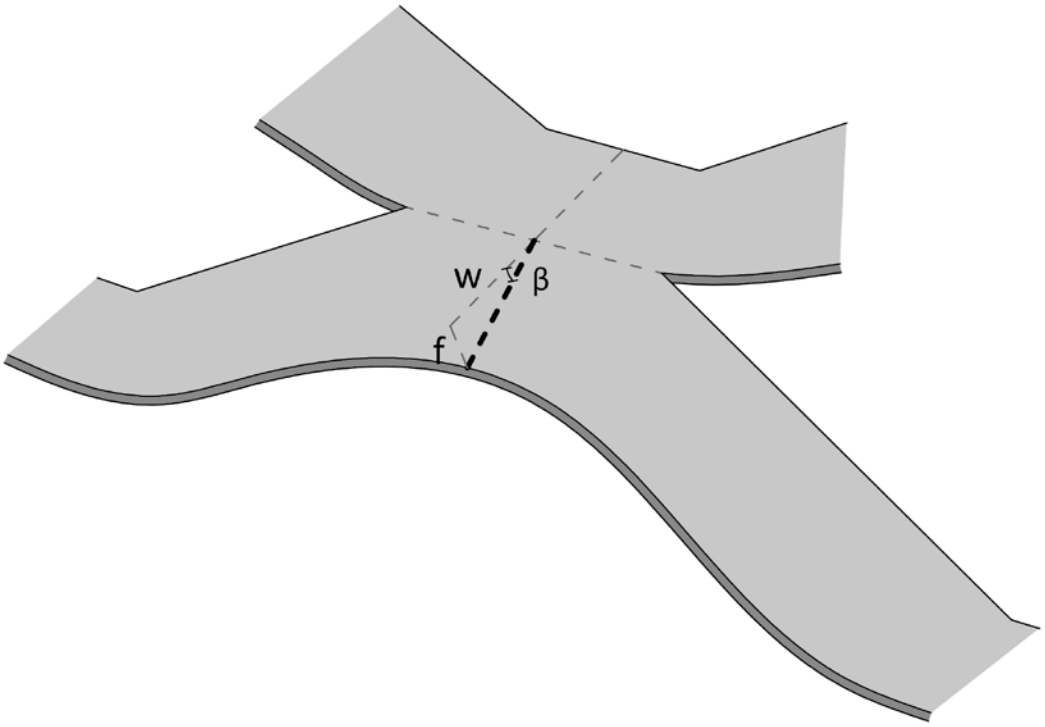

Fig. 4.7. Descent (*f*) of the front of the strand in the main section from the opening direction (*σ*) of the strands

So the angle β that varies the direction of one of the strands in the main section with respect to its original direction can be obtained from the following expression:

$$\beta = \arctan\left(\mathrm{f}/\mathrm{w}\right) = \arctan\left(K_f d / c\right)$$

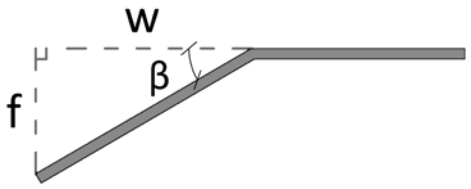

Fig. 4.8. Relation between *w*, *f* and β

This β angle depends on parameters *d* and *c* that, which even though they are not difficult to obtain, they are not usually provided by manufacturers. In case of knowing them angle β can be deduced and taken into account for a better approximation in the calculation of the direction of incident radiation with highest transmittance through the main section of an EM mesh.

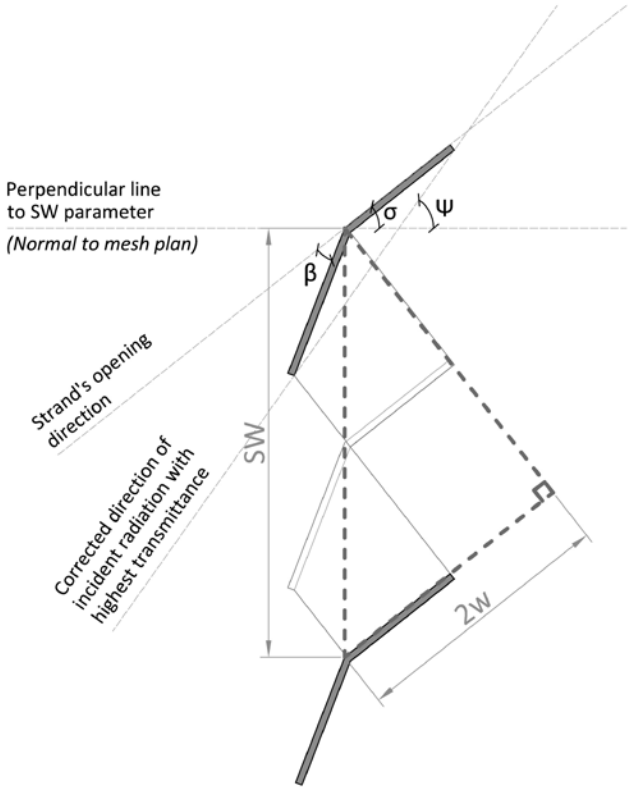

Fig. 4.9. Corrected direction of incident radiation with highest transmittance for the main section of an EM

The corrected incidence angle with highest transmittance (from now on Ψ) will be calculated based on σ and a correction depending on β.

The corrected angle (Ψ) will be the angle formed by the tangent to both ends of the strands in the main section and the normal to the mesh plan.

Based on the relationship between angles represented in the previous figure, Ψ angle can be defined in the following way:

$$\psi = \frac{\beta}{2} + \sigma = \frac{\arctan\left(K_f d / c\right)}{2} + \arcsin\left(2w / SW\right)$$

4.3 Conclusions

Some quick conclusions can be extracted from the obtained results:

- The higher the ratio *SW*/*w*, the closer the direction of highest specular transmittance to the normal of the plane of the mesh (the angle defining this direction will be lower)
- If the ratio *SW*/*w* has a high value, the transmittance for all specular directions through that mesh will tend to have a more symmetric behavior with respect to a horizontal plane. Alternatively, if *SW*/*w* has a low value, a rear-bottom radiation (e.g. 105º) or a front-top radiation (e.g. 75º) would imply a very low or null transmittance.

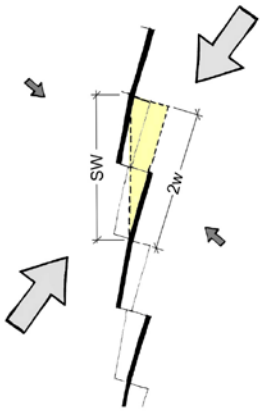

Fig. 4.10. Transmittance trough a mesh with a low *SW*/*w* ratio

- If the ratio *SW*/*w* increases, the range of angles of incident radiation with lack of specular transmittance decreases

Remember that, as mentioned in section 4.1, the previous observations are based on rough simplifications as the specular character of metal's reflectance, the analysis of just the mesh main section and the consideration of a null mesh thickness. Disregarding the influence of the sheet's thickness (*e*) is acceptable when its value is much lower than strand's width (*w*). These conclusions should be reconsidered for meshes with a high value of the ratio *e*/*w* which typically are meshes with very small openings (values higher than approximately 1/5).

Therefore, by knowing the parameters usually provided by manufacturers as *SW* and *w*, some first basic approximations to the behavior of a specific expanded metal mesh referring to transmittance can be done.

Each of the two following graphs summarizes some information about light transmission through the main section of a given mesh. Once the validity of this assessment is verified, this kind of representation could be a valuable and intuitive chart to describe an EM mesh because it allows comparing the following relevant information:

1. The width and location of the range of incident directions with lack of direct (specular) transmittance.
2. The incident direction for maximum transmittance.

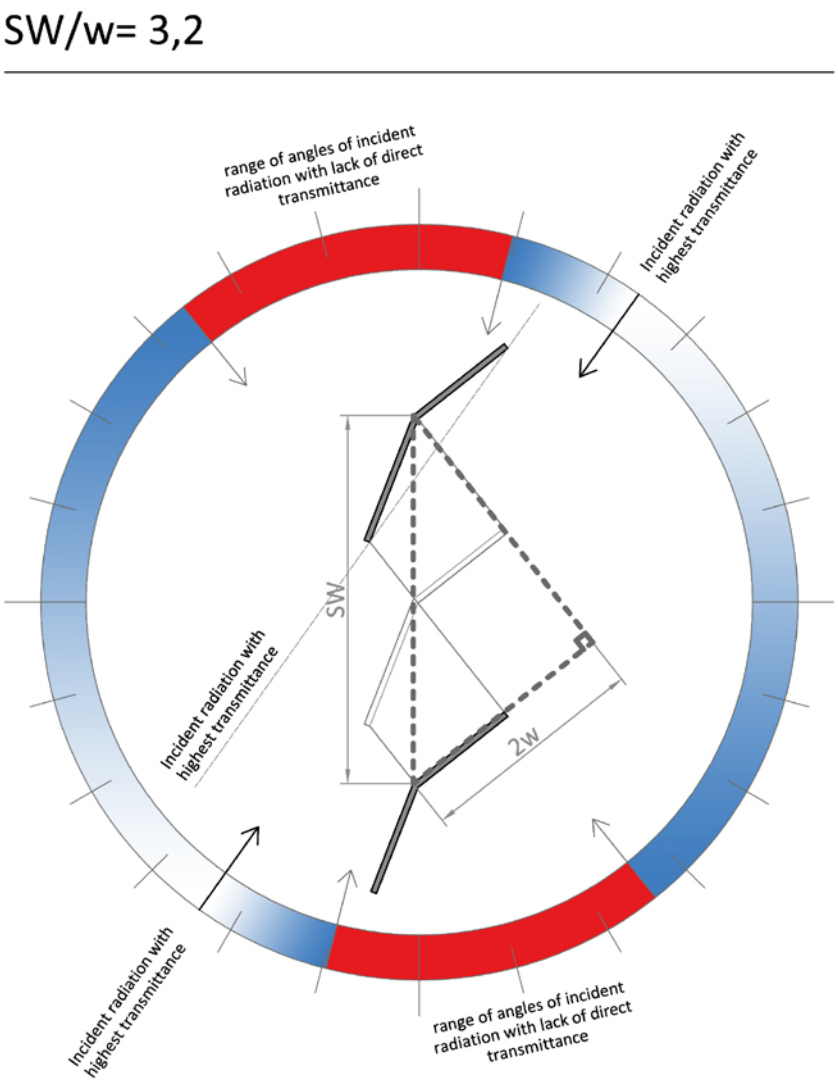

Fig. 4.11. Direction of highest transmittance and range of angles with lack of direct transmission; *SW*/*w* = 3.2. Mesh thickness is disregarded

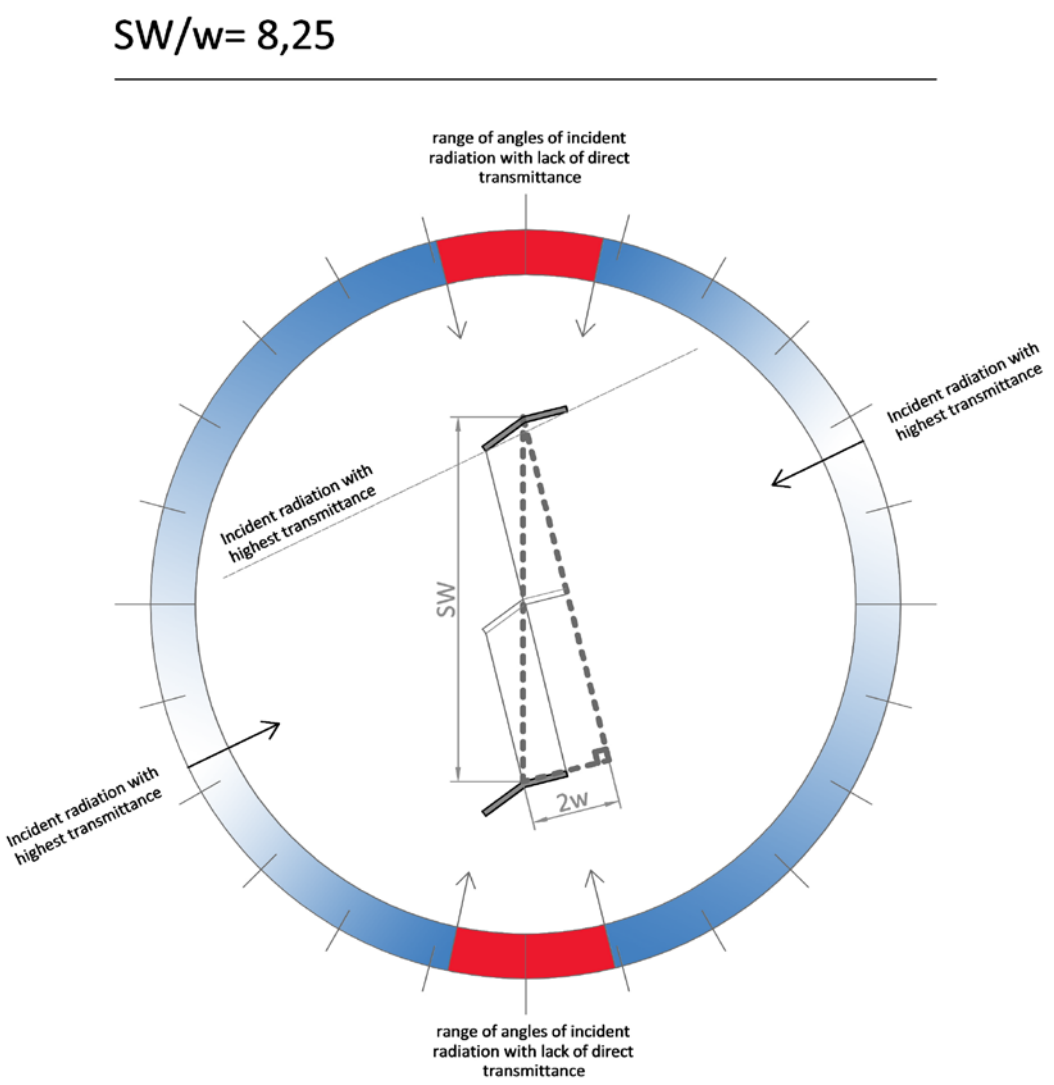

Fig. 4.12. Direction of highest transmittance and range of angles with lack of direct transmission; SW/w = 8.25. Mesh thickness is disregarded

References

Specular Reflection
2014 Wikipedia, the Free Encyclopedia.
http://en.wikipedia.org/w/index.php?title=Specular_reflection&oldid=634251263, accessed November 26, 2014.

5.1 Goniophotometry and other methods

Nowadays goniophotometers are the most advanced and complete devices to carry out daylight performance laboratory analysis of sheet materials. These devices are capable of obtaining BSDF data from fenestration samples by relative movements of every part of the goniophotometers (light source, light detector and sample) and monitoring all the outgoing light flux for every incoming light source direction.

The first device with these characteristics was developed in the late eighties at the Lawrence Berkeley National Laboratory (USA). Since then, different bidirectional goniophotometers have been developed to achieve more accurate and efficient studies of CFS. (Andersen and de Boer 2006)

The latest goniophotometer devices have a rotating table where a lamp is placed on a rotating arm with a mirror at the end and a light measuring device. The mirror at the end of the rotating arm reflects the light coming from the lamp or light source directly to the measuring device. This system rotates and stops every few degrees to register the measurements so this process is repeated until an entire map of the lamp is obtained. (Apian-Bennewitz 2010)

Other methods use a digital video capture to detect the light going through the sample or CFS.

5.2 Homemade specular transmittance assessment device

Solar and daylight transmittance of glass is normally measured by precision spectrophotometers which are usually designed for small samples (10x10 cm approx.).

We have made measurements with a spectrophotometer in collaboration with Tecnalia Technology Corporation (see section 5.5) for expanded metal samples with small

openings but expanded metal meshes used in facades often have larger opening dimensions and wider strands to make the bended forms appreciable, thus providing a deeper texture to the façade. These larger meshes cannot be assessed in regular spectrophotometers because the measuring area does not cover a representative surface of the mesh (measuring area is smaller than the holes in the mesh).

As Goniophotometry is beyond our possibilities, we chose to build our own device for laboratory assessment. As our capacity and budget to build a lab system was limited, we opted for a low tech and modest system. The aim of this system is not to characterize EM meshes in all of their variables or to consider all of the complexities of light behavior. The main limitation of this method and system is that the measurements of the transmitted light are made only in the direction of specular transmission. As we aimed to assess the daylight transmittance of EM devices, we had to consider a representative amount of directions of illuminance and assume that the transmittance (the % of incident radiation going through the device) would not change depending on the total amount of incident illuminance. Other features and limitations related to this laboratory system will be explained when describing those elements. The accuracy of the system was proved by means of a precision spectrophotometer (see section 5.5.1).

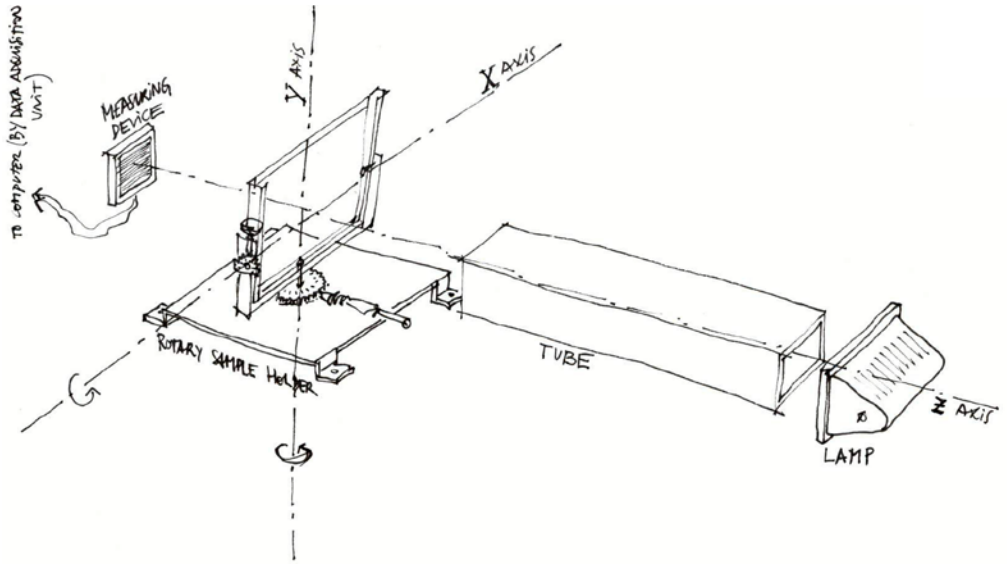

Fig. 5.1. First sketch for laboratory set

The device was conceived as a set of: lamp, black tube, sample holder and measuring device, as illustrated in the previous sketch.

This set was constructed inside a big black box and is composed by seven principal elements placed in this order: lamp, circular section pipe, rotary sample holder, EM mesh sample, light diffuser, luxmeter and computer.

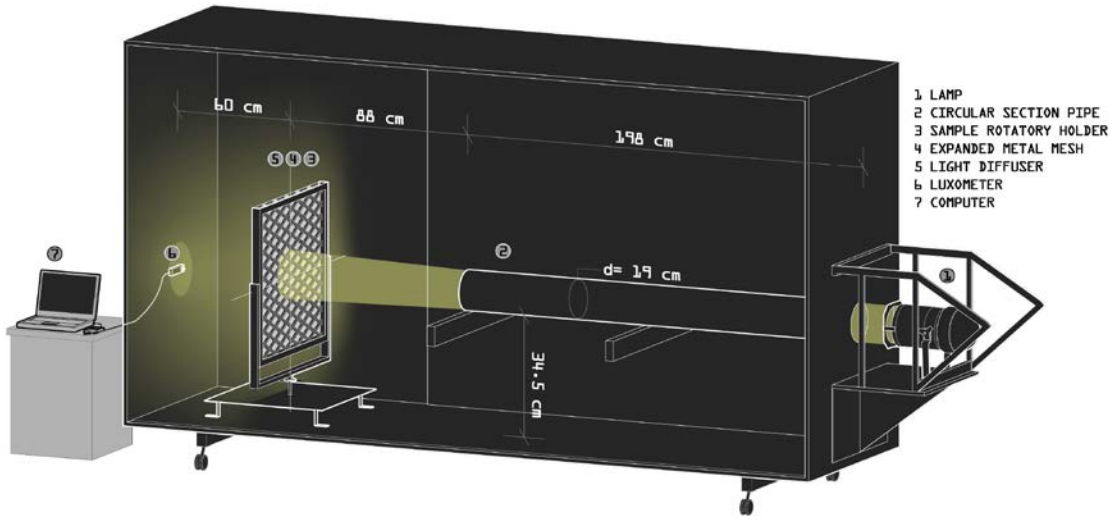

Fig. 5.2. Final laboratory set drawing

Fig. 5.3. Final laboratory set

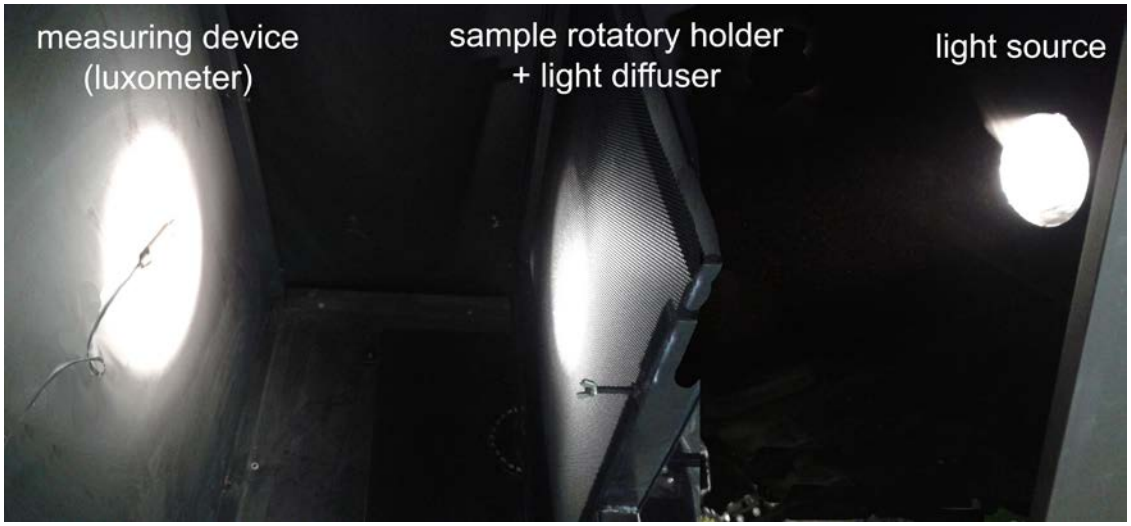

Fig. 5.4. Final laboratory set inside picture

5.2.1 Lamp and pipe

The lamp's radiation must be as similar as possible as real solar radiation. This similarity has two sides: geometrical and spectral.

From the geometrical point of view, to get a radiation as similar as possible to direct solar radiation (beam radiation), we need a set of rays as parallel as possible. We could achieve this objective by means of a parabolic aluminized reflector (PAR) or a big lens. Another less precise but more modest method consists on spacing out a small powerful lamp from the tested sample, thus reducing the cone effect and removing the perimeter part of the ray beam, keeping only the centre of the solid angle, which will be conducted through a black (to avoid reflection) 198cm long circular pipe (diameter of 19cm). Even if this central part of the ray beam will be the most parallel, this represents an error source or deviation from real direct solar light.

Fig. 5.5. Lamp and pipe set test

Besides the non collimated light, another limitation of this lighting system is the variations of the light emitted by the lamp. The spectral similarity of real and simulated radiation has a minor significance because we do not look for precise illuminance values but for the percentage of incident illuminance going through the device.

So the main characteristic we required from the lamp was to have good beam control. We choose the lamp Super PAR64 1000W-230V CP/60 EXE GENERAL ELECTRICS:

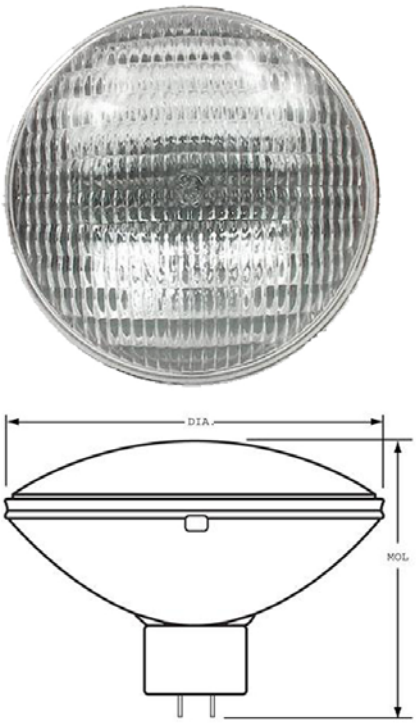

GENERAL CHARACTERISTICS

Lamp Type	Sealed Beam - PAR
Bulb	PAR64
Base	Extended Mogul End Prong (GX16d EXT)
Filament	C-7A
Rated Life (Vert)	800.0 h
Rated Life	800.0 hrs
Primary Application	Stage & Studio;Narrow Spot

PHOTOMETRIC CHARACTERISTICS

Initial Lumens (Vert)	330000.0
Initial Lumens (Hor)	330000.0
Beam Spread - Horizontal	26.0 - 10.0 °/14.0 - 50.0 °
Beam Spread - Vertical	7.0 - 50.0 °/14.0 - 10.0 °
Center Beam Candlepower (CBCP)	330000.0
Color Temperature	3200.0 K
Max. Beam Candlepower (MBCP) (MAX)	330000.0
Nominal Initial Lumens per Watt	330

ELECTRICAL CHARACTERISTICS

Wattage	1000.0
Voltage (MIN)	1000.0
Voltage	120.0

DIMENSIONS

Maximum Overall Length (MOL)	6.0000 in(152.4 mm)
Bulb Diameter (DIA)	8.000 in(203.2 mm)

Fig. 5.6. PAR64 CP60 lamp characteristics and images

Before carrying out any measurement for EM meshes once the set was ready, we took some registers of the illuminance of the lamp without sample or diffuser layer between the measuring device (luxmeter) and the lamp. In this way, we took measurements on different days and at different hours of those days of the illuminance emitted by this lamp arriving to the luxmeter with the aim of having an approximate idea of its behavior and constancy. Some variations were detected from one measurement to the other, but not significant to calculate daylight transmittance. Nevertheless, this fact may imply an error source in our assessment.

Day	06/02/2013	14/02/2013			21/02/2013	
Time	*12:00*	*11:20*	*12:10*	*15:30*	*10:15*	*12:00*
Measurmement (lux)	18058.00	20108.33	20125.00	19800.00	21122.22	20720.00
	MIN				MAX	

AVERAGE	19988.93

RELATIVE ERROR OF THE EXTREME VALUES TO AVERAGE::		
Minimum value:	**- 9,66%**	(Variation of the minimum value from average)
Maximum value:	**+ 5,67%**	(Variation of the maximum value from average)

Table 5.1. Lamp illuminance values obtained on different days and hours, illuminance average and variation from that average value of the minimum and maximum values

This lamp was placed inside an aluminum PAR 64 can that allows to connect it and to adjust the beam in the direction required as well as straightening the ray beam so to be more parallel.

Fig. 5.7. PAR 64 Polish can

5.2.2 Black box and sample holder

As mentioned we wanted to check several incident light directions for each sample. For this purpose we had two options: to turn the lamp and the luxmeter fixing the sample or to turn the sample fixing the lamp and the luxmeter. As we need to work inside a black box to avoid reflection phenomena and other light sources, moving the lamp at a given distance from the sample would entail a very big black box. Instead, making a rotary sample holder allows keeping the lamp, black tube and measuring device in fixed positions. An automatism for turning the sample holder and recording the measurements would speed up the process, but was unaffordable. Instead, we turned the sample holder manually for each position and recorded the incident and transmitted radiation to calculate the consequent transmittances.

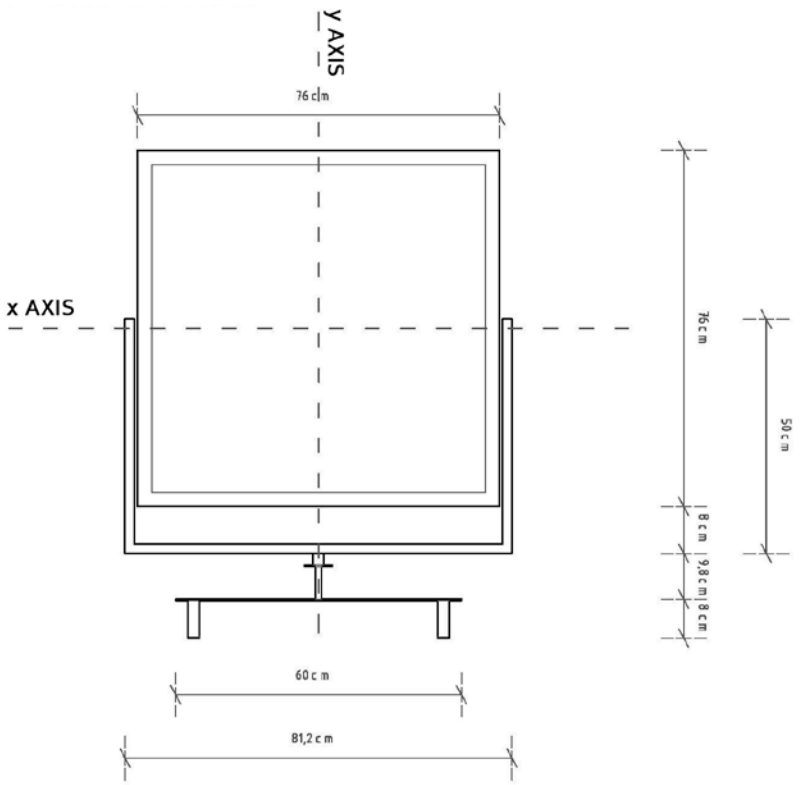

Fig. 5.8. Sample holder dimensions

This rotary sample holder has two rotation axes. In each one, there are some flaps that allow fixing the sample holder in a range of 180º every 15º. Making these rotations in a range of angles of just 180º we can deduce the behavior to transmittance in 360º due to the

symmetry of the EM mesh respect to a vertical plane that divides the mesh through the main section (see section 4.1). Combining these positions of each rotation axis, the sample can be fixed in 169 different positions with regard to the fixed light beam, producing this amount of incident radiation directions.

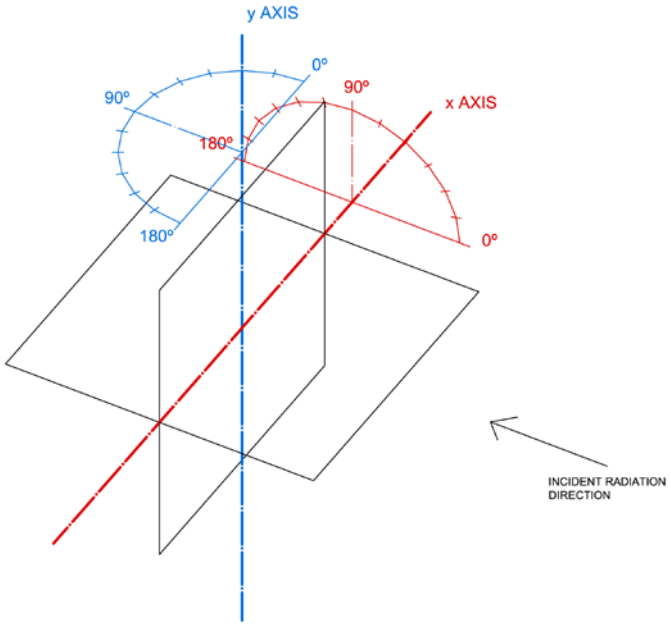

Fig. 5.9. Sample holder's rotation axes and fixing positions

Fig. 5.10. Left: Rotary sample holder. Right: Sample holder's rotation and fixing systems

However, some of these 169 positions produce non valid measurements because in those positions, the sample holder itself obstructs the incident radiation. For instance we obtain null measurements with the following positions:

- 0^o and 180^o in *x* axis

- 90^o on *y* axis

Besides those null measurements, the following four combined (*x*,*y*) positions produce also non-valid measurements for the same reason: (15^o,75^o), (15^o,105^o), (165^o,75^o) and (165^o,105^o). Consequently, we obtained valid results for 128 positions.

All the non-valid positions correspond to incident directions forming very small angles with the mesh plan, i.e. directions with very low transmittances for most meshes.

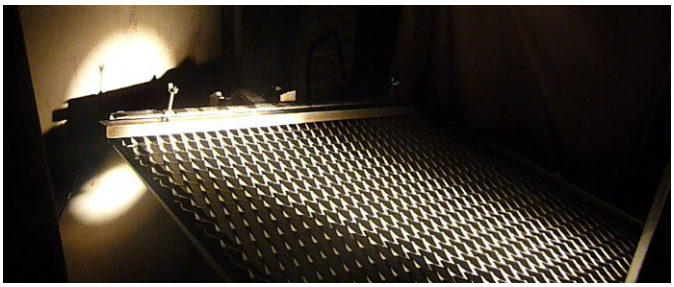

Fig. 5.11. Example of sample holder oblique position resulting in null register.

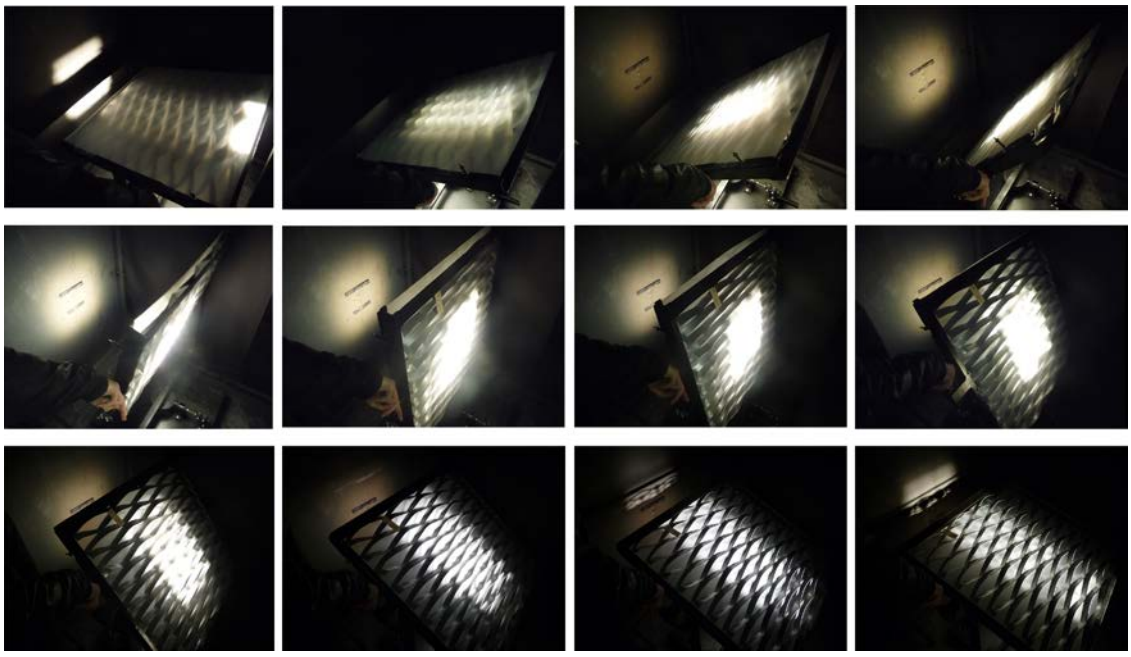

Fig. 5.12. Rotation sequence around horizontal *x* axis of the sample holder

A video showing the laboratory set and our data registering process can be seen at: http://youtu.be/n4jq1P4PT6o

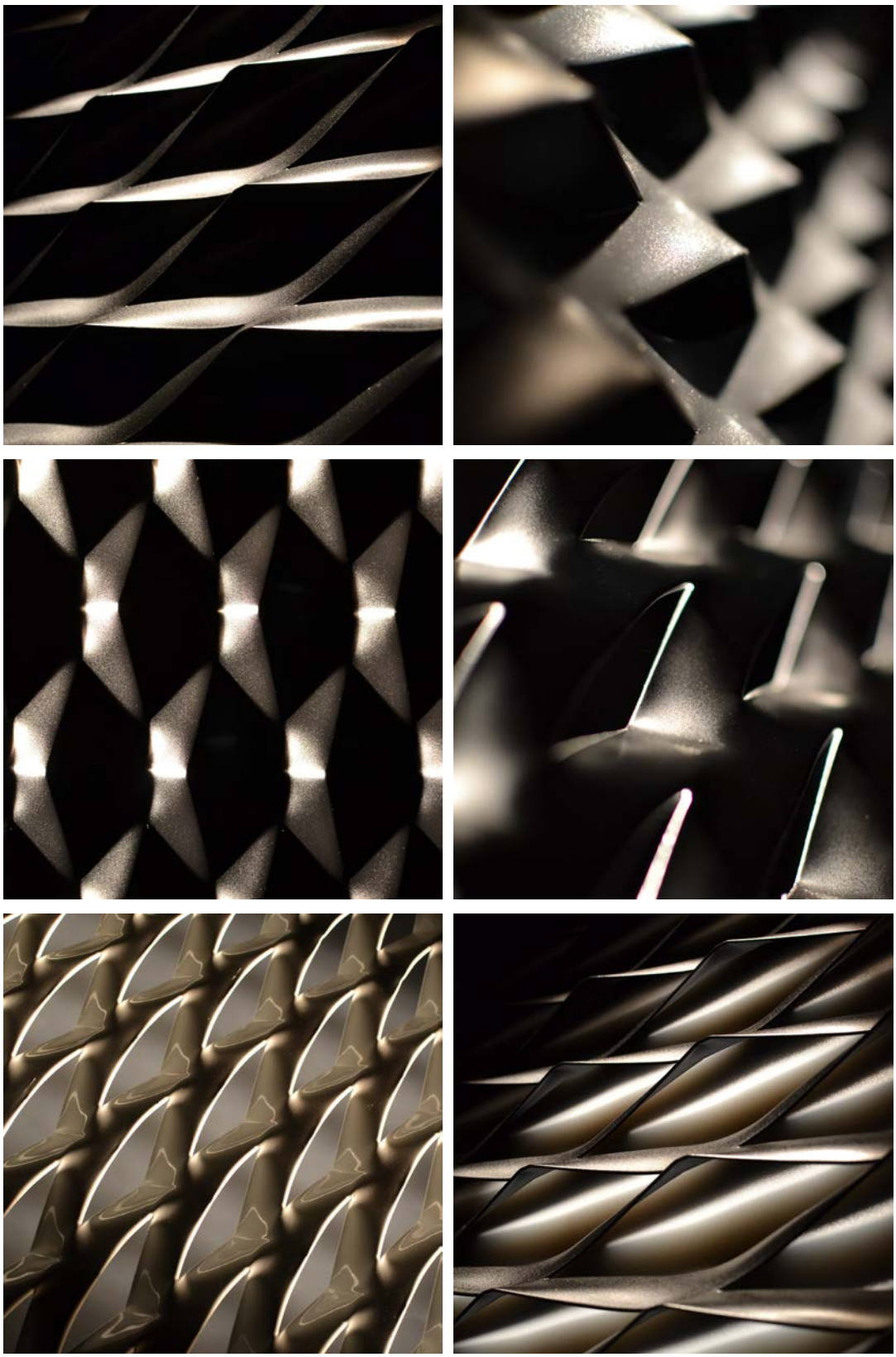

Fig. 5.13. Lit meshes in the laboratory set

5.2.3 Diffuser

The existing precision devices for measuring light offer a small measuring surface, normally a hemisphere approximately one or two centimeters wide. This represents a problem when it comes to measure the overall light transmission through a mesh with wider holes and opaque parts than that diameter. The measuring surface could be almost completely illuminated by beam radiation or completely covered by the projected shades. Even if the diffraction that light undergoes going through the mesh blurs the projected shadows and the luxmeter was situated at a prudent distance from the mesh of 60 cm (which increases that diffraction effect), meshes with very big holes still projected a pattern of illuminated and shadowed areas with very different illuminances (see fig.5.13), resulting in unacceptable register deviations.

Fig. 5.14. Projected shadow pattern projected through a mesh (without diffuser layer)

As we need to measure the mean transmitted illuminance through the mesh, we needed a solution. We could not create a large enough measuring surface (we tried with a solar cell, but it was not sufficiently precise) so we decided to place a plastic diffuser immediately behind the mesh so that the transmitted light through the mesh -which includes

beam and diffuse radiation- is all converted to diffuse radiation. We used a common spiral notebook binding Polypropylene translucent sheet.

Fig. 5.15. Diffuser layer placed behind a mesh and resulting diffuse light incident on luxmeter

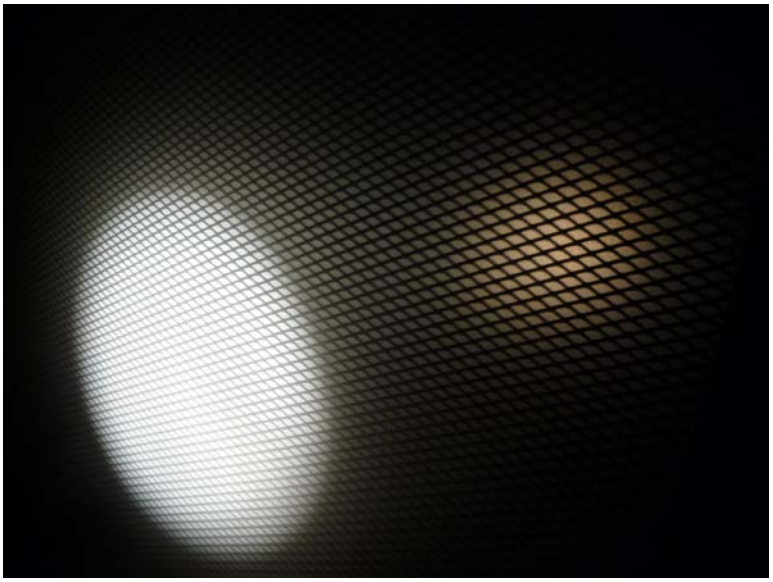

Fig. 5.16. Light through an EM mesh and the diffuser layer

Obviously the radiation arriving to the measuring device was filtered by this diffuser layer and there was a loss of radiation due to absorption and reflection. We also had to consider that the further the angle of incidence is from perpendicular to the mesh-diffuser set,

the greater the backward reflection of radiation in the diffuser, and this reflected radiation can hit back on the mesh and produce some distortion. To control these deviations we made some tests with a mesh with very small openings (mesh sample 10b, the one with smallest openings from our collection). The openings of that mesh were so small that they produced a transmitted light homogeneous enough to be measured by the luxmeter without the need of using the diffuser layer. We did compare the results of assessing it with and without diffuser and we detected acceptable maximum deviations of 3.43 % in the resulting transmittances.

The parameters and properties of the mesh sample used to do this verification are specified, together with those of the rest of the samples, in section 5.3. The results obtained in this test can be found in Appendix A, section A.2. As we can see in the tables shown in section A.2, most of the deviations are smaller than 1%, having a maximum deviation of 3.43%. As expected most of the deviations have a negative value, meaning that the transmittance registered with diffuser layer are slightly higher to those obtained without diffuser layer.

5.2.4 Measuring device (luxmeter)

We selected a luxmeter (MAVOLUX 5032 C USB) as a measuring device, in accordance with class C per DIN 5032-7, appendix B of IEC 13032-1 and CIE 69. It is equipped with a silicon photodiode light sensor with V (*λ*) filtering as well as cosine correction, and measures the illuminance of daylight and artificial sources of light with reliability. Even in the case of very bright sunlight or light from headlights, no accessories are required.

Fig. 5.17. Luxmeter MAVOLUX 5O32C USB

This device has a high measuring precision in 4 ranges with luminance attachment from 0.1lx to 199.900 lx and from 1cd/m2 to 1999000cd/m2, selecting measuring ranges automatically or manually. Meter control, as well as acquisition, display and storage of measured values, is managed with specific software in a computer via a USB port.

Strictly speaking, transmittance is the relationship between the incident light *outside* the mesh and the transmitted light *inside* it. Instead of placing the luxmeter in both outside and inside positions we left it in a fixed inside position at a distance of 60 cm from the sample holder's center point. This procedure was acceptable as the illuminance without obstacles did not change considerably from the sample holder's position to the luxmeter position.

Once we calibrated the luxmeter we could measure the light reaching the luxmeter with the diffuser layer situated in the sample holder and save all the data for every sample holder position without any EM mesh. Then, we placed an EM sample and measured the light transmitted through the sample-diffuser set in every position to compare both values and get the transmittances for that given mesh and all the incident directions.

5.2.5 Data reader and data process (Computer)

As aforementioned, all the values received from the luxmeter were saved in a computer via USB with specific software. This data was saved in text files, exported to spreadsheet files and automatically ordered in different data tables. These tables have 13 columns for each position of the sample holder's *x* axis, in ranges of 15º, from 0º to 180º, and 13 rows for each position in *y* axis, also in ranges of 15º from 0º to 180º.

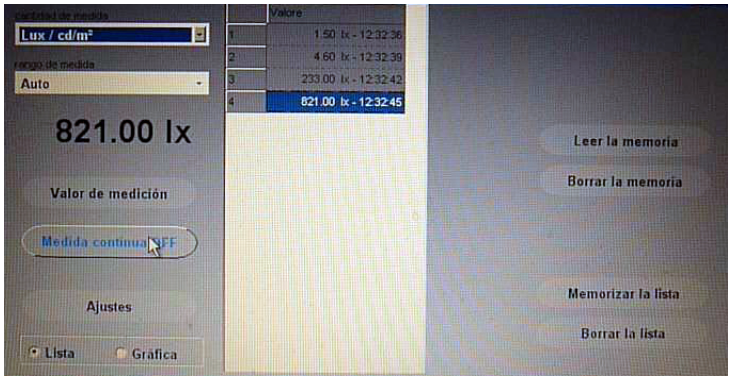

Fig. 5.18. Luxmeter data reader interface

On one hand, we had the data tables for the illuminance values with diffuser layer but without EM sample for any sample holder position. We did repeat these measurements some times to obtain a median data table of illuminance values with diffuser layer in any position of the sample holder. On the other hand, we had some data tables with the illuminance values for each sample of EM, in all positions. To obtain the transmittance of the EM mesh samples, we had to divide the samples illuminance data with the diffuser median illuminance data, deducing a percentage that indicates the transmittance of the assessed mesh for every position.

5.3 Analyzed meshes

With the aim of analyzing some different meshes with varying properties, we took 15 samples of EM mesh with different parameters in three different colors: white, gray and black (with some exceptions because of supply problems). Referring to the material, most of the analyzed EM meshes are made of galvanized steel, except for a few aluminum meshes, again due to supply availability. In the following table we can see the parameters and color of each assessed mesh and its nomenclature:

SAMPLE NOMENCLATURE

	Parameters						Colour		
	LW	SW	w	e	b	i	White	Gray	Black
01	200	73	24	1	7	33	01w	01g	01b
02	16	8	2	2	1	4.5	02w	02g	02*b
03	62.5	23	8	1	2	25	03w	03g	03b
04	10	6.5	2.1	1	1	4.5	04w	04g	04b
05	6	4.5	1.5	1	1	2	05w	05g	05b
06	60	21	10	1.5	2	33	06w	06g	06b
07	115	52	23	1	2	43.5	07w	07g	07b
08	110	50	24	2	3.5	50	08w		08b
09	110	40	15	2	2	33	09w		09b
10	6	4	1.2	1	1	2.5	10w		10b
11	60	22	7	2	2	18	11w		11b
12	115	48	20	1.5	2	39	12w		12b
13	280	76	23.5	1.5	10	50		p13g	p13b
14	280	70	20	1.5	10	50	p14w		
15	20	17	6	1	3	7	f15w		f15b

Table 5.2. Assessed sample parameters and nomenclature.*Black sample number 02 (02*b) has two different parameters from the other 02 samples: *e*=1,5 and *i*=3,5

We assessed a total of 36 different samples. Samples containing numbers 13, 14 or 15 can be considered special meshes of expanded metal: the first two are made from a previously perforated metal sheet, named with an initial "p", while the third one is a flattened EM mesh, named with an initial "f".

The amount of samples that has been assessed in laboratory is quite reduced. Compared to the great variety of possible EM meshes, this group of samples is small due to supply limitations and to the aforementioned laborious manual assessment procedure.

The following datasheets show some scaled pictures of each assessed mesh, the colors in which it is available and its parameters. As explained in section 2.3.2, these are the abbreviations of the parameters: *LW*- Long Way of mesh; *SW*- Short Way of mesh; *w*- strand width; *e*- strand thickness; *b*- blade bevel width; *i*- intercut; *c*- cut width and *d*-blade descent.

MESH SAMPLES 01

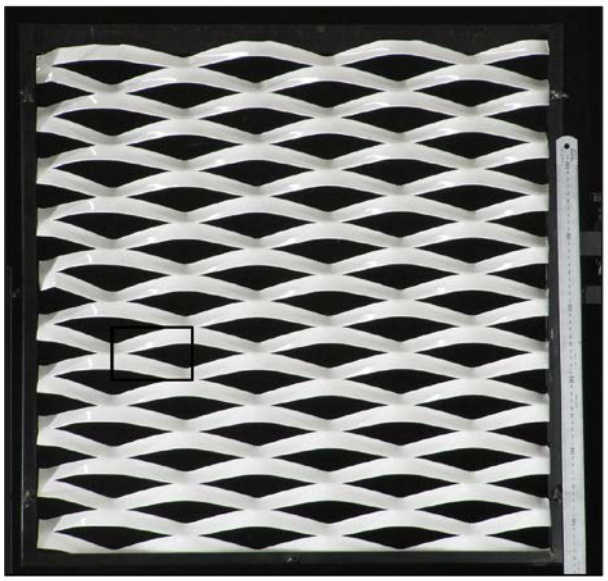

10cm 50cm

Detail:

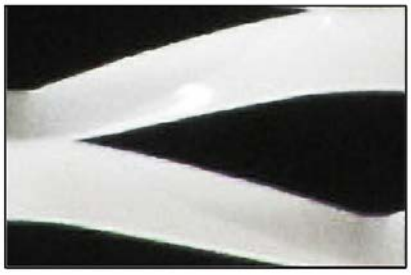

1cm 5cm 10cm

Colours:

01w 01g 01b

Parameters:

LW	SW	w	e	b	i	c	d
200	73	24	1	7	33	167	27,5

MESH SAMPLES 02

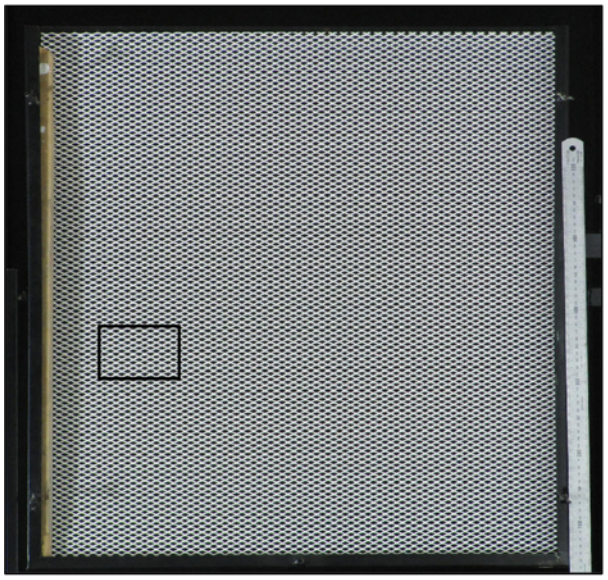

10cm 50cm

Detail:

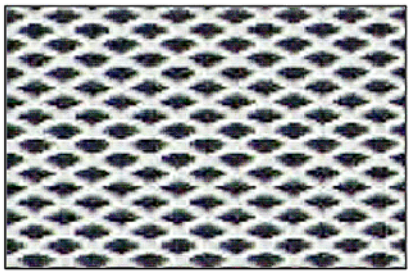

1cm 5cm 10cm

Colours:

02w 02g 02b*

Parameters:

LW	SW	w	e	b	i	c	d
16	8	2	2 /*1,5*	1	4,5/*3,5*	11,5/*12,5*	3,46

MESH SAMPLES 03

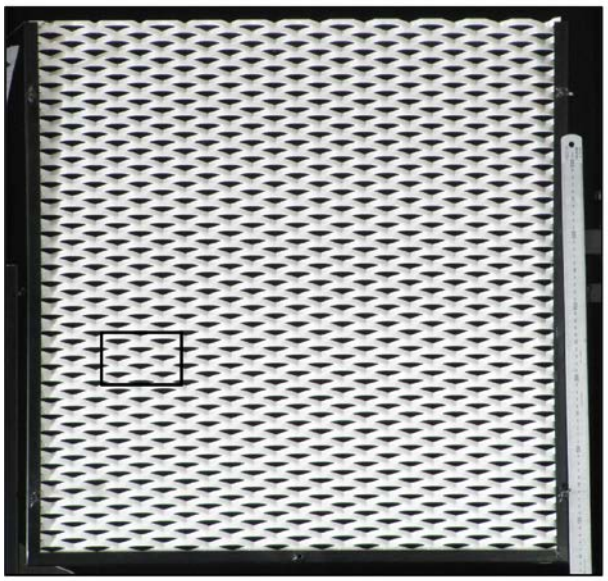

10cm 50cm

Detail:

1cm 5cm 10cm

Colours:

03w 03g 03b

Parameters:

LW	SW	w	e	b	i	c	d
62,5	23	8	1	2	25	37,5	8,26

MESH SAMPLES 04

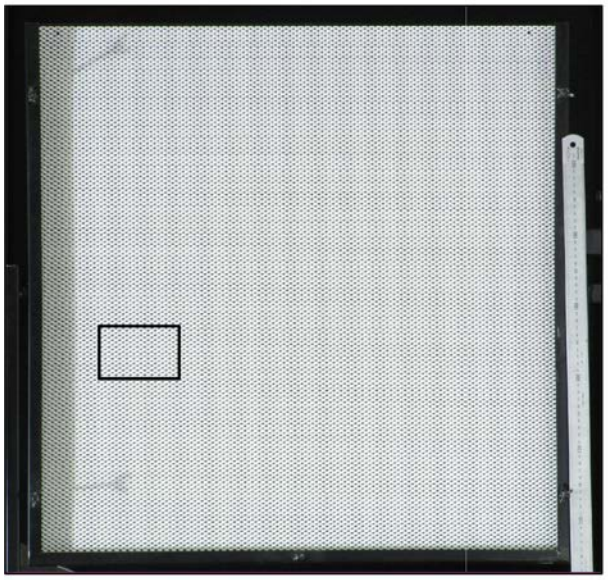

10cm 50cm

Detail:

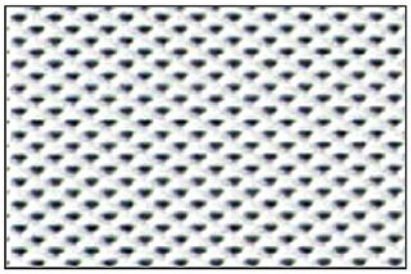

1cm 5cm 10cm

Colours:

04w 04g 04b

Parameters:

LW	SW	w	e	b	i	c	d
10	6,5	2,1	1	1	4,5	5,5	2,48

MESH SAMPLES 05

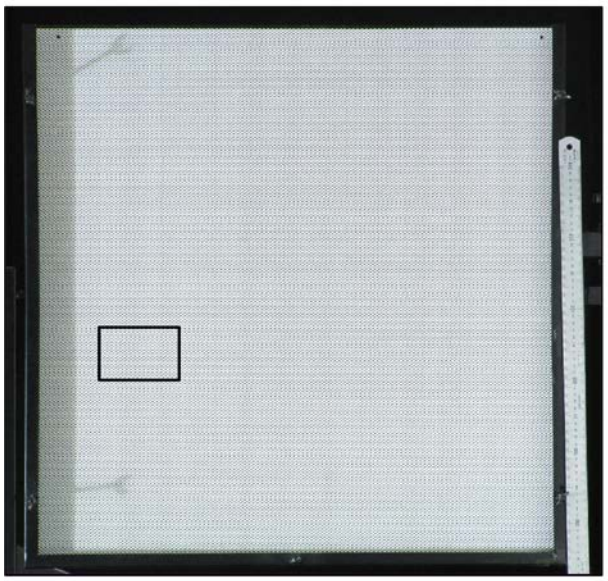

10cm 50cm

Detail:

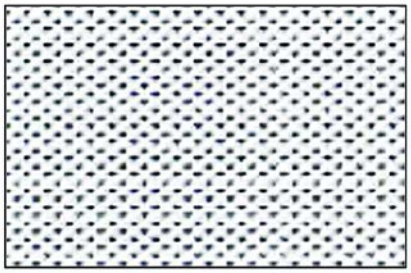

1cm 5cm 10cm

Colours:

05w 05g 05b

Parameters:

LW	SW	w	e	b	i	c	d
6	4,5	1,5	1	1	2	4	1,68

MESH SAMPLES 06

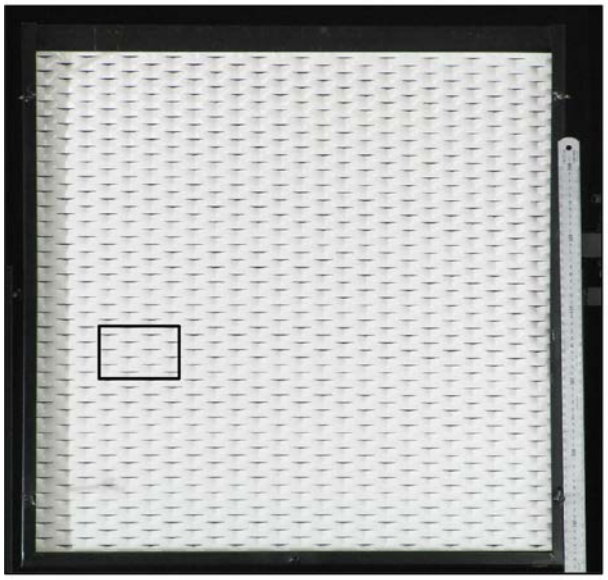

10cm 50cm

Detail:

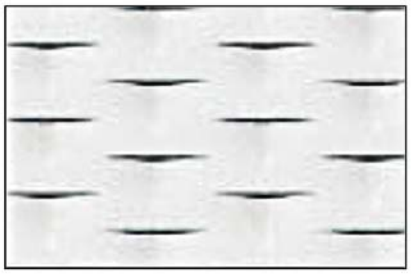

1cm 5cm 10cm

Colours:

06w 06g 06b

Parameters:

LW	SW	w	e	b	i	c	d
60	21	10	1,5	2	33	27	3,2

MESH SAMPLES 07

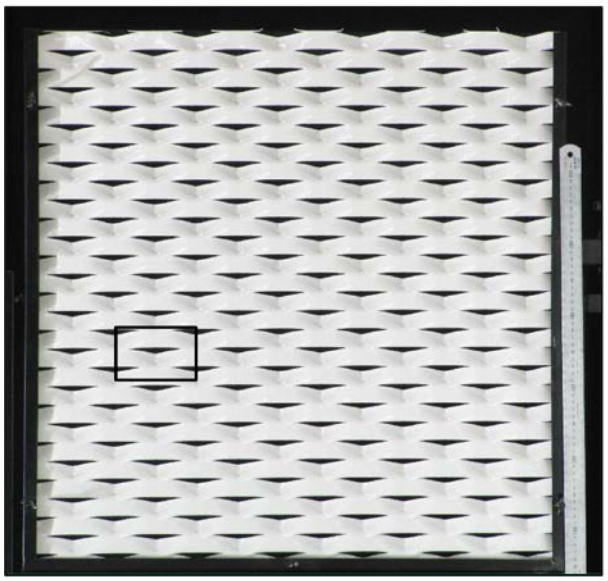

10cm 50cm

Detail:

1cm 5cm 10cm

Colours:

07w 07g 07b

Parameters:

LW	SW	w	e	b	i	c	d
115	52	23	1	2	43,5	71,5	12,12

MESH SAMPLES 08

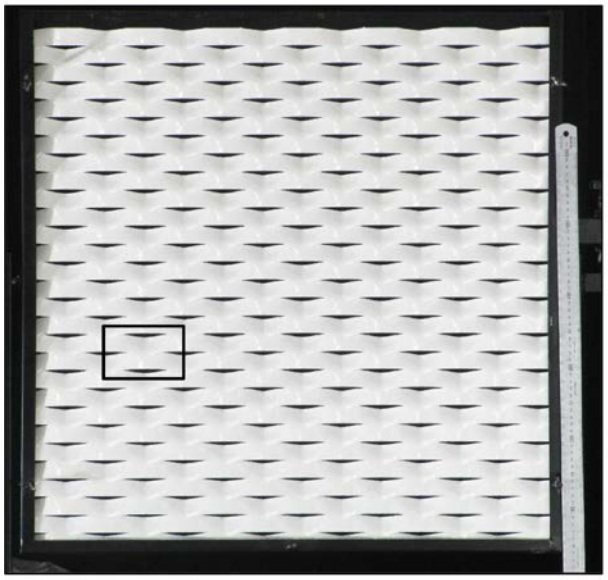

10cm 50cm

Detail:

1cm 5cm 10cm

Colours:

08w - 08b

Parameters:

LW	SW	w	e	b	i	c	d
110	50	24	2	3,5	50	60	7

MESH SAMPLES 09

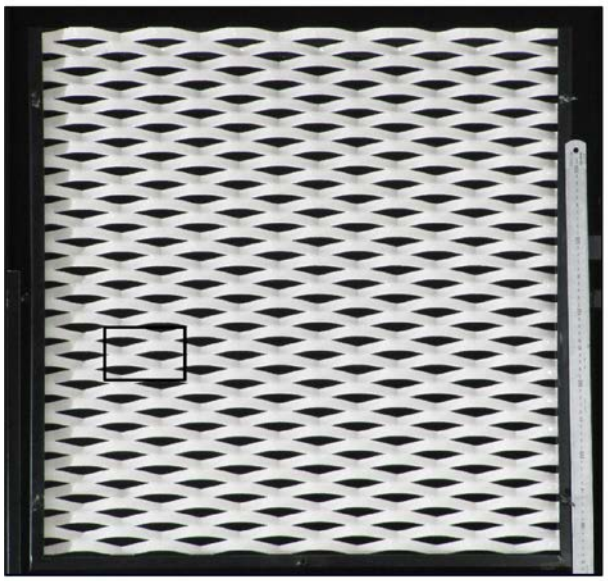

10cm 50cm

Detail:

1cm 5cm 10cm

Colours:

09w - 09b

Parameters:

LW	SW	w	e	b	i	c	d
110	40	15	2	2	33	77	13,23

MESH SAMPLES 10

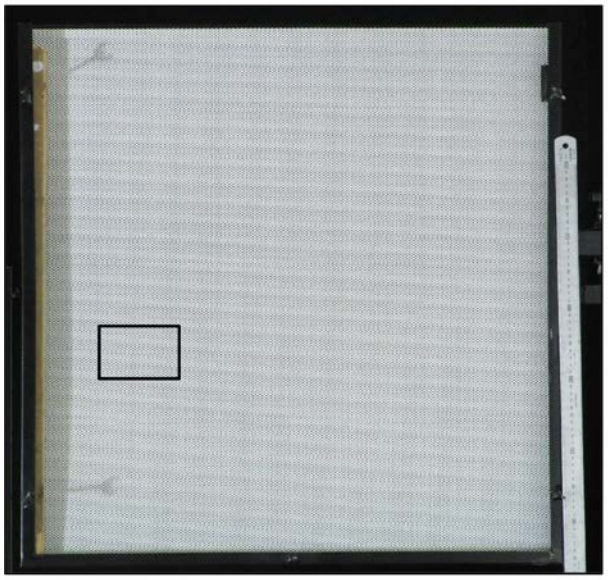

10cm 50cm

Detail:

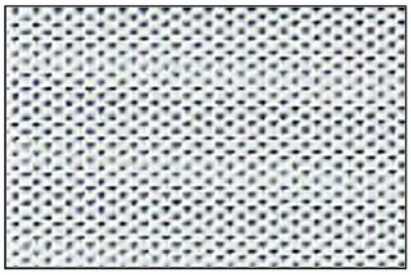

1cm 5cm 10cm

Colours:

10w - 10b

Parameters:

LW	SW	w	e	b	i	c	d
6	4	1,2	1	1	2,5	3,5	1,6

MESH SAMPLES 11

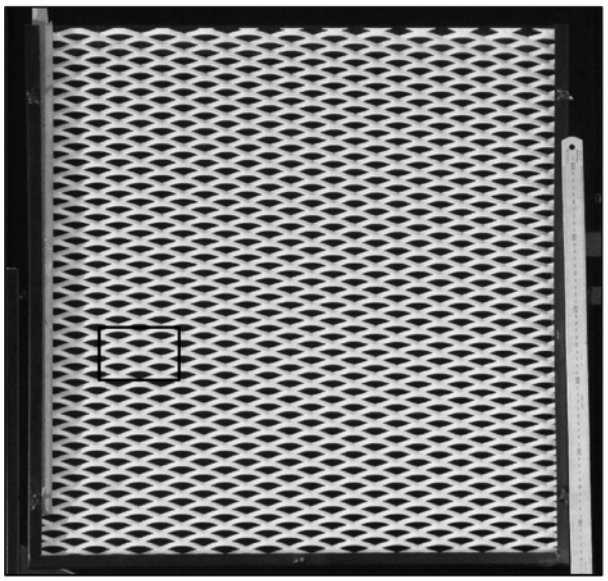

10cm 50cm

Detail:

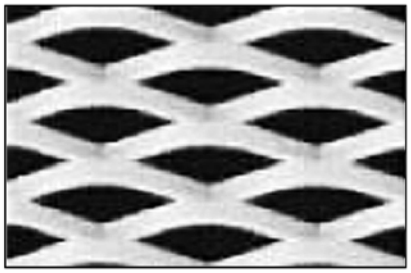

1cm 5cm 10cm

Colours:

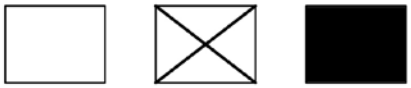

11w - 11b

Parameters:

LW	SW	w	e	b	i	c	d
60	22	7	2	2	18	42	8,48

MESH SAMPLES 12

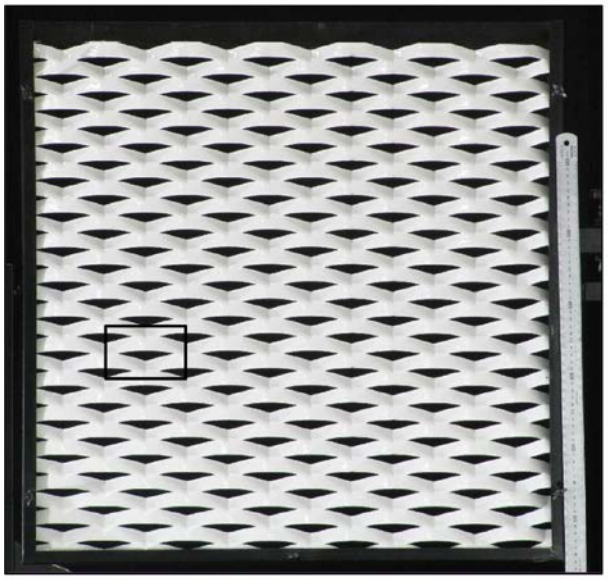

10cm 50cm

Detail:

1cm 5cm 10cm

Colours:

12w - 12b

Parameters:

LW	SW	w	e	b	i	c	d
115	48	20	1,5	2	39	76	13,26

MESH SAMPLES p13

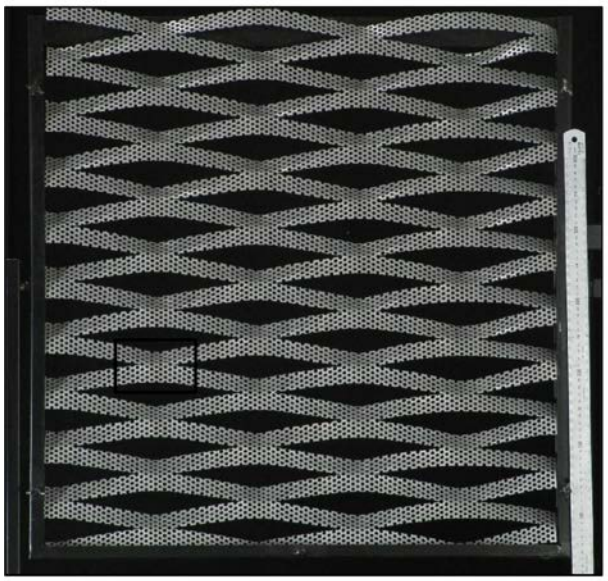

10cm 50cm

Detail:

1cm 5cm 10cm

Colours:

\- p13g p13b

Parameters:

LW	SW	w	e	b	i	c	d
280	76	23,5	1,5	10	50	230	29,87

MESH SAMPLES p14

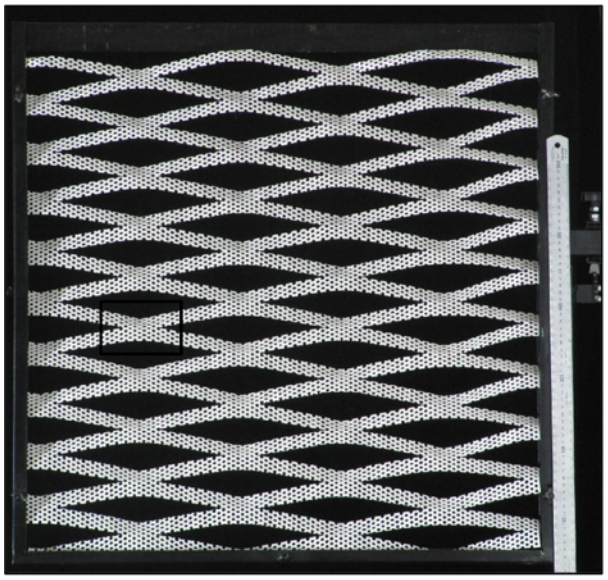

10cm 50cm

Detail:

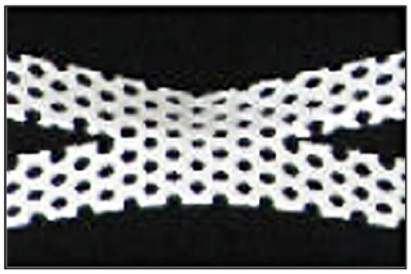

1cm 5cm 10cm

Colours:

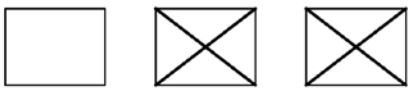

p14w - -

Parameters:

LW	SW	w	e	b	i	c	d
280	70	20	1,5	10	50	230	28,72

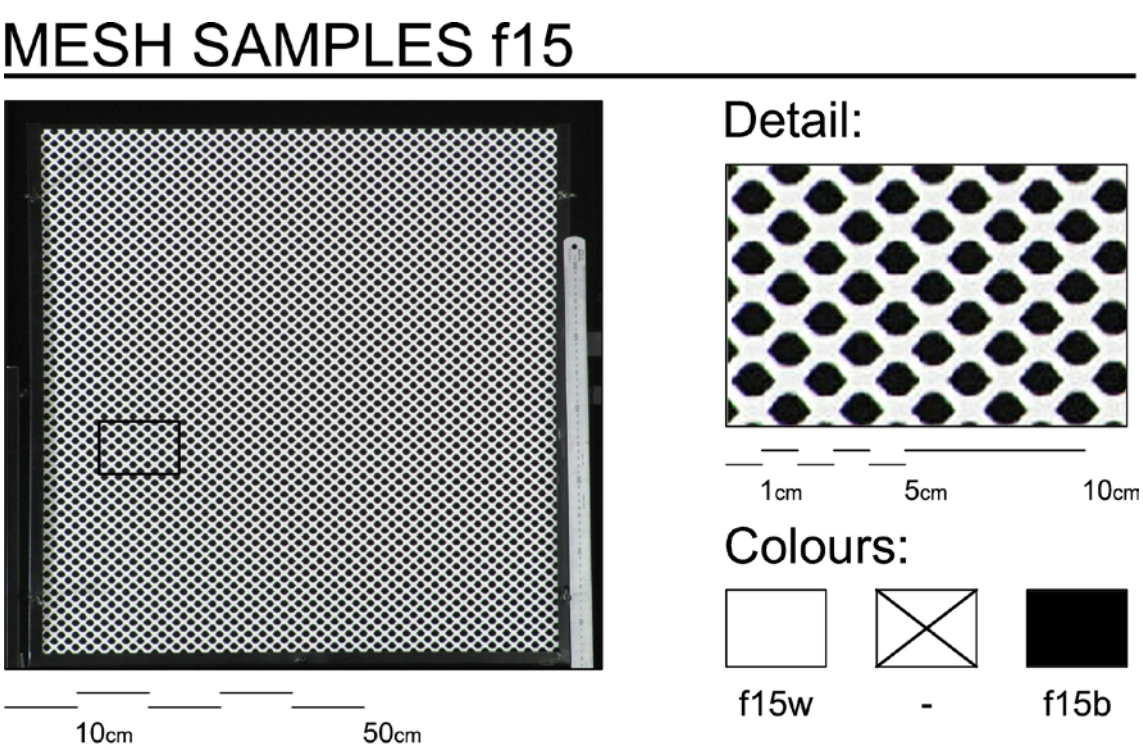

Fig. 5.19. Assessed sample datasheets with scaled pictures, geometrical parameters and colors available for each sample.

5.4 Laboratory assessment results

5.4.1 Comparative analysis between meshes

Keeping in mind all the limitations of the lab methodology previously described, the results obtained gave us a preliminary idea of the behavior of the EM in light transmittance and verified the validity of other assessment methods as the “rough geometrical analysis of transmittance” described in chapter 4 and the “computer aid assessment” described in chapter 6. Remember that the measurements of transmitted illuminance are done only in the direction of specular transmission.

5.4.1.1 Geometry

The results are given in data tables that can be found in Appendix A, section A.3. There is one table for each assessed sample that helps us make a first approach to its transmittance performance. Due to the limited amount of assessed meshes and the limitations of the assessment method itself, we can not infer general statements about the transmittance performance of EM based on the results. However, some first conclusions can be extracted from this data. We can also use it to verify some of the previously made hypotheses.

First of all, we took the average transmittance and maximum transmittance values of each sample to try to understand the factors that influence the transmittance through the meshes. We drew the following two tables where we ordered the EM samples by average daylight transmittance on one hand and by maximum daylight transmittance on the other. Both tables are in descending order, from highest to lowest transmittances. In the case of the table containing the ranking of maximum transmittance values, we also included the position of the sample holder in which that maximum was registered.

As expected, the mesh samples named ”special” (perforated and flattened ones) have the highest transmittance values. Taking into account the rest of EM meshes, we could presume that these rankings depend on how open the strands of each mesh are or on the proportion between hollow and solid space in them. With the aim of verifying these points, we have also completed two rankings expressing both facts. As said in the previous chapter, the opening of the strands depends on the relationship between *SW* and *w*. The greater the ratio *SW/w*, the more open the strands are.

To make an approximation of the proportion between hollow and solid space in a mesh, we have taken as reference a repetitive rectangular area of the mesh in its front elevation (fig. 5.19) and we have made and approximate calculation of the hollow and solid areas in it in order to obtain the ratio. This repetitive area is the one defined by a square whose sides are *LW* and *SW*.

We have made a simplification of the form of the hollow area envisaging it as a rhombus. This way the hollow area has a surface equal to two hollow rhombuses in the *LW*x*SW* rectangle (gray colored in fig 5.19). The hollow rhombus has one diagonal defined by *c* and the other by *SW-2w'*.

mesh Nº	AVERAGE Daylight Transmittance
p14w	50.45
p13b	44.91
p13g	43.83
f15w	37.31
01w	36.58
f15b	36.38
01b	35.14
01g	33.44
02w	30.16
11w	29.81
02*b	29.24
11b	29
02g	28.78
09w	26.26
09b	25.89
12w	23.66
03w	23.45
03b	21.95
12b	21.62
03g	20.43
07w	13.94
07b	13.49
07g	13.27
10w	12.39
05w	12.3
08w	12.15
05b	11.6
08b	11.42
05g	10.7
10b	10.45
04w	9.73
04b	9.24
04g	8.86
06w	4.95
06g	4.84
06b	4.77

		SAMPLE POSITION	
mesh Nº	MAXIMUM Daylight Transmittance	rotation around x axis	rotation around y axis
p14w	85,24	150	15
p13b	82,70	150	15
01g	82,44	150	15
01b	80,92	150	15
01w	79,69	150	180
p13g	79,07	150	150
09b	69,97	150	15
09w	69,86	150	135
11b	68,90	135	0
11w	68,23	135	0
03g	67,45	150	180
12w	67,43	150	15
02*b	66,92	150	15
12b	66,67	150	15
08w	65,54	165	135
02w	65,22	135	0
03w	64,12	150	15
02g	63,25	135	180
03b	58,18	150	165
f15w	55,22	105	45
f15b	53,08	60	45
08b	52,34	165	150
07w	49,91	165	135
07g	45,31	165	150
07b	43,38	165	180
10w	32,44	135	0
05w	30,94	135	0
05b	29,49	120	0
10b	28,70	135	180
05g	26,84	135	165
04b	24,20	120	180
04w	24,19	120	0
04g	23,46	120	0
06b	22,43	165	0
06w	21,17	165	150
06g	20,36	165	180

Table 5.3. Average daylight transmittance values ranking, maximum daylight transmittance values ranking and sample holder position in which the maximum was registered

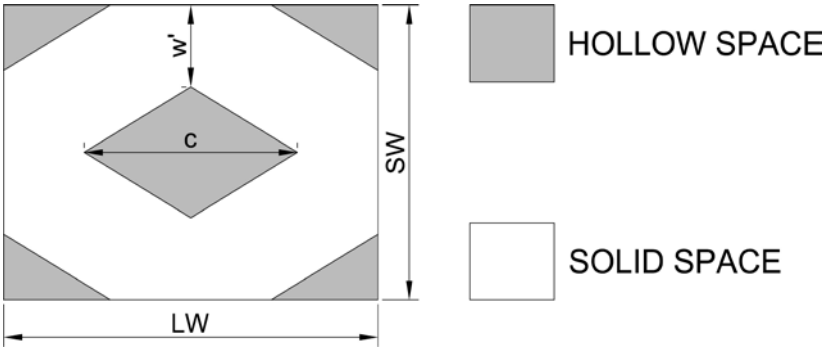

Fig. 5.20. Simplification of a pattern unit front view, hollow and solid areas and parameters defining them

Thus, we obtain the area of hollow space (h_s) in the following way:

$$h_s = 2\frac{c\left(SW - 2w'\right)}{2} = c\left(SW - 2w'\right)$$

w' is the projection of the strand width (*w*) in the front elevation of the mesh, so we can define it as a function of the strands opening angle (σ) mentioned in chapter 5:

$$w' = w\sin\sigma$$

Given that $\sigma = \arcsin\frac{2w}{SW}$ we deduce that $\sin\sigma = \frac{2w}{SW}$ and $w' = \frac{2w^2}{SW}$

so:

$$h_s = c\left(SW - \frac{4w^2}{SW}\right)$$

To obtain the area of solid space (S_s) we just subtract the area of hollow space from the whole area of the pattern:

$$S_s = SW \times LW - h_s = SW \times LW - c\left(SW - \frac{4w^2}{SW}\right)$$

We made the ranking of the relationship between hollow and solid space from dividing the area of hollow space (h_s) by the area of solid space (S_s).

MESH SAMPLE NUMBER	SW/w RELATION
02	4,000
10	3,333
11	3,143
04	3,095
01	3,042
03	2,875
09	2,667
12	2,400
07	2,261
06	2,100
08	2,083
05	1,800

MESH SAMPLE NUMBER	hs/Ss RELATION
02	1,169
01	0,901
11	0,714
10	0,596
05	0,588
04	0,472
03	0,449
09	0,441
12	0,253
07	0,156
08	0,045
06	0,044

Table 5.4. *SW/w* ratio based ranking and hollow/solid ratio based ranking

In spite of the fact that some of the meshes are positioned in the top of the previous two transmittance rankings as in this last two geometry related tables, some others are placed in very different places in all the tables, so we cannot conclude that the strands opening angle or the relation between hollow and solid space are directly related with the transmittance average or maximum, or that at least they are not the only affecting factors. This fact confirms once again that quick conclusions cannot be drawn when trying to understand the transmittance through EM and that its complex geometry makes its performance difficult to predict and summarize.

5.4.1.2 Mesh surface finish

As aforementioned, we have assessed meshes with three different finishes: white, gray and black. The reflectance of these finishes has been measured (see section 5.5.2) and, as expected, it decreases from white to black (as absortance increases). If we compare the data tables in appendix A, section A.3, for each of the meshes in their three colors we can observe that the initially logical supposition of having a higher transmittance for the white sample, intermediate for the gray and lower for the black one is not confirmed.

The first conclusion from these observations is that the color does not significantly affect the specular transmittance. This is a logical statement as light transmitted in that direction has not been subjected to reflections in the mesh strands. The differences between the three colored mesh's transmittances are probably due to inaccuracies of the assessment devices (lamp and luxmeter consistency) and to light differences in the mesh's geometries due to manufacture, overall deformations and coating density and thickness. Anyway the differences between the three colored mesh's transmittances are not representative.

We should expect different results from the analysis of scattered light (see section 6.7.1) where the reflections produced in the strands of the mesh will result in very different transmittances in non specular directions depending on the reflectance (i.e. the color) of the mesh.

5.4.2 Comparative analysis with rough geometrical assessment (vertical variation of specular transmittance)

In chapter 4, we tried to predict the direction of incident radiation with highest transmittance. The prediction was based on the geometrical properties of the EM *main section*. This fact represented a limitation because the rest of sections of the mesh were not taken into account. Another limitation was that the analysis predicted the angle of incident direction with highest transmittance on only one vertical plane.

The following table shows two types of data for each mesh: on the one hand the predicted direction with highest transmittance and on the other the position in *x* axis of the sample holder at which the maximum transmittance was registered in the laboratory. This calculation has been done for mesh samples 01 to 12, leaving the *special* ones aside (meshes 13, 14 and 15). In chapter 4 we defined the angle of incident radiation with highest transmittance (Ψ) and it was measured from the normal to the EM mesh plan. To be able to compare this prediction with the results obtained from our laboratory assessment, the

calculation must be made adding 90º (the norm) to the predicted angle (Ψ). Remember how Ψ was obtained:

$$\psi = \frac{\beta}{2} + \sigma = \frac{\arctan\left(K_f d / c\right)}{2} + \arcsin\left(2w / SW\right)$$

MESH SAMPLE NUMBER	PREDICTION OF INCIDENT RADIATION DIRECTION WITH HIGHEST TRANSMITTANCE (90º+ψ)	POSITION OF x AXIS WHEN TRANSMITTANCE VALUE IS MAXIMUM IN LABORATORY ASSESMENT		
		WHITE (w)	GRAY (g)	BLACK (b)
01	110,57	150	150	150
02	**116,22**	**150**	**135**	**135**
03	113,65	150	150	150
04	**131,36**	**120**	**120**	**120**
05	**135,59**	**120**	**135**	**135**
06	114,33	165	165	165
07	120,45	165	165	165
08	120,65	165		165
09	112,79	150		150
10	**130,28**	**135**		**135**
11	111,62	135		135
12	117,42	150		150

Table 5.5. Predicted direction of incident radiation with highest transmittance of each mesh and position of the sample holder in *x* axis at which maximum daylight transmittance value was registered in the laboratory

As can be observed in the previous table, the prediction made in chapter 4 does not concur with the results obtained in the laboratory. In spite of that, some meshes have more accurate predictions than others. The most accurate predictions are those made for meshes 02, 04, 05 and 10, precisely those with smallest holes. This fact might be explained as follows:

- In meshes with the smallest holes, the mesh thickness is bigger in proportion to the rest of the parameters (mesh thickness is almost the same in all meshes, between 1 and 2 mm, while other parameters are significantly smaller in these meshes). This proportionally greater thickness restricts the bending deformations

and therefore the shape of the main section might gain importance in transmittance.

- The ratio *LW*/*SW* in these meshes is lower than in the rest. This means that the number of main sections per mesh area increases. They are proportionally closer from each other, increasing the effect of what happens in the main section.

At the end of the previous chapter some quick conclusions were extracted from the geometrical properties of the main section and the ratio *SW*/*w*:

- The higher the ratio *SW*/*w*, the closer the direction of highest transmittance to the normal to the plane of the mesh
- If the ratio *SW*/*w* increases, the specular transmittance will tend to have a more symmetric behavior with respect to a horizontal plane.
- If the ratio *SW*/*w* increases, the range of angles of incident radiation with lack of specular transmittance decreases

With the aim of contrasting these statements, we have completed some graphs with values obtained in the laboratory to describe the performance of three meshes with different *SW*/*w* ratios for incident radiation directions included along some vertical plans. We chose samples number 02 (*SW*/*w*=4), 11(*SW*/*w*=3,143) and 06 (*SW*/*w*=2,1). These graphs can be found in section A.4.

Those graphs correlate with the conclusions drawn in chapter 4, being mesh number 02 (highest ratio *SW*/*w*) the one with maximum transmittance value nearer to the normal to the mesh plane (90º position in *x* axis of the sample holder), with more symmetric graphs and with fewer null or nearly null values. On the contrary, the mesh with the lowest ratio *SW*/*w*, mesh number 06, is the one with its maximum transmittance value farther from the normal to the mesh plane, with less symmetric graphs and with highest amount of null or nearly null values.

5.4.3 Analysis of horizontal variation of specular transmittance

With the aim of analyzing the transmission performance for incident directions included along planes intersecting the mesh through a horizontal line, we have produced some other graphs. In spite of the fact that these graphs do not have a specific purpose of contrasting previous hypotheses, they can help to understand the transmittance behavior of EM meshes in general. These graphs can be also found in section A.4.

As we can observe, all these last graphs are similar in shape to each other. They have a decreasing tendency from both ends to the centre, having a null value when the sample holder is rotated to 90º in *y* axis (incident light parallel to mesh plane). The maximums of these graphs are at or near 0º and 180º in *y* axis (incident light normal to mesh plane) and the values get lower as they approach to 90º (incident light oblique). As expected, the highest transmittance is registered when the mesh is facing the incident radiation and as it leans, the transmittance decreases. We can also observe that all the graphs are quite symmetric, meaning that the behavior of the transmittance through one face or the other of the mesh is quite similar.

5.5 Spectrophotometer aided assessment

5.5.1. EM Mesh assessment

With the aim of validating the results obtained in the home made specular transmittance assessment lab device, we made an assessment with a precision spectrophotometer, in collaboration with Tecnalia Technology Corporation. This measuring device has some limitations:

- It only allows the analysis of quite small samples, about 10cm x 10cm
- The incident light beam affects a small surface of the sample

- The incident light has a quasinormal angle respect to the sample, with a deviation from the normal of 8º to avoid the reflected radiation from escaping through the light entrance.

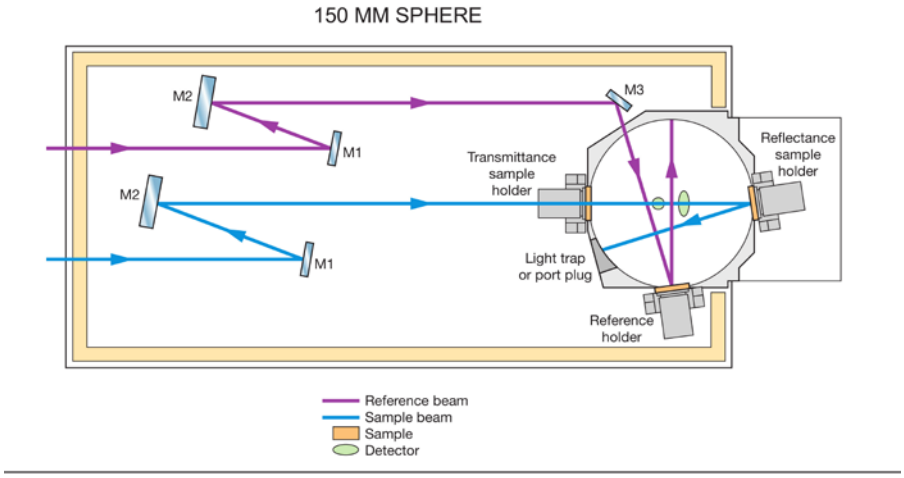

Fig. 5.21 Optical design of 150 mm integrating sphere. **©PerkinElmer, Inc. All rights reserved. Printed with permission.**

Therefore, we chose the mesh with smallest holes from lab set (mesh number 05); we cut small samples of its three colors: white, gray and black (05w, 05g and 05b) and we assessed its transmittance with the spectrophotometer. We could not make tests of other meshes due to the dimension of their openings.

We assessed the transmittance and reflectance for the quasinormal incident radiation. The measurement was done three times from each face of the mesh sample, moving it a small horizontal distance in every measurement to assure that changing the illuminated mesh surface would not change significantly the results. Indeed, the results obtained from these three measurements did not greatly change.

This process was done for both faces of the mesh, i.e. for 0º and 180º rotation positions in *y* axis in our home made lab device, more precisely for the 8º and 172º positions of this axis. The rotation position of the sample holder in *x* axis for that incident direction would be 90º.

We used the Spectrophotometer Lambda 900 UV/VIS/NIR of Perkin-Elmer with a 150mm integrating sphere, quartz pattern and white color. This spectrophotometer is able to obtain data of all the solar range (from 280nm to 2500nm), but for this case we took only the wave lengths of visible range (from 380nm to 780nm). These wave lengths were weighted depending on the importance of each wave length in solar spectrum.

The method used had the following characteristics:

- Wave lengths interval: 5nm
- Scanning speed: 284,6nm/min
- Slit UV/VIS: 1
- Detectors gaining NIR: 4

The results obtained with the spectrophotometer also required a correction due to the device characteristics.

So, for the registered transmittances obtained from this method we took into account the following three factors:

- The 3 different measurements of the same mesh in different positions for each face of the sample
- The weighting of different wave lengths depending on their importance in solar spectrum
- The measuring device's own correction factor.

The results of these measurements are shown in the following table. We have two values of transmittance and reflectance for each mesh sample, one for each face of the mesh. The face of the mesh is defined in the table by the equivalent position in the rotation axis of the sample holder of our own built lab device, giving a value for rotation in *x* and *y* axes (mesh front face x=90 º, y=8 º; mesh back face x=90 º, y=172º).

MESH	FACE	TRANSMITTANCE (%)			REFLECTANCE (%)		
05w	x 90º ; y 8º	26.4	+/-	0.2	55.8	+/-	0.3
	x 90º ; y 172º	24.5	+/-	0.3	57.7	+/-	0.4
05g	x 90º ; y 8º	23	+/-	0.3	24.6	+/-	0.3
	x 90º ; y 172º	21.4	+/-	0.5	25.4	+/-	0.3
05b	x 90º ; y 8º	24	+/-	0.3	2.9	+/-	0.1
	x 90º ; y 172º	23.7	+/-	0.3	3	+/-	0.1

Table 5.6. Transmittance and reflectance obtained by means of spectrophotometer for both faces of mesh 05 in its three colors (white, gray and black)

Having these results as reference, we compared them with the values obtained in the home made specular transmittance assessment device for the same samples and for the same positions of these samples. We had to deduce from the values obtained with the home made device the values corresponding to the rotation positions of 8º and 172º in the sample holder's *y* axis, and 90º in *x* axis. To do that we used linear interpolation of the nearest values of rotation positions (*x,y*): values from (90º,0º) and (90º,15º) were interpolated to obtain a value for (90º,8º) and values from (90º,165º) and (90º,180º) were interpolated to obtain a value for (90º,172º). In the following table we can observe the absolute error between the values obtained in both methods. Knowing the limitations of this brief verification by our home made device and having as reference the more precise values obtained by the spectrophotometer, we can deduce that our system is quite accurate, having a maximum deviation of 2,65% in transmittances obtained from both devices.

MESH	FACE	TRANSMITTANCE (%)		ABSOLUTE ERROR (%)
		spectrometer	own built lab device	
05w	x 90º ; y 8º	26.4	26.14	0.26
	x 90º ; y 172º	24.5	25.31	0.81
05g	x 90º ; y 8º	23	22.76	0.24
	x 90º ; y 172º	21.4	22.8	1.4
05b	x 90º ; y 8º	24	26.65	2.65
	x 90º ; y 172º	23.7	25.7	2

Table 5.7. Transmittances obtained by means of spectrophotometer and homemade device and absolute error between them

5.5.2. Metal sheet assessment

The spectrophotometer was also used to assess some flat lacquered sheets of metal. These sheets were finished with the same lacquers as the analyzed EM meshes; in white, gray and black. The aim of assessing those flat sheets was to quantify the reflectance of each different finish of the tested EM meshes to obtain its properties and simulate them by ray-tracing software during computer aided assessment.

This test was done in the same aforementioned conditions, with the same corrections and weightings. The reflectance of each finish (lacquering color) is expressed in the following table, differentiating the total reflectance from the reflectance without specular component. This way we can deduce the % of specular reflectance. To obtain the reflectance without specular component in the spectrophotometer, a window is opened inside the measuring device in the direction of the specular reflection, so that radiation leaves the integrating sphere and is not registered. Some of the diffuse radiation leaves also in a small quantity from that window, so the values obtained of the reflectance without specular component are slightly smaller than they should.

COLOUR	REFLECTANCE (%)			REFLECTANCE WITHOUT SPECULAR COMPONENT (%)		
White	84.1	+/-	0.3	80.9	+/-	0.6
Gray	43.1	+/-	0.2	39.5	+/-	0.3
Black	4.4	+/-	0.1	4.2	+/-	0.1

Table 5.8. Total reflectance and reflectance without specular component of analyzed EM meshes (measured with spectrophotometer)

As we can observe there is a clear difference between the reflectances depending on the color of the lacquer and the ratio specular reflection to total incident light is 3.2% for white, 3.6% for gray and 0.2% for black lacquer.

References

Andersen, Marilyne, and Jan de Boer
2006 Goniophotometry and Assessment of Bidirectional Photometric Properties of Complex Fenestration Systems. Energy and Buildings 38(7): 836–848.

Apian-Bennewitz, Peter
2010 New Scanning Gonio-Photometer for Extended BRTF Measurements. *In* . Zu-Han Gu and Leonard M. Hanssen, eds. P. 77920O–77920O–20. http://proceedings.spiedigitallibrary.org/proceeding.aspx?articleid=1347498, accessed November 26, 2014.

6.1 Parametric modeling and architecture

Any good design is parametrical as it must have some premise for its shape. These premises can be related to the use, manufacture, geometry, etc. they are, after all, the determining factors of the design.

Parametric modeling is nowadays known as the design that allows us to define a form by means of parameters instead of drawing it directly. Instead of drawing, we define in abstraction attributes of the parts and relations between parts or between parts and the environment. For instance, we can define a line tangent to a curve *C* and passing by a point *A*. We can then alter the curve *C* and point *A*, and therefore our line will change but will maintain its attributes.

Traditional architecture has been conditioned by infinite ideas dancing in builder's brains in a more or less conscious manner. When we want to exploit the power of an information processor we must define the parameters in programming language. Human thoughts are difficult to translate into that language, but the field of geometry is easier to deal with because of its precise mathematical expression.

Abstract modeling of a shape's attributes and relationships offers some advantages compared to modeling the concrete shape because it allows:

- Obtaining product variations rapidly

- Adapting a design to changes in the starting conditions

- Exploiting the calculation power of digital tools defining shape by computing terms

- Re-using parts of a model in several projects in a similar way to the use of code paragraphs in different applications, or the use of shapes or concepts in different architectural projects.

In the following section we'll explain how we can define expanded metal by means of these modeling techniques.

6.2 Parametric modeling of expanded metal

6.2.1 Definition of basic arm with NURBS

As the objective of this research is to define assessment methods for the performance of a large amount of expanded metal models, a parametric definition of expanded metal becomes especially useful.

We have used Rhinoceros[1] modeling application and its extension Grasshopper, which provides the capacity for parametric design.

Obviously, the construction of the digital 3D model will not follow the same process as the manufacturing of the real sheet described in section 2.2. The way we build the shape consists of drawing the kind of sinusoid lines that limit the surfaces, create the surface that binds those lines and extrude them to the thickness of the mesh.

Because expanded metal is a product based on a repeated form, we must find the minimal unit of the form that is repeated in the space. In the following image we can see the upper right yellow colored bow shaped piece which is repeated as a matrix. But this unit is composed by 4 identical pieces, each one in a different position; those pieces are the strands of the mesh and we name them *basic arms*. This minimal *basic arm* is repeated symmetrically to form the whole product.

The design of the *basic arm* depends on two basic curves: straight lines and NURBs. The straight lines are defined with specific points, whereas the NURBs have 4 control points (with a specific weight) and a degree of 3.

A NURB (Non Uniform Rational Basis Spline) is a mathematical manner of defining geometry created by CAD industries in the 70's to unify in one standard the mathematical

[1] Rhinoceros is a three-dimensional modelling program based in NURBs. Other modelling programs as Sketchup, 3DStudio, etc use meshes based in straight lines.

models to represent curves and free surfaces. They offer a unified representation of spline and conic geometries. They were developed starting from Bézier curves (defined by Pierre Bézier) and the mathematical work done by Paul de Faget de Casteljau in the early 60's. (Farin, Hoschek, and Kim 2002)

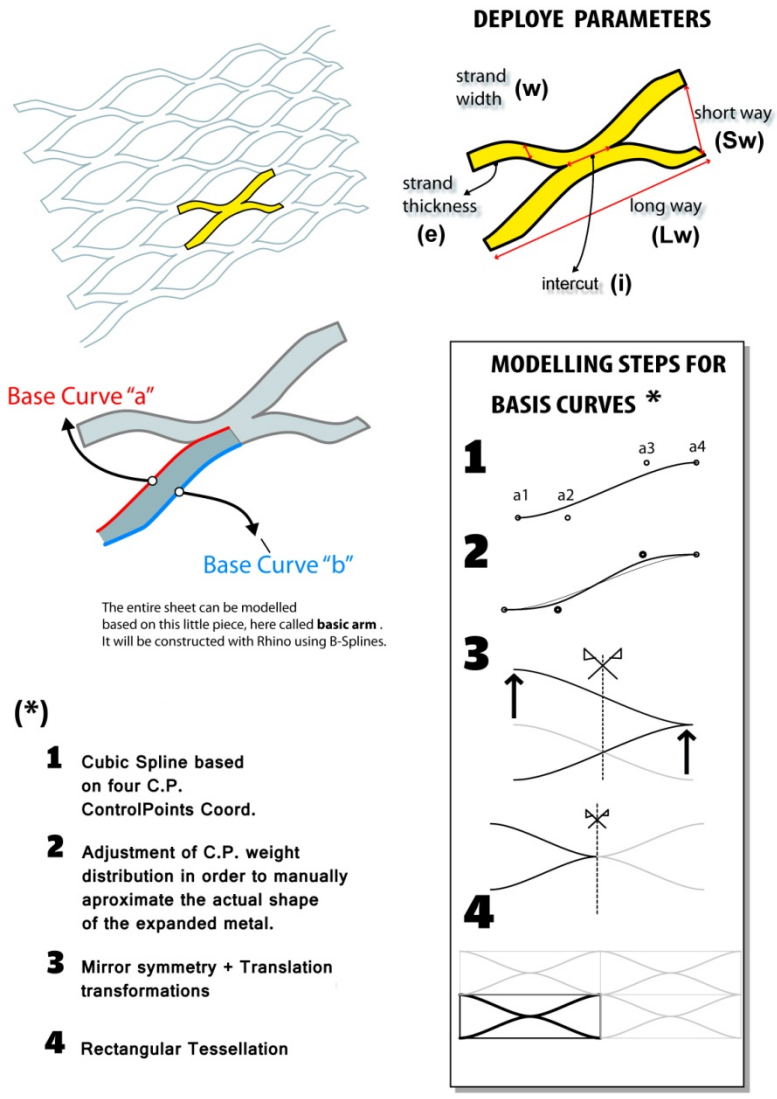

Fig. 6.1. Modeling basic arm

Once we have the basic arm we just need to repeat it with symmetry operations to get the next picture's yellow colored bow and then copy this piece by rectangular tessellation.

As the shape of the folds of the mesh depends on the elastic properties of metals, we needed further analysis of the real product's form by photography and 3D scanning to adjust

the resulting Rhinoceros models. This allowed us to find some kind of rule to define the bending angles.

6.2.2 Ratios to automate the deformation degree

We followed the procedure described in the previous section to build the 3D models of each of the real meshes we assessed in the laboratory and adjusted the control point's position and weight in order to make the resulting virtual mesh's shape match the real one. The control point's weight dictates the "force" with which the control point pulls the curve towards the control point itself. The attraction that each point's weight produces is related to the weights of the other control points of the curve. Consequently, varying the weight of a control point does not only change the distance between the curve and that control point but also, to a lesser extent, between the curve and the other control points, as shown in the following figure

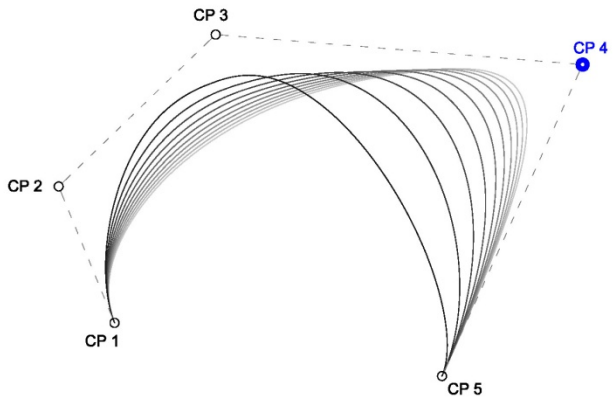

Fig. 6.2. Variation in the weight of a control point

As we had two parameters of the control points to vary (position and weight), we decided to first fix the appropriate weight for each control point (the same for all the meshes) and adjust the position. From this manually introduced data we extracted some approximate ratios, described below, to automate the 3D model builder. With automation we lose precision but simplify the process.

As our modeler is dedicated to build most usual rhombus shaped E.M. meshes manufactured with saw shaped blades whose edges are straight lines, one of the lines that form the *basic arm* -named *basic curve a* in the previous figure- is an exact trace of the contour of the blade. Therefore this line is drawn as a succession of three straight lines (from *D* to *A'* in next figure):

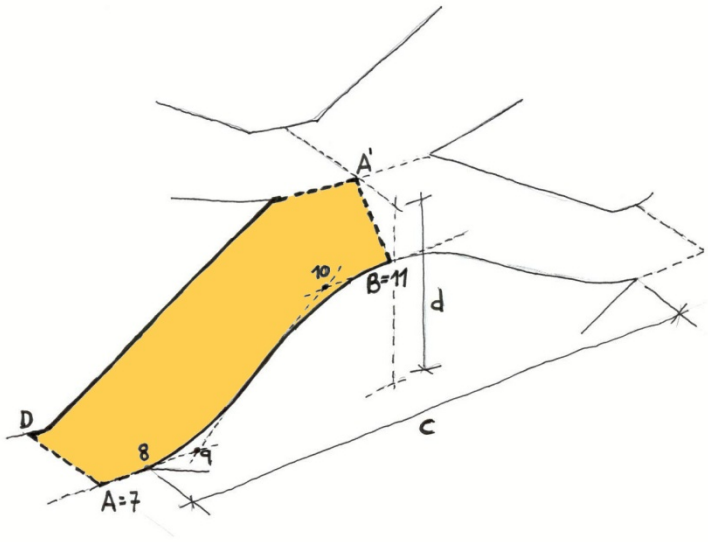

Fig. 6.3. Basic curves and control points

The *basic curve b* (or curve *A-B* in the previous figure*)* is composed by a straight line from *A* to *8* and a NURB with four control points: *8*, 9, *10* and *11*. This curve passes by points *8* and *11* and is attracted by points *9* and *10*. Point *8* is the joining point of *cut* and *intercut*. Point *11* (or *B*) is the joining point of two symmetrical units of *basic curve b*.

Measurements of the shape of the meshes tested in laboratory were made on pictures photographed with a zoom lens from a distance of 20 meters in order to obtain a nearly orthogonal projection of the mesh. With these measurements we were able to determine the control points position, that is, distances *8-9* and *10-11* (fixing the control points weight to 50 for point *9* and 30 for point *10*) to obtain a model as similar as possible to the real mesh.

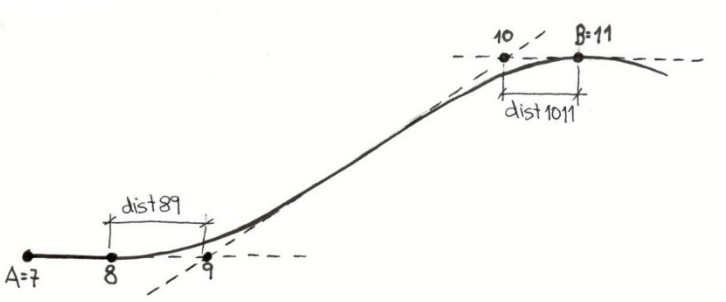

Fig. 6.4. Base curve b and control points

As can be appreciated in figure 6.3, point *A* and *A'* appear in both basic curves (*D-A'* and *A-B*). This is due to the fact that the mesh is composed by the basic arm which is repeated with copy-displacement and symmetry operations. Copying and displacing the basic arm from *A* to *A'* we obtain half a bow:

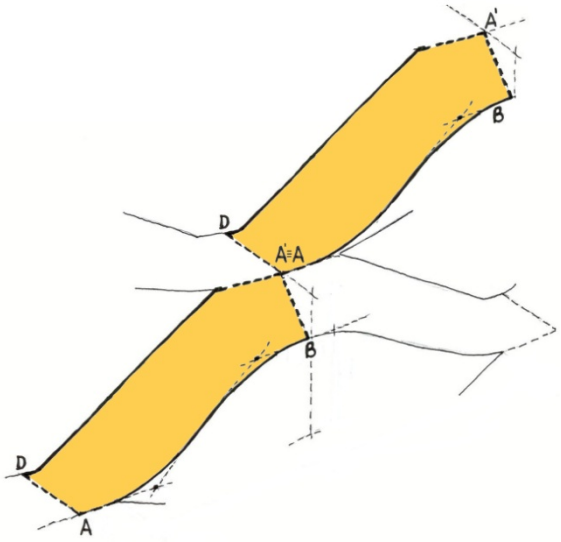

Fig. 6.5. Basic arm copied and displaced

From the symmetry of the previous two basic arms we can obtain a complete bow.

To automate the definition of the curve we searched a way to relate the distance between point *8* and *9* with the known parameters of the mesh. From observation of the manufacture deformations we can deduce that *8-9* distance is directly proportional to the cut length (*c*) and strand width (*w*) and inversely proportional to the blade descent (*d*):

The wider the cut (*c*) is the smoother the curve, and consequently the greater the distance *8-9*.

The larger the descent (*d*) is, the greater the deformation of the mesh (expansion) and the smaller the distance *8-9*.

The larger the strand width (*w*) is, the smaller the descent of point *B* from point *A* (*f*) and therefore the smoother the deformation and greater distance *8-9*.

In short *8-9* distance can be expressed as a function of *c, w, d* and a constant K_{8-9}:

$$dist8-9 = K_{8-9}\frac{c \cdot w}{d}$$

From the values of *8-9* distance obtained from measured real meshes we obtained a statistical average of $\boldsymbol{K_{8-9}}$**= 2,59 x 10^{-4}**.

Similarly, we can deduce that the distance *10-11* keeps the same kind of proportionalities for *c*, *w* and *d*:

$$dist10-11 = K_{10-11}\frac{c \cdot w}{d}$$

The average value of K_{10-11} obtained from measured real meshes is $\boldsymbol{K_{10-11}}$ **= 0,111**.

In manufacture, when the blade cuts and pushes down the strand, *D* and *A* points go down the distance *d*, named *descent*, *A'* point remains unmoved because it is just on the edge of the press-bench and *B* point descends a certain distance, pulled by the strand. We name *f* the distance that *B* descends and we measured it in the nearly orthogonal photographs of all the real meshes available in laboratory. We also did a 3D scan of some of the meshes to have more accurate data and validate the measurements of the pictures. This was especially useful to measure that deformation. To automate the value of *f*, we also searched a relation with the known parameters of the mesh. The value of *f* must be directly proportional to strand width (*w*) and descent (*d*) and inversely proportional to cut length (*c*). Therefore *f* can be expressed as a function of *w, d, c* and a constant K_f:

$$f = K_f \frac{d \cdot w}{c}$$

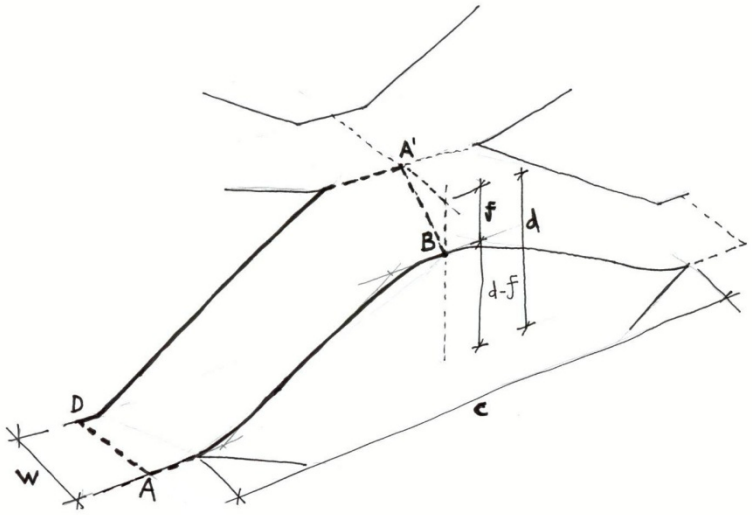

Fig. 6.6. Definition of *B* point's descent, *f*

The average value of K_f obtained from measured real meshes is $\boldsymbol{K_f}$ **= 1,444**.

As mentioned before, this way we reduce precision but we obtain automation. The following images show the difference between some of the models constructed using measurements of real meshes' photographs and 3d scanning (red colored); and the more imprecise automated modeling of the same meshes (gray colored).

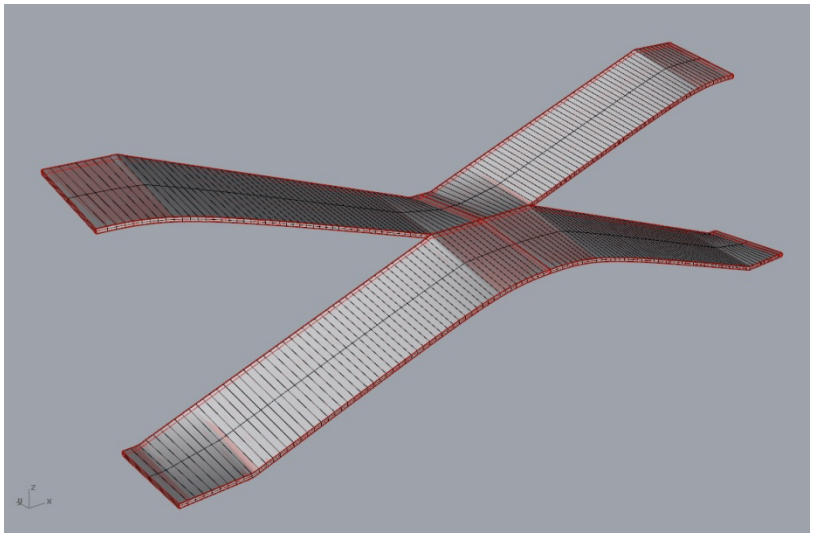

Mesh nº	LW	SW	w	i	b	e
01	200	73	24	33	7	1

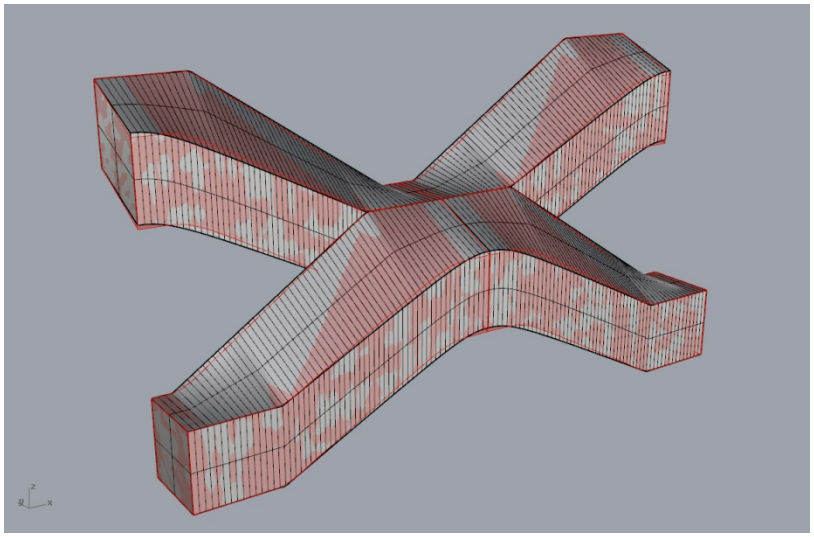

Mesh nº	LW	SW	w	i	b	e
02	16	8	2	4,5	1	2

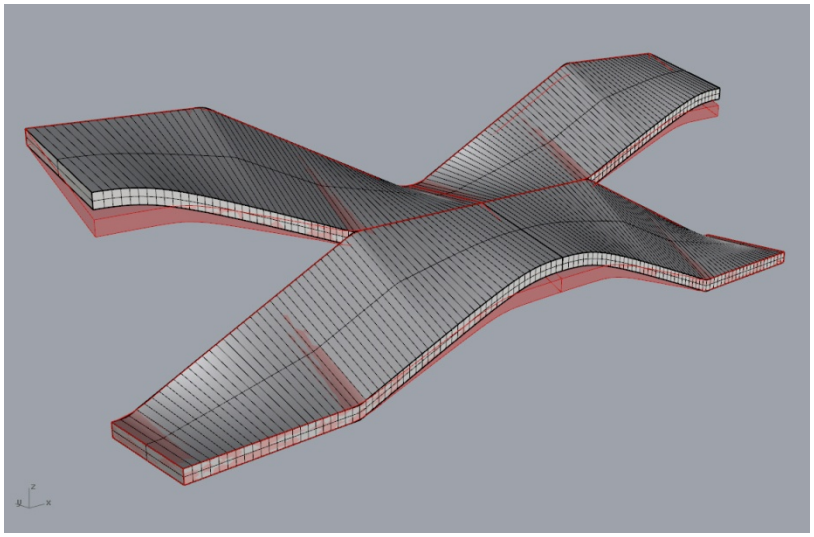

Mesh nº	LW	SW	w	i	b	e
03	62,5	23	8	25	2	1

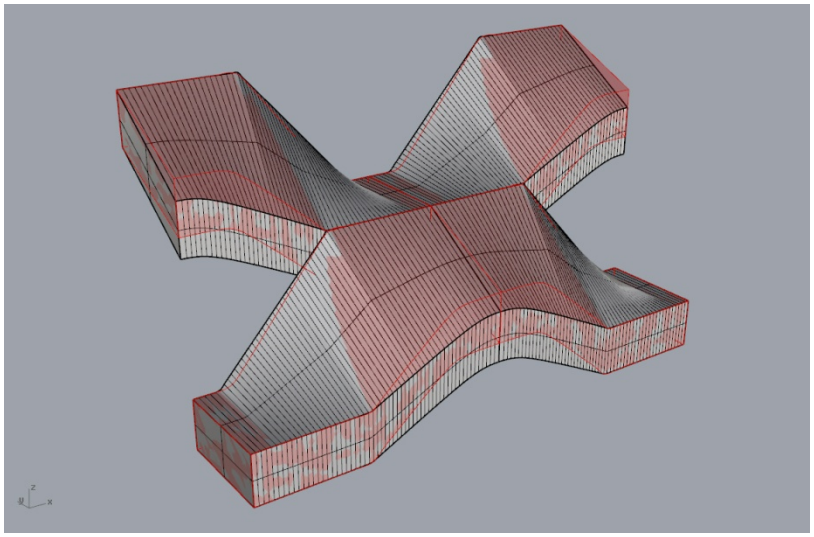

Mesh nº	LW	SW	w	i	b	e
04	10	6,5	2,1	4,5	1	1

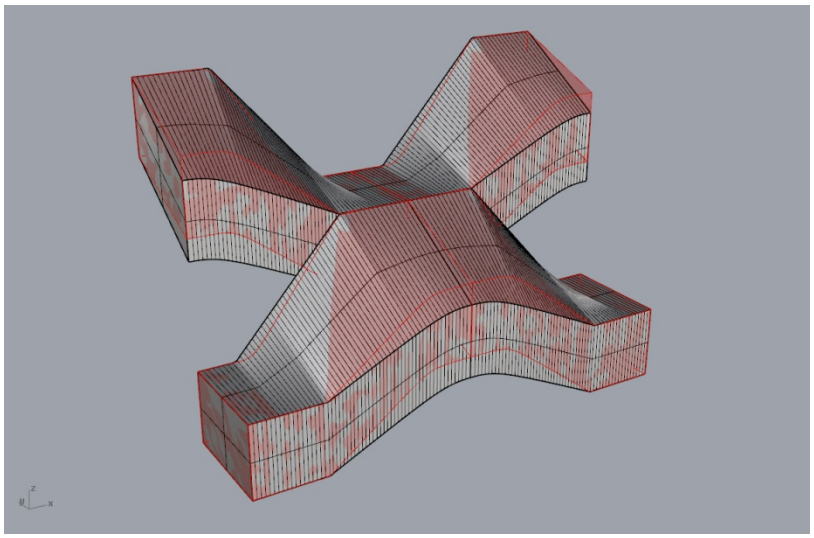

Mesh nº	LW	SW	w	i	b	e
05	6	4,5	1,5	2	1	1

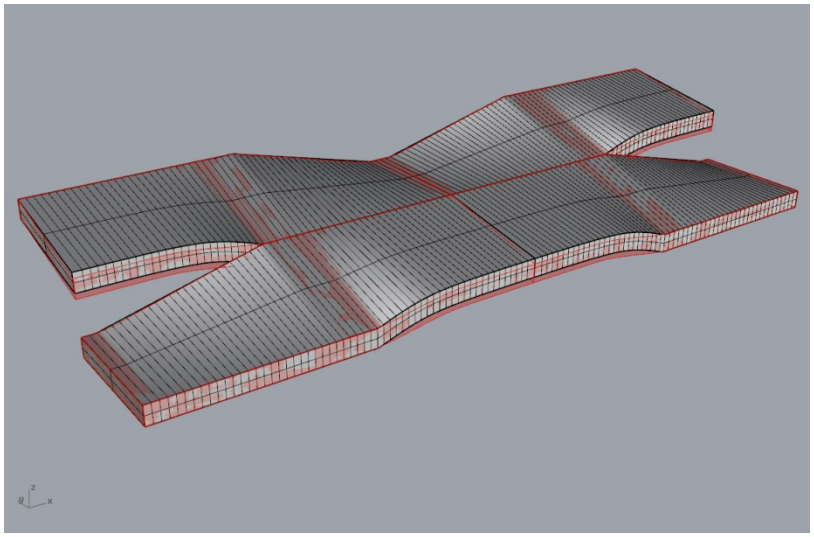

Mesh nº	LW	SW	w	i	b	e
06	60	21	10	33	2	1,5

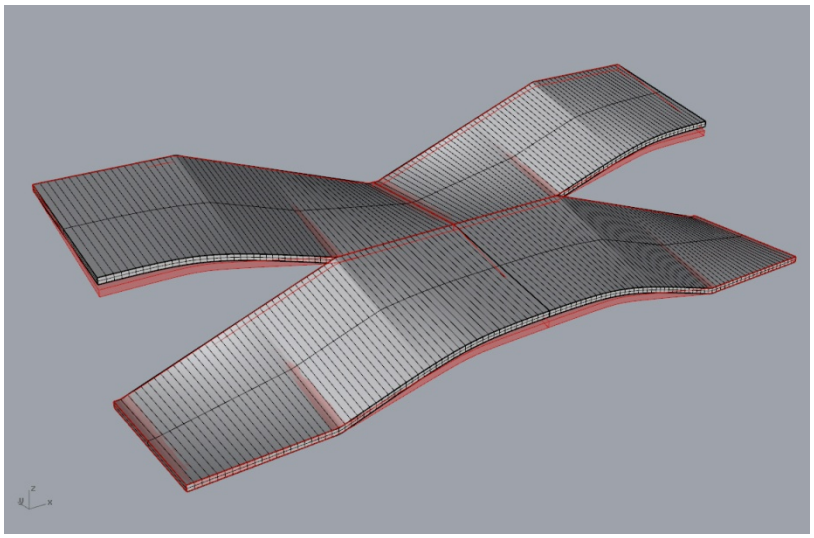

Mesh nº	LW	SW	w	i	b	e
07	115	52	23	43,5	2	1

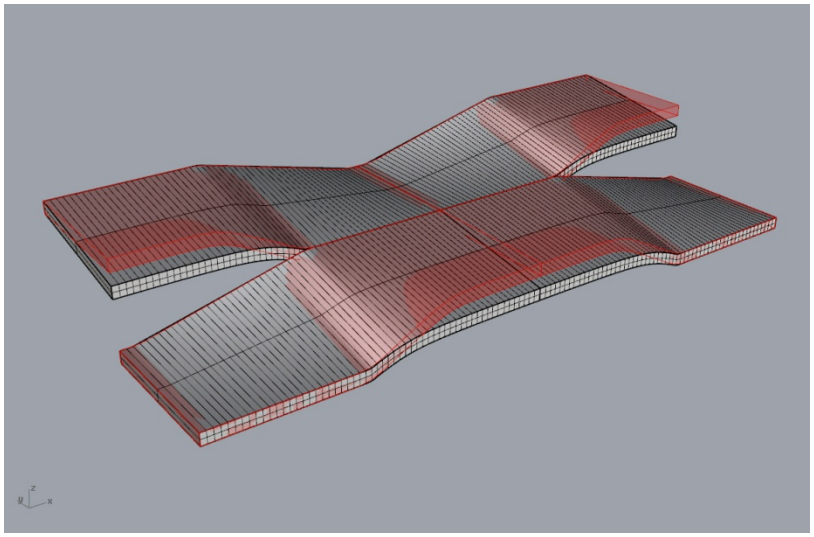

Mesh nº	LW	SW	w	i	b	e
08	110	50	24	50	3,5	2

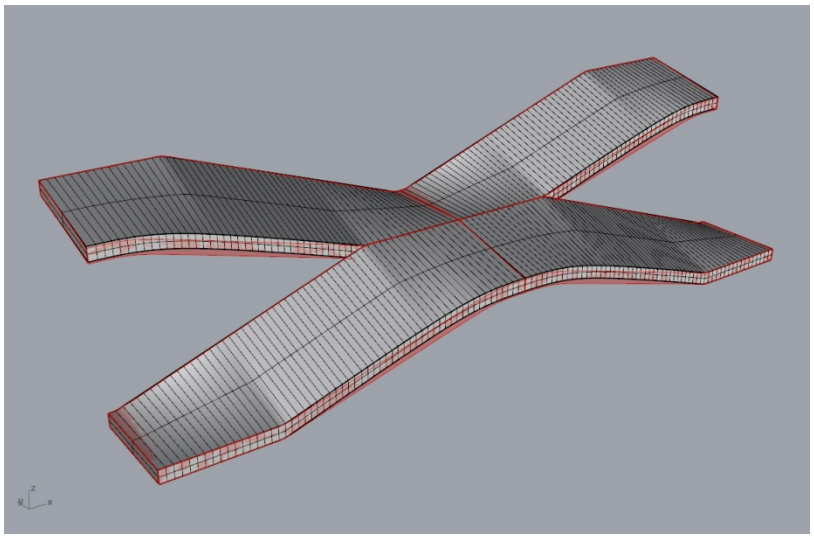

Mesh nº	LW	SW	w	i	b	e
09	110	40	15	33	2	2

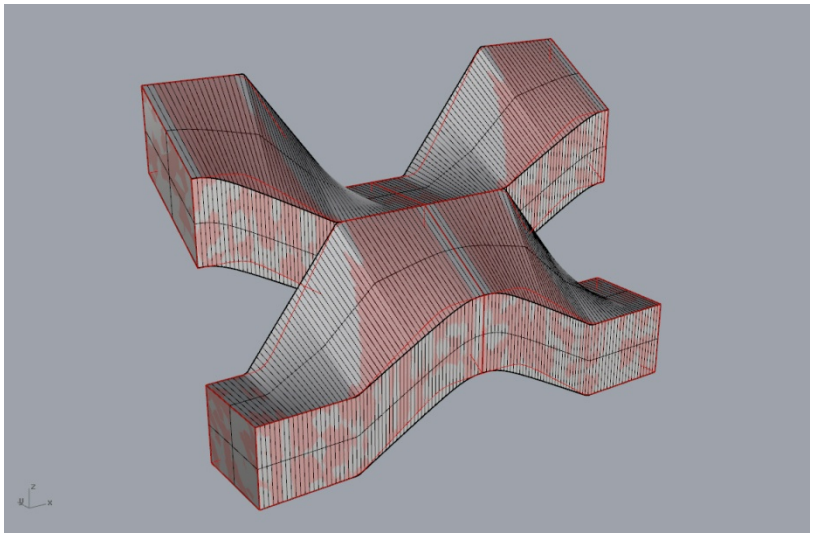

Mesh nº	LW	SW	w	i	b	e
10	6	4	1,2	2,5	1	1

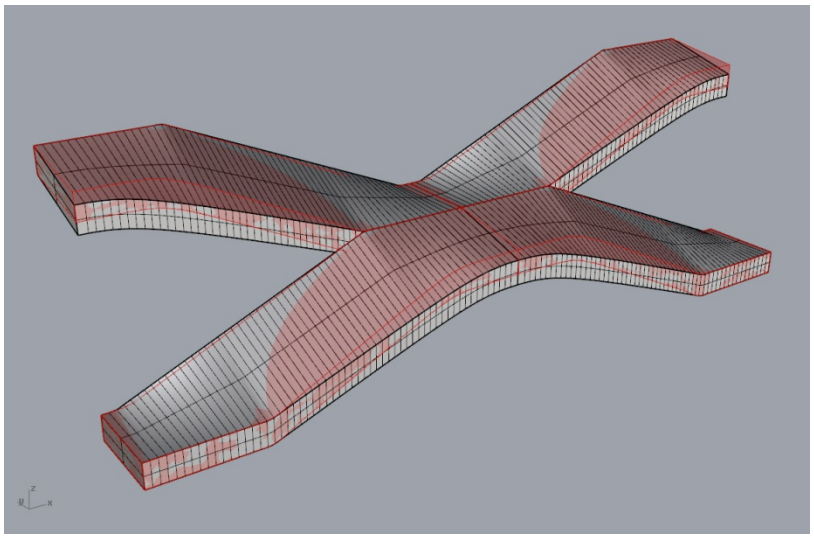

Mesh nº	LW	SW	w	i	b	e
11	60	22	7	18	2	2

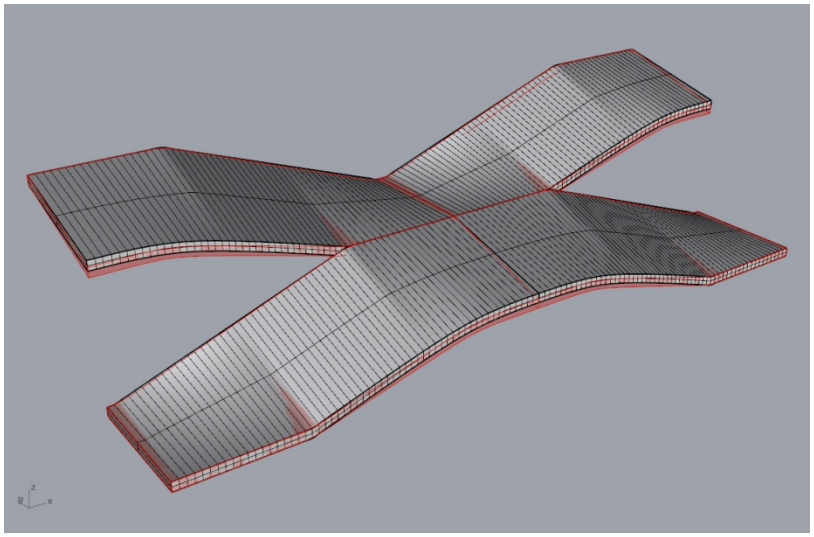

Mesh nº	LW	SW	w	i	b	e
12	115	48	20	39	2	1,5

Fig. 6.7. Superimposed images of automated models (gray) and more precise models (red)

The tool we created to model E.M. will ask the user for 6 of the geometrical parameters defined in section 2.3.2: strand width (*w*), short way (*SW*), long way (*LW*), intercut (*i*), sheet thickness (*e*) and blade bevel (*b*). As mentioned, a 7th parameter would be necessary for a more precise model: blade thickness (*t*). The effect of blade thickness has been disregarded in our tool as only a slight punch in the middle of the knuckle depends on that parameter, which is not expected to affect noticeably daylight transmittance.

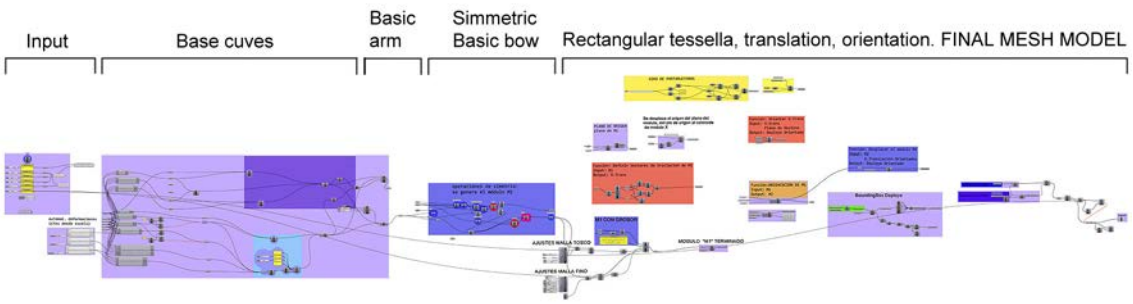

Fig. 6.8. Grasshopper interface for the E.M. 3D modeler

Once we have provided those 6 values to the E.M. builder it will automatically draw the 3D model of the resulting mesh.

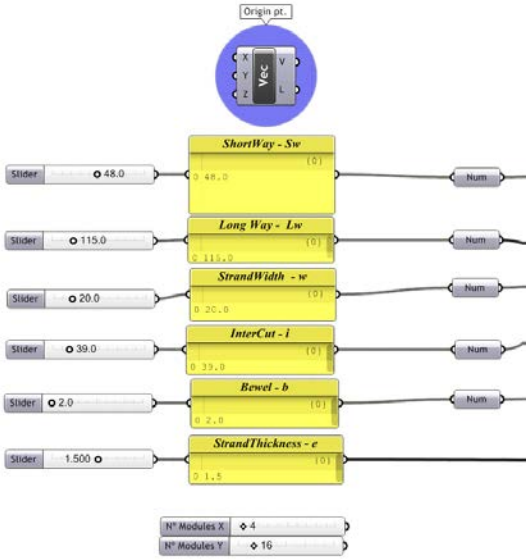

Fig. 6.9. Closer view of the 3D modeler interface. Input data

6.2.3 Discarded shape aspects

There are some shape aspects that were discarded when the parametric modeler was programmed due to their complex design and, specially, because a precise analysis of the elastic behavior of the material is beyond the aim of this research.

Some of those deformations, such as, irregular bending points and the appearance of bumps in the knuckle, are described in section 6.3, where we discuss 3D scanning.

Other deformations observed in the meshes, such as convexities and section changes due to Poisson effect, are shown in the following figure.

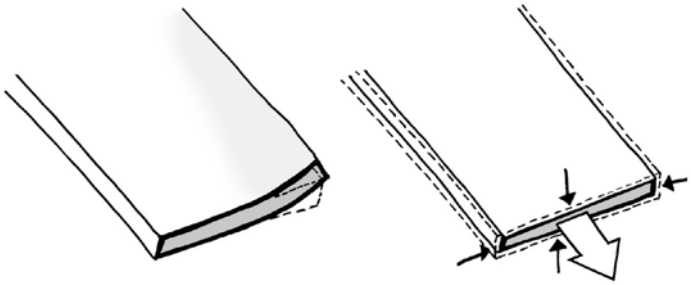

Fig. 6.10. Discarded shape aspects: convexities and Poisson effect

In some meshes, when strand thickness (*e*) is small compared to strand width(*w*), a little warp can be observed on one side of the arm (left drawing in previous figure). The strand

tries to adapt itself to fabrication movement and deformations, but it cannot create a perfect ruled surface, and as the sheet is quite thin, some convexity appears.

In addition, when the rib is stretched in the fabrication process (when the blade descends), the Poisson effect causes a small shrinking of the section (right drawing).

6.3 Geometry analysis by means of 3D scanning.

As mentioned before, in order to improve the parametric E.M. 3D modeler and correct possible errors in the models created measuring photographs, a 3D scanning of some samples was done. The scan used for this purpose was an *ATOS Compact Scan 5M* (ATOS Compact Scan: GOM n.d.).

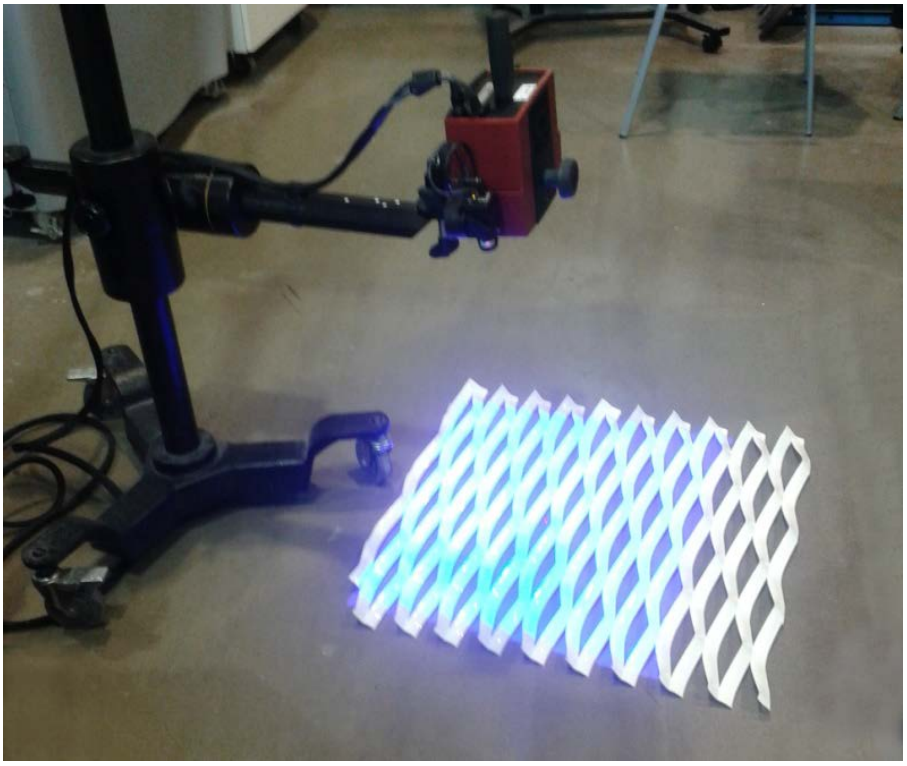

Fig. 6.11. Scan process.

Only one of the faces of the meshes was scanned, the front one. In the process, starting from a reference point, the relative position of a finite amount of geometric points on the surface of the subject is calculated (depending on the needed accuracy).

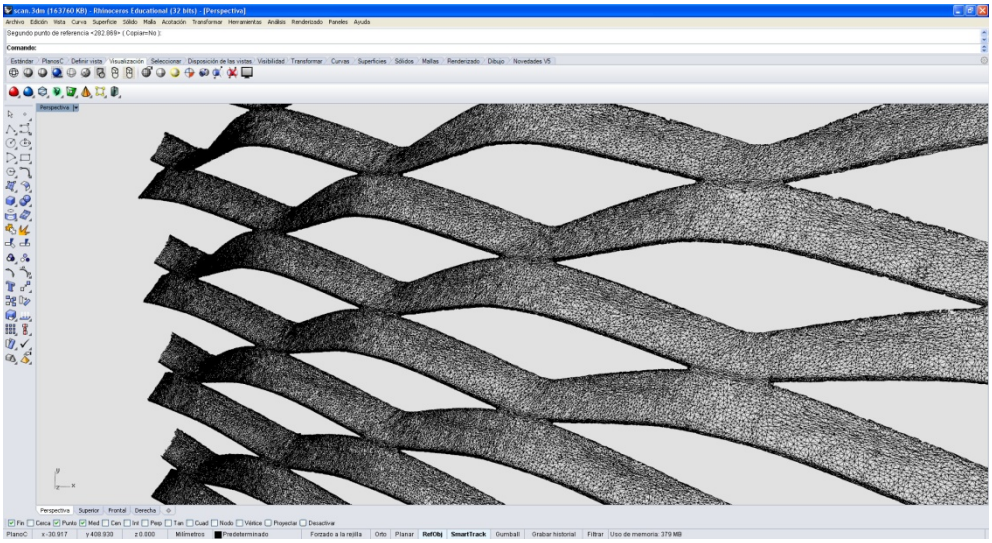

Fig. 6.12. Triangulated surface created from 3D scan

The result is a point cloud that can be extrapolated in order to create a continuous surface using a modeling program. In this case, connecting the points generated in the scanning, triangulated surfaces were created.

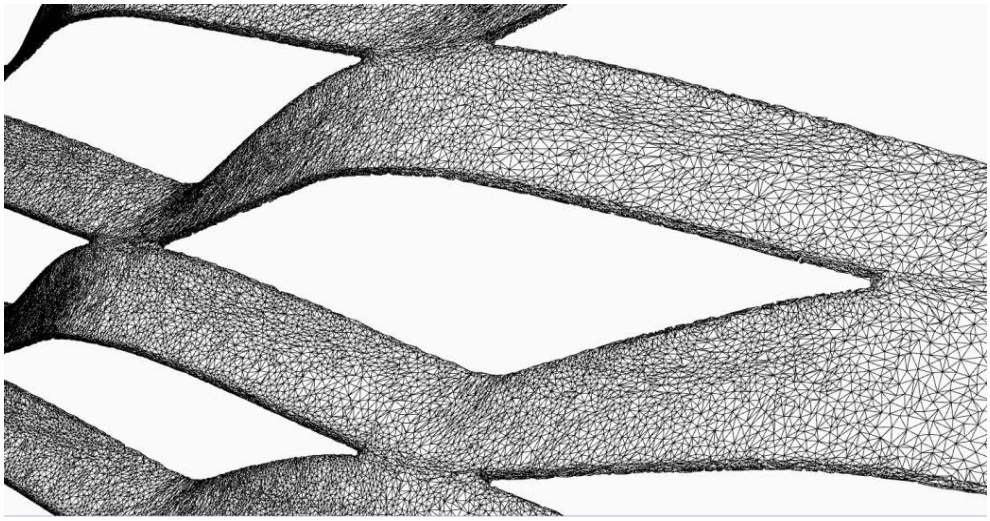

Fig. 6.13. Closer view of a scanned mesh

These geometries were compared to those created from parameters and measurements on photographs, in order to improve the modeler. The comparison between vertical sections in the following image enabled us to correct some errors in the beta version of the modeler (red colored), comparing to scanned samples (blue colored).

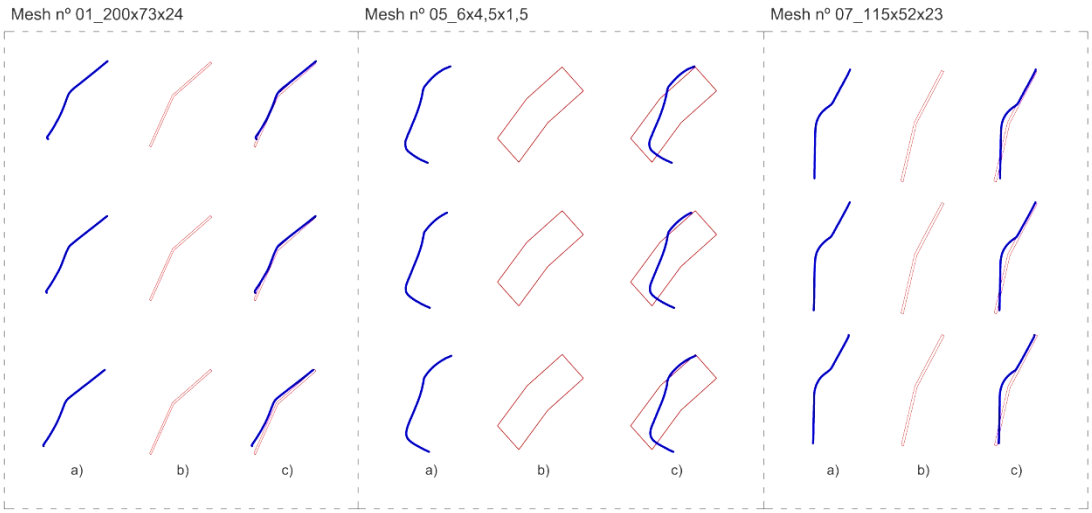

Fig. 6.14. 3D scan – beta modeler comparison for meshes 01, 05 and 07: a) Scanned mesh, b) Modeled mesh, c) Superimposed

From that analysis we can draw the following conclusions:

- In some meshes, e.g. the mesh nº1, we can observe that the precision of the modeler is dependable enough for our purpose. The vertical section of the model is very similar to the real one.

- When the thickness of the sheet is high in proportion to the other parameters, some deviations related to distinctive deformations that occur in the fabrication process can be observed. On the one hand, a greater descent of the front strand (that we call *f* deformation) is observed. On the other hand, it seems that in samples with large thickness, when the blade pushes down and expands the metal sheet in the fabrication process, the previously mentioned bending does not happen exactly on the edge of the press-bench, but behind the cutting line.

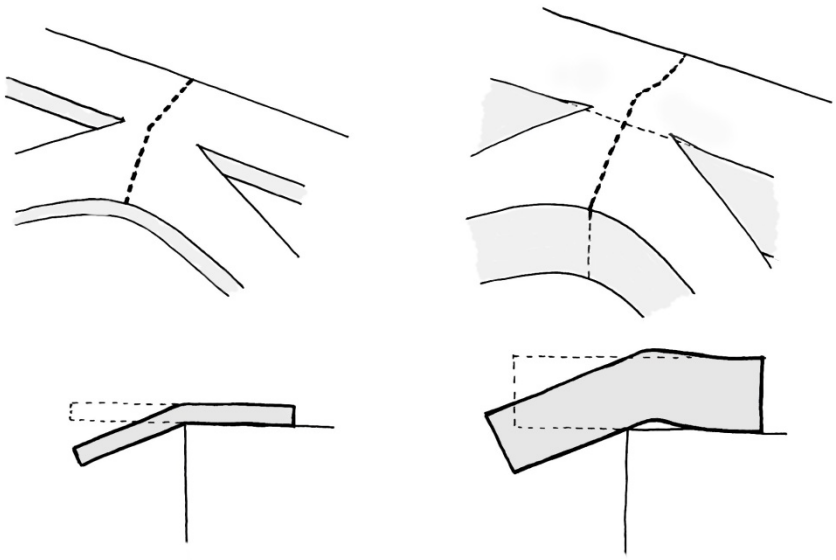

Fig. 6.15. Bending behind the cutting line

In the third sample (mesh nº07), we can observed that when the strand width (*w*) is larger than the thickness of the cutting blade, a little bump appears due to the blade's bite.

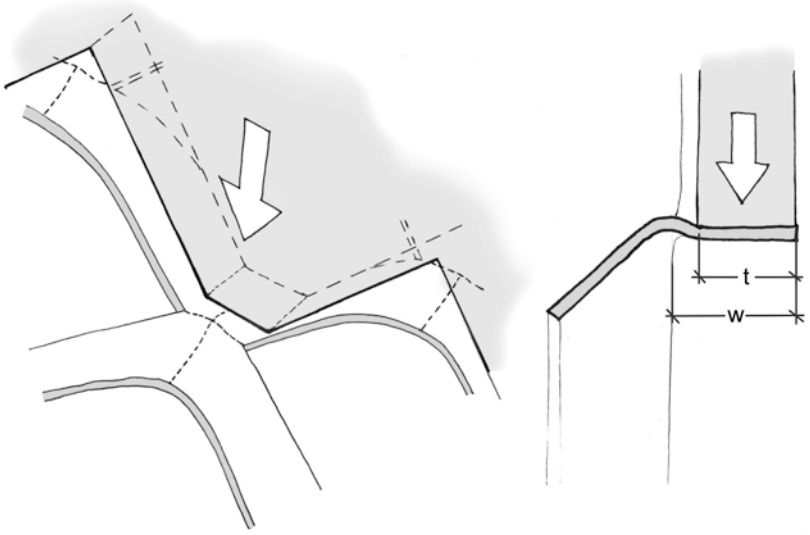

Fig. 6.16. Bump due to blade's bite

Some of these deformations were not taken into account for the parametric 3D modeler due to the design complexity and minor effect on the daylight transmittance of the meshes.

6.4 Resulting models

With the improvements mentioned above, we obtained the last version of the Rhinoceros/Grasshopper EM 3D modeler. As any 3D model, the generated mesh can be used for the usual purposes: as part of a whole building model, for rendering, for energetic / lighting / thermal simulations, etc. It can also be exported to almost any modeling software.

The EM 3D modeler (2015/03) can be downloaded from:

https://www.dropbox.com/s/cty7yrkydj901xw/Deploye.gh?dl=0

You can also write to j.rico@ehu.eus to request the file.

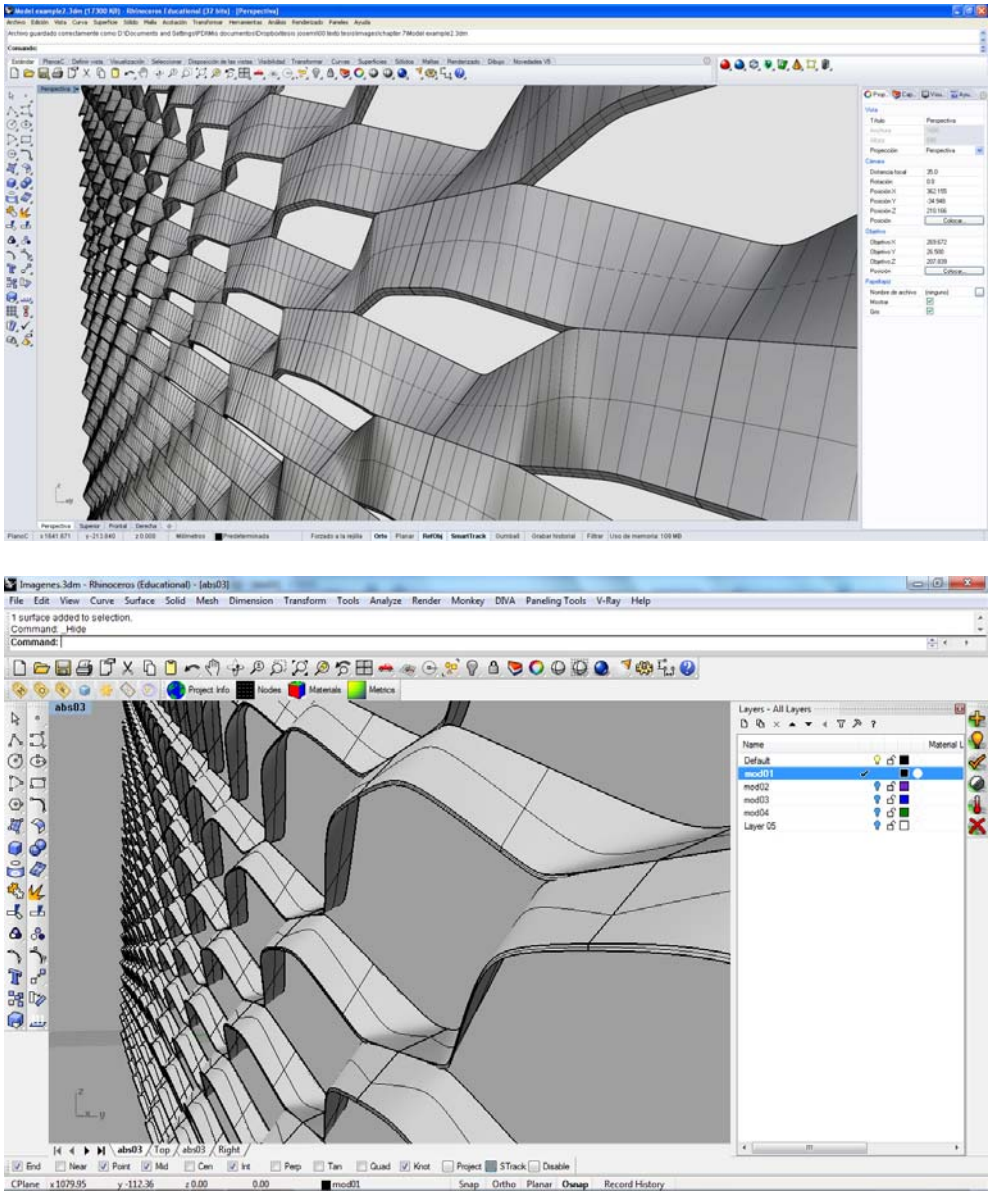

Fig. 6.17. Examples of resulting models

6.5 Rendered models

Rendering programs can be used for fast visualization purposes that give an intuitive idea of the daylight transmittance performance of a specific mesh. The following images were rendered using V-ray for Rhino as ray-tracing solution.

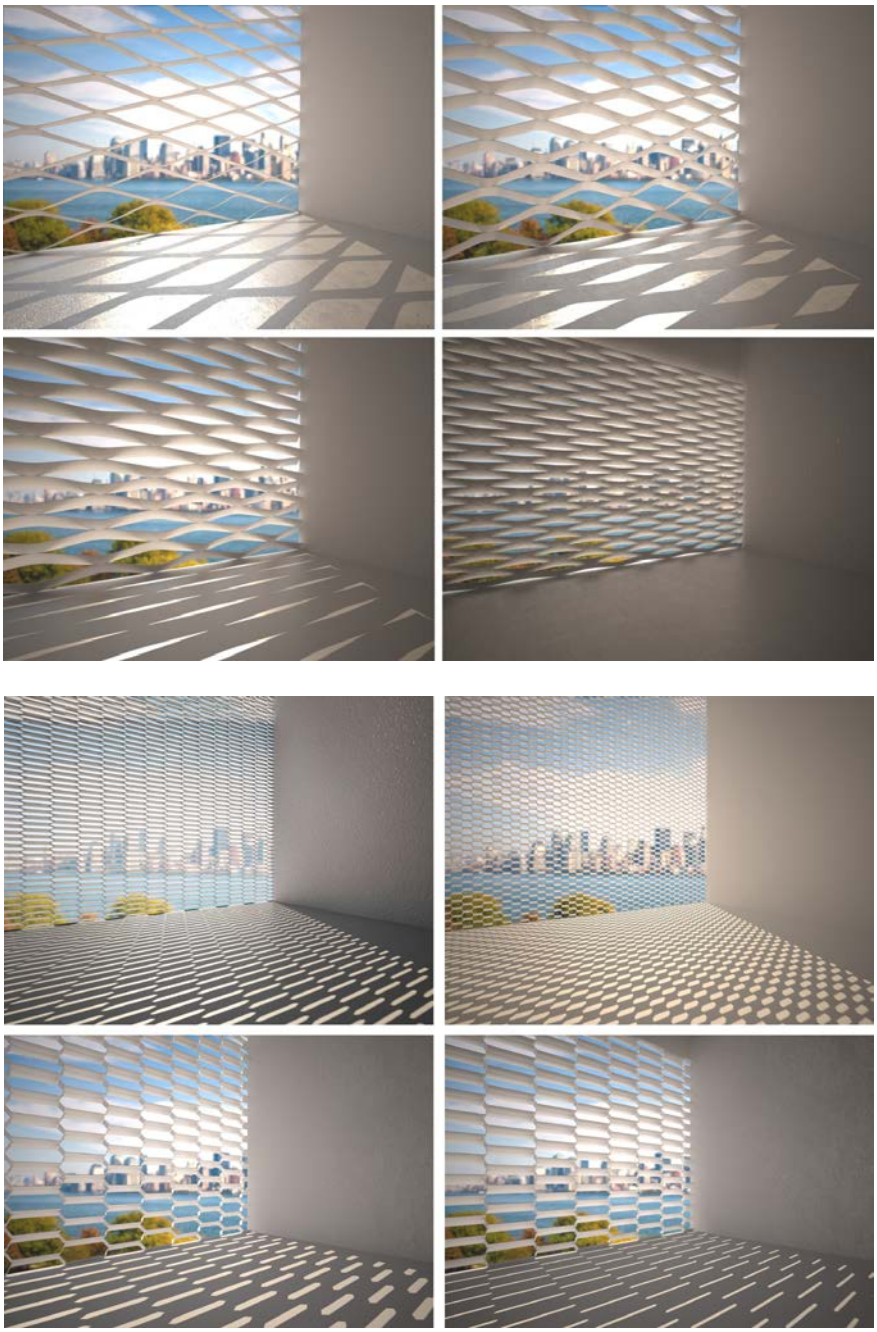

Fig. 6.18. Render of 8 different meshes with the same lighting conditions

6.6 Computer-aided daylight transmittance assessment with BTDF

For our daylight assessment purposes, the most precise and complete approach is the use of BSDF (BSDF 2014). Based on Nicodemus and Klems works (Nicodemus 1965) (Klems 1994) a method was created to compile the directional behavior of complex fenestration systems as regards reflection and transmission of radiation in a matrix. When radiation reaches a surface it can be reflected and/or transmitted in all directions. The distribution of that reflected and transmitted (i.e. scattered) radiation depends on the characteristics of the surface. The BSDF of a surface is a four dimensional function that comes to describe the behavior of radiation reaching that surface; in other words: how does that surface scatter radiation. In practice the scattering is usually split into the reflected (backward) and transmitted (forward) components, referred as BRDF (Bidirectional Reflectance Distribution Function - Wikipedia, the Free Encyclopedia n.d.) for opaque surfaces and BTDF (Bidirectional transmittance distribution function) for the transmitted part of translucent surfaces. BSDF offers a complete description of reflection and transmission for translucent surfaces. In the strict sense, the data we will manage will be the BTDF as the purpose of our work is the assessment of daylight transmittance of EM.

The function takes an incoming light direction and outgoing light direction, both defined with respect to the surface normal, and returns the ratio of scattered radiance exiting along the outgoing direction to the irradiance incident on the surface from incoming direction. Each direction is defined by azimuth and zenith angles; therefore the BSDF is 4 dimensional (2 angles for each direction). If we want to assess the whole spectrum of light we can add a 5^{th} dimension: wavelength. Therefore it cannot be thoroughly described in a 2D or 3D representation. Any 2D or 3D representation we can imagine will show only a part of the function. The BSDF has units sr^{-1}, with steradians (sr) being a unit of solid angle.

Even if expanded metal and other typical fenestration layers such as louvers are not continuous surfaces because of their gaps, BSDF can be used to define them (the gaps will be

areas of the surface where radiation is not subjected to changes in direction and magnitude, i.e. specular transmission will happen through the gaps and backwards/forwards scattering where radiation reaches the solid parts of the layer).

6.6.1 Calculation of BTDF

6.6.1.1 Physical definition of BSDF

In order to interpret the meaning of the data included in a BSDF (Bidirectional Scattering Distribution Function), its physical definition should be considered.

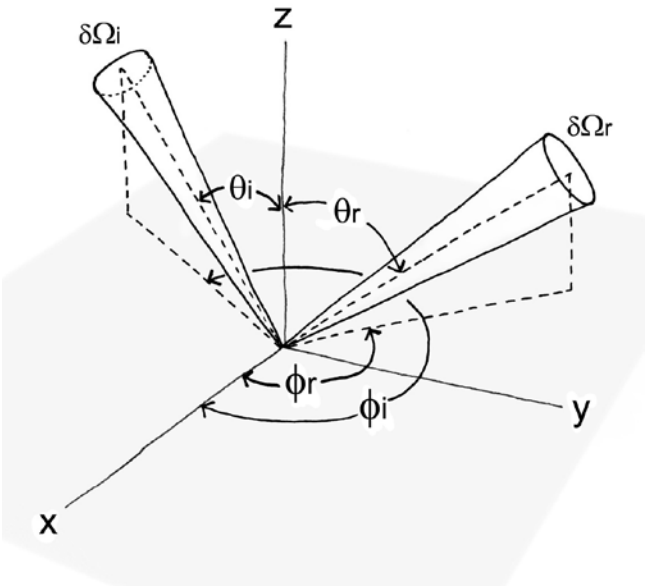

Fig. 6.19. Geometry of incident and reflected elementary beams as explained by Nicodemus. *z* axis along the normal to the surface at 0

According to Fred Nicodemus (Nicodemus 1965):

$$f_r(\omega_i, \omega_r) = \frac{dL_r(\omega_r)}{dE_i(\omega_i)} = \frac{dL_r(\omega_r)}{L_i(\omega_i)\cos\theta_i d\omega_i}$$

Where:

L= Radiance (W/m^{2}xsr)

E= Irradiance (W/m^2)

θ= Polar angle between light beam and surface normal (rad)

ω= Direction vector of a light beam

The suffix "*i*" refers to "incident" and "*r*" to "reflected" but the latter can be understood as "transmitted" for BTDF.

Therefore, the unit of BSDF is sr^{-1}.

In order to better understand the meaning of the function, let us remember the definitions of Radiance and Irradiance:

Radiance (*L*) is the quantity of radiation that passes through or is emitted from a surface and falls within a given solid angle in a specified direction (W/m^{2}xsr).

Irradiance (*E*) is the power of radiation per unit area (radiative flux) incident on a surface or radiated by a surface (W/m^2).

Radiance is associated to a direction vector and Irradiance is associated to a plane.

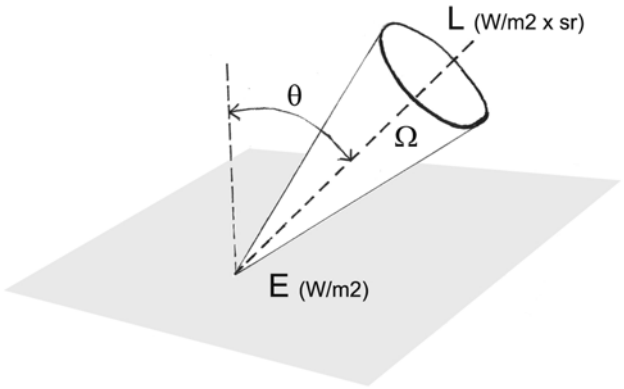

Fig. 6.20. Relation between Irradiance and Radiance

Considering a lambertian surface and a regular irradiance, in a simplified way, we can accept that both magnitudes can be related as follows:

$$E = L\cos\theta \cdot \Omega$$

Where:

θ= Polar angle between light beam and surface normal (rad)

Ω= Solid angle (sr)

When talking about visible electromagnetic spectrum, in light terms we talk of Illuminance (E_v) and Luminance (L_v):

$$E_v = L_v \cos\theta \cdot \Omega$$

The cosine is necessary to obtain the magnitude of the Irradiance/Illuminance in the surface, because the perpendicular component (parallel to the surface normal) of the radiance (L) is needed to obtain that value. Remembering Lambert's Cosine Law**:** the irradiance or illuminance falling on any surface varies as the cosine of the incident angle (θ); the perceived measurement area orthogonal to the incident flux is reduced at oblique angles causing light to spread out over a wider area than it would if perpendicular to the measurement plane.

6.6.2 Management of BTDF

Two tools we have used for our analysis are:

- *genBSDF*, a program designed to work within Radiance[2] (Ward et al. 2011) (McNeil, Jonsson, and Appelfeld 2011)

- *BSDF viewer*, a program designed to display BSDF data in an intuitive and comprehensive way. (McNeil 2013)

[2] RADIANCE is a highly accurate ray-tracing software system for UNIX computers that is licensed at no cost in source form. Radiance was developed with primary support from the U.S. Department Of Energy and additional support from the Swiss Federal Government. Copyright is held by the Regents of the University of California.

6.6.2.1 Handling GenBSDF

By means of genBSDF we illuminate a sample in Radiance and get a list of BSDF (L_s/E_i) values for each combination of directions of incidence and scattering. That is, given a certain incident luminous flux reaching the sample, its behaviour is characterized and described, the sample understood as a surface.

As the possible combinations of incident and scattering directions are boundless, the program discretizes the solution for the 145 patches defined by Klems (Klems 1994), both for incidence and for scattering. More complex patch systems have been developped for more precise descriptions of radiation, increasing the amount of patches (Ward et al. 2011) or changing the patch sizes adapted to light transmittance variability (e.g., tensor tree BSDFs) (Ward, Kurt, and Bonneel 2012), but this surpasses our objectives here.

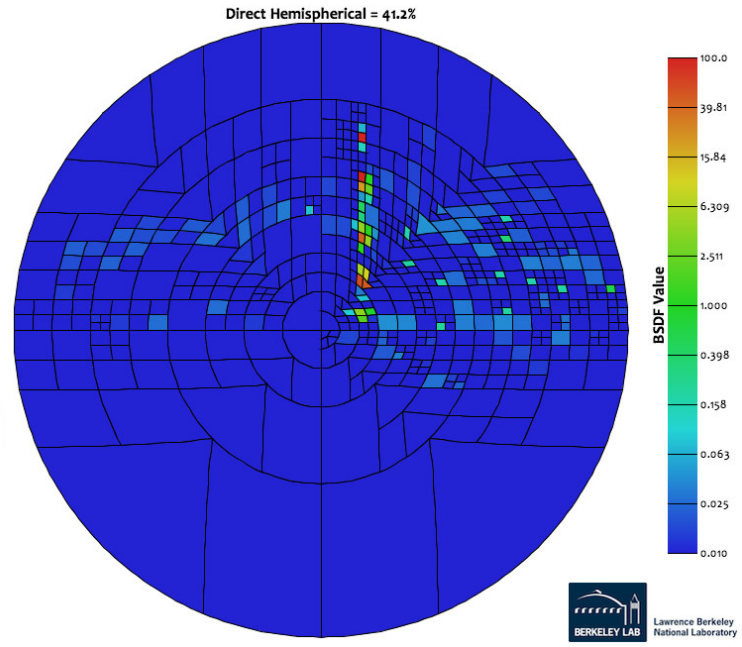

Fig. 6.21. Other patch systems: Tensor tree BSDF, BSDF viewer. (McNeil 2013)

The pattern proposed by Klems, divides the hemisphere on each side of the surface in 145 patches, returning 145 x 145 = 21 025 transmittance values for each surface sample.

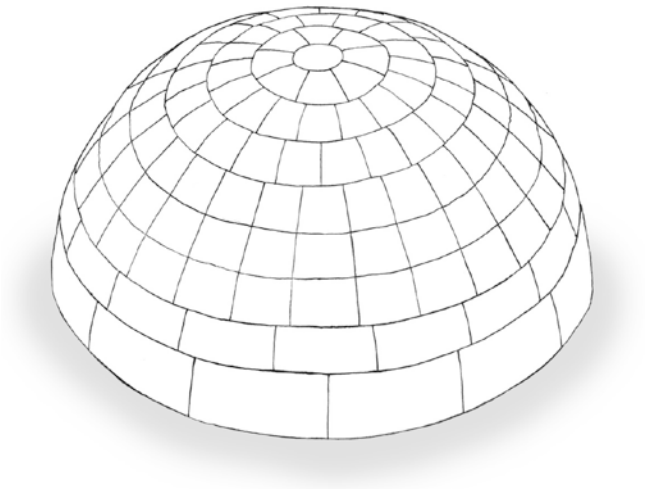

Fig. 6.22. Klems patches

One of these hemispheres is shown in the drawing, divided as described earlier. This division of the hemisphere follows such a logic that if luminance (lm/(m^2 x sr)) is constant in hemisphere, illuminance is similar on each patch.

The output file generated by genBSDF is a data list in ".xml" format. In order to improve data handling, a parser which converts these 21 025 BSDF values to a ".txt" format was created, ordering all data in a list of values, as follows:

Incident patch 1 scattering patch 1
Incident patch 2 scattering patch 1
…
…
…
Incident patch 145 scattering patch1

Incident patch 1 scattering patch 2
Incident patch 2 scattering patch 2
…
…
…
Incident patch 145 scattering patch 2
…
…
…

Incident patch 1 scattering patch 145
Incident patch 2 scattering patch 145
…
…
…
Incident patch 145 scattering patch145

This way, for each patch of incidence and scattering, one transmittance value is obtained. Each column of grouped data refers to an outgoing patch.

6.6.2.2 Meaning of BSDF viewer graphs

With BSDF viewer (loading a ".xml" file generated by genBSDF) we obtain one graph representing light behaviour for each incident light direction reaching the surface of the sample. Additionally, the percentage of transmitted or reflected light to incident light is obtained.

The percentages given by BSDFviewer (*Es/Ei*), and the data obtained from genBSDF (*Ls/Ei*) can be related this way:

$$E_s / E_i = L_s / E_i \cos\theta_s \cdot \Omega_s(sr) \cdot 100$$

That is, starting with a BSDF value (related to an incident patch and to an outgoing one) and multiplying it by the cosine and polar angle of the outgoing patch, the ratio between outgoing patch's and incident patch's illuminances is obtained.

6.6.2.3 Definition of each patch

The characteristic data related to each patch is:

- The cosine of the polar angle formed by the radius passing through the centre of the patch and the surface normal ($cos\theta$),

- The solid angle related to the patch (Ω).

Both values can be defined for each patch in Klems pattern. The hemisphere is divided by lines of latitude and meridians.

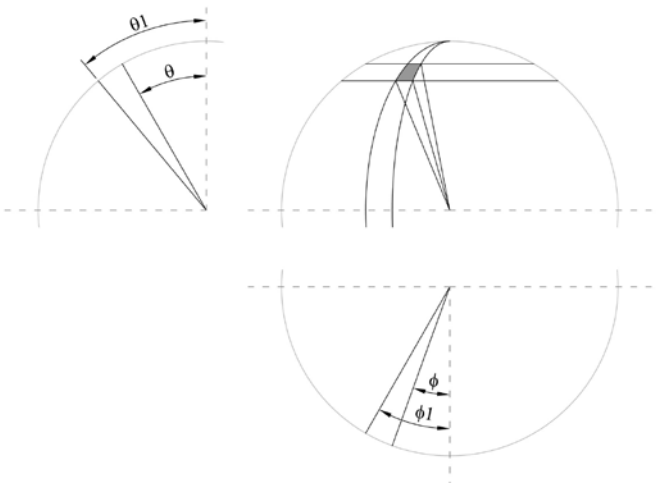

Fig. 6.23. Latitude-longitude rectangle definition

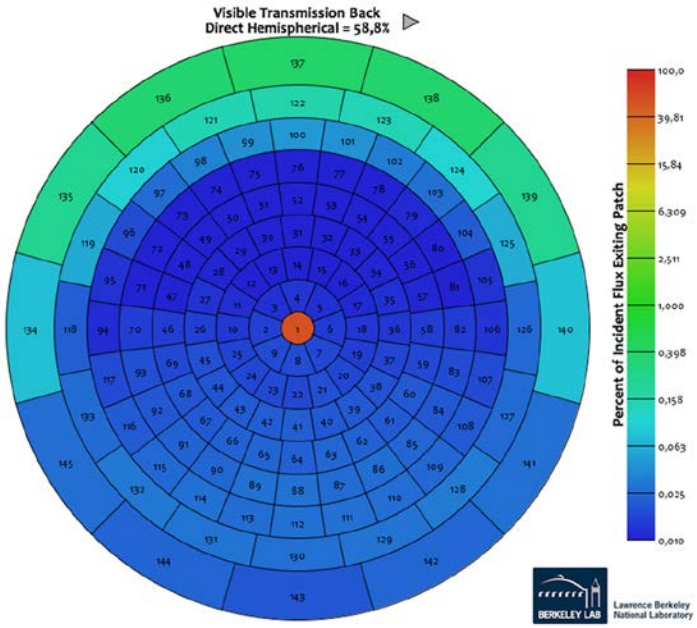

Fig. 6.24. Resulting graph example of BSDF viewer. (McNeil 2013)

The hemisphere is divided into 9 latitude ranges creating 8 rings of patches and a central circular patch. The angles (θ) between each latitude range and the surface normal are the following: 0^o-5^o, 5^o-15^o, 15^o-25^o, 25^o-35^o, 35^o-45^o, 45^o-55^o, 55^o-65^o, 65^o-75^o, 75^o-90^o. These latitude rings are also divided in equal longitude values different for each range, creating equal patches for each ring:

Latitude range	Latitude angles(θ)	Subdivisions	Longitude angle (ϕ) for each patch
1	0^o-5^o	1	360^o
2	5^o-15^o	8	45^o
3	15^o-25^o	16	22.5^o
4	25^o-35^o	20	18^o
5	35^o-45^o	24	15^o
6	45^o-55^o	24	15^o
7	55^o-65^o	24	15^o
8	65^o-75^o	16	22.5^o
9	75^o-90^o	12	30^o

Table 6.1. Klems patch's definition angles

As mentioned previously, this division of the hemisphere follows such a logic that if luminance (lm/m^2 x sr) is constant in hemisphere, illuminance is similar on each patch.

In order to obtain the $\cos\theta$ value of each patch, the medium angle of the related range can be used. This value is the same for all patches of a given range.

Regarding the solid angle, it can be calculated as follows:

- for the patch in the first range, the solid angle of a cone (or the area of a spherical cap) should be calculated as follows:

$$\Omega = 2\pi(1-\cos\theta)$$

where θ is half the apex angle of the cone.

- for all remaining ranges, the solid angle of a latitude-longitude rectangle should be obtained as follows (ϕ angle in radians). The value for each angle is shown in Table 6.1.

$$\Omega = (\phi_1 - \phi)(\cos\theta - \cos\theta_1)$$

The value of the solid angle is the same for all patches in a range. The following table shows the resulting data for each patch:

Latitude range	Patch number (Klems)	cosθ	Solid angle Ω (sr)	cosθ x Ω
1	1	1	0.02391	0.02391
2	2-9	0.9848	0.02377	0.02341
3	10-25	0.9397	0.02341	0.02200
4	26-45	0.866	0.02738	0.02371
5	46-69	0.766	0.02933	0.02247
6	70-93	0.6428	0.03496	0.02247
7	94-117	0.5	0.03952	0.01976
8	118-133	0.342	0.06432	0.02200
9	134-145	0.1305	0.13552	0.01768

Table 6.2. Klems patch's characterization data

6.6.3 Obtained results and data management

After obtaining BSDF values for each required sample, it is possible to manage all the information. All data is organized in an orderly way, showing information about the incident and outgoing patches for each value and always related to Klems pattern.

6.6.3.1 Values for specular transmission

A specific table was created to summarize the transmittances for each of the 145 available specular transmission trajectories of light.

Klems pattern is defined in such a way that two patches linked by a specular transmittance direction are named with the same number. If a light beam arrives from an incident patch named with a certain number in the incoming hemisphere and it goes through the surface with no changes in its direction (specular transmission), it will cross a patch named with same number in the outgoing hemisphere as shown in the following figure.

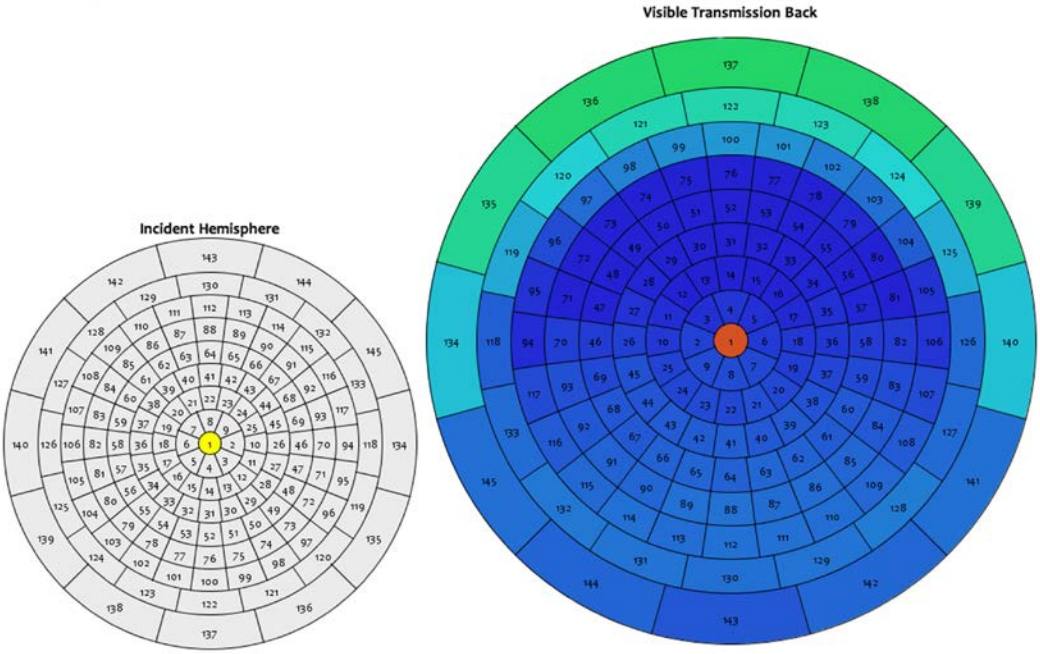

Fig. 6.25. Incident and outgoing hemispheres. BSDF viewer (McNeil 2013)

As explained later, this specular transmittance data are especially useful when comparing computer and laboratory results.

6.6.3.2 Data related to a certain incident patch

When studying the behavior of light transmitted through expanded metal, it is useful to know what happens when light arrives from a precise direction. We created a data table with that purpose. If a certain incident patch number is introduced, 145 values of E_s/E_i (%) are obtained, one for each outgoing patch.

In addition, some specific values for this particular incident patch are obtained:

a) Maximum transmittance value, and the outgoing patch receiving that transmittance. It is usually the value referred to the specular transmission.

b) Minimum transmittance value, and the outgoing patch receiving that transmittance.

c) Absolute arithmetic mean. Average of all transmittance values in outgoing hemisphere, related to the solid angle of each patch.

$$\frac{\sum_{a=1}^{145} Ta \, x \, \Omega a}{\Omega total}$$

Where,

T_a = *Es/Ei* (%) value of each patch

Ω_a = solid angle of each patch (sr)

Ω_{total} = solid angle of the outgoing hemisphere, 2π (sr)

d) Scattering arithmetic mean. It is the same value from the expression above, but subtracting the value of the specular transmission. It is useful to obtain an approximate value of the scattered portion of the light.

$$\frac{(\sum_{a=1}^{145} Ta \, x \, \Omega a) - Tspec \, x \, \Omega spec}{\Omega total - \Omega spec}$$

Where,

T_a = E_s/E_i (%) value of each patch

T_{spec} = *Es/Ei* (%) value of the specular transmission

Ω_a = solid angle of each patch (sr)

Ω_{spec} = solid angle of the patch in the specular direction (sr)

Ω_{total} = solid angle of the outgoing hemisphere, 2π (sr)

e) Sum. It is the sum of all the transmittance values for a certain incident direction, i.e. the total light transmittance for that incident direction.

6.6.3.3 Graphic representation of transmittance values

We have to remember that the results compiled in these assessments are always related to transmittance, omitting reflectance values.

At first glance, the spatial nature of the outgoing hemisphere makes the graphic representation and the correct interpretation of the light behavior a difficult task.

As mentioned before, *BSDFviewer* shows, for a certain incident patch, a representation of the transmittance in the outgoing hemisphere. The color of each outgoing patch is related to its transmittance value. Additionally, the percentage of transmitted to incident light is obtained. See figure 6.24.

Another valid graphic representation is to create a three-dimensional surface related to transmittance values, a "transmittance bulb". A vector for each direction of outgoing light beam (from the center of the hemisphere to the center of each patch) is defined. The magnitude of the vector is referred to the transmittance on that direction.

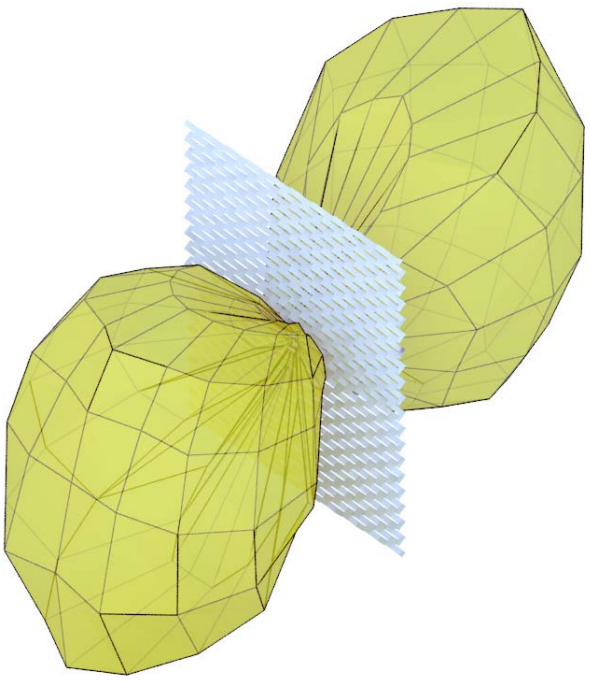

Fig. 6.26. “Transmittance bulb” for specular transmission

As an example, we modeled these vectors and the mentioned "transmittance bulb" with Rhino and Grasshopper, using the results obtained by genBSDF and obtaining images like the previous one.

The figure above summarizes obtained specular transmittance values for a certain mesh. Different types of “bulbs” can be created, representing, for example, all transmittance values for a certain incident direction.

In some ways, it is similar to the photometric curves shown by lamp manufacturers but in three-dimensional format. However, this kind of representation is very useful and complete when analyzing light behavior in a particular sample, but it can be confusing when comparing different sheets or results. 2D graphics or charts are much more useful and intuitive for this purpose.

Anyway, with both previous representation types we obtain just a small part of the information included in the whole BSDF.

In order to facilitate the analysis of these concepts we decided to work with charts/diagrams and our study was limited to two perpendicular planes. These planes are both perpendicular to the plane of the sample mesh, one vertical and the other horizontal.

The symmetry plane of the mesh (see figure 6.1) is considered the "vertical plane". The "horizontal plane" is perpendicular to the vertical one. The vertical section of the hemisphere crosses the central patch (number one) and all others that are located on the "vertical plane". The horizontal section crosses the central patch and all patches located on the "horizontal plane".

In both sections, each patch is identified with its polar angle. That is, the polar angle in the scatter direction measured from surface normal.

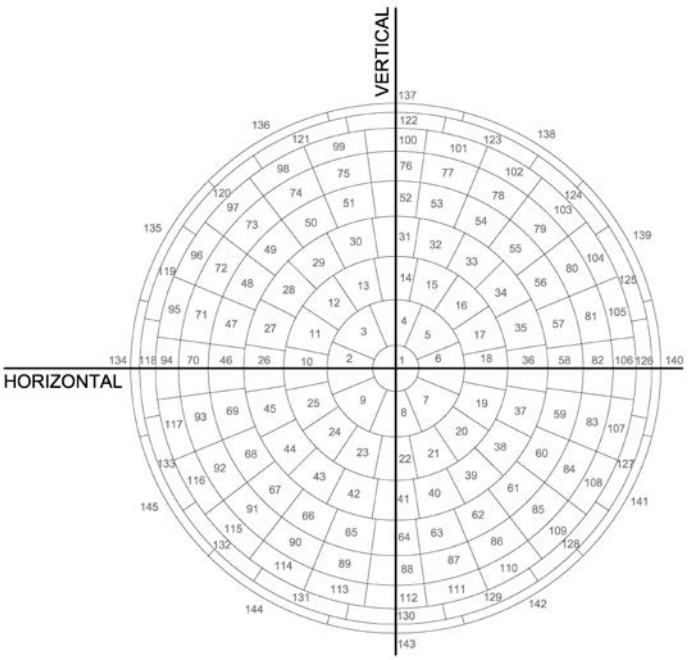

Fig. 6.27. Vertical and horizontal section of the outgoing hemisphere

Two types of charts are created from each section:

a) Line chart. In this chart type, E_s/E_i (%) percentage values of each patch in a section are shown in vertical axis. The values on the horizontal axis are referred to the polar angle of each patch (figure 6.28).

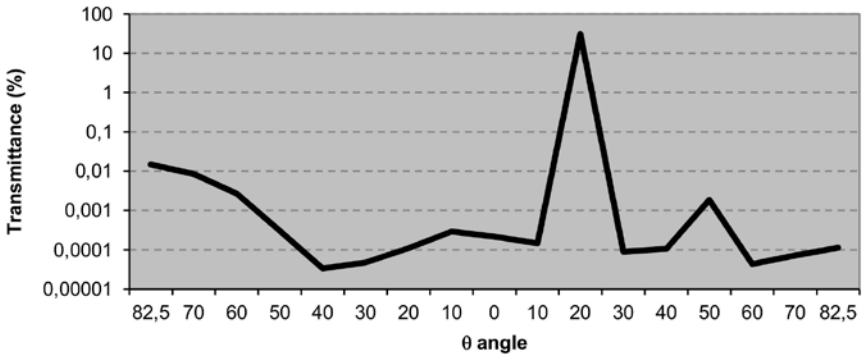

Fig. 6.28. Line chart

b) Polar chart. This chart type represents the same data that the previous one, but the percentage values are represented in the radius, starting from a central point (figure 6.29). The position of each value in the chart is related with the polar angle of each patch. A better

representation (more intuitive) of light behavior is achieved. It can be interpreted as something similar to a 2D section of the "transmittance bulb" mentioned before.

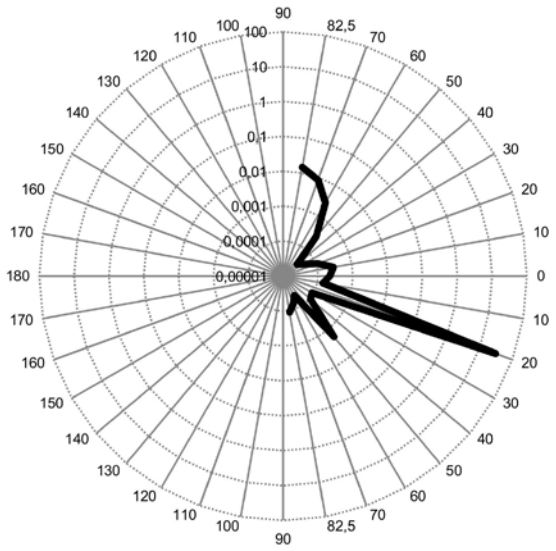

Fig. 6.29. Polar chart

In both charts, logarithmic scale (base 10) is used. The use of the logarithms of the transmittance values rather than the actual transmittance values reduces a wide range to a more manageable size. Moreover, human senses and perception are supposed to work in a logarithmic way (hearing, sight, etc).

6.6.3.4 Example datasheet with obtained results

A “hemispherical transmittance datasheet” was designed and can be generated for each modeled mesh and incident patch. The datasheet summarizes all the information mentioned above and identifies the incident patch on the incoming hemisphere.

One possible application of that datasheet could consist on creating a set of technical datasheets for a particular EM mesh, describing its hemispherical transmittance for specific incident directions.

We generated 3D models of all the meshes assessed in laboratory in order to run a comparative analysis of lab and computer aid assessment methods (see section 6.8). These 3D

models have also been used to create one hemispherical transmittance datasheet for each of them. As one chart represents data for only one incident light direction, we chose one specific incident direction for all these datasheets (corresponding to incident patch number 41 in Klems basis). These datasheets can be found in Appendix B.2.

In the following two illustrations we show two applications of the described hemispherical transmittance datasheets, corresponding to mesh number 09w for incident patch number 88 and mesh number 10g for incident patch number 76. (for information about the meshes see section 5.3)

MESH SAMPLE NUMBER

09w

PARAMETERS

LW	SW	w	e	b	i	color
110	40	15	2	2	33	

TRANSMITTANCE

INCIDENT PATCH	88

	Es/Ei (%)	OUTG. PATCH
MÁX	7,135	88
MÍN	0,013	130
ABS. MEAN	0,104	
SCATT. MEAN	0,064	
SUM (%)	12,554	

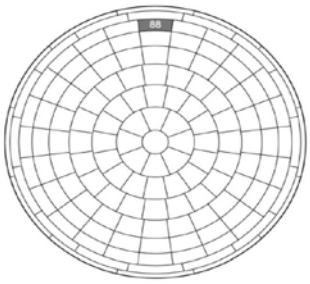

incoming hemisphere

VERTICAL SECTION

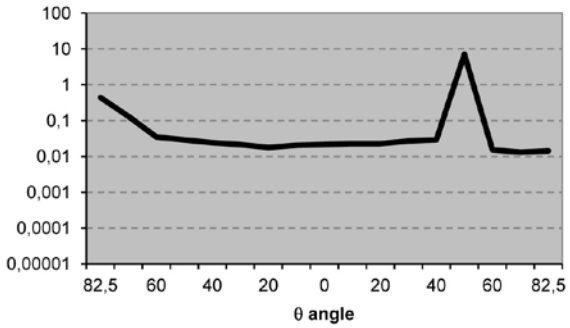

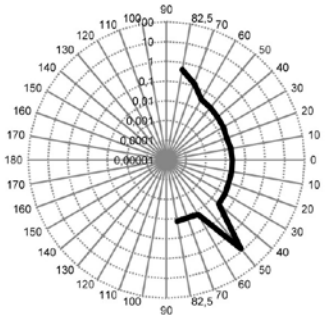

HORIZONTAL SECTION

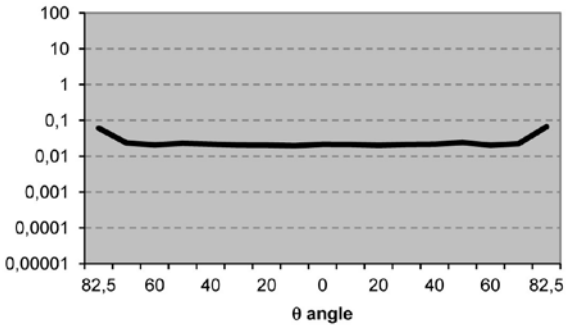

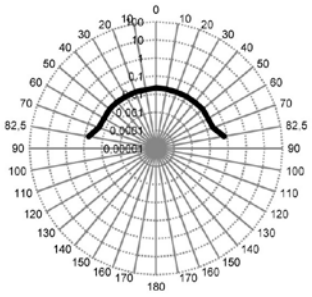

MESH SAMPLE NUMBER

10g

PARAMETERS

LW	SW	w	e	b	i	color
6	4	1,2	1	1	2,5	

TRANSMITTANCE

INCIDENT PATCH	76

	Es/Ei (%)	OUTG. PATCH
MÁX	33,664	76
MÍN	0,001	7
ABS. MEAN	0,215	
SCATT. MEAN	0,028	
SUM (%)	36,235	

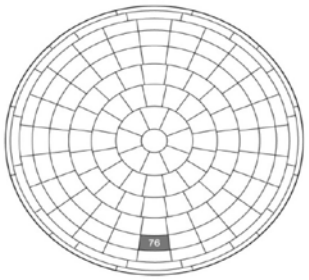

incoming hemisphere

VERTICAL SECTION

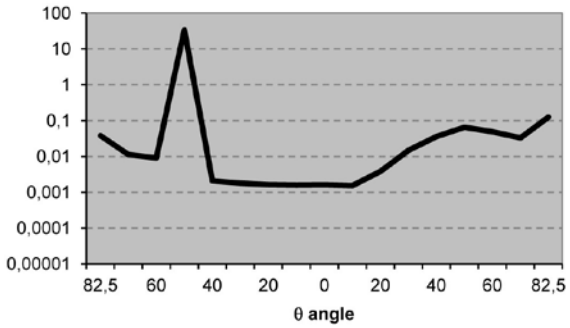

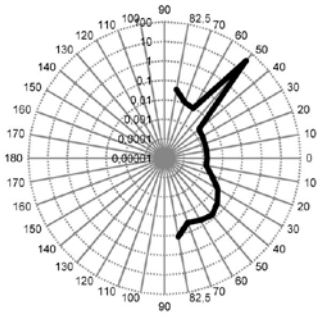

HORIZONTAL SECTION

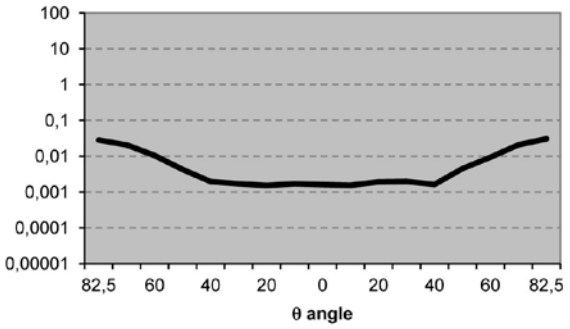

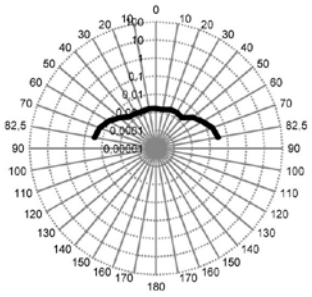

From the analysis of the hemispherical transmittance datasheets of the assessed EM meshes we can point out some observations:

1. As expected, the highest transmittance value occurs with specular transmission. This corresponds to the "peak" in the charts. The rest of values, surrounding this “peak”, refer to scattered transmission. The main source of scattered transmission is expected to be the reflection of light in the mesh’s strands. Among these values, we can observe the most significant reflection directions where transmittance values are higher. Anyway the specular transmission takes more than 90% of the whole transmission.

2. An increased value of the transmittance in the most oblique scattering angles (approximately from 60^{o} to 90^{o}) is observed. The charts shown above are related to a certain direction of incidence, so scattered transmission is what is increasing in these oblique directions. These changes in transmittance values could be due to the reflections in the mesh’s strands and/or diffractions on the edges of the meshes. But the program Radiance does not consider wave optic phenomenon including diffraction (McNeil, Jonsson, and Appelfeld 2011), so the second supposition should be discarded. Another possible reason could be some kind of “edge effect” in the operation of genBSDF when dealing with the edges of the mesh. Analyzed 3D models consist of a 3x3 tessellation of the basic bow. The boundary of these samples could create some disturbance on the results. Even so, remember that a logarithmic scale is used, and these variations are very small. Anyway they represent a behavior that could be further studied.

6.7 Comparative analysis of modeled meshes

One of the greatest advantages of computer modeling is that, both the performance and the luminous behavior of certain meshes can be compared before they are manufactured or installed in a facade.

Moreover, thanks to parametric modeling, it is very easy to create as many samples as needed. After obtaining BSDF values for each mesh, their transmittance can be compared.

As the possible comparisons are endless, the following features have been chosen as comparison criteria: mesh surface finish and strand width. These analyses serve, in a way, to validate the results of the process. Further tasks could be to compare samples with different shapes (rhomboidal, hexagonal, square), different orientations, other geometric variations, etc.

6.7.1 Mesh surface finish

We cannot forget that when studying light transmittance of EM, besides the geometry of a mesh, there are some other important and necessary aspects to take into account for its optical characterization related to its finish, i.e. its texture, color, etc. When a simulation model is constructed, suitable material should be applied to it, in accordance with those optical properties.

With the aim of simulating the real finishes in the laboratory samples (white, gray and black meshes), the data obtained in the test with spectrophotometer were used. As mentioned in section 5.5, the spectrophotometer was also used to assess some flat lacquered metal sheets in order to quantify the reflectance of each different finish of the tested EM meshes and simulate them with computer aided assessment.

These optical properties (see table 5.8) are used when generating any of the BSDF data obtained in our assessment, in order to compare modeled and real meshes.

The following example charts show the results when simulating the same mesh with different finishes. Different models are compared, using different incident directions:

MESH SAMPLE NUMBERS

01b/01g/01w

INCIDENT PATCH

01

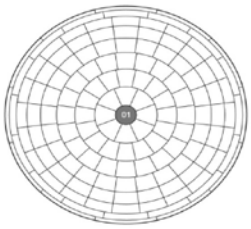

PARAMETERS

LW	SW	w	e	b	i
200	73	24	1	7	33

TRANSMITTANCE

VERTICAL SECTION

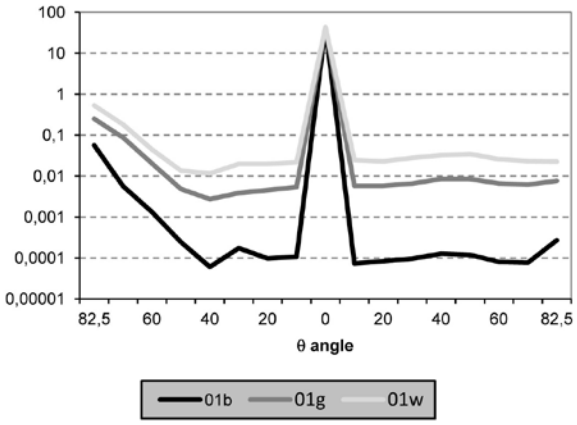

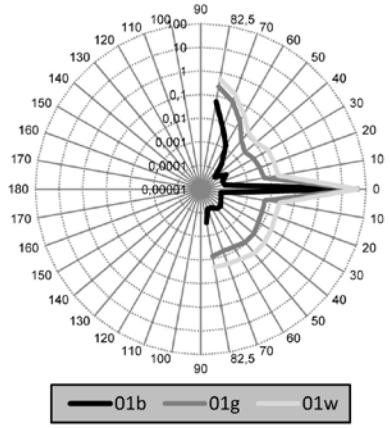

HORIZONTAL SECTION

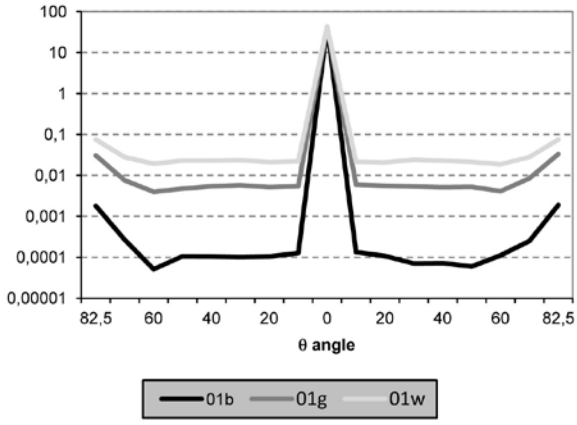

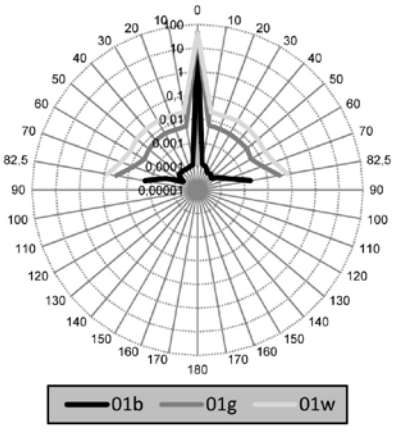

MESH SAMPLE NUMBERS

01b/01g/01w

INCIDENT PATCH

76

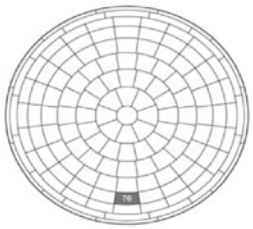

PARAMETERS

LW	SW	w	e	b	i
200	73	24	1	7	33

TRANSMITTANCE

VERTICAL SECTION

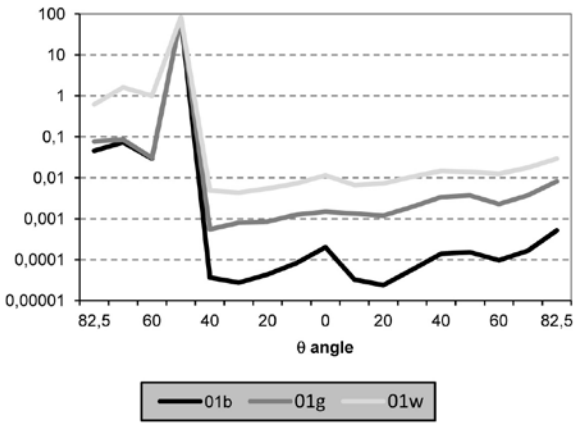

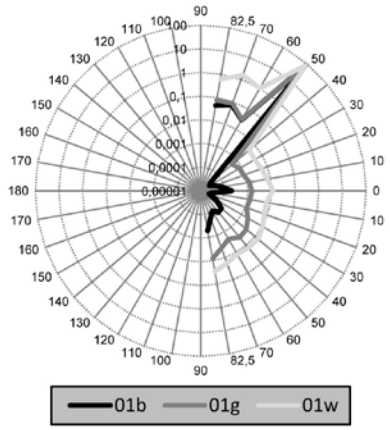

HORIZONTAL SECTION

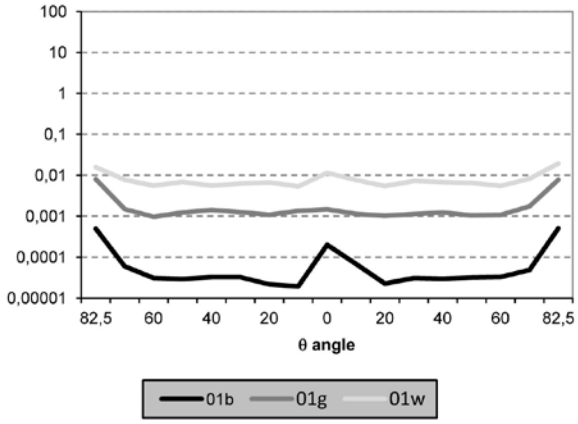

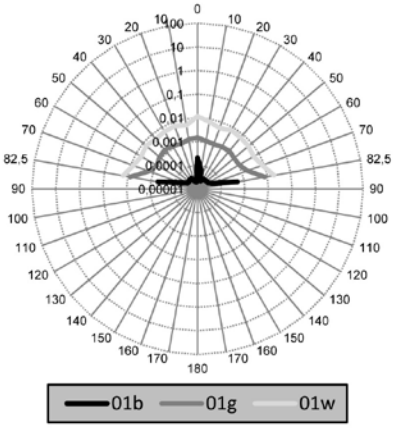

MESH SAMPLE NUMBERS

08b/08g/08w

INCIDENT PATCH

41

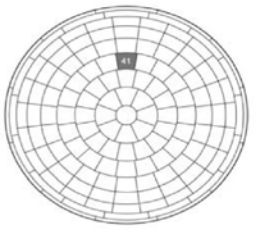

PARAMETERS

LW	SW	w	e	b	i
110	50	24	2	3,5	50

TRANSMITTANCE

VERTICAL SECTION

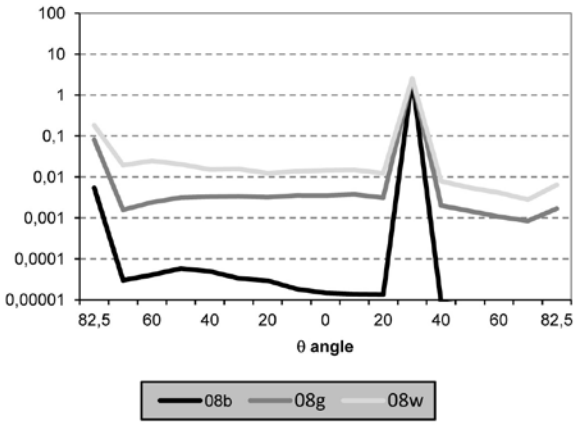

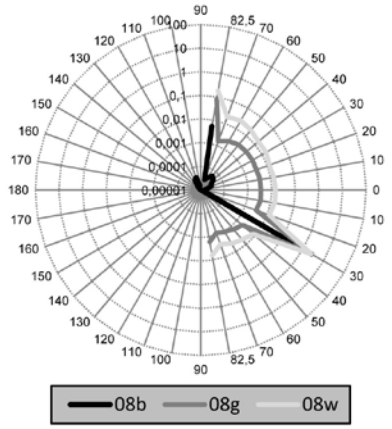

HORIZONTAL SECTION

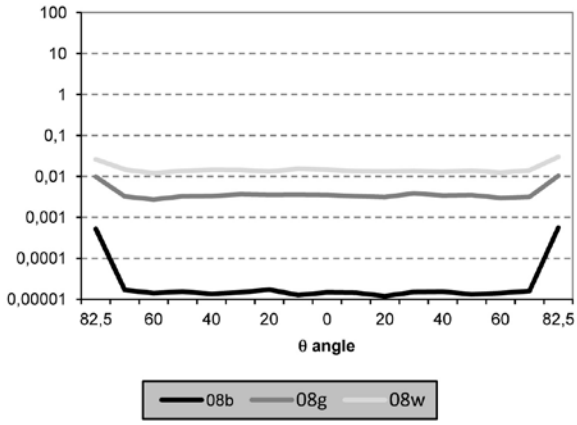

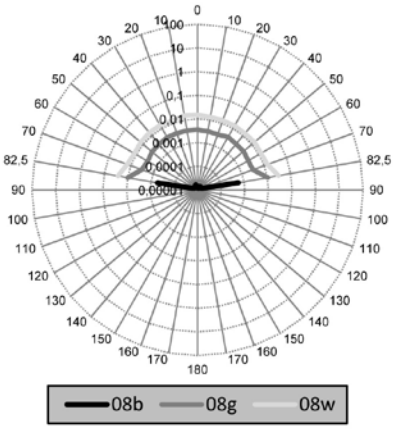

MESH SAMPLE NUMBERS

08b/08g/08w

INCIDENT PATCH

94

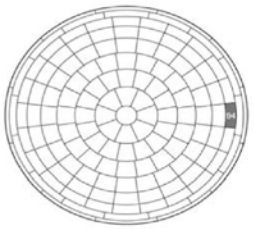

PARAMETERS

LW	SW	w	e	b	i
110	50	24	2	3,5	50

TRANSMITTANCE

VERTICAL SECTION

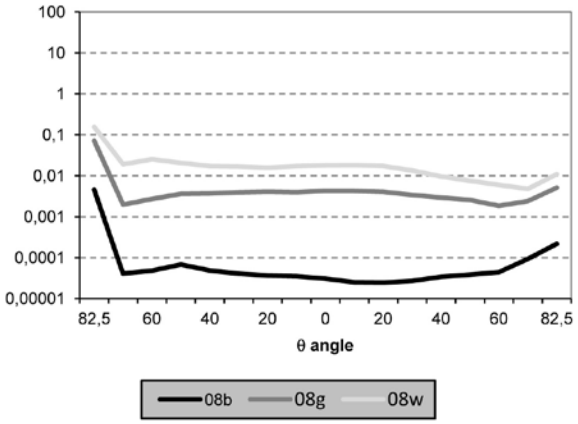

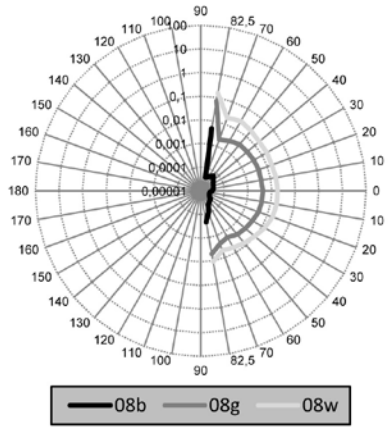

HORIZONTAL SECTION

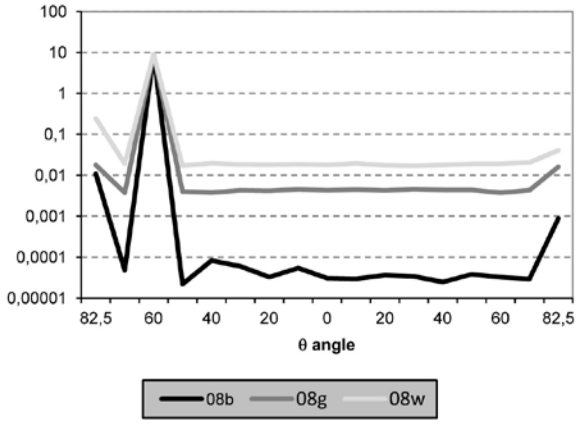

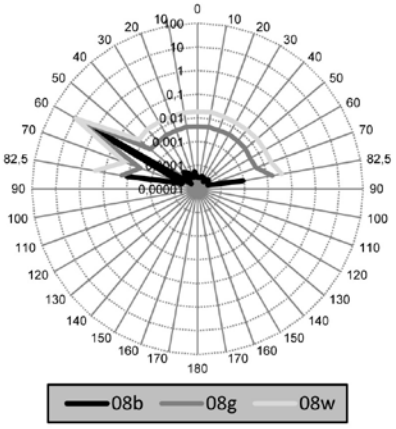

As expected, the same behavior can be observed in all these cases: the transmittance in the specular direction is nearly the same for the three finishes (white, gray and black). The results are consistent with those obtained from lab-assessment (section 5.4.1.2). This is logical, because most of the light passes directly through the openings of the mesh without any contact with the lacquered strands of the meshes.

However, the data obtained for other output directions describe the scattered light, that is, transmitted light resulting from reflections in the mesh. Here we can observe logical decreasing values from white to black and, again, all these values far from the specular direction show very low transmittance values, lower than 1%.

6.7.2 Influence of strand width

Any variation in the geometric parameters of an EM mesh implies changes in the ratio between opaque and translucent parts and therefore influences the light transmission through it.

The variation of the strand width (*w*) is one of the most visual and intuitive. This variation produces a change in the opacity of the sample. As explained in sections 2.3.2 and 4.1 the following three EM parameters: *SW*, *d* and *w*, form a right triangle. In consequence, keeping the dimension of the Short Way (*SW*) constant, any variation in strand width (*w*) results in a change in the manufacture's blade descent (*d*):

$$\left(\frac{SW}{2}\right)^2 = d^2 + w^2$$

In addition, the slope of the blade (α) also varies if the strand width is changed and all other parameters are fixed.

In this specific case, the limits for *w* would be:

a) *w*>*e*. This is an approximate limit due to fabrication conditions.

b) *w*<*SW*/2. Elsewhere, the blade doesn't descend; therefore the expansion of the mesh doesn't occur.

Starting with the model of an existing laboratory sample (mesh 01w, white finish), the following 5 new models were created, with different strand widths.

MESH	LW	SW	w	E	b	i	d	α
01	200	73	24	1	7	33	27,500	18,97º
01a	200	73	6	1	7	33	36,003	24,23º
01b	200	73	12	1	7	33	34,471	23,31º
01c	200	73	18	1	7	33	31,753	21,65º
01d	200	73	30	1	7	33	20,791	14,57º
01e	200	73	35	1	7	33	10,356	7,38º

Table 6.4. Strand width variation – parameters of the meshes

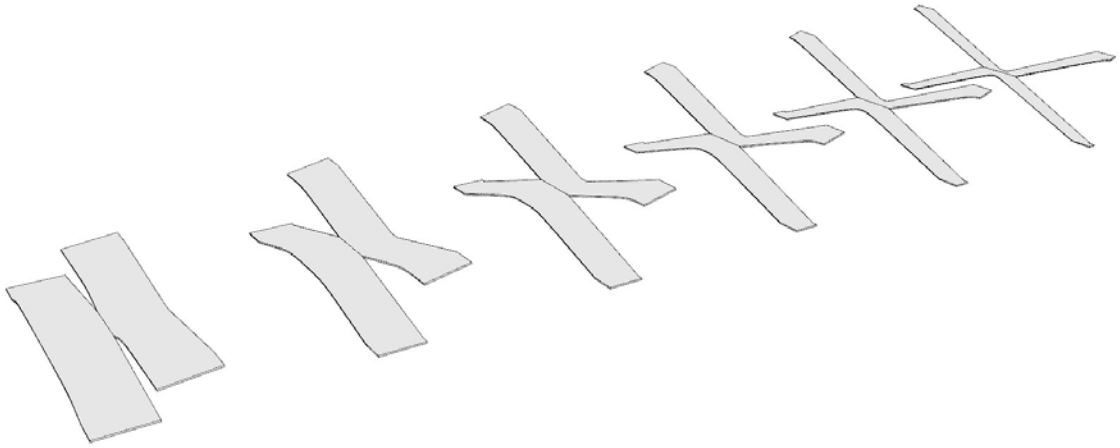

Fig. 6.30. Strand width variation – created models

The analysis of the BSDFs of each model and the comparison between them allows analyzing the effect of the variation in the strand width. This should help the designer and manufacturer to foresee what kind of mesh is needed for a specific use. Showing and analyzing all the incoming light directions is a vast task and it is more illustrative to choose some selected ones. The incident direction patches (on incoming hemisphere) used to obtain the data are shown in the following figure:

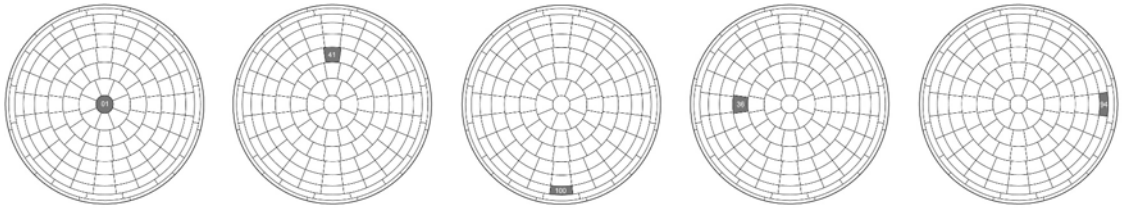

Fig. 6.31. Incident patches 01, 41, 100, 36 and 94 for strand with variation comparison

The comparison is summarized on the following datasheets. Total and specular transmittance of each mesh sample is also shown.

MESH SAMPLE NUMBERS

01w strand width variation

INCIDENT PATCH

01

PARAMETERS

	LW	SW	w	e	b	i	TOTAL TRANSM. (%)	SPEC. TRANSM. (%)
01a	200	73	6	1	7	33	83,05	81,23
01b	200	73	12	1	7	33	76,59	72,21
01	200	73	18	1	7	33	67,30	61,37
01c	200	73	24	1	7	33	53,28	46,57
01d	200	73	30	1	7	33	32,78	25,59
01e	200	73	35	1	7	33	12,52	7,44

TRANSMITTANCE

VERTICAL SECTION

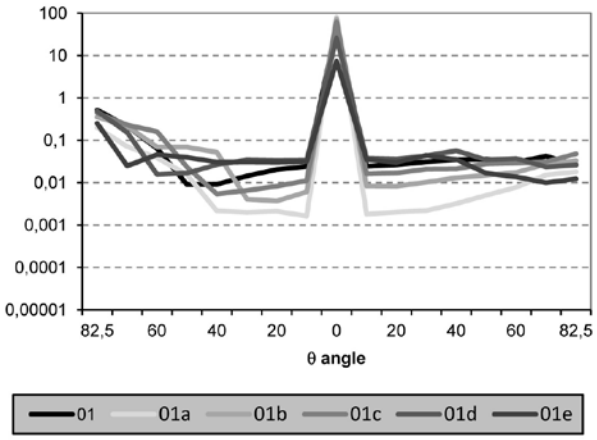

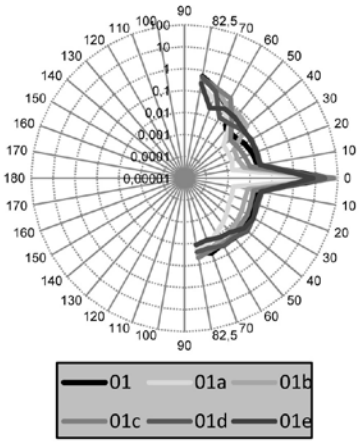

HORIZONTAL SECTION

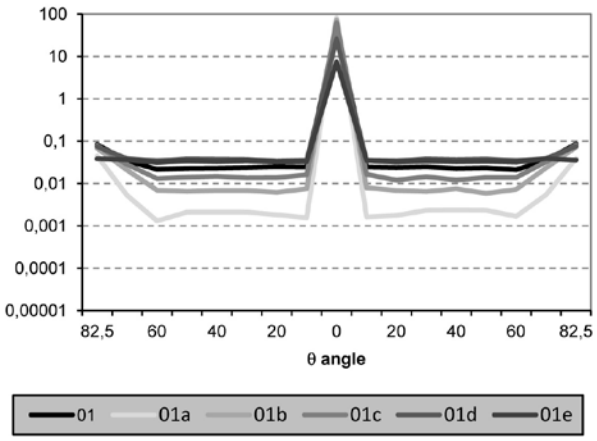

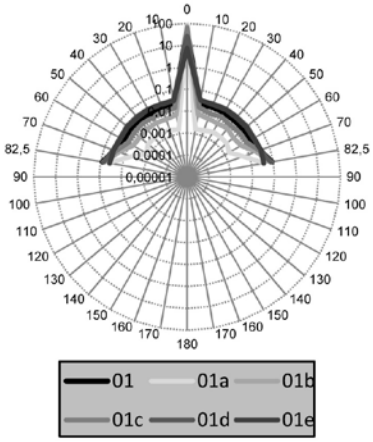

MESH SAMPLE NUMBERS

01w strand width variation

INCIDENT PATCH

41

PARAMETERS

	LW	SW	w	e	b	i	TOTAL TRANSM. (%)	SPEC. TRANSM. (%)
01a	200	73	6	1	7	33	76,20	73,45
01b	200	73	12	1	7	33	66,20	60,46
01c	200	73	18	1	7	33	52,16	44,12
01	200	73	24	1	7	33	34,58	25,34
01d	200	73	30	1	7	33	16,18	7,47
01e	200	73	35	1	7	33	5,54	1,34

TRANSMITTANCE

VERTICAL SECTION

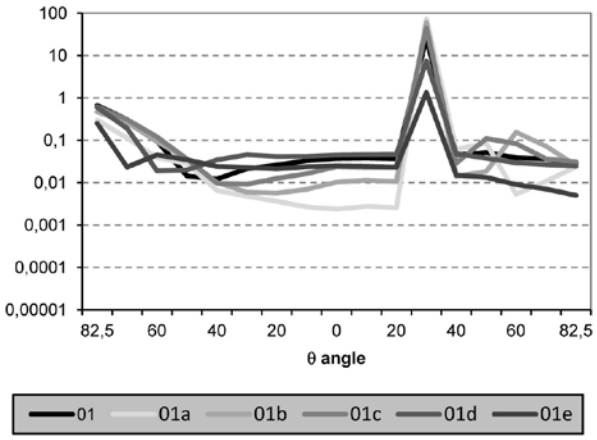

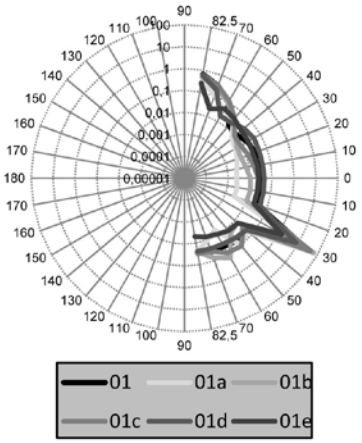

HORIZONTAL SECTION

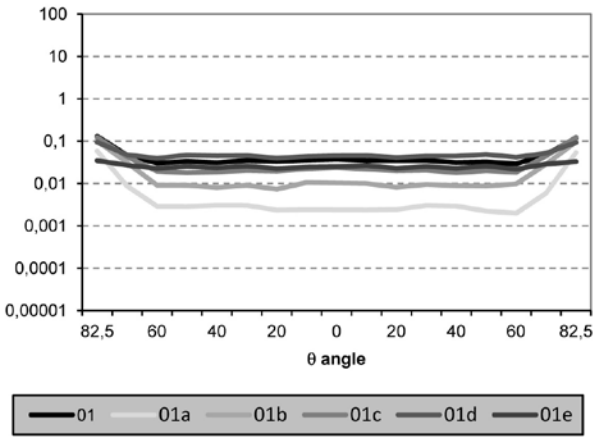

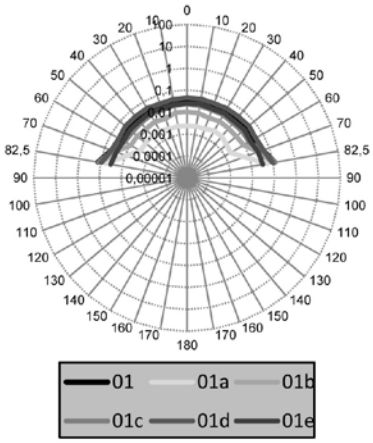

MESH SAMPLE NUMBERS

01w strand width variation

INCIDENT PATCH

100

PARAMETERS

	LW	SW	w	e	b	i	TOTAL TRANSM. (%)	SPEC. TRANSM. (%)
01a	200	73	6	1	7	33	94,36	89,75
01b	200	73	12	1	7	33	91,72	80,27
01c	200	73	18	1	7	33	92,17	78,34
01	200	73	24	1	7	33	94,12	83,30
01d	200	73	30	1	7	33	94,17	89,99
01e	200	73	35	1	7	33	58,90	50,01

TRANSMITTANCE

VERTICAL SECTION

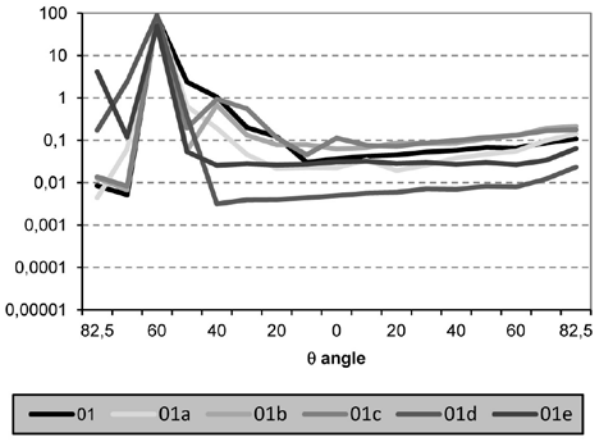

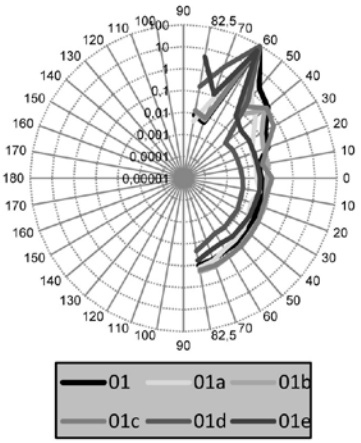

HORIZONTAL SECTION

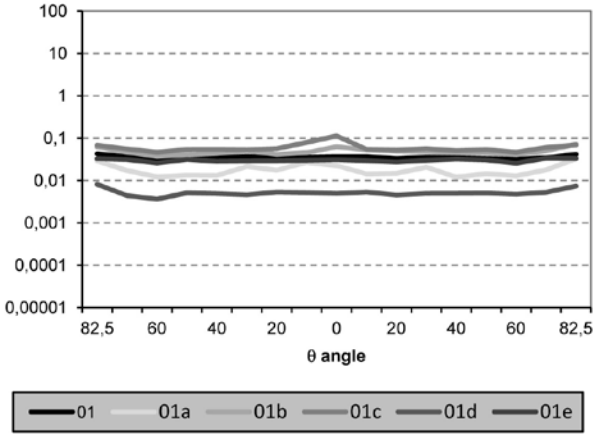

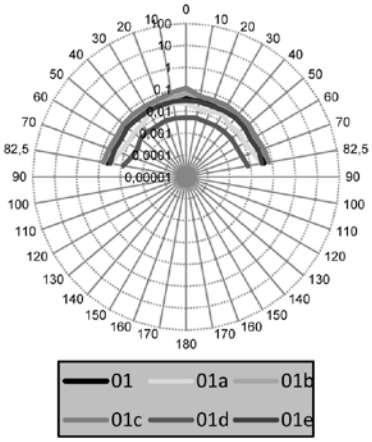

MESH SAMPLE NUMBERS

01w strand width variation

INCIDENT PATCH

36

PARAMETERS

	LW	SW	w	e	b	i	TOTAL TRANSM. (%)	SPEC. TRANSM. (%)
01a	200	73	6	1	7	33	82,08	79,86
01b	200	73	12	1	7	33	76,97	72,44
01c	200	73	18	1	7	33	66,91	60,56
01	200	73	24	1	7	33	52,12	44,73
01d	200	73	30	1	7	33	33,79	26,86
01e	200	73	35	1	7	33	12,63	7,75

TRANSMITTANCE

VERTICAL SECTION

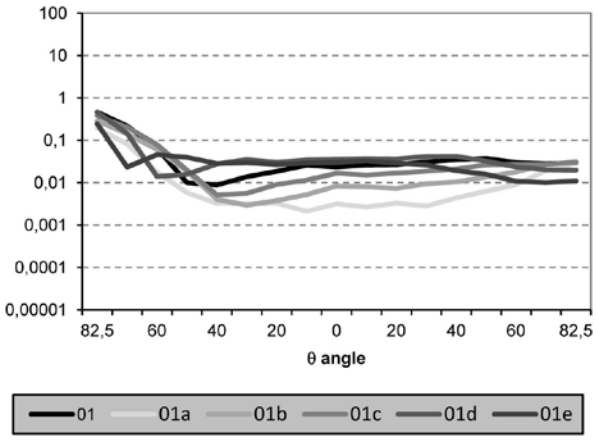

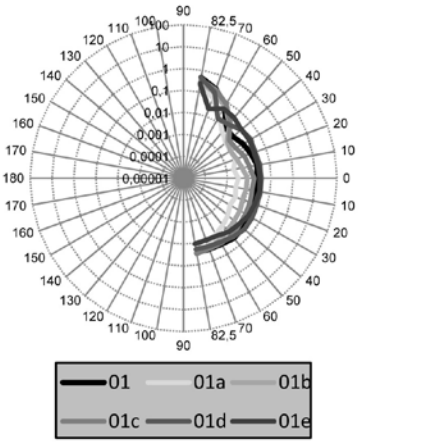

HORIZONTAL SECTION

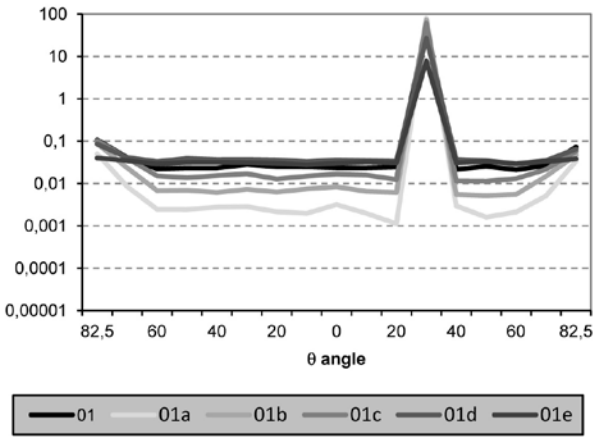

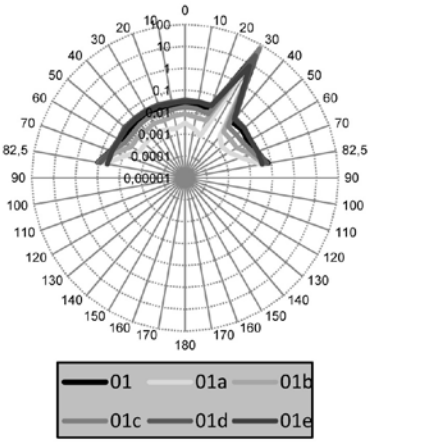

MESH SAMPLE NUMBERS

01w strand width variation

INCIDENT PATCH

94

PARAMETERS

	LW	SW	w	e	b	i	TOTAL TRANSM. (%)	SPEC. TRANSM. (%)
01a	200	73	6	1	7	33	85,80	83,11
01b	200	73	12	1	7	33	78,12	73,14
01c	200	73	18	1	7	33	70,22	63,74
01	200	73	24	1	7	33	57,75	49,39
01d	200	73	30	1	7	33	39,27	30,52
01e	200	73	35	1	7	33	14,17	9,37

TRANSMITTANCE

VERTICAL SECTION

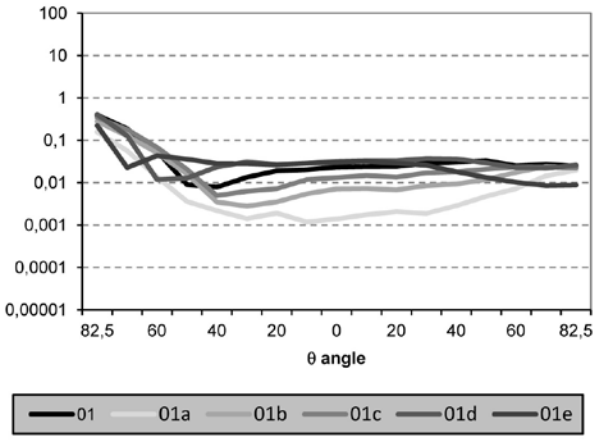

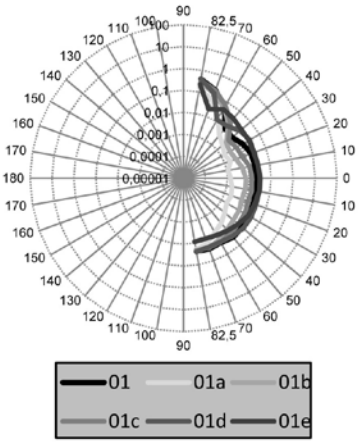

HORIZONTAL SECTION

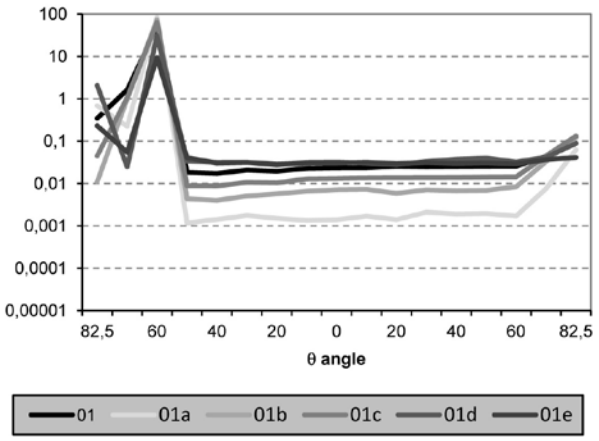

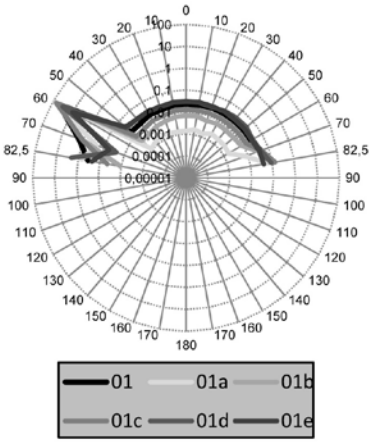

From previous comparative sheets, the following can be deduced:

Obviously, when strand width (*w*) increases, the opacity of the sample is increased and, in turn transmittance decreases. In addition, the ratio of specular to total transmittance decreases, that is, an increase of the proportion of scattered light is observed. The charts do not allow to accurately discerning the decrease in specular component due to the use of a logarithmical scale, that is why they are shown in the upper right panel. As expected we observe very drastic variations of specular transmission among the meshes (the difference between maximum and minimum specular transmission is 74% in the highest case and 39% in the lowest. Total transmission values show similar differences, which is logical as in general, specular transmission is much higher than scattered transmission.

Let us focus on the scattered component of transmitted light. For light arriving from the upper part of the incoming hemisphere (patch 41) or from the horizon (patch 1, 36 and 94) we find very different curves in the vertical section for the scattered part of transmission. The maximum values in the scattered range are registered in different directions for each mesh. This is probably due to the variations in the slope of the strands resulting from changing the ternion *SW-w-d*. Obviously these differences are related to the reflection of light in the strands. The strand's slope variations result in more noteworthy scattered light differences in the vertical section. In the horizontal section curves are more homogeneous because the vertical symmetrical nature of EM blurs to a certain extent the scattering in the horizontal section.

If light comes from below (patch 100), results seem to be more confusing. Specular transmission direction changes for some of the meshes. Choosing an incoming light direction that fits the slope of the strands of one of the meshes results in a much greater value of the specular transmittance compared with the rest of meshes.

6.8 Comparative analysis with lab. Results

6.8.1 Bases for comparison. Relationship between data

The computer simulation enables us to compare light behavior in a certain modeled mesh, with the tests done in laboratory for the same sample. As seen in Chapter 5, all laboratory measurements are referring only to specular transmission. We obtained valid results for 128 incoming light beams, related to different rotation angles of the sample-holder on the predefined *x* and *y* axis. Now, computer simulation results are related to Klems pattern defining patches. Each patch could be related to its solid angle's central vector direction but these directions are not coincident with the laboratory directions.

Laboratory measuring angles (red) and distribution of patches in Klems pattern (blue) are shown in the following diagram:

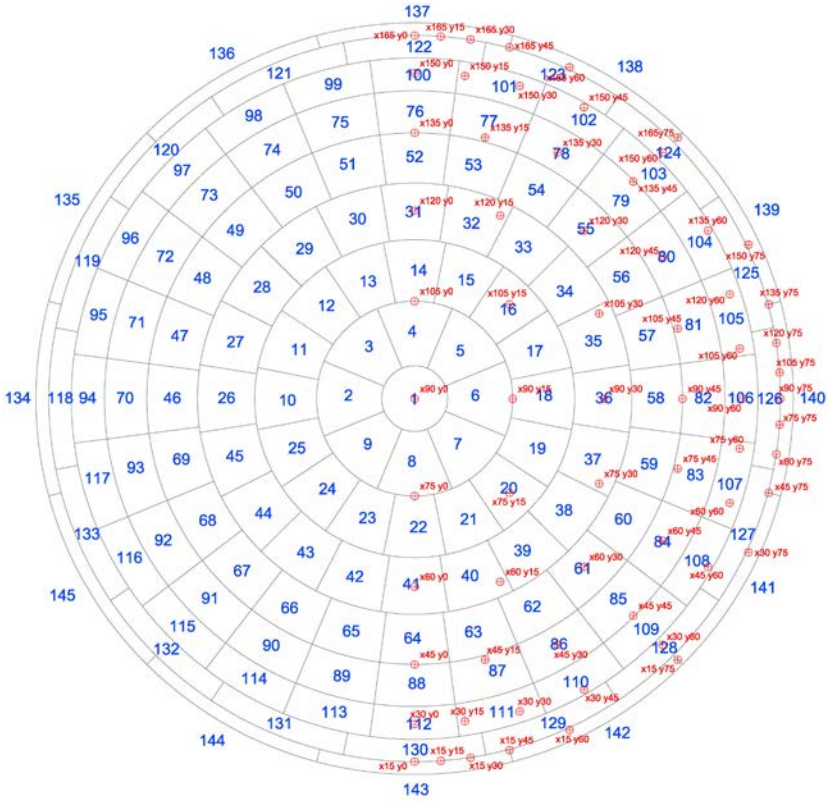

Fig. 6.32. Laboratory measurement points and Klems basis. Outgoing hemisphere

The following table summarizes the relation between laboratory test angles and Klems pattern. Here we follow the data table structure created for the laboratory results, where each box corresponds to a certain direction of incoming light expressed as a rotation of the sample-holder around the horizontal (*x*) and vertical (*y*) rotation axes, see figure 5.9. In this table, instead of listing transmittance values, we have listed the Klems patches that are crossed by the corresponding laboratory direction. The points that are close to or on the limit between two or more patches are associated with these two or more patches. In those cases, the average mean of the transmittance for those patches is calculated for the comparison.

RELATION BETWEEN LABORATORY MEASUREMENT POINTS AND KLEMS BASIS													
y \ x	0º	15º	30º	45º	60º	75º	90º	105º	120º	135º	150º	165º	180º
0º		130-143	**112**	64-88	**41**	8-22	**1**	4-14	**31**	52-76	**100**	122-137	
15º		130-143	111	87	40	**20**	6-18	**16**	32	77	101	122-137	
30º		130-143	111	**86**	**61**	37	**36**	35	**55**	**78**	101	122-137	
45º		129-142-143	110	85-109	**84**	83	58-82	81	**80**	79-103	102	123-137-138	
60º		142	128	108	107	107	**106**	105	105	104	124	138	
75º			141	127-140-141	126-140	126-140	126-140	126-140	126-140	125-139-140	139		
90º													

Table 6.5. Relationship between laboratory measurement angles and Klems basis

When any laboratory measurement direction matches with the center of a certain patch, the number of this patch is shown in boldface. These values are supposed to offer a more accurate comparison.

6.8.2 Comparative tables

Starting from specular transmission data of the modeled meshes, a table that summarizes all values (following Table 6.5 above) was created for each sample, in order to facilitate the comparison with laboratory results. That is, the table shows the results obtained in the simulation for each laboratory tested angle.

Another table shows the absolute deviation between the transmittance values obtained in both methods. Below this table certain key values are summarized; maximum and

minimum values, average value, and average value based on data from matching incoming directions in both methods (those assumed to be more accurate).

Gray colored shading is applied to identify deviation values that are above average value.

A sample of three of the data sheets generated for this comparative assessment is shown below. The complete set of data sheets can be found in Appendix B.3.

MESH SAMPLE NUMBER

06w

PARAMETERS

LW	SW	w	e	b	i	color
60	21	10	1,5	2	33	

SPECULAR TRANSMITTANCE (%)

COMPUTER AID ASSESMENT RESULT

y \ x	0º	15º	30º	45º	60º	75º	90º	105º	120º	135º	150º	165º	180º
0º		10,30	**3,29**	2,49	**1,90**	2,05	**3,39**	5,44	**6,29**	9,68	**15,15**	27,99	
15º		10,30	2,99	2,79	1,80	**2,00**	3,73	**4,79**	6,88	9,88	13,69	27,99	
30º		10,30	2,99	**1,50**	**2,10**	2,50	**3,18**	5,59	**6,59**	**10,67**	13,69	27,99	
45º		11,60	2,69	2,89	**3,39**	2,50	4,96	5,50	**6,19**	10,18	14,77	28,62	
60º		13,72	4,49	3,39	3,29	3,29	**4,19**	6,33	6,33	9,79	17,43	31,79	
75º			13,57	10,74	10,16	10,16	10,16	10,16	10,16	17,29	25,13		
90º													

LABORATORY ASSESMENT RESULT

y \ x	0º	15º	30º	45º	60º	75º	90º	105º	120º	135º	150º	165º	180º
0º		0,49	0,22	0,10	0,20	2,17	4,56	5,95	7,05	8,65	11,85	15,03	
15º		0,71	0,17	0,10	0,20	2,11	4,50	5,79	6,91	8,44	12,29	13,37	
30º		1,08	0,12	0,10	0,19	2,06	4,47	5,67	6,92	8,74	12,39	12,78	
45º		0,79	0,09	0,11	0,22	2,15	4,61	5,99	7,18	9,26	12,62	10,70	
60º		0,68	0,17	0,12	0,27	2,25	5,51	6,12	7,51	9,00	10,29	6,08	
75º			1,01	0,39	0,48	2,05	4,99	5,69	6,26	6,14	4,70		
90º													

ABSOLUTE DEVIATION BETWEEN BOTH METHODS

y \ x	0º	15º	30º	45º	60º	75º	90º	105º	120º	135º	150º	165º	180º
0º		9,81	**3,07**	2,39	**1,70**	0,13	**1,18**	0,52	**0,77**	1,03	**3,31**	12,96	
15º		9,59	2,82	2,69	1,60	**0,11**	0,77	**1,00**	0,03	1,43	1,40	14,62	
30º		9,22	2,87	**1,39**	**1,90**	0,44	**1,29**	0,08	**0,34**	**1,94**	1,30	15,21	
45º		10,81	2,61	2,78	**3,17**	0,35	0,36	0,49	**0,99**	0,92	2,15	17,93	
60º		13,03	4,32	3,28	3,02	1,04	**1,31**	0,21	1,18	0,79	7,15	25,71	
75º			12,55	10,34	9,68	8,11	5,17	4,47	3,90	11,16	20,43		
90º													

MAXIMUM DEVIATION (%)	25,71
MINIMUM DEVIATION (%)	0,03
AVERAGE DEVIATION (%)	4,66
AV. DEVIATION - COINCIDING MEASUREMENT ANGLES (%)	1,56

MESH SAMPLE NUMBER

07g

PARAMETERS

LW	SW	w	e	b	i	color
115	52	23	1	2	43,5	

SPECULAR TRANSMITTANCE (%)

COMPUTER AID ASSESMENT RESULT

y \ x	0º	15º	30º	45º	60º	75º	90º	105º	120º	135º	150º	165º	180º
0º		11,63	**4,07**	2,19	**1,73**	6,67	**10,05**	16,68	**21,97**	30,62	**43,33**	56,51	
15º		11,63	4,78	3,26	2,14	**6,01**	10,89	**15,97**	20,95	32,34	42,72	56,51	
30º		11,63	4,78	**3,05**	**2,65**	8,14	**11,60**	15,87	**21,87**	**32,24**	42,72	56,51	
45º		13,34	4,17	3,66	**3,46**	6,11	13,07	18,11	**21,77**	31,68	39,77	54,15	
60º		16,65	6,21	4,68	5,39	5,39	**14,34**	21,36	21,36	29,09	45,16	51,87	
75º			18,90	15,96	18,67	18,67	18,67	18,67	18,67	32,11	41,40		
90º													

LABORATORY ASSESMENT RESULT

y \ x	0º	15º	30º	45º	60º	75º	90º	105º	120º	135º	150º	165º	180º
0º		0,38	0,15	0,04	1,07	6,95	11,81	16,30	21,61	29,06	39,40	43,54	
15º		0,36	0,12	0,04	1,16	6,81	11,52	15,64	20,97	28,46	38,35	41,69	
30º		0,36	0,08	0,04	1,11	6,79	11,56	15,53	20,57	28,35	37,72	37,37	
45º		0,26	0,06	0,06	1,19	6,76	11,51	15,57	20,79	28,44	36,80	31,63	
60º		0,56	0,12	0,08	1,42	8,17	11,98	15,97	20,74	25,71	27,10	10,90	
75º			0,88	0,34	1,90	6,44	13,26	13,88	16,36	15,87	7,02		
90º													

ABSOLUTE DEVIATION BETWEEN BOTH METHODS

y \ x	0º	15º	30º	45º	60º	75º	90º	105º	120º	135º	150º	165º	180º
0º		11,26	**3,92**	2,15	**0,66**	0,29	**1,75**	0,38	**0,36**	1,55	**3,93**	12,97	
15º		11,28	4,66	3,21	0,98	**0,81**	0,63	**0,33**	0,02	3,89	4,37	14,83	
30º		11,28	4,70	**3,01**	**1,54**	1,35	**0,04**	0,33	**1,30**	**3,89**	5,00	19,14	
45º		13,08	4,11	3,60	**2,27**	0,66	1,57	2,54	**0,97**	3,24	2,97	22,52	
60º		16,09	6,09	4,61	3,97	2,77	**2,36**	5,39	0,62	3,38	18,06	40,97	
75º			18,02	15,62	16,77	12,23	5,41	4,79	2,32	16,24	34,38		
90º													

MAXIMUM DEVIATION (%)	40,97
MINIMUM DEVIATION (%)	0,02
AVERAGE DEVIATION (%)	6,62
AV. DEVIATION - COINCIDING MEASUREMENT ANGLES (%)	1,81

MESH SAMPLE NUMBER

11b

PARAMETERS

LW	SW	w	e	b	i	color
60	22	7	2	2	18	

SPECULAR TRANSMITTANCE (%)

COMPUTER AID ASSESMENT RESULT

y \ x	0º	15º	30º	45º	60º	75º	90º	105º	120º	135º	150º	165º	180º
0º		25,01	**12,40**	16,16	**26,92**	34,09	**39,35**	47,55	**56,48**	65,94	**64,83**	36,80	
15º		25,01	13,11	12,30	28,14	**35,56**	41,66	**45,92**	56,08	68,89	63,91	36,80	
30º		25,01	13,11	**14,53**	**26,42**	36,98	**39,11**	43,18	**56,29**	**67,36**	63,91	36,80	
45º		26,88	13,72	16,82	**26,72**	35,36	41,30	47,45	**55,17**	64,72	65,34	38,27	
60º		30,41	16,76	21,03	33,43	33,43	**40,44**	51,31	51,31	59,24	51,11	36,84	
75º			34,18	30,76	37,17	37,17	37,17	37,17	37,17	40,79	40,00		
90º													

LABORATORY ASSESMENT RESULT

y \ x	0º	15º	30º	45º	60º	75º	90º	105º	120º	135º	150º	165º	180º
0º		1,05	0,02	9,70	24,60	39,31	41,79	50,11	59,24	68,90	59,95	10,83	
15º		1,03	0,02	10,26	24,75	39,34	40,40	49,02	57,59	67,17	68,45	5,46	
30º		0,70	0,02	9,96	23,48	34,24	41,67	49,25	57,87	67,77	58,62	11,29	
45º		0,77	0,03	1,68	23,88	28,28	41,37	50,08	57,60	64,43	59,08	19,94	
60º		0,46	0,10	7,30	24,88	33,10	42,32	47,31	50,81	50,29	37,87	5,09	
75º			0,97	8,39	19,51	28,43	31,68	31,91	25,85	13,21	3,75		
90º													

ABSOLUTE DEVIATION BETWEEN BOTH METHODS

y \ x	0º	15º	30º	45º	60º	75º	90º	105º	120º	135º	150º	165º	180º
0º		23,96	**12,38**	6,45	**2,32**	5,22	**2,44**	2,57	**2,76**	2,95	**4,88**	25,97	
15º		23,99	13,09	2,03	3,39	**3,78**	1,25	**3,10**	1,51	1,72	4,53	31,34	
30º		24,32	13,08	**4,57**	**2,93**	2,74	**2,55**	6,08	**1,59**	**0,40**	5,29	25,51	
45º		26,11	13,68	15,14	**2,85**	7,08	0,07	2,63	**2,43**	0,30	6,26	18,33	
60º		29,94	16,67	13,73	8,55	0,33	**1,88**	4,00	0,50	8,94	13,23	31,75	
75º			33,22	22,37	17,67	8,74	5,50	5,26	11,32	27,57	36,25		
90º													

MAXIMUM DEVIATION (%)	36,25
MINIMUM DEVIATION (%)	0,07
AVERAGE DEVIATION (%)	10,36
AV. DEVIATION - COINCIDING MEASUREMENT ANGLES (%)	3,39

6.8.3 Conclusions

Analyzing the comparative data sheets we observe that for all the assessed meshes the values corresponding to direction angles comprised between 45º and 135º on *x* axis and 0º and 60º on *y* axis show deviations lower than the average deviation and are in any case very acceptable. Those directions are surrounding the normal to the mesh plane and are placed in the upper centre boxes of the tables.

The most significant deviations are always related to the same set of directions: those forming small angles with the plane of the mesh. A similar concentration of less reliable values was also observed when analyzing the scattered transmittance of a mesh in section 6.6.3.4: scattered transmittance values in direction forming small angles with the mesh plane (oblique angles) showed higher values than in adjacent directions, closer to the normal to the mesh plane.

We can point out several possible reasons for those seemingly erroneous registers:

Results obtained from genBSDF show higher scattered transmittance values in oblique directions that might be due to the reflections in the mesh's strands, or some kind of edge effect in genBSDF operation when dealing with the edges of the mesh. The same reason could explain the increase of specular transmittance registered by genBSDF in the previous tables for oblique angles.

In laboratory results a similar tendency is observed. There we have to consider the existence of a diffuser layer just behind the mesh. In principle, we would expect that the most oblique the direction the greater the reflectance of the diffuser layer, which would result in a lower transmittance of the set mesh-diffuser. But we also observe an increase of transmittance for most oblique angles in some cases; for instance in values of (*x,y*) from (30º,60º) to (30º,75º) or from (45º,60º) to (45º,75º). These values correspond to directions coming from the upper-lateral part of the mesh, where radiation can be close to the normal to the strand's surface, reinforcing the hypothesis based on the reflections on the strands. The

existence of a diffuser layer in laboratory could be the reason of having a much slighter increase in the laboratory table than in the computer aid table for oblique directions.

For a general view of the comparative analysis the following table compiles all the calculated deviation data:

SAMPLE	MAXIMUM deviation (%)	MINIMUM deviation (%)	AVERAGE DEVIATION (%)	AV. DEVIATION - coinciding measurement angles (%)
01w	29,02	0,06	7,80	4,38
01g	30,00	0,06	7,81	3,36
01b	25,96	0,02	7,37	2,42
02w	34,61	0,01	13,17	10,20
02g	36,51	0,27	12,61	8,04
03w	35,34	0,33	7,83	2,80
03g	38,07	0,64	9,99	3,98
03b	43,78	0,00	8,59	2,45
04w	42,33	0,00	18,64	11,65
04g	**43,80**	6,34	**19,22**	12,18
04b	43,24	6,10	18,92	11,85
05w	36,81	0,38	14,00	5,90
05g	37,62	0,03	16,22	9,23
05b	37,43	0,20	14,77	6,78
06w	25,71	0,03	4,66	1,56
06g	26,83	0,01	4,60	1,57
06b	26,46	0,10	4,65	1,72
07w	37,26	0,05	6,42	2,16
07g	40,97	0,02	6,62	1,81
07b	37,08	0,01	6,33	1,71
08w	33,49	0,01	6,58	2,35
08b	34,50	0,05	6,46	2,51
09w	32,62	0,08	7,66	3,02
09b	38,43	0,05	8,41	2,65
10w	33,89	1,08	14,06	7,15
10b	34,32	4,94	15,71	9,41
11w	35,96	0,16	9,15	2,60
11b	36,25	0,07	10,36	3,39
12w	33,76	0,34	8,37	5,18
12b	40,25	0,13	8,10	4,64
Average	**35,41**	**0,72**	**10,17**	**4,96**

Table. 6.6. Comparison between computer and lab assessment. Deviation values

The differences are acceptable as the global average is 10.17% and descends to 4.96% when it comes to the directions where the comparison is more precise in theory (boldface values).

The maximum deviations for each mesh vary from 25% and 44% (with an average of 35.41%) and always correspond to some specific directions.

There seems to be no relation between the magnitude of the deviations and the type of geometry or finish of the mesh.

6.9 Comparative analysis with rough geometrical assessment

From BSDF data obtained in computer aided simulations, we can extract the incident direction with highest transmittance for each sample. The aim of this section is to compare this direction angles with those obtained in chapter 4, “Rough geometrical analysis of transmittance”, and chapter 5, “Laboratory assessment”.

In chapter 4, the direction of incidence radiation with highest transmittance was predicted, based on the geometrical properties of the EM *main section*. Therefore, those directions are referred to only this “main” vertical plan, where the angle for *y* axis is 0^{o} (according to laboratory set).

In section 5.4, a table compared predicted directions with highest transmittance from chapter 4, and the position in *x* axis of the sample holder at which the maximum transmittance was registered in laboratory. In the following table a new column is added with values obtained from computer aided assessment. Remember that all angles are referred to laboratory basis.

As we can observe in the following table, all the values obtained from computer aided assessment are almost identical to those obtained in laboratory assessment. For further considerations about the accuracy of the geometrical prediction refer to section 5.4.

MESH Nº	GEOMETRICAL PREDICTION	LABORATORY ASESSMENT			COMPUTER AIDED ASSESMENT		
		WHITE (w)	GRAY (g)	BLACK (b)	WHITE (w)	GRAY (g)	BLACK (b)
01	110,57	150	150	150	150	150	150
02	116,22	150	135	135	135	135	-
03	113,65	150	150	150	150	150	150
04	131,36	120	120	120	150	150	150
05	135,59	120	135	135	135	135	135
06	114,33	165	165	165	165	165	165
07	120,45	165	165	165	165	165	165
08	120,65	165		165	165		165
09	112,79	150		150	150		150
10	130,28	135		135	135		135
11	111,62	135		135	135		135
12	117,42	150		150	150		150

Table. 6.7. Incident radiation angle with highest transmittance of each mesh from geometrical prediction, laboratory and computer aided assessment

References

ATOS Compact Scan: GOM
N.d. http://www.gom.com/metrology-systems/system-overview/atos-compact-scan.html, accessed November 6, 2014.

Bidirectional Reflectance Distribution Function - Wikipedia, the Free Encyclopedia
N.d. http://en.wikipedia.org/wiki/Bidirectional_reflectance_distribution_function, accessed July 2, 2014.

BSDF
2014 Wikipedia, the Free Encyclopedia. http://en.wikipedia.org/w/index.php?title=Bidirectional_scattering_distribution_function&oldid=612813141, accessed July 2, 2014.

Farin, Gerald E., Josef Hoschek, and Myung-Soo Kim
2002 Handbook of Computer Aided Geometric Design. Elsevier.

Klems, J. H.
1994 New Method for Predicting the Solar Heat Gain of Complex Fenestration Systems- 2. Detailed Description of the Matrix Layer Calculation. ASHRAE Transactions 100(1): 1073–1086.

McNeil, Andrew
2013 BSDF Viewer — Radsite. Radsite. http://www.radiance-online.org/download-install/bsdf-viewer, accessed July 2, 2014.

McNeil, Andy, Jacob Jonsson, and David Appelfeld, dir.
2011 Validation of genBSDF.

Nicodemus, Fred E.
1965 Directional Reflectance and Emissivity of an Opaque Surface. Applied Optics 4(7): 767–773.

Ward, G., M. Kurt, and M. Bonneel
2012 Practical Framework Sharing Rendering Real-World BSDF.

Ward, G., R. Mistrick, E. S. Lee, A. McNeil, and J. Jonsson
2011 Simulating the Daylight Performance of Complex Fenestration Systems Using Bidirectional Scattering Distribution Functions within Radiance. LEUKOS 7(4): 241–261.

7.1 Conclusions

All the procedures we followed to assess light transmittance of Expanded Metal meshes have provided us with useful information for both a better understanding of the transmittance performance itself as for validating and improving the assessment procedures. All along the text, some partial conclusions have been extracted. We will summarize them and add new reflections on the problem in the following sections.

7.1.1 Methods and tools for EM light transmittance assessment

Besides its industrial wide application, Expanded Metal is present in a great amount of building envelopes but there is no specific knowledge available about its performance beyond the mechanical features as flexion resistance. This lack of insight entails a risk of inappropriate and inefficient use of the product. Nowadays, as a general fact, the building design trade lacks enough proper simulation work prior to construction. But even when simulation procedures are implemented, designers do not have specific knowledge and tools to deal with many existing industrial products and materials. That is the case of Expanded Metal.

Even if there are other methods available such as working outdoors with real radiation or by means of goniophotometry, we have used two other methods, own built lab device and computer aided assessment, intending to provide some know-how about EM light transmittance assessment. When adopting our assessment methods, we adapted them to our possibilities being aware of the diversity of aspects that must be taken into account to define or improve light transmittance control through EM.

7.1.1.1 Expanded metal specificity and diversity

One of the aspects that had to be taken into account is the shape complexity. EM is a product that needs a complex assessment method to achieve accurate daylight transmittance

data due to its varying geometry. This geometry makes the accurate modeling and its automation a relevant task, but it also implies the necessity of a three dimensional assessment, both in laboratory and computer aided methods. The assessment of just one section of the mesh or one incident light direction is insufficient. As an advantage, EM's geometry results from the repetition of one and the same curved metal strand, which enables 3D automated modeling.

Besides the complex geometry of a specific EM mesh we have to deal with a boundless range of EM types. As proven when studying the results of achieved assessments, the performances of different EM types are very diverse; therefore, the need of a specific EM 3D modeler is undeniable and becomes one of the key components of the computer aided method.

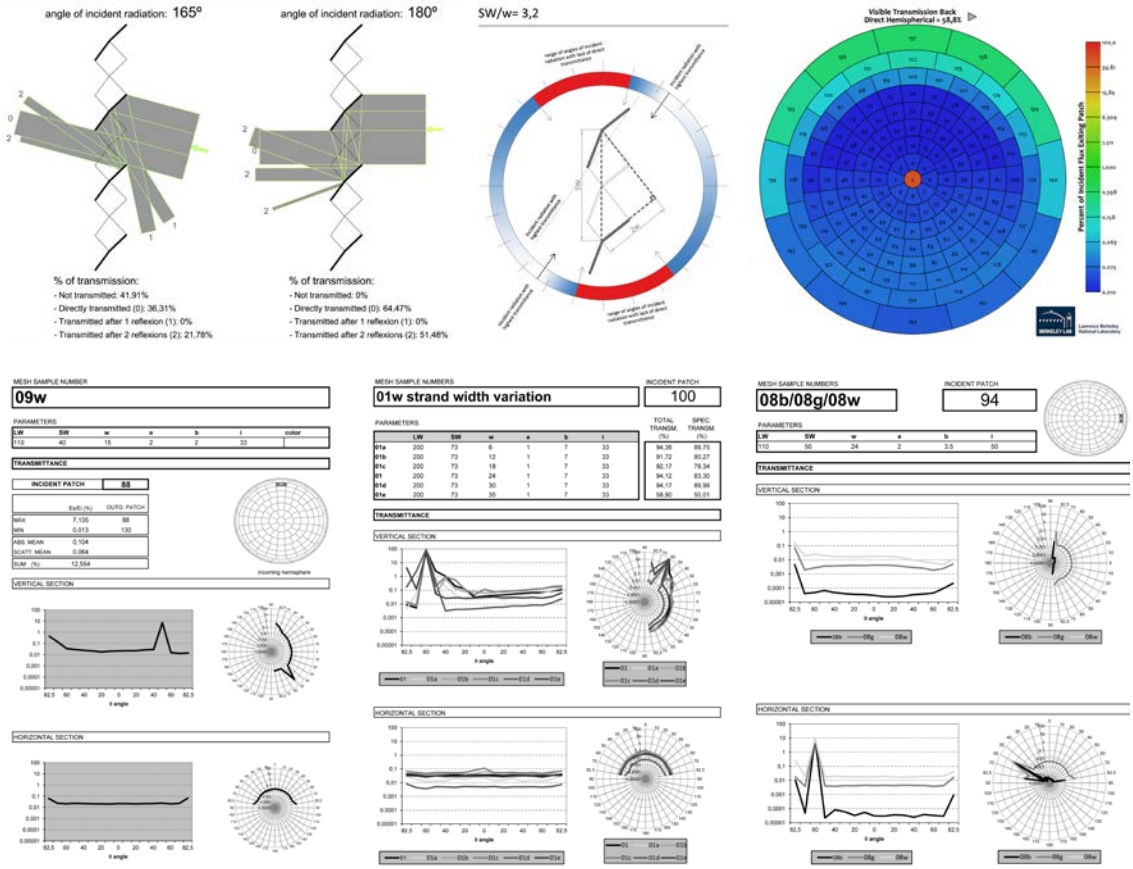

Fig. 7.1 Data visualization for decision-making. Charts, datasheets and graphs used in this research.

Our EM 3D automated modeler has been proved to be sufficiently accurate for specular transmittance assessment of modeled meshes, when comparing results obtained from our handmade lab device and BSDF management.

Depending on the objectives we were facing, we have used and drawn several data visualization charts and graphs. Reaching an agreement on unified visualization methods for a broad application seems to be necessary.

7.1.1.2 Validity and application of geometrical and lab assessment

Based on geometrical parameters usually provided by manufacturers such as *SW* and *w*, some first basic approximations to the performance of a specific EM mesh referring to daylight transmittance were done. This first intuitive approach to transmittance performance is obviously not sufficient for a rigorous assessment, but it can be helpful for designers when trying to choose the EM mesh that fits their objectives, quickly reducing the range of meshes for selection.

The rough geometrical analysis we carried out and explained in chapter 4 was intended to provide some arithmetical expression and graphs based on the known parameters of EM meshes for a useful and easy interpretation of light transmittance. Even if the results were later proved to not be always precise, they still explain in simple manner general features such as a rough approximation to the direction of maximum specular transmittance and the position and extension of the range of incident directions with lack of specular transmittance (section 4.2.2). These results were more accurate for meshes with small openings and are suitable for straightforward design decisions. Statements that could be intuitively predicted without any analysis were proved to be valid and expressed in a measurable manner such as for instance, obliquity of maximum specular transmission direction, higher symmetry (i.e. homogeneity) of specular transmissions and fewer null transmission directions for meshes

with high values of the ratio *SW*/*w* (section 4.3). In fact, the ratio *SW*/*w* appeared as a depictive feature of EM meshes.

The more abundant and accurate specular transmittance data obtained in our handmade lab assessment device proved that it is difficult to predict and summarize transmittance behavior for EM and that we cannot relate it simply and directly to geometrical mesh features such as *SW*/*w* or the openings surface (section 5.4.1.1). The coating features of the meshes were proven to have no appreciable effect in specular transmittance. White, gray and black coatings with very different reflectance were assessed (section 5.4.1.2).

7.1.1.3 BSDF management and interpretation

The Bidirectional Scattering Distribution Function based assessment of EM has different types of applications. We can use the raw BSDF data for the simulation of specific situations (specific spaces and times). It could also serve to prove the fulfillment of a given standard or regulation. But for a more generic approach to the product's performance, a simpler management of the BSDF data seemed to be necessary. In fact we believe that some standard should harmonize the way of summarizing that information for specific products as EM. The criterions we have proposed when choosing the assessed planes and directions and the graphic presentation were proven to be revealing.

BSDF based assessment allowed us to analyze the relationship between transmission in the scattered region and in the specular direction. This analysis was possible thanks to the adoption of a logarithmical scale for transmittance values which corresponds with the ability of human sight to adapt to light availability. Therefore even if the scattering is much lower than the specular transmission, the former has to be taken into account.

From BSDF based assessment we could observe very different transmittance values in non specular (i.e. scattered) directions depending on the coating color of the mesh and following the logic descent of transmittance from white to black coated meshes. These

scattered transmittance values were lower than 1% but appreciable thanks to the mentioned logarithmic representation (section 6.7.1).

When it came to the influence of strand width, BSDF based assessment accompanied by the selection of some representative incident directions and representation planes, was also proved illustrative. Very drastic reduction of specular transmittance resulted from the strand width variation and changing scattering patterns could be observed depending on the strands slope, which is linked to its width (section 6.7.2).

7.2 Next steps, limitations and challenges

7.2.1 Other requirements

This research has been focused on how incident beam light is transmitted through EM but as a facade element we have to address other requirements such as thermal performance, visual transparency, glare, rain screen performance if used in ventilated facades, etc.

For the appropriate agreement of all these requirements a more holistic point of view is needed. Anyway we can affirm that, in general, EM with large openings is not suitable for facades of work spaces as the projected shadow patterns would involve glare and sight problems. Therefore it is more often installed in facades as for sport, leisure, commercial or circulation spaces.

7.2.2 New software development

Building simulation procedures must be simplified to achieve a broad and effective application. We have to consider that the design period of a building can’t last indefinitely and designers can’t tackle the diversity of software used in the research level. Therefore, for an adequate implementation of this kind of tools in architecture design and building engineering procedures must be simplified and compact computing tools created.

Next steps related to this research could include developing a compact software that upon requesting the geometrical parameters of an EM mesh, would involve the whole process of generating the three dimensional model of the expanded metal mesh, obtaining its BSDF and returning a graphic summary. Additionally we could think about some application that entering the location, orientation and position of the façade would return useful data about total and specular daylight transmittance all along the year or any other period of time. Appendix C is dedicated to the geometric calculation needed to apply the assessment registers to real cases. The automation of all the process and operations is yet to be done.

This could be materialized in easy to use software where the designers could just introduce geometrical parameters of the desired mesh, position, location, orientation, date and time to automatically obtain the daylight specular and scattered transmittance.

Another interesting road to take in this sense could be a software with an invert operation, where specifying location, orientation and position of a facade in a specific day and time and entering the desired daylight transmittance we would obtain the geometrical parameters of the EM mesh or meshes required to fulfill those transmittance objectives. This second possible software faces up to some other difficulties, such as the amount of possible EM meshes that can achieve the results, the geometrical limitations of the EM meshes due to its manufacture process, the impossibility of achieving our desired transmittance values, etc. Besides, the user should not undertake the enormous job of entering the whole BSDF data set but should think about selecting some transmission directions to take into account. These specifications could be defined by a standard or regulation.

7.2.3 Outdoor assessment

This research is based on laboratory and computer aided assessment. Nowadays, computer aided assessment is usually the most practical, as it is not necessary to obtain physical samples of the product (no waste of money or material) and it is easily accessible

based on widely spread hardware and software tools. The development of specific software allows designers to obtain useful data in their own working space from their common working tools. But it is also very appropriate to use other assessment methods to validate and improve the computer aided assessment. For instance, an outdoor assessment with real radiation is deemed to be quite clarifying. In fact our lab assessment has been focused on incident direct light but Daylight, is a combination of direct and indirect including: direct sunlight, diffuse sky radiation and light reflected by earth and objects. Assessment with outdoors real radiation allows working with the whole phenomenon, with the difficulty of handling continuous changes in atmospheric conditions.

7.2.4 Extending the field of action of this research, its methods and tools

As aforementioned, due to the need of limiting the field of action and to supply limitations, just a small amount of the wide range of possible EM meshes has been analyzed in this research, all of them being rhombus shaped with the aim of focusing at least in one typical type of EM. Therefore, another task to carry out could be analyzing some other types of expanded metal, such as other types of translucent metal screens.

For the same reasons, we limited the research to Daylight but there is obviously much to do with thermal behavior and with visual comfort in spaces with expanded metal envelopes.

7.2.5 Improving the parametric modeling of EM

As explained, a specific 3D modeler is a key component when it comes to assess a product like EM. The accuracy of the modeler decreases with automation as that automation has been created on the basis of the analysis of a limited amount of samples. We could develop the photography based analysis and the 3D scans of more meshes to increase the data base and accuracy of the coefficients used in the automation of the 3D modeler. The process

could be adapted also to other types of EM. This scanning and photographing process has been done with the previously mentioned rhombus shaped EM meshes and all the automation has been designed based on the specific geometry and manufacture conditions of this type of mesh. There is also work to do trying to achieve an improved modeling of some meshes that presented shape accuracy problems, such as those with small holes or high strand thicknesses (high ratio *e*/*w*).

As explained in section 7.1.1.1 the adequacy of our 3D models for specular light transmittance assessment was proved comparing BSDF and lab results. The adequacy has not been proven for the scattered portion of light, as we could only assess it by BSDF. The use of goniophotometry could help to contrast those results and confirm the 3D models as a good base also for the scattered transmittance assessment.

7.2.6 Adaptability

As the immense majority of contemporary facade products, EM is not very adaptive, i.e. it does not change its shape, position or performance upon varying ambient conditions. Thermosensitive and photosensitive materials and products are good examples of highly adaptive contemporary facade elements. EM was invented in the XIX century and we cannot pretend to transform it into a product at the cutting edge of technology, but while improving its efficiency and exploitation, we could obtain inspiration for new products and ideas. The case of Basel Exhibition Center presented in section 2.4 can be understood as a further step in product adaptability as it takes a kind of facade solution and it adapts its shape to the different positions all along the envelope. This is what we could define as an adaptive facade in three dimensions. The challenge nowadays is to leap to the fourth dimension, time, and develop facade elements capable to adapt to changing ambient conditions over time inspired in natural phenomena that we observe in living beings. In the mean time, we can also work to exploit the

possibilities of EM manufacture, parametric design and digital manufacture to design adaptive facades that vary depending on position, inclination and orientation, which is not small feat.

APPENDIX A LABORATORY ASSESSMENT RESULTS

A.1 Appendix introduction

This appendix contains the data obtained in the laboratory assessment explained in chapter 5 “Laboratory assessment”. Remember that the registers of the transmitted illuminance are measured only in the direction of the specular transmission and therefore, they are valid only to obtain an initial idea of the behavior of the EM in luminous transmittance and to verify the validity of other assessment methods.

The results are given in tables with 13 rows and 13 columns (one for every fixed position of the sample holder in rotation around *x* and *y* axis), where each box contains a number expressing the transmittance (%) for each combination of rotations, i.e. for each light incident direction (see section 5.2.2 for the meaning of x and y). The boxes related to the positions where the sample holder obstructed the incident radiation voiding those registers, are empty and crossed out.

A.2 Laboratory assessment registers for diffuser layer validation

In section 5.2.3 we mentioned a test to validate the use of a diffuser layer. Here we can find the registers of this test made with mesh sample 10b (see section 5.3 for the properties of this mesh). We show one table for the daylight transmittance through this sample without diffuser layer, another one for the daylight transmittance through the same sample and the adjacent diffuser layer and a last one comparing both registers. This last table shows the absolute deviation between both tests and identifies the maximum deviation detected.

DAYLIGHT TRANSMITTANCE OF MESH: 10b - WITHOUT DIFFUSER -												
y \ x	0º	15º	30º	45º	60º	75º	90º	105º	120º	135º	150º	165º	180º
0º		0.01	0.00	5.37	14.51	18.96	21.46	23.81	25.41	25.16	17.11	0.00	
15º		0.01	0.00	5.16	14.16	18.51	21.16	23.11	24.56	23.76	15.66	0.01	
30º		0.00	0.00	4.85	13.26	17.31	19.96	21.81	22.36	20.51	12.11	0.01	
45º		0.00	0.00	4.10	13.16	17.41	19.81	21.06	19.91	15.51	3.39	0.01	
60º		0.01	0.00	2.33	9.51	13.76	15.26	14.11	9.81	1.96	0.01	0.01	
75º			0.01	0.17	1.94	2.83	1.44	0.14	0.01	0.01	0.04		
90º													
105º			0.01	0.04	0.80	1.61	0.98	0.05	0.01	0.01	0.02		
120º		0.01	0.00	1.53	8.34	12.81	14.51	13.91	10.11	1.94	0.01	0.01	
135º		0.00	0.00	3.16	12.41	17.21	19.36	20.61	19.66	15.76	3.93	0.00	
150º		0.00	0.00	4.14	13.31	17.66	20.76	22.41	23.36	21.86	13.86	0.03	
165º		0.00	0.00	4.68	14.26	18.76	21.51	23.66	24.91	24.51	17.26	0.00	
180º		0.00	0.00	5.34	15.71	20.51	23.41	25.71	27.47	27.52	19.81	0.00	
											AVERAGE DAYLIGHT TRANSMITTANCE		9.76

Table A.1. Daylight transmittances measured without diffuser

DAYLIGHT TRANSMITTANCE OF MESH: 10b - WITH DIFFUSER -												
y \ x	0º	15º	30º	45º	60º	75º	90º	105º	120º	135º	150º	165º	180º
0º		0.32	0.02	5.57	14.98	19.84	22.82	25.40	27.92	28.06	18.49	0.27	
15º		1.03	0.02	5.24	14.56	19.18	22.30	24.45	26.31	26.11	18.07	0.34	
30º		0.89	0.02	5.02	14.53	19.77	22.83	24.04	25.26	23.94	14.14	0.22	
45º		0.49	0.02	3.87	13.46	18.28	20.79	22.25	21.13	17.31	4.51	0.13	
60º		0.37	0.04	1.76	9.79	14.55	16.48	15.48	11.62	3.02	0.10	0.31	
75º			0.60	0.41	2.05	3.27	2.02	0.61	0.22	0.16	0.33		
90º													
105º			0.32	0.24	1.26	2.08	1.21	0.23	0.14	0.21	0.72		
120º		0.31	0.04	1.97	9.05	13.88	15.69	14.33	9.59	2.03	0.14	0.76	
135º		0.04	0.02	3.65	12.85	17.84	20.60	21.78	20.54	16.12	3.18	0.16	
150º		0.05	0.01	4.51	13.78	18.64	21.08	23.71	24.67	23.33	13.95	0.25	
165º		0.03	0.01	5.11	14.62	19.22	22.08	24.68	26.61	25.89	17.10	0.27	
180º		0.03	0.01	5.55	15.91	20.61	23.74	26.57	28.61	28.70	19.48	0.16	
											AVERAGE DAYLIGHT TRANSMITTANCE		10.45

Table A.2. Daylight transmittances measured with diffuser

10b SAMPLES TRANSMITTANCE DIFFERENCE WHEN MEASURING WITH OR WITHOUT DIFFUSER												
ABSOLUT ERROR: TRANSMITTANCE VALUES WITHOUT DIFFUSER - TRANSMITTANCE VALUES WITH DIFFUSER												
y \ x	0º	15º	30º	45º	60º	75º	90º	105º	120º	135º	150º	165º	180º
0º		-0.31	-0.01	-0.20	-0.47	-0.88	-1.36	-1.59	-2.50	-2.90	-1.38	-0.26	
15º		-1.02	-0.01	-0.07	-0.40	-0.67	-1.14	-1.34	-1.75	-2.35	-2.41	-0.32	
30º		-0.89	-0.02	-0.17	-1.27	-2.46	-2.87	-2.23	-2.90	**-3.43**	-2.03	-0.20	
45º		-0.49	-0.02	0.23	-0.30	-0.87	-0.98	-1.19	-1.22	-1.80	-1.12	-0.13	
60º		-0.37	-0.03	0.57	-0.28	-0.79	-1.22	-1.37	-1.81	-1.06	-0.09	-0.30	
75º			-0.59	-0.24	-0.11	-0.45	-0.58	-0.47	-0.20	-0.15	-0.30		
90º													
105º			-0.31	-0.20	-0.45	-0.47	-0.23	-0.18	-0.13	-0.20	-0.70		
120º		-0.30	-0.03	-0.44	-0.71	-1.07	-1.18	-0.42	0.51	-0.09	-0.13	-0.75	
135º		-0.04	-0.02	-0.49	-0.44	-0.63	-1.24	-1.17	-0.88	-0.36	0.74	-0.16	
150º		-0.05	-0.01	-0.37	-0.48	-0.98	-0.32	-1.30	-1.30	-1.46	-0.10	-0.22	
165º		-0.03	-0.01	-0.43	-0.36	-0.45	-0.56	-1.02	-1.70	-1.38	0.15	-0.27	
180º		-0.03	-0.01	-0.21	-0.20	-0.10	-0.32	-0.86	-1.14	-1.19	0.33	-0.15	
											AVERAGE DAYLIGHT TRANSMITTANCE DIFFERENCE		-0.69

Table A.3. Difference or deviation table of the daylight transmittances obtained with and without diffuser. This table is the result of deducting the measurements with diffuser to the ones without diffuser

A.3 Laboratory assessment registers for daylight transmittance of each assessed mesh

There is one table for each assessed sample, marking the position and value of the maximum and minimum transmittance and the average transmittance of all directions. The list of the assessed samples and their properties (geometry and color) are specified in section 5.3.

DAYLIGHT TRANSMITTANCE OF MESH: 01w

y \ x	0º	15º	30º	45º	60º	75º	90º	105º	120º	135º	150º	165º	180º
0º		1.59	1.09	12.95	24.57	38.05	41.57	49.77	58.85	70.90	73.38	23.37	
15º		1.44	1.11	13.30	26.23	33.72	41.98	49.13	58.38	69.18	76.84	21.29	
30º		1.64	1.19	13.92	24.59	38.63	42.52	49.13	58.44	69.96	74.80	31.05	
45º		1.76	1.24	14.53	26.25	38.54	42.40	50.38	60.47	70.93	76.00	49.42	
60º		2.04	1.61	13.42	25.27	34.37	48.73	50.62	59.12	63.53	61.45	32.38	
75º			4.19	14.67	28.33	34.33	45.17	46.07	45.73	37.64	22.67		
90º													
105º			1.50	10.16	34.27	41.43	45.72	51.37	53.12	48.25	29.47		
120º		1.16	0.89	11.34	25.50	35.45	43.68	53.88	59.46	64.87	66.65	42.24	
135º		0.80	1.10	10.57	24.37	38.67	41.89	50.32	59.35	70.12	77.30	47.05	
150º		0.68	0.87	12.37	24.71	33.75	40.17	48.66	58.54	71.18	79.65	44.55	
165º		**0.61**	0.85	12.60	24.18	37.77	40.07	47.85	58.44	70.35	79.09	40.28	
180º		0.68	0.86	12.74	27.17	33.00	40.39	47.76	57.74	70.77	**79.69**	44.46	

AVERAGE DAYLIGHT TRANSMITTANCE 36.58

MAX 79.69

MIN 0.61

DAYLIGHT TRANSMITTANCE OF MESH: 01g

y \ x	0º	15º	30º	45º	60º	75º	90º	105º	120º	135º	150º	165º	180º
0º		0.63	0.13	10.39	23.57	32.76	40.90	49.08	58.45	71.40	79.38	38.78	
15º		0.52	0.14	10.54	23.92	33.26	41.64	49.48	58.77	71.86	**82.44**	33.43	
30º		0.52	0.16	11.12	23.47	32.95	40.44	48.26	58.72	72.53	78.25	32.20	
45º		0.51	0.23	11.41	24.53	33.13	41.37	49.47	60.64	71.37	73.54	35.06	
60º		0.90	0.49	10.55	24.73	33.62	41.12	49.17	57.51	61.18	51.55	17.95	
75º			2.90	14.94	26.57	35.06	38.78	35.57	40.99	32.13	14.91		
90º													
105º			0.87	7.71	24.28	34.11	39.40	41.91	44.73	40.61	27.13		
120º		0.51	0.33	8.29	22.51	32.13	40.26	48.94	55.95	60.29	53.68	26.21	
135º		0.18	0.15	8.79	22.29	31.43	38.89	46.35	54.26	64.94	67.73	48.93	
150º		0.11	0.09	9.09	21.79	30.98	37.99	44.69	53.64	65.18	70.35	26.62	
165º		0.10	0.08	9.63	22.04	31.17	37.75	45.40	54.60	66.14	71.58	20.35	
180º		0.13	**0.07**	10.10	22.52	31.56	38.78	45.18	54.86	67.01	72.92	21.65	

AVERAGE DAYLIGHT TRANSMITTANCE 33.44

MAX 82.44

MIN 0.07

DAYLIGHT TRANSMITTANCE OF MESH: 01b

y \ x	0º	15º	30º	45º	60º	75º	90º	105º	120º	135º	150º	165º	180º
0º		1.52	0.04	12.78	25.27	35.17	43.00	51.38	62.25	74.58	79.86	33.70	
15º		1.19	0.08	11.23	25.72	35.01	42.87	51.21	61.13	73.20	**80.92**	29.33	
30º		0.84	0.05	11.20	26.19	39.79	43.26	51.87	61.70	74.36	78.51	29.95	
45º		0.68	0.07	11.22	25.54	34.98	42.98	53.56	62.16	71.58	72.92	36.45	
60º		1.11	0.23	9.24	25.14	35.25	43.10	52.27	58.89	61.18	51.79	20.48	
75º			1.80	10.97	27.27	34.13	40.56	43.22	38.36	29.73	23.65		
90º													
105º			0.55	8.89	26.01	33.39	40.38	40.47	41.94	32.80	20.10		
120º		0.39	0.13	10.28	23.92	34.75	48.80	51.29	59.19	61.65	55.48	18.41	
135º		0.10	0.05	10.02	24.14	38.21	42.19	50.63	59.17	69.41	71.63	40.18	
150º		0.07	0.02	11.72	24.14	38.29	40.78	49.55	58.99	70.99	75.58	32.14	
165º		0.03	0.02	10.49	23.93	38.34	41.61	50.06	60.63	72.81	79.09	28.72	
180º		0.03	**0.02**	12.00	23.82	33.67	41.78	49.44	59.32	72.14	78.13	35.76	

AVERAGE DAYLIGHT TRANSMITTANCE 35.14

MAX 80.92

MIN 0.02

DAYLIGHT TRANSMITTANCE OF MESH: 02w

y \ x	0º	15º	30º	45º	60º	75º	90º	105º	120º	135º	150º	165º	180º
0º		1.89	2.07	25.03	39.42	41.38	46.53	52.76	60.03	**65.22**	50.12	6.52	
15º		1.90	2.13	23.36	39.30	41.22	47.14	51.79	58.51	61.64	49.11	4.04	
30º		2.16	2.41	24.78	39.53	41.73	47.92	52.61	57.87	60.44	47.96	12.63	
45º		2.13	2.45	26.47	35.09	47.21	48.83	52.04	54.05	53.15	43.69	9.94	
60º		1.98	3.10	19.45	33.00	40.25	51.69	46.69	41.57	36.56	20.24	2.09	
75º			4.88	14.56	22.42	25.84	30.55	24.26	15.78	5.53	1.70		
90º													
105º			2.31	13.01	22.34	24.46	22.80	18.86	11.71	4.90	2.82		
120º		1.30	1.88	22.21	35.18	41.91	50.77	45.88	43.22	35.02	13.81	4.44	
135º		1.08	2.07	24.49	39.86	42.06	47.15	51.59	52.81	50.59	40.28	7.03	
150º		0.90	1.70	23.50	39.69	41.31	45.75	50.19	55.42	55.13	45.09	11.38	
165º		0.81	1.79	24.86	34.53	40.50	44.92	50.06	56.79	58.07	45.34	5.04	
180º		**0.77**	1.80	24.13	39.33	40.53	45.44	49.89	55.77	60.34	46.61	6.29	

AVERAGE DAYLIGHT TRANSMITTANCE 30.16

MAX 65.22

MIN 0.77

DAYLIGHT TRANSMITTANCE OF MESH: 02g

y \ x	0º	15º	30º	45º	60º	75º	90º	105º	120º	135º	150º	165º	180º
0º		0.41	0.25	21.56	33.90	40.92	45.53	50.92	55.57	58.70	45.32	5.78	
15º		0.27	0.27	21.11	34.45	40.98	45.57	49.94	53.93	56.28	45.60	4.45	
30º		0.25	0.28	20.92	33.33	40.31	44.49	47.76	51.35	51.47	39.52	7.65	
45º		0.23	0.33	21.05	33.70	40.40	45.32	47.96	47.30	44.90	32.46	4.86	
60º		0.46	0.43	17.42	33.97	41.18	45.15	39.67	35.87	28.24	11.84	3.50	
75º			1.61	12.57	22.59	25.84	25.93	16.50	9.62	4.87	6.14		
90º													
105º			1.16	7.36	14.30	23.75	25.67	29.01	24.70	12.63	4.50		
120º		0.61	0.67	15.58	29.07	39.19	44.64	48.94	49.24	45.63	29.23	4.40	
135º		0.31	0.63	18.24	30.94	39.91	45.80	51.90	54.99	55.53	50.32	19.82	
150º		0.24	0.48	18.71	31.29	39.92	45.63	51.60	58.10	60.93	53.63	18.62	
165º		0.19	0.43	18.59	30.68	38.68	44.59	50.29	58.16	61.75	54.69	7.98	
180º		**0.18**	0.42	18.40	30.27	38.21	44.36	49.66	57.35	**63.25**	55.73	11.35	

AVERAGE DAYLIGHT TRANSMITTANCE 28.78

MAX 63.25

MIN 0.18

DAYLIGHT TRANSMITTANCE OF MESH: 02*b

y \ x	0º	15º	30º	45º	60º	75º	90º	105º	120º	135º	150º	165º	180º
0º		1.31	0.75	24.41	35.09	41.95	48.18	54.14	60.29	63.04	48.68	5.19	
15º		1.39	0.73	23.73	39.57	42.74	48.48	53.75	59.16	61.64	**66.92**	2.06	
30º		0.94	1.03	23.78	34.37	43.54	48.04	53.61	57.73	58.06	45.89	9.86	
45º		0.82	1.50	23.77	30.43	48.30	47.22	53.10	54.22	52.06	40.62	8.60	
60º		0.40	1.78	21.39	33.50	41.09	49.79	46.07	43.65	36.15	18.79	0.86	
75º			3.32	14.47	21.80	25.91	26.11	22.95	14.50	5.13	0.90		
90º													
105º			0.92	7.31	17.82	18.99	18.55	15.09	8.15	2.17	1.00		
120º		0.53	0.92	18.16	31.41	39.35	44.20	44.24	41.49	31.58	8.97	1.23	
135º		0.15	1.57	21.92	33.04	41.14	47.15	50.79	51.54	48.71	35.74	3.58	
150º		0.05	0.69	20.98	40.26	40.93	46.60	50.96	55.72	55.71	43.02	8.55	
165º		0.05	0.19	24.61	39.41	40.96	46.80	52.04	57.34	58.60	44.77	1.99	
180º		**0.02**	0.58	24.15	39.83	41.42	47.05	51.57	57.09	62.91	47.14	4.09	

AVERAGE DAYLIGHT TRANSMITTANCE 29.24

MAX 66.92

MIN 0.02

DAYLIGHT TRANSMITTANCE OF MESH: 03w

y \ x	0º	15º	30º	45º	60º	75º	90º	105º	120º	135º	150º	165º	180º
0º		0.82	0.62	1.02	11.75	18.20	29.55	32.53	40.37	51.84	59.23	25.91	
15º		0.86	0.67	1.17	12.25	19.98	30.64	33.45	40.97	51.76	**64.12**	35.73	
30º		1.26	0.72	1.19	11.84	20.03	27.57	33.71	41.42	52.56	63.66	43.54	
45º		1.30	0.74	1.22	11.18	19.86	26.59	39.49	41.55	52.49	62.46	42.50	
60º		1.73	1.02	1.22	13.16	20.32	26.94	34.13	40.85	46.35	45.85	24.23	
75º			2.07	2.87	9.12	15.97	22.97	26.78	25.53	17.42	8.02		
90º													
105º			0.78	1.32	9.64	20.89	22.23	23.66	21.90	12.80	5.12		
120º		0.94	0.64	1.11	12.41	20.18	26.41	32.85	40.03	44.73	47.29	14.08	
135º		0.72	0.70	0.97	11.80	19.17	25.75	31.97	38.66	48.94	62.06	35.09	
150º		0.59	0.54	0.90	10.68	18.73	25.53	30.86	38.19	48.16	61.05	37.66	
165º		0.45	0.51	1.06	11.50	19.03	25.28	31.43	38.68	48.42	60.59	34.54	
180º		**0.43**	0.49	1.03	11.74	19.32	29.11	31.17	38.45	48.38	59.64	35.32	

AVERAGE DAYLIGHT TRANSMITTANCE 23.45

MAX 64.12

MIN 0.43

DAYLIGHT TRANSMITTANCE OF MESH: 03g

y \ x	0°	15°	30°	45°	60°	75°	90°	105°	120°	135°	150°	165°	180°
0°		0.80	0.08	0.45	10.04	17.91	23.59	29.54	36.57	45.48	50.60	24.53	
15°		0.71	0.08	0.26	10.16	17.88	24.02	29.64	35.99	44.22	53.18	28.37	
30°		0.65	0.09	0.23	12.06	18.97	24.75	29.85	36.45	44.69	55.70	29.95	
45°		0.39	0.09	0.52	12.34	18.95	24.91	30.86	35.98	44.03	48.92	25.76	
60°		0.59	0.16	0.53	10.50	18.33	23.76	26.18	33.65	36.15	32.13	10.33	
75°			0.88	1.50	7.59	17.43	22.02	21.97	18.60	11.98	4.81		
90°													
105°			0.40	0.93	5.08	19.64	20.96	22.43	19.76	15.61	4.35		
120°		0.33	0.12	0.63	10.33	18.88	25.21	31.62	38.08	42.19	38.97	11.81	
135°		0.11	0.08	0.40	11.28	18.20	24.47	30.51	41.38	46.59	56.31	22.50	
150°		0.10	**0.04**	0.26	11.11	17.83	23.75	29.45	35.96	46.42	66.86	23.72	
165°		0.11	0.05	0.40	11.58	16.72	26.93	29.34	36.49	45.09	54.96	24.04	
180°		0.16	0.05	0.47	10.79	17.98	23.85	28.92	36.22	45.13	**67.45**	24.03	

AVERAGE DAYLIGHT TRANSMITTANCE 20.43

MAX 67.45

MIN 0.04

DAYLIGHT TRANSMITTANCE OF MESH: 03b

y \ x	0°	15°	30°	45°	60°	75°	90°	105°	120°	135°	150°	165°	180°
0°		0.28	0.03	0.39	13.15	19.03	26.24	32.07	39.58	48.83	53.96	9.01	
15°		0.49	0.03	0.30	11.36	19.10	29.07	31.60	38.61	47.91	56.49	20.79	
30°		0.43	0.03	0.33	10.44	19.47	26.00	31.84	38.72	47.44	54.11	32.87	
45°		0.38	0.03	0.28	12.37	19.01	26.32	32.83	38.85	47.29	53.54	30.64	
60°		0.68	0.05	0.39	11.64	20.05	26.03	31.49	37.16	41.79	46.47	29.52	
75°			0.74	1.22	8.91	15.84	22.38	23.66	21.42	15.32	5.53		
90°													
105°			0.38	0.84	7.97	15.65	21.02	21.12	18.83	10.06	3.40		
120°		0.33	0.06	0.47	10.20	19.28	26.50	33.88	38.86	42.58	38.45	9.96	
135°		0.06	0.02	0.29	11.82	19.54	25.96	36.67	38.48	47.06	56.03	31.70	
150°		0.05	0.01	0.26	11.45	18.50	29.00	31.88	38.63	47.78	57.27	47.59	
165°		0.09	0.01	0.32	11.31	18.90	28.37	31.78	39.09	47.89	**58.18**	51.77	
180°		0.05	**0.01**	0.37	11.13	18.96	29.00	31.39	38.45	48.03	56.51	36.55	

AVERAGE DAYLIGHT TRANSMITTANCE 21.95

MAX 58.18

MIN 0.01

DAYLIGHT TRANSMITTANCE OF MESH: 04w

y \ x	0°	15°	30°	45°	60°	75°	90°	105°	120°	135°	150°	165°	180°
0°		0.80	0.32	2.88	14.34	18.68	19.98	22.25	**24.19**	23.98	17.43	0.94	
15°		0.77	0.32	2.05	14.19	18.57	20.37	21.66	23.04	22.75	17.23	0.90	
30°		1.05	0.35	3.30	14.62	18.24	20.40	21.04	21.52	20.26	12.57	0.77	
45°		1.03	0.36	1.92	14.31	17.62	19.21	19.76	18.72	13.99	2.89	0.53	
60°		1.08	0.50	1.22	11.25	14.59	16.24	13.86	8.64	1.40	0.35	0.44	
75°			1.24	0.86	2.47	3.34	2.39	0.81	0.34	0.27	0.44		
90°													
105°			0.78	0.88	2.44	3.46	2.33	1.28	1.02	1.00	1.48		
120°		0.63	0.50	1.89	13.12	15.63	16.19	15.06	9.59	2.50	1.14	1.41	
135°		0.28	0.47	2.31	15.00	17.98	19.29	20.02	19.11	14.99	4.63	2.17	
150°		**0.25**	0.33	2.50	14.47	18.15	19.83	20.87	21.49	20.41	13.75	2.87	
165°		0.25	0.30	2.18	15.38	18.20	19.67	21.15	22.70	22.54	18.71	2.38	
180°		0.27	0.28	2.08	14.55	18.15	19.96	21.02	22.90	23.50	19.84	1.67	

AVERAGE DAYLIGHT TRANSMITTANCE 9.73

MAX 24.19

MIN 0.25

DAYLIGHT TRANSMITTANCE OF MESH: 04g

y \ x	0°	15°	30°	45°	60°	75°	90°	105°	120°	135°	150°	165°	180°
0°		0.71	0.06	2.55	15.26	18.47	19.77	21.57	**23.46**	22.34	15.20	0.25	
15°		0.67	0.06	2.21	14.19	18.13	19.88	21.19	22.36	21.54	14.83	0.20	
30°		0.81	0.06	2.18	14.59	18.33	19.93	20.57	21.23	19.43	10.13	0.18	
45°		0.55	0.05	1.01	14.49	17.24	18.76	18.96	17.35	12.52	1.42	0.09	
60°		0.59	0.11	1.03	8.88	13.03	15.17	12.36	7.16	0.84	0.05	0.31	
75°			0.78	0.47	1.75	2.50	1.63	0.41	0.12	0.14	0.33		
90°													
105°			0.64	0.35	1.48	2.13	1.12	0.49	0.37	0.45	0.91		
120°		0.37	0.11	1.43	10.65	14.04	14.46	13.08	7.68	1.14	0.33	0.79	
135°		0.08	0.09	1.73	13.08	17.00	18.09	18.68	17.35	13.18	2.22	0.62	
150°		0.08	0.05	1.99	13.63	17.14	18.39	19.36	19.97	19.03	11.10	0.82	
165°		0.10	0.05	2.23	14.13	17.29	18.58	19.97	21.41	21.12	16.25	0.68	
180°		0.12	**0.04**	2.15	14.54	17.76	19.01	20.21	21.71	22.41	15.78	0.37	

AVERAGE DAYLIGHT TRANSMITTANCE 8.86

MAX 23.46

MIN 0.04

DAYLIGHT TRANSMITTANCE OF MESH: 04b

y \ x	0º	15º	30º	45º	60º	75º	90º	105º	120º	135º	150º	165º	180º
0º		1.39	0.03	2.30	15.64	18.74	20.35	22.31	23.83	23.19	16.45	0.08	
15º		1.67	0.03	1.44	14.78	18.81	20.44	21.75	23.18	22.24	15.57	0.11	
30º		1.15	0.03	1.54	13.73	19.11	20.43	21.24	21.73	19.84	11.11	0.14	
45º		0.72	0.03	1.22	14.64	18.14	19.58	19.70	18.87	12.89	1.97	0.09	
60º		0.59	0.05	0.57	8.83	13.80	14.83	13.33	7.41	0.81	0.04	0.42	
75º			0.78	0.34	1.67	2.64	1.61	0.34	0.17	0.43	0.41		
90º													
105º			0.32	0.26	1.14	1.68	0.86	0.21	0.14	0.22	0.81		
120º		0.31	0.08	0.94	11.03	14.28	15.30	13.55	7.22	0.60	0.10	0.69	
135º		0.10	0.04	1.32	14.11	17.94	19.49	20.17	19.36	13.51	1.68	0.17	
150º		0.12	0.02	0.97	14.79	18.48	20.06	21.18	21.44	21.47	11.66	0.69	
165º		0.05	0.01	0.92	15.75	18.59	20.26	21.76	23.80	22.49	16.84	0.30	
180º		0.03	**0.01**	0.90	14.83	17.86	20.10	21.39	**24.20**	23.08	19.74	0.29	
											AVERAGE DAYLIGHT TRANSMITTANCE		9.24

MAX 24.20

MIN 0.01

DAYLIGHT TRANSMITTANCE OF MESH: 05w

y \ x	0º	15º	30º	45º	60º	75º	90º	105º	120º	135º	150º	165º	180º
0º		0.88	0.51	5.85	16.86	22.06	28.56	27.82	30.67	**30.94**	26.59	1.55	
15º		0.82	0.50	2.32	16.12	20.46	24.03	26.64	28.66	28.64	21.88	1.57	
30º		1.09	0.54	5.08	16.03	21.47	24.24	26.37	27.66	26.74	17.43	1.00	
45º		1.09	0.50	4.59	16.88	20.42	23.08	24.66	26.18	20.46	5.57	0.67	
60º		1.27	0.63	3.05	12.30	17.22	20.42	19.65	15.96	5.85	0.68	0.53	
75º			1.57	1.88	5.08	7.08	8.74	4.35	1.15	0.72	0.64		
90º													
105º			1.01	1.88	5.18	7.64	6.69	4.05	1.92	1.50	2.01		
120º		0.81	0.72	4.07	14.85	17.91	19.23	18.16	14.05	5.56	1.82	2.71	
135º		0.39	0.66	4.69	15.44	19.77	21.86	22.75	22.07	16.35	7.13	3.15	
150º		0.34	0.49	6.03	15.96	20.55	22.09	23.98	25.02	22.98	16.83	3.65	
165º		**0.30**	0.46	6.26	15.75	20.18	25.17	24.80	26.89	26.49	21.47	3.97	
180º		0.32	0.44	5.52	16.22	20.38	25.46	24.78	27.17	28.03	22.55	2.99	
											AVERAGE DAYLIGHT TRANSMITTANCE		12.30

MAX 30.94

MIN 0.30

DAYLIGHT TRANSMITTANCE OF MESH: 05g

y \ x	0º	15º	30º	45º	60º	75º	90º	105º	120º	135º	150º	165º	180º
0º		0.22	7.70	19.81	22.08	23.25	23.93	23.45	20.48	12.26	0.20	**0.00**	
15º		0.73	0.08	4.85	14.13	18.85	21.75	23.76	25.00	24.20	17.30	0.75	
30º		0.94	0.08	4.71	13.86	18.97	21.75	22.81	23.66	22.01	12.23	0.30	
45º		0.72	0.07	3.50	13.24	17.82	20.70	21.38	20.51	15.81	2.93	0.12	
60º		0.56	0.12	2.05	10.60	14.80	17.74	16.18	11.82	3.39	0.14	0.33	
75º			0.69	0.91	3.15	5.04	5.64	2.37	0.58	0.27	0.85		
90º													
105º			0.40	1.56	5.02	6.15	5.58	2.50	0.73	0.57	1.05		
120º		0.39	0.24	4.15	14.15	16.68	17.99	16.85	12.62	3.99	0.52	0.94	
135º		0.10	0.14	5.13	14.35	18.78	20.98	22.13	20.94	16.85	5.03	0.76	
150º		0.09	0.08	5.14	14.59	19.40	21.75	23.27	24.37	22.88	15.87	1.10	
165º		0.09	0.06	5.21	14.76	19.35	21.72	23.98	25.65	**26.84**	22.87	1.66	
180º		0.12	0.06	5.71	14.88	19.37	24.06	23.88	25.72	25.37	20.89	0.94	
											AVERAGE DAYLIGHT TRANSMITTANCE		10.70

MAX 26.84

MIN 0.00

DAYLIGHT TRANSMITTANCE OF MESH: 05b

y \ x	0º	15º	30º	45º	60º	75º	90º	105º	120º	135º	150º	165º	180º
0º		1.56	0.04	4.69	16.37	24.60	24.92	27.70	**29.49**	28.60	20.89	0.23	
15º		1.90	0.07	4.32	15.99	21.38	28.17	26.87	28.14	27.30	20.28	2.25	
30º		1.14	0.16	4.00	15.29	21.32	23.66	26.00	26.67	25.09	14.62	0.22	
45º		0.88	0.04	3.43	15.78	19.77	22.28	24.15	23.61	19.31	3.32	0.08	
60º		0.96	0.07	2.03	10.70	16.11	18.10	17.67	12.49	3.59	0.10	0.68	
75º			0.88	0.83	3.51	5.92	6.29	2.51	0.41	0.24	0.39		
90º													
105º			0.38	0.60	2.73	4.60	4.19	1.93	0.37	0.25	0.81		
120º		0.31	0.17	2.69	12.49	16.10	18.23	17.76	12.03	3.23	0.17	0.69	
135º		0.05	0.07	4.02	15.75	20.15	22.64	23.83	22.00	17.13	3.97	0.21	
150º		0.05	0.02	4.86	15.08	20.68	23.52	28.30	26.00	24.10	15.81	0.31	
165º		0.04	0.01	4.69	15.46	20.94	27.04	26.08	27.71	27.32	21.77	1.49	
180º		0.03	**0.01**	5.29	15.50	21.04	24.17	26.35	28.35	28.63	23.83	0.50	
											AVERAGE DAYLIGHT TRANSMITTANCE		11.60

MAX 29.49

MIN 0.01

DAYLIGHT TRANSMITTANCE OF MESH: 06w

y \ x	0°	15°	30°	45°	60°	75°	90°	105°	120°	135°	150°	165°	180°
0°		0.49	0.22	0.10	0.20	2.17	4.56	5.95	7.05	8.65	11.85	15.03	
15°		0.71	0.17	0.10	0.20	2.11	4.50	5.79	6.91	8.44	12.29	13.37	
30°		1.08	0.12	0.10	0.19	2.06	4.47	5.67	6.92	8.74	12.39	12.78	
45°		0.79	0.09	0.11	0.22	2.15	4.61	5.99	7.18	9.26	12.62	10.70	
60°		0.68	0.17	0.12	0.27	2.25	5.51	6.12	7.51	9.00	10.29	6.08	
75°			1.01	0.39	0.48	2.05	4.99	5.69	6.26	6.14	4.70		
90°													
105°			0.52	0.42	0.93	3.05	4.50	5.54	6.67	7.34	6.46		
120°		0.43	0.12	0.15	0.34	2.52	4.75	6.16	7.41	9.00	11.48	13.68	
135°		0.20	0.10	0.10	0.23	2.22	4.47	5.78	6.84	8.73	12.66	20.98	
150°		0.14	0.06	0.08	0.19	2.14	4.32	5.58	6.70	8.45	12.18	**21.17**	
165°		0.15	0.06	0.07	0.18	2.10	4.28	5.60	6.84	8.33	12.04	21.06	
180°		0.15	**0.06**	0.07	0.17	2.04	4.27	5.47	6.64	8.12	11.88	20.50	

AVERAGE DAYLIGHT TRANSMITTANCE 4.95

MAX 21.17

MIN 0.06

DAYLIGHT TRANSMITTANCE OF MESH: 06g

y \ x	0°	15°	30°	45°	60°	75°	90°	105°	120°	135°	150°	165°	180°
0°		1.22	0.20	0.03	0.05	2.17	4.47	5.57	7.02	8.76	12.23	18.34	
15°		1.18	0.14	0.03	0.05	2.18	4.44	5.71	6.88	8.64	12.90	17.70	
30°		1.16	0.08	0.03	0.06	2.16	5.11	5.67	6.87	8.72	12.49	11.72	
45°		0.68	0.03	0.03	0.09	2.33	5.12	5.85	6.93	9.00	12.00	7.79	
60°		0.53	0.08	0.04	0.15	2.34	5.30	5.95	7.23	8.56	9.03	3.55	
75°			0.69	0.19	0.41	1.92	4.48	5.34	5.69	5.59	3.14		
90°													
105°			0.38	0.31	0.72	2.43	4.49	6.52	6.43	6.82	5.55		
120°		0.35	0.05	0.05	0.18	2.37	4.66	6.38	7.68	8.85	11.03	9.96	
135°		0.05	0.02	0.03	0.09	2.20	4.52	5.94	6.90	8.73	12.48	19.82	
150°		0.08	0.02	**0.02**	0.06	2.13	4.36	5.75	6.78	8.51	12.15	19.59	
165°		0.08	0.02	0.02	0.05	2.09	4.36	5.73	6.87	8.40	12.17	20.07	
180°		0.10	0.02	0.02	0.05	2.10	4.32	5.61	6.76	8.36	12.21	**20.36**	

AVERAGE DAYLIGHT TRANSMITTANCE 4.84

MAX 20.36

MIN 0.02

DAYLIGHT TRANSMITTANCE OF MESH: 06b

y \ x	0°	15°	30°	45°	60°	75°	90°	105°	120°	135°	150°	165°	180°
0°		1.33	0.09	0.01	0.10	2.43	4.80	6.20	7.29	8.68	11.56	**22.43**	
15°		1.44	0.07	0.01	0.11	2.10	4.71	6.01	7.09	8.48	12.09	17.13	
30°		1.13	0.04	0.01	0.09	2.31	5.36	5.88	7.08	8.68	11.62	10.00	
45°		0.67	0.02	0.02	0.22	1.67	4.71	6.25	7.28	8.96	11.60	8.02	
60°		0.43	0.05	0.03	0.19	2.36	5.30	6.16	7.30	8.47	9.47	3.90	
75°			0.69	0.19	0.35	2.34	4.16	5.23	5.72	5.53	3.91		
90°													
105°			0.38	0.26	0.66	2.86	4.74	6.52	6.14	6.61	4.88		
120°		0.35	0.03	0.03	0.18	2.49	5.60	6.66	7.38	8.71	10.00	7.00	
135°		0.04	0.01	0.01	0.10	2.40	5.48	6.22	7.17	8.75	11.67	14.77	
150°		0.04	0.01	0.01	0.09	2.35	4.81	6.18	7.16	8.63	11.57	16.97	
165°		0.03	0.01	0.01	0.08	2.22	4.65	6.07	7.15	8.40	11.31	19.79	
180°		0.03	0.01	**0.01**	0.07	2.30	4.53	6.09	7.11	8.56	11.51	17.27	

AVERAGE DAYLIGHT TRANSMITTANCE 4.77

MAX 22.43

MIN 0.01

DAYLIGHT TRANSMITTANCE OF MESH: 07w

y \ x	0°	15°	30°	45°	60°	75°	90°	105°	120°	135°	150°	165°	180°
0°		0.78	0.50	0.45	2.40	8.23	11.71	15.89	20.62	27.01	36.04	35.19	
15°		0.77	0.47	0.45	1.86	8.21	12.05	16.12	20.13	26.63	38.47	48.71	
30°		0.85	0.48	0.46	2.30	8.32	12.05	15.83	20.72	27.82	38.28	38.18	
45°		0.75	0.47	0.50	1.49	8.42	12.46	16.57	20.49	28.94	38.34	37.27	
60°		1.18	0.63	0.52	2.74	7.78	11.10	16.74	21.52	27.32	29.32	17.62	
75°			1.61	1.10	3.12	7.38	14.80	14.97	17.83	17.72	8.33		
90°													
105°			0.55	0.49	1.90	6.70	11.21	15.16	19.29	15.92	9.57		
120°		0.53	0.29	0.36	1.65	8.61	12.01	16.52	21.70	28.35	30.26	22.09	
135°		0.40	0.33	0.34	2.23	8.94	11.82	15.78	20.73	28.02	41.24	**49.91**	
150°		0.40	0.27	0.31	1.56	6.95	11.48	15.54	20.30	27.39	40.20	43.93	
165°		0.32	0.27	0.30	1.54	7.88	11.50	15.45	20.60	27.11	39.57	37.80	
180°		0.31	**0.26**	0.30	2.00	7.83	11.79	15.59	20.45	27.28	39.17	38.71	

AVERAGE DAYLIGHT TRANSMITTANCE 13.94

MAX 49.91

MIN 0.26

DAYLIGHT TRANSMITTANCE OF MESH: 07g

y \ x	0º	15º	30º	45º	60º	75º	90º	105º	120º	135º	150º	165º	180º
0º		0.38	0.15	0.04	1.07	6.95	11.81	16.30	21.61	29.06	39.40	43.54	
15º		0.36	0.12	0.04	1.16	6.81	11.52	15.64	20.97	28.46	38,35	41.69	
30º		0.36	0.08	0.04	1.11	6,79	11.56	15.53	20.57	28.35	37.72	37.37	
45º		0.26	0.06	0.06	1.19	6.76	11.51	15.57	20.79	28.44	36.80	31.63	
60º		0.56	0.12	0.08	1.42	8.17	11.98	15.97	20.74	25.71	27.10	10.90	
75º			0.88	0.34	1.90	6.44	13.26	13.88	16.36	15.87	7.02		
90º													
105º			0.35	0.26	1.67	6.92	11.10	19.41	18.83	17.60	9.04		
120º		0.31	0.05	0.06	1.16	7.13	11.77	17.11	21.62	27.71	29.16	21.91	
135º		0.08	0.04	0.04	0.96	6.63	11.19	15.84	20.34	27.69	38.65	45.09	
150º		0.09	0.04	**0.02**	1.33	7.17	10.63	14.93	19.94	26.56	38.69	**45.31**	
165º		0.10	0.03	0.03	0.92	6.47	10.85	15.09	19.92	25.60	36.38	43.97	
180º		0.11	0.03	0.02	0.74	6.35	10.67	14.50	19.13	25.62	36.74	42.88	

AVERAGE DAYLIGHT TRANSMITTANCE 13.27

MAX 45.31

MIN 0.02

DAYLIGHT TRANSMITTANCE OF MESH: 07b

y \ x	0º	15º	30º	45º	60º	75º	90º	105º	120º	135º	150º	165º	180º
0º		0.71	0.06	0.01	1.08	7.93	12.15	16.67	22.36	29.63	40.29	37.85	
15º		0.69	0.04	0.01	1.20	7.79	11.90	16.19	21.41	28.68	40.79	41.24	
30º		0.80	0.02	0.01	1.26	8.01	11.73	16.11	21.46	29.03	38.89	39.62	
45º		0.56	0.01	0.01	1.35	8.14	11.90	16.60	21.45	29.28	39.08	34.36	
60º		0.46	0.03	0.02	1.51	8.01	11.43	16.16	21.27	27.35	28.74	14.78	
75º			0.60	0.20	1.96	6.34	10.40	14.54	17.64	17.79	7.81		
90º													
105º			0.32	0.21	1.36	6.64	10.44	18.52	17.24	15.30	7.03		
120º		0.31	0.02	0.02	1.10	7.85	11.73	16.80	20.97	26.63	25.29	14.58	
135º		0.04	0.01	0.01	1.12	7.92	11.74	16.29	20.74	27.86	37.23	35.63	
150º		0.06	0.01	0.01	1.10	7.68	11.66	16.30	20.89	27.81	38.98	40.55	
165º		0.06	0.01	0.01	1.11	7.66	11.56	15.98	21.14	27.53	39.03	36.03	
180º		0.09	0.01	**0.00**	0.99	6.85	11.60	15.68	20.92	27.61	38.54	**43.38**	

AVERAGE DAYLIGHT TRANSMITTANCE 13.49

MAX 43.38

MIN 0.00

DAYLIGHT TRANSMITTANCE OF MESH: 08w

y \ x	0º	15º	30º	45º	60º	75º	90º	105º	120º	135º	150º	165º	180º
0º		0.80	0.28	0.29	0.39	3.43	7.65	11.52	16.47	22.98	34.29	38.29	
15º		0.83	0.28	0.28	0.37	1.19	7.93	11.81	16.11	22.73	35.98	33.43	
30º		0.98	0.28	0.29	0.39	4.01	7.79	11.60	15.97	23.10	35.15	45.17	
45º		0.93	0.28	0.34	0.41	3.48	7.85	11.85	16.28	23.47	34.86	37.21	
60º		0.96	0.43	0.36	0.45	3.83	8.44	12.38	17.00	23.18	32.37	17.18	
75º			1.43	0.75	0.82	3.57	8.46	10.95	13.73	14.41	9.51		
90º													
105º			0.52	0.33	0.55	3.17	7.44	11.39	15.94	19.32	18.52		
120º		0.53	0.21	0.26	0.37	3.63	8.97	12.33	17.38	23.84	31.03	27.80	
135º		0.22	0.19	0.21	0.31	3.76	7.58	11.49	16.19	23.48	37.98	**65.54**	
150º		0.20	0.15	0.19	0.29	3.24	7.29	11.00	15.35	21.86	35.84	58.48	
165º		0.18	0.14	0.19	0.28	3.67	7.34	10.81	15.68	21.95	34.72	55.96	
180º		0.20	**0.14**	0.18	0.28	3.70	7.57	10.92	15.96	21.97	34.32	54.89	

AVERAGE DAYLIGHT TRANSMITTANCE 12.15

MAX 65.54

MIN 0.14

DAYLIGHT TRANSMITTANCE OF MESH: 08b

y \ x	0º	15º	30º	45º	60º	75º	90º	105º	120º	135º	150º	165º	180º
0º		0.49	0.09	0.03	0.02	2.87	7.52	11.61	16.40	22.74	33.33	48.29	
15º		0.60	0.09	0.03	0.01	3.37	7.47	11.52	16.11	22.45	34.55	47.30	
30º		0.56	0.04	0.01	0.01	2.86	7.35	11.34	16.03	22.53	33.24	43.01	
45º		0.61	0.03	0.02	0.01	2.65	8.03	11.69	16.49	23.15	33.29	37.21	
60º		0.99	0.05	0.02	0.03	3.38	8.80	11.78	16.17	21.71	27.20	14.54	
75º			0.69	0.14	0.17	2.60	7.30	10.55	14.24	13.79	10.49		
90º													
105º			0.32	0.12	0.19	2.19	6.52	11.73	14.38	16.80	11.67		
120º		0.31	0.03	0.02	0.05	2.76	8.47	12.12	16.43	22.69	26.26	16.86	
135º		0.06	0.02	0.01	0.02	2.74	7.30	11.44	15.72	22.33	33.62	47.41	
150º		0.07	0.01	0.01	0.01	3.07	7.10	11.18	15.41	21.61	33.14	**52.34**	
165º		0.11	0.01	0.01	0.01	2.95	7.23	11.32	15.97	21.67	33.24	52.06	
180º		0.12	0.01	0.01	**0.00**	2.88	7.36	11.39	15.75	21.97	33.18	48.20	

AVERAGE DAYLIGHT TRANSMITTANCE 11.42

MAX 52.34

MIN 0.00

DAYLIGHT TRANSMITTANCE OF MESH: 09w

y \ x	0°	15°	30°	45°	60°	75°	90°	105°	120°	135°	150°	165°	180°
0°		1.13	0.74	2.06	13.21	21.89	32.52	35.40	42.99	53.34	65.47	36.74	
15°		1.19	0.75	2.00	13.19	21.56	32.55	34.60	41.36	52.09	67.18	42.75	
30°		1.51	0.79	2.15	12.91	21.30	32.23	33.96	40.99	51.83	66.58	42.25	
45°		1.63	0.84	2.64	13.21	21.18	27.88	39.33	41.89	53.80	65.85	52.85	
60°		1.76	1.10	2.84	15.33	21.88	28.99	35.95	43.83	50.26	53.09	27.97	
75°			2.40	4.67	13.39	23.66	31.68	31.53	33.87	27.93	14.29		
90°													
105°			0.69	2.21	11.85	21.96	27.05	30.52	31.31	24.52	12.63		
120°		0.75	0.48	1.80	15.03	22.94	29.23	36.89	45.22	51.51	51.55	20.69	
135°		0.45	0.56	2.01	14.21	22.00	26.68	34.03	42.11	55.06	**69.86**	39.64	
150°		0.41	0.47	1.77	13.03	21.28	31.07	33.67	41.16	52.80	69.77	38.00	
165°		**0.37**	0.47	1.80	12.86	21.06	31.35	33.76	41.70	52.11	68.63	37.73	
180°		0.38	0.45	1.78	14.06	21.22	27.60	33.18	40.94	51.79	68.49	42.45	

AVERAGE DAYLIGHT TRANSMITTANCE 26.26

MAX 69.86

MIN 0.37

DAYLIGHT TRANSMITTANCE OF MESH: 09b

y \ x	0°	15°	30°	45°	60°	75°	90°	105°	120°	135°	150°	165°	180°
0°		0.58	0.07	1.26	13.47	21.68	32.97	35.63	44.17	54.85	65.71	38.90	
15°		0.64	0.06	0.94	13.27	21.11	32.21	35.18	43.32	54.44	**69.97**	45.51	
30°		0.56	0.03	0.82	13.67	22.26	29.04	35.07	43.12	55.13	68.17	38.04	
45°		0.48	0.03	1.04	13.79	21.08	28.98	41.00	43.24	55.10	64.31	38.95	
60°		0.59	0.07	1.41	14.54	20.66	28.80	35.83	43.28	49.97	47.15	19.76	
75°			0.83	2.62	13.25	20.61	29.54	32.30	31.05	22.82	8.41		
90°													
105°			0.81	1.41	10.17	23.10	28.66	35.39	29.73	21.66	9.33		
120°		0.41	0.05	1.11	14.02	22.44	30.28	37.29	45.22	50.97	45.48	12.96	
135°		0.05	0.02	0.79	13.72	22.17	29.46	38.57	44.10	56.24	64.89	40.98	
150°		0.06	0.01	0.83	13.53	22.09	33.13	35.85	43.54	54.55	67.73	32.21	
165°		0.04	0.01	0.81	13.30	21.49	33.33	35.39	43.76	54.21	69.44	31.70	
180°		0.03	**0.01**	1.09	13.81	21.73	33.19	35.31	43.44	54.36	68.75	40.94	

AVERAGE DAYLIGHT TRANSMITTANCE 25.89

MAX 69.97

MIN 0.01

DAYLIGHT TRANSMITTANCE OF MESH: 10w

y \ x	0°	15°	30°	45°	60°	75°	90°	105°	120°	135°	150°	165°	180°
0°		0.90	0.59	2.28	15.06	20.53	27.56	27.70	30.80	**32.44**	23.69	1.27	
15°		0.99	0.55	5.73	15.57	20.62	24.07	26.99	29.71	30.65	23.99	1.46	
30°		1.33	0.60	4.84	15.12	20.54	24.19	25.87	27.94	27.60	19.28	1.25	
45°		1.32	0.62	4.84	15.87	19.67	22.88	24.72	24.38	21.50	8.74	0.75	
60°		1.11	0.74	3.16	10.81	16.52	19.45	18.49	14.92	5.91	0.70	0.64	
75°			1.61	1.11	2.77	4.01	3.59	1.45	0.77	0.52	1.26		
90°													
105°			0.81	0.80	1.85	2.98	2.11	1.27	0.97	0.89	1.39		
120°		0.77	0.64	3.07	13.62	17.26	19.10	18.31	13.76	4.66	1.35	1.34	
135°		0.64	0.70	4.71	15.44	20.88	23.15	25.29	25.25	22.38	7.87	2.06	
150°		0.35	0.52	5.60	16.02	21.31	23.69	30.09	28.38	27.85	18.40	2.79	
165°		**0.31**	0.52	6.13	16.41	21.38	27.59	27.47	30.45	31.09	23.73	2.46	
180°		0.32	0.49	5.39	16.28	21.20	24.06	26.46	30.18	31.79	23.93	1.51	

AVERAGE DAYLIGHT TRANSMITTANCE 12.39

MAX 32.44

MIN 0.31

DAYLIGHT TRANSMITTANCE OF MESH: 10b

y \ x	0°	15°	30°	45°	60°	75°	90°	105°	120°	135°	150°	165°	180°
0°		0.32	0.02	5.57	14.98	19.84	22.82	25.40	27.92	28.06	18.49	0.27	
15°		1.03	0.02	5.24	14.56	19.18	22.30	24.45	26.31	26.11	18.07	0.34	
30°		0.89	0.02	5.02	14.53	19.77	22.83	24.04	25.26	23.94	14.14	0.22	
45°		0.49	0.02	3.87	13.46	18.28	20.79	22.25	21.13	17.31	4.51	0.13	
60°		0.37	0.04	1.76	9.79	14.55	16.48	15.48	11.62	3.02	0.10	0.31	
75°			0.60	0.41	2.05	3.27	2.02	0.61	0.22	0.16	0.33		
90°													
105°			0.32	0.24	1.26	2.08	1.21	0.23	0.14	0.21	0.72		
120°		0.31	0.04	1.97	9.05	13.88	15.69	14.33	9.59	2.03	0.14	0.76	
135°		0.04	0.02	3.65	12.85	17.84	20.60	21.78	20.54	16.12	3.18	0.16	
150°		0.05	0.01	4.51	13.78	18.64	21.08	23.71	24.67	23.33	13.95	0.25	
165°		0.03	0.01	5.11	14.62	19.22	22.08	24.68	26.61	25.89	17.10	0.27	
180°		0.03	**0.01**	5.55	15.91	20.61	23.74	26.57	28.61	**28.70**	19.48	0.16	

AVERAGE DAYLIGHT TRANSMITTANCE 10.45

MAX 28.70

MIN 0.01

DAYLIGHT TRANSMITTANCE OF MESH: 11w

y \ x	0º	15º	30º	45º	60º	75º	90º	105º	120º	135º	150º	165º	180º
0º		1.16	1.21	10.46	24.48	37.24	40.46	47.93	57.27	**68.23**	63.07	16.35	
15º		1.27	1.21	9.26	23.50	36.77	39.84	47.64	55.89	66.00	66.67	8.76	
30º		1.80	1.27	9.16	23.33	36.56	40.07	47.01	56.17	67.22	62.33	18.18	
45º		2.23	1.32	10.53	22.59	32.45	39.47	47.81	55.41	64.64	59.69	25.87	
60º		2.23	1.62	8.00	23.47	32.60	36.73	52.69	52.66	53.24	42.66	9.05	
75º			2.81	8.35	11.17	22.93	30.20	34.37	30.60	18.62	4.06		
90º													
105º			1.07	7.57	21.98	29.23	29.06	27.37	22.09	11.99	5.02		
120º		1.14	0.93	8.72	24.82	34.15	41.14	53.65	50.81	56.27	34.00	7.94	
135º		1.00	1.14	9.43	25.80	33.90	40.69	47.46	55.72	62.82	54.61	15.27	
150º		0.78	0.93	10.24	24.21	37.03	39.93	46.73	55.57	66.34	60.47	14.48	
165º		0.65	0.95	9.70	25.20	32.99	39.85	47.03	56.93	66.32	63.27	9.01	
180º		**0.64**	0.93	10.66	22.05	37.43	39.85	46.30	55.38	66.15	66.15	16.55	

AVERAGE DAYLIGHT TRANSMITTANCE 29.81

MAX 68.23

MIN 0.64

DAYLIGHT TRANSMITTANCE OF MESH: 11b

y \ x	0º	15º	30º	45º	60º	75º	90º	105º	120º	135º	150º	165º	180º
0º		1.05	0.02	9.70	24.60	39.31	41.79	50.11	59.24	**68.90**	59.95	10.83	
15º		1.03	0.02	10.26	24.75	39.34	40.40	49.02	57.59	67.17	68.45	5.46	
30º		0.70	0.02	9.96	23.48	34.24	41.67	49.25	57.87	67.77	58.62	11.29	
45º		0.77	0.03	1.68	23.88	28.28	41.37	50.08	57.60	64.43	59.08	19.94	
60º		0.46	0.10	7.30	24.88	33.10	42.32	47.31	50.81	50.29	37.87	5.09	
75º			0.97	8.39	19.51	28.43	31.68	31.91	25.85	13.21	3.75		
90º													
105º			0.55	4.54	17.53	25.89	28.78	28.53	19.01	8.89	2.73		
120º		0.39	0.07	3.98	23.59	34.17	42.74	57.65	50.54	46.20	28.19	3.00	
135º		0.06	0.03	8.33	24.69	34.21	42.34	50.00	56.81	61.65	49.29	11.52	
150º		0.05	0.01	9.08	25.16	34.01	41.26	49.17	57.36	67.31	56.10	8.34	
165º		0.04	0.01	10.08	24.30	37.77	40.40	48.89	58.16	66.84	60.59	4.33	
180º		0.03	**0.01**	8.89	24.40	33.44	41.03	47.53	56.56	66.15	64.06	10.36	

AVERAGE DAYLIGHT TRANSMITTANCE 29.00

MAX 68.90

MIN 0.01

DAYLIGHT TRANSMITTANCE OF MESH: 12w

y \ x	0º	15º	30º	45º	60º	75º	90º	105º	120º	135º	150º	165º	180º
0º		1.39	0.66	0.94	9.07	16.91	23.63	30.69	39.06	51.17	62.59	29.83	
15º		1.33	0.67	0.86	9.66	15.97	23.79	30.10	38.22	50.25	**67.43**	42.92	
30º		1.47	0.68	0.87	9.91	16.65	23.80	34.08	38.01	50.18	64.19	54.40	
45º		1.40	0.68	0.97	10.51	16.42	24.04	30.88	39.36	51.19	63.38	56.05	
60º		1.55	0.90	1.13	10.16	16.70	24.75	30.83	39.31	47.68	49.57	24.45	
75º			2.07	1.96	7.78	16.30	24.04	27.98	31.11	27.83	14.11		
90º													
105º			0.66	1.64	9.60	20.60	23.15	25.72	26.37	18.47	7.13		
120º		0.73	0.43	0.91	10.73	17.65	24.35	30.85	38.92	43.87	40.65	25.45	
135º		0.44	0.53	0.74	9.02	16.43	23.24	29.62	41.92	49.18	61.35	47.95	
150º		0.40	0.43	0.67	8.83	16.39	22.61	28.81	36.70	48.55	65.12	46.55	
165º		**0.38**	0.43	0.65	9.60	16.38	25.39	29.10	37.59	47.89	67.02	49.65	
180º		0.41	0.44	0.65	9.47	16.45	25.89	28.92	37.14	48.21	66.67	50.07	

AVERAGE DAYLIGHT TRANSMITTANCE 23.66

MAX 67.43

MIN 0.38

DAYLIGHT TRANSMITTANCE OF MESH: 12b

y \ x	0º	15º	30º	45º	60º	75º	90º	105º	120º	135º	150º	165º	180º
0º		0.32	0.07	0.09	8.04	16.31	21.78	29.43	38.14	50.33	64.99	54.70	
15º		0.34	0.07	0.08	9.00	13.19	21.90	32.41	37.30	49.25	**66.67**	56.18	
30º		0.25	0.03	0.07	7.85	15.78	21.24	33.33	37.45	49.27	62.60	51.20	
45º		0.19	0.02	0.25	7.84	16.44	22.94	29.24	41.72	47.07	54.46	39.24	
60º		0.84	0.05	0.27	9.06	15.29	22.28	28.33	34.78	39.53	37.29	13.08	
75º			0.74	0.99	7.80	15.37	19.42	24.37	23.80	18.42	6.48		
90º													
105º			0.35	0.60	5.57	11.51	20.16	28.05	23.21	19.27	6.36		
120º		0.37	0.03	0.24	6.81	15.25	22.39	29.98	34.73	38.75	33.61	15.02	
135º		0.04	0.02	0.15	8.58	15.39	22.18	29.08	35.59	44.92	51.70	37.23	
150º		0.05	0.01	0.12	7.70	15.47	20.45	32.14	35.81	46.03	58.72	39.31	
165º		0.03	0.01	0.14	8.68	15.28	22.19	28.99	36.63	46.67	60.59	39.57	
180º		0.02	**0.01**	0.11	7.74	15.59	25.03	28.59	35.96	46.84	61.72	47.12	

AVERAGE DAYLIGHT TRANSMITTANCE 21.62

MAX 66.67

MIN 0.01

DAYLIGHT TRANSMITTANCE OF MESH: p13g

y \ x	0°	15°	30°	45°	60°	75°	90°	105°	120°	135°	150°	165°	180°
0°		14.16	27.77	49.21	51.12	55.06	57.00	59.08	62.25	69.73	74.82	14.59	
15°		12.50	26.93	41.65	50.61	54.33	56.00	58.25	61.91	69.68	77.35	18.93	
30°		9.09	23.37	38.31	47.49	52.58	54.29	57.09	61.99	70.51	76.13	21.00	
45°		5.72	15.41	33.20	43.48	48.14	50.88	56.58	60.98	70.28	75.08	31.34	
60°		4.74	10.37	22.91	36.79	43.82	54.64	53.72	60.28	67.06	66.33	27.42	
75°			6.41	21.96	32.04	38.17	43.75	49.62	49.26	45.35	28.02		
90°													
105°			3.18	11.41	31.61	39.88	40.90	43.55	47.53	43.95	32.11		
120°		**1.93**	7.58	21.40	34.95	41.97	47.26	52.71	59.73	64.87	64.77	24.77	
135°		3.85	14.14	29.78	40.91	47.00	50.90	54.13	59.17	68.47	74.11	40.98	
150°		6.70	18.46	37.01	46.37	51.39	53.76	56.34	60.33	69.44	**79.07**	35.17	
165°		5.95	24.22	46.23	48.91	53.24	55.08	56.93	61.32	68.07	78.55	33.90	
180°		7.54	24.84	41.77	50.25	54.15	55.75	57.40	62.20	67.86	78.39	35.76	

AVERAGE DAYLIGHT TRANSMITTANCE 43.83

MAX 79.07

MIN 1.93

DAYLIGHT TRANSMITTANCE OF MESH: p13b

y \ x	0°	15°	30°	45°	60°	75°	90°	105°	120°	135°	150°	165°	180°
0°		8.46	26.31	42.53	52.69	57.93	60.53	63.33	66.71	74.25	81.77	29.28	
15°		7.09	26.77	40.42	51.01	56.56	59.71	61.13	64.14	72.53	**82.70**	32.92	
30°		5.59	25.04	37.27	47.94	54.26	57.23	59.33	63.40	72.53	79.31	28.23	
45°		4.26	16.31	32.48	42.57	48.92	52.63	56.88	60.64	71.15	76.31	31.98	
60°		2.91	8.82	22.39	34.65	43.01	50.21	53.10	58.66	64.71	66.18	36.12	
75°			7.51	21.83	36.63	38.70	49.73	48.36	50.48	46.75	31.85		
90°													
105°			1.24	8.75	26.72	34.52	41.87	51.92	45.11	38.06	24.78		
120°		**0.94**	4.73	16.54	32.09	42.15	55.80	57.65	60.27	64.87	63.16	24.48	
135°		2.20	12.81	26.92	45.80	48.07	53.00	57.46	61.34	71.06	75.89	36.88	
150°		3.34	16.89	34.91	52.35	52.64	56.31	59.03	62.26	71.76	80.81	32.90	
165°		5.46	25.35	44.72	49.81	55.06	58.39	60.88	64.33	71.23	81.23	40.71	
180°		6.94	24.13	47.10	51.61	56.81	59.29	60.99	63.12	70.26	81.51	43.53	

AVERAGE DAYLIGHT TRANSMITTANCE 44.91

MAX 82.70

MIN 0.94

DAYLIGHT TRANSMITTANCE OF MESH: p14w

y \ x	0°	15°	30°	45°	60°	75°	90°	105°	120°	135°	150°	165°	180°
0°		21.24	35.71	52.72	57.82	60.92	62.84	65.75	71.69	81.77	82.25	38.40	
15°		17.69	34.19	49.74	59.89	59.02	61.84	63.90	69.37	80.90	**85.24**	38.99	
30°		15.54	30.88	48.04	54.13	58.01	60.54	62.56	68.94	80.40	80.90	28.80	
45°		11.67	22.64	44.06	51.81	55.26	57.89	62.48	68.24	79.18	79.38	31.10	
60°		13.03	19.12	33.85	47.60	53.17	57.38	60.33	67.21	74.12	71.40	43.83	
75°			23.23	42.16	52.16	59.11	62.17	58.09	56.70	53.95	39.67		
90°													
105°			7.54	27.46	39.66	47.80	51.06	57.89	55.36	50.96	37.22		
120°		**3.34**	11.42	28.54	41.71	55.16	54.70	61.41	68.65	73.12	65.48	30.22	
135°		5.16	17.52	36.41	47.20	52.54	56.76	60.79	67.33	77.65	73.05	34.46	
150°		7.37	22.70	40.76	49.22	54.28	57.28	60.95	65.82	76.02	76.45	24.48	
165°		7.68	27.74	52.43	53.66	56.77	59.49	62.40	68.04	76.84	78.82	23.69	
180°		9.33	28.35	47.10	54.59	57.59	58.97	61.32	65.35	75.38	77.86	28.99	

AVERAGE DAYLIGHT TRANSMITTANCE 50.45

MAX 85.24

MIN 3.34

DAYLIGHT TRANSMITTANCE OF MESH: f15w

y \ x	0°	15°	30°	45°	60°	75°	90°	105°	120°	135°	150°	165°	180°
0°		25.59	40.99	51.85	46.25	46.78	47.74	48.05	47.84	45.48	42.45	22.43	
15°		24.62	36.35	48.86	45.63	46.60	47.14	47.75	46.73	45.06	39.77	16.74	
30°		20.21	41.96	43.14	43.95	45.35	45.96	45.40	45.25	43.22	37.14	12.54	
45°		25.55	45.57	52.51	53.99	54.33	54.82	**55.22**	53.89	51.19	43.08	15.23	
60°		11.52	31.12	34.15	41.10	42.81	42.17	40.50	38.57	35.74	25.56	**2.03**	
75°			16.41	23.87	32.39	31.28	36.06	29.51	24.31	16.82	4.63		
90°													
105°			13.32	31.29	34.91	34.82	32.40	32.30	24.04	16.53	6.03		
120°		10.98	40.52	43.89	45.13	50.00	43.54	43.06	42.27	35.27	23.74	3.94	
135°		24.87	43.11	51.76	46.85	46.38	44.89	45.24	42.11	39.76	33.72	7.13	
150°		26.85	40.39	51.81	46.37	46.85	46.36	46.09	44.43	42.55	37.82	11.31	
165°		25.95	42.45	47.24	46.73	46.87	46.47	46.68	46.23	43.16	37.53	15.67	
180°		24.49	43.51	53.55	45.66	46.84	46.51	46.19	46.19	44.96	38.80	18.35	

AVERAGE DAYLIGHT TRANSMITTANCE 37.31

MAX 55.22

MIN 2.03

DAYLIGHT TRANSMITTANCE OF MESH: f15b												
y \ x	0º	15º	30º	45º	60º	75º	90º	105º	120º	135º	150º	165º	180º
0º		20.80	39.32	52.90	47.96	49.43	50.17	49.89	49.15	47.49	41.49	27.68	
15º		19.30	39.73	51.49	47.91	48.95	49.49	48.67	47.91	45.90	41.98	27.70	
30º		14.91	38.68	50.98	47.35	48.97	48.77	48.38	47.09	45.97	40.74	18.80	
45º		9.57	32.93	42.96	53.08	47.37	47.37	48.11	47.64	44.03	39.14	12.33	
60º		4.43	27.04	33.52	42.53	43.39	49.58	43.80	42.03	38.88	29.57	3.26	
75º			12.58	21.93	31.95	31.61	38.48	31.75	27.20	19.02	6.84		
90º													
105º			4.68	16.42	28.45	28.10	29.64	27.16	27.49	16.32	5.02		
120º		2.75	28.44	35.33	40.23	42.00	43.72	43.29	41.38	37.24	27.10	6.86	
135º		8.10	32.48	40.84	44.58	45.61	46.70	48.41	44.83	42.12	38.30	8.60	
150º		13.23	32.67	48.91	45.95	47.48	47.82	46.86	46.36	44.29	39.22	16.48	
165º		17.84	36.39	46.06	47.11	48.01	48.45	48.66	47.33	44.74	40.75	17.66	
180º		20.38	37.78	46.29	47.39	48.62	48.87	48.43	47.38	45.64	40.96	20.86	
											AVERAGE DAYLIGHT TRANSMITTANCE		36.38

MAX 53.08

MIN 2.75

Table A.4. Daylight transmittance results of assessed meshes

A.4 Conclusions contrasting graphs

As mentioned in section 5.4, with the aim of contrasting some conclusions obtained in chapter 4, we have drawn some graphs with the values obtained in the laboratory in order to describe the variation of transmittance through three different meshes with different *SW*/*w* ratios for incident radiation directions included along some vertical planes. We chose samples number 02 (*SW/w*=4), 11 (*SW/w*=3,143) and 06 (*SW/w*=2,1).

The following graphs show the registers for each color of the mentioned meshes. Each graph represents the values of specular transmittance for a given fixed rotation angle around *y* axis of the sample holder and for every position around *x* axis, from 15º to 165º (0º and 180º positions on *x* axis give null values). We have drawn the graphs for the next positions of the sample holder in *y* axis: 0º, 45º, 135º and 180º. As aforementioned, these graphs describe the specular light transmission trough a mesh for several the incident directions included in a vertical plane.

MESH 02 (y=0º)

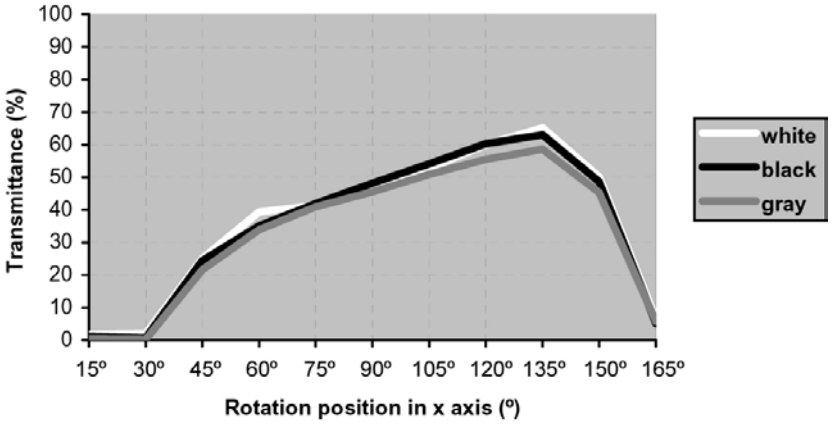

MESH 02 (y=45º)

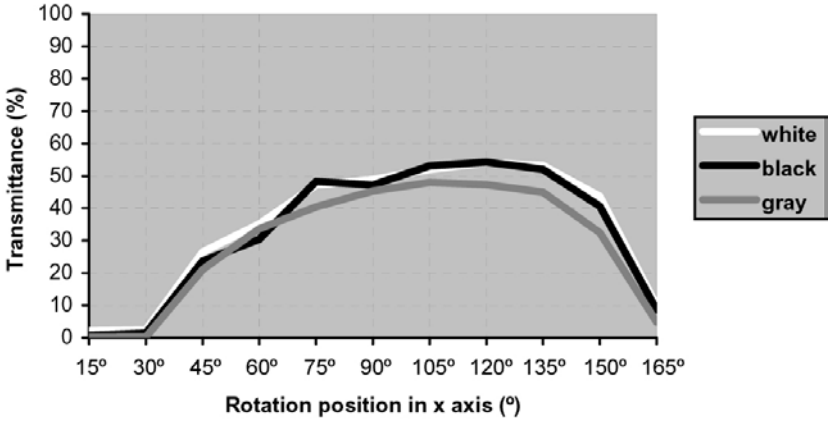

MESH 02 (y=135º)

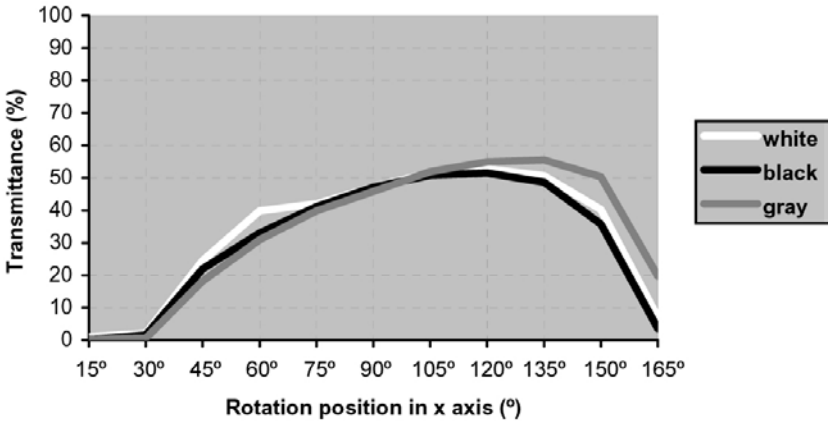

MESH 02 (y=180º)

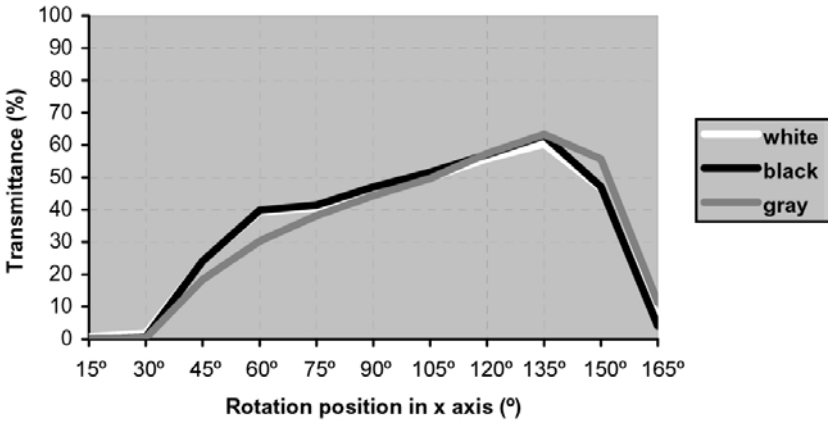

MESH 11 (y=0º)

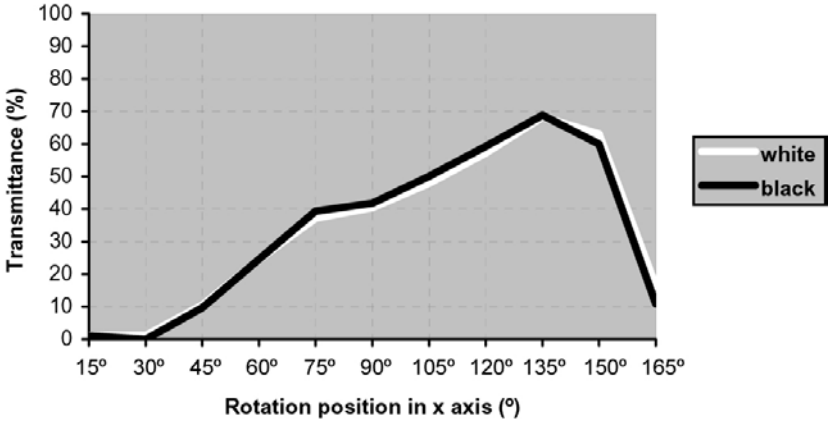

MESH 11 (y=45º)

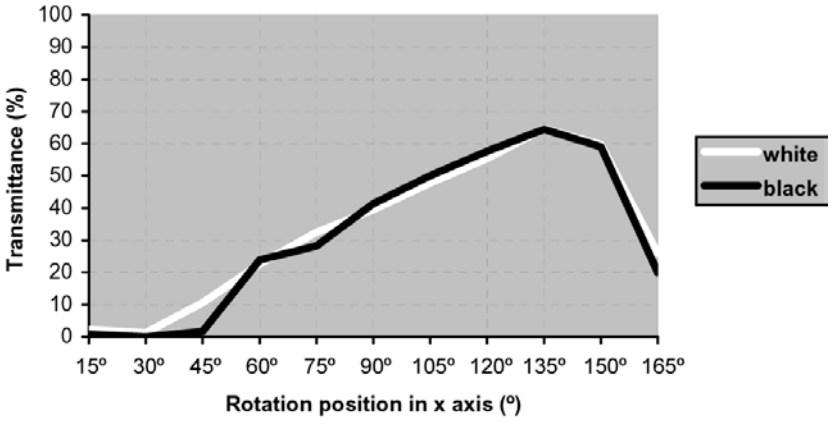

MESH 11 (y=135º)

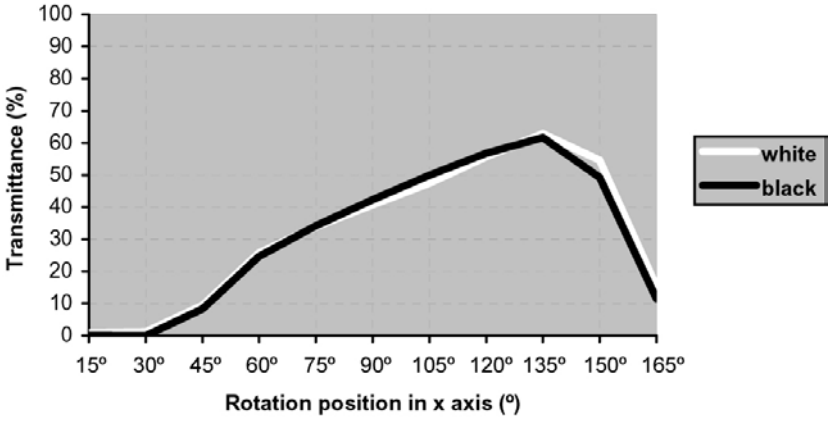

MESH 11 (y=180º)

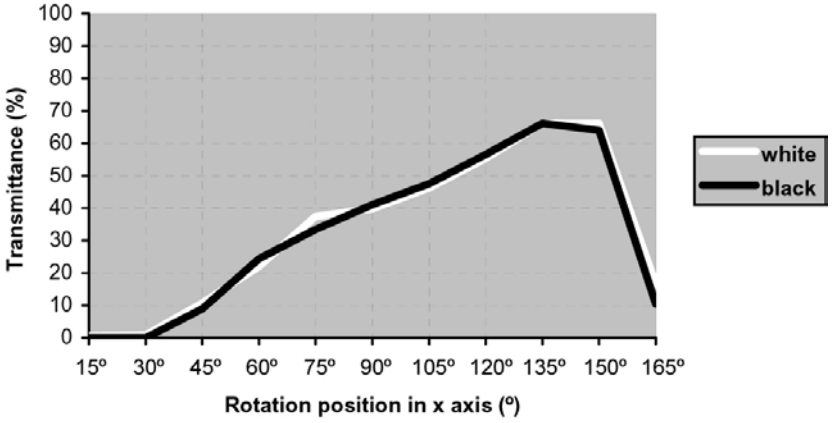

MESH 06 (y=0º)

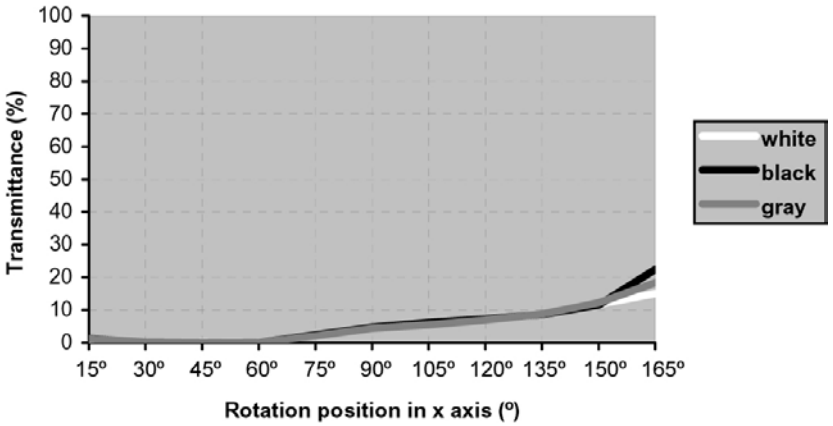

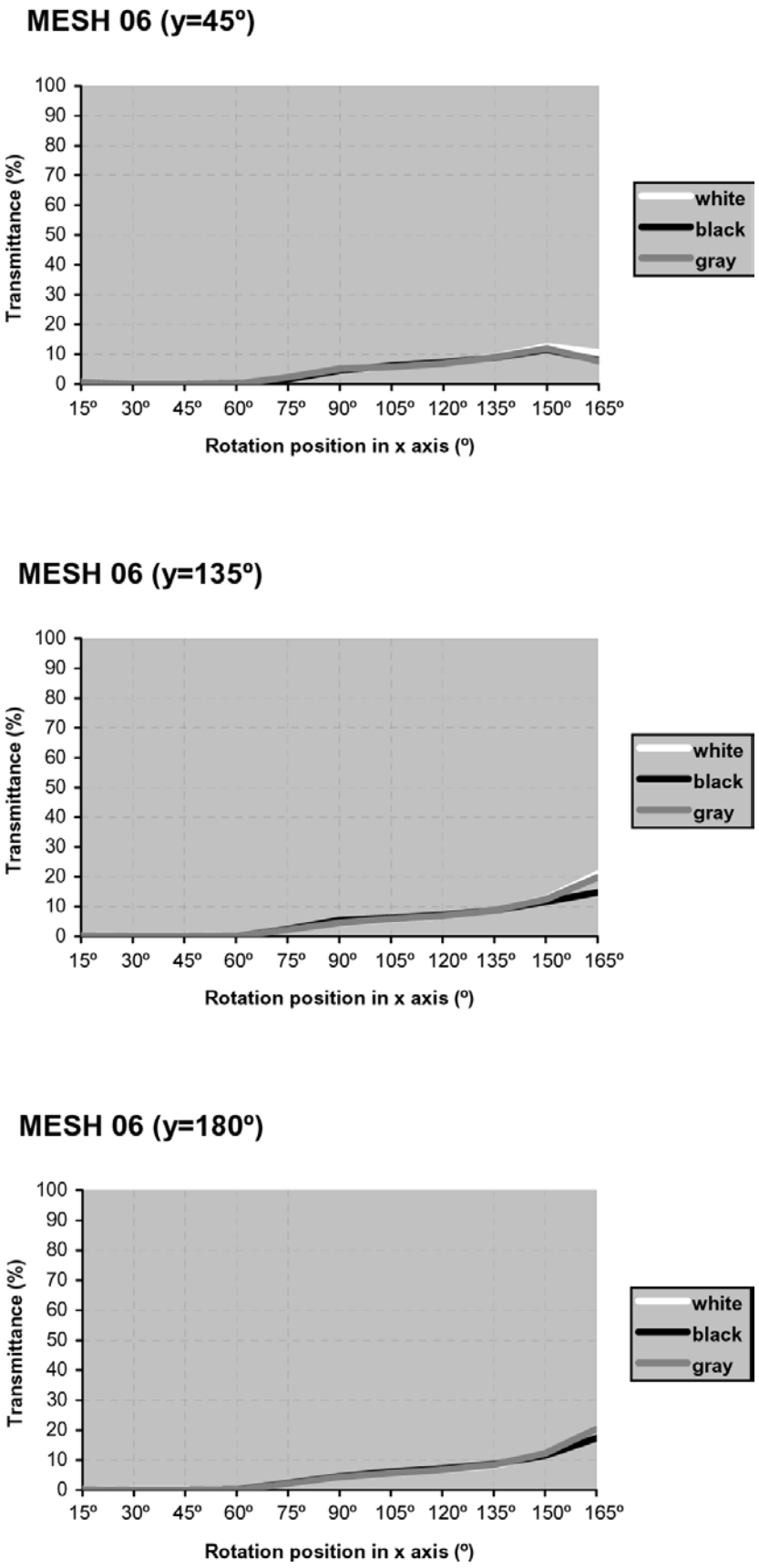

Fig. A.1. Luminous specular transmittance through EM meshes 02, 11 and 06 for incident directions included in several vertical planes; i.e., planes with fixed value in *y* axis and varying values in *x* axis.

We have also drawn some graphs with the aim of visualizing the variation of specular transmittance through EM meshes for incident directions included along a horizontal plane. These graphs include the different values corresponding to all the rotation angles of the sample holder around *y* axis (from 0º to 180º) for some given fixed rotation angles around *x* axis. Those fixed positions in *x* axis are the ones corresponding to 90º and 150º. The chosen samples are the same from the previous graphs (samples number 02, 11 and 06).

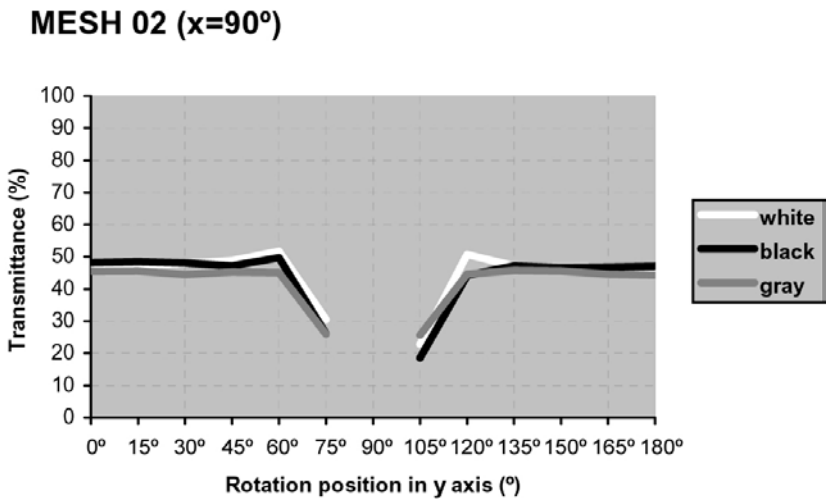

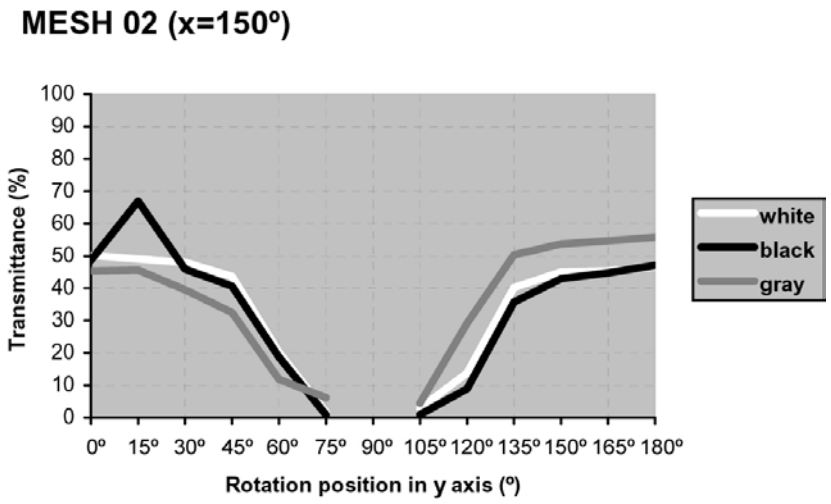

MESH 11 (x=90º)

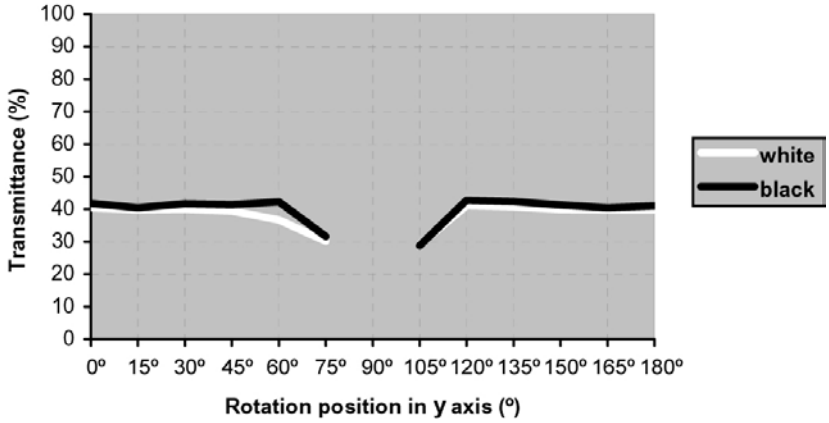

MESH 11 (x=150º)

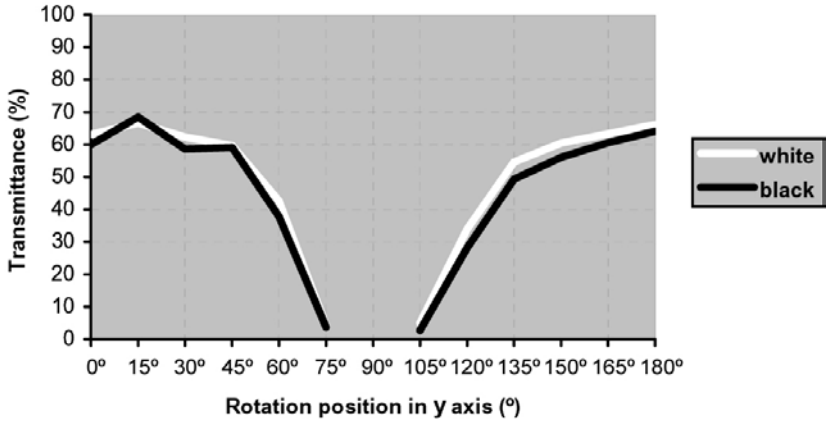

MESH 06 (x=90º)

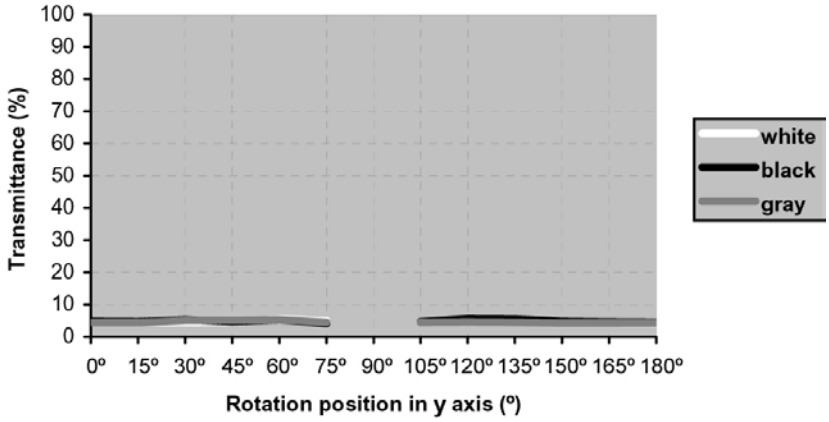

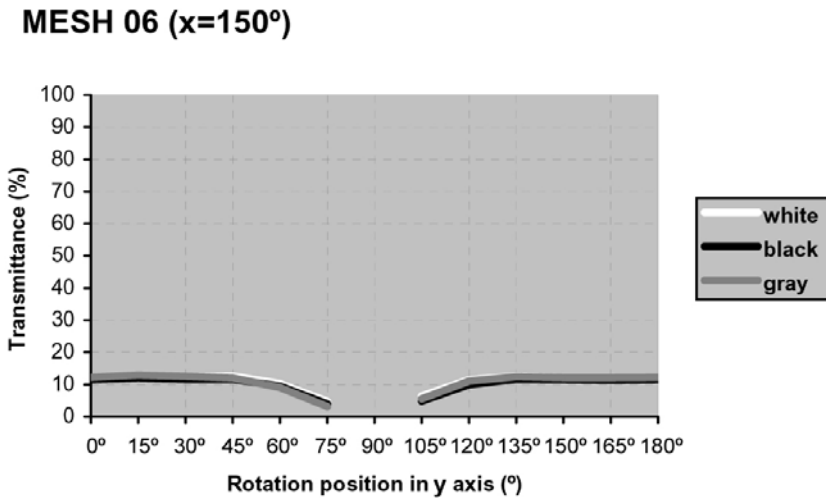

Fig. A.2. Luminous specular transmittance through EM meshes 02, 11 and 06 for incident radiation directions included in several planes intersecting the mesh through a horizontal line; i.e., planes with fixed value in *x* axis and varying values in *y* axis.

APPENDIX B COMPUTER AIDED ASSESSMENT RESULTS

B.1 Appendix introduction

This appendix contains extended data with the results obtained in computer aided simulations explained in chapter 6 “Computer aided assessment”. On one hand, the complete series of datasheet for all assessed meshes are listed. On the other hand, all the tables generated from the comparative analysis with lab results are shown.

B.2 Computer simulation results

As mentioned in chapter 6, Radiance and genBSDF were used to obtain a list of BSDF (*Ls/Ei*) values for each combination of directions of incidence and scattering. Possible incidence and scattering directions are always related to Klems basis.

Based on these BSDF values, a series of datasheet can be generated for each analyzed mesh and incident patch. On each sheet, all data mentioned in sections 6.6.3.2 and 6.6.3.3 is summarized.

All values on datasheets are related to the same incident patch, in order to enable a better comparison between different samples. To simulate a possible position of the sun in the sky as light-source, incident patch 41 was chosen.

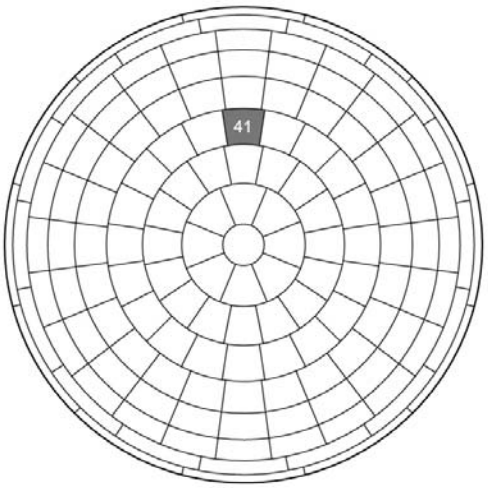

Fig. B.1. Incident patch 41 on incoming hemisphere

MESH SAMPLE NUMBER

01w

PARAMETERS

LW	SW	w	e	b	i	color
200	73	24	1	7	33	

TRANSMITTANCE

INCIDENT PATCH	41

	Es/Ei (%)	OUTG. PATCH
MÁX	22,388	41
MÍN	0,017	52
ABS. MEAN	0,194	
SCATT. MEAN	0,097	
SUM (%)	30,567	

VERTICAL SECTION

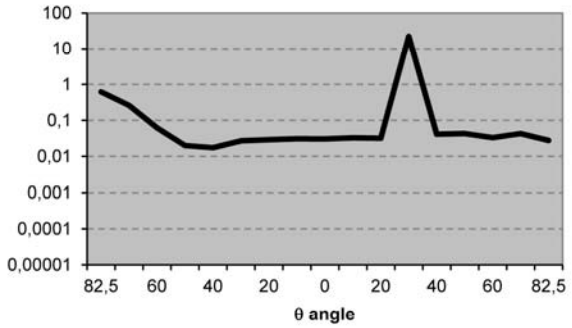

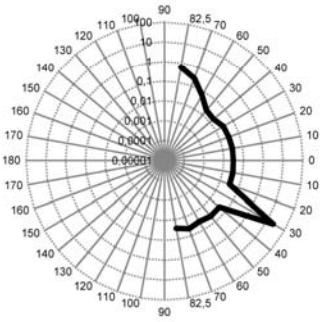

HORIZONTAL SECTION

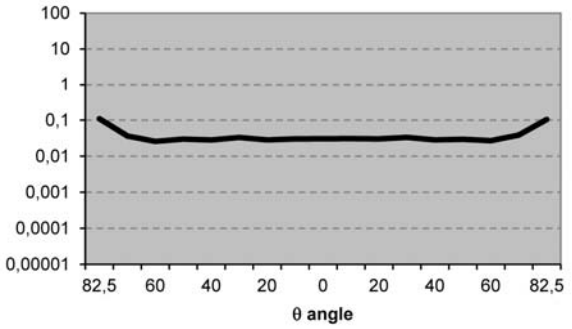

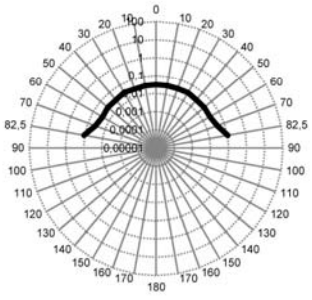

MESH SAMPLE NUMBER

01g

PARAMETERS

LW	SW	w	e	b	i	color
200	73	24	1	7	33	

TRANSMITTANCE

INCIDENT PATCH	41

	Es/Ei (%)	OUTG. PATCH
MÁX	22,359	41
MÍN	0,004	53
ABS. MEAN	0,137	
SCATT. MEAN	0,039	
SUM (%)	25,236	

VERTICAL SECTION

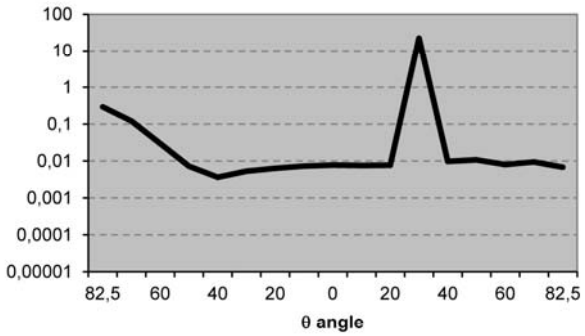

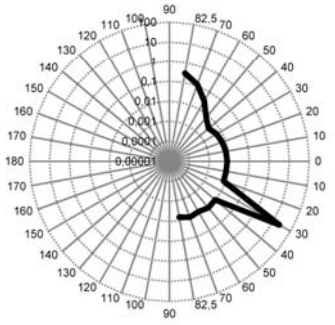

HORIZONTAL SECTION

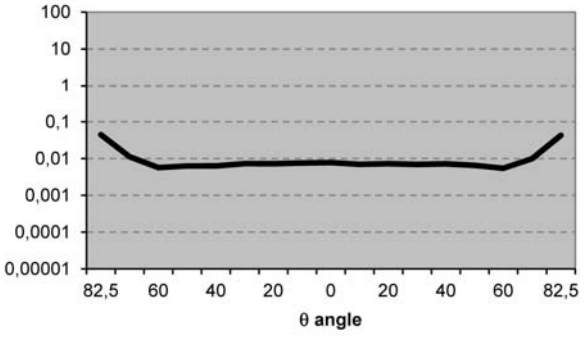

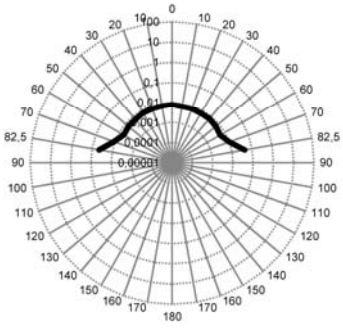

MESH SAMPLE NUMBER

01b

PARAMETERS

LW	SW	w	e	b	i	color
200	73	24	1	7	33	

TRANSMITTANCE

INCIDENT PATCH	41

	Es/Ei (%)	OUTG. PATCH
MÁX	22,350	41
MÍN	0,000	106
ABS. MEAN	0,100	
SCATT. MEAN	0,002	
SUM (%)	22,489	

VERTICAL SECTION

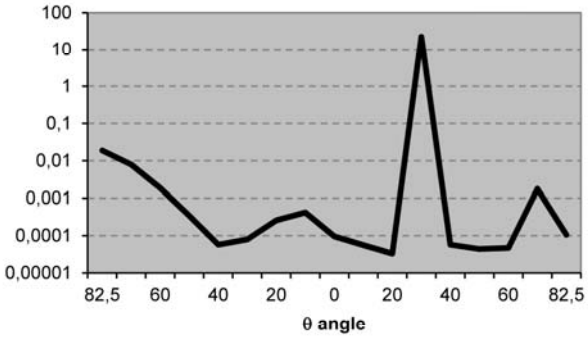

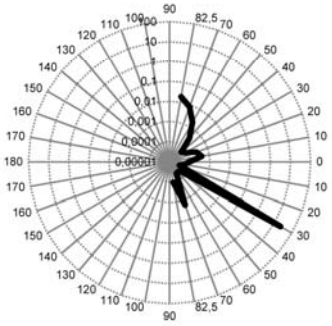

HORIZONTAL SECTION

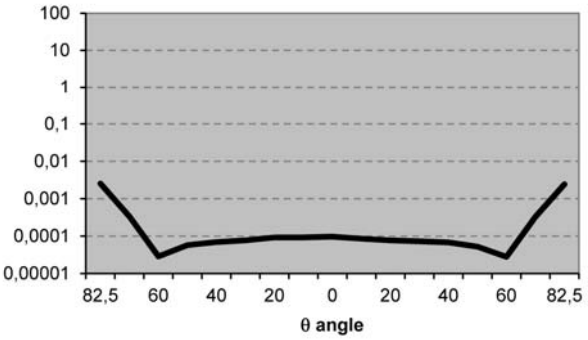

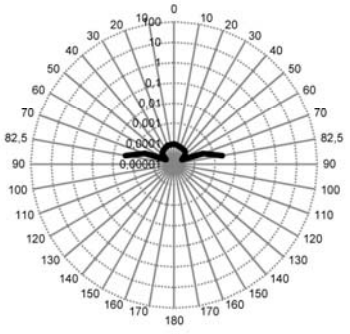

MESH SAMPLE NUMBER

02w

PARAMETERS

LW	SW	w	e	b	i	color
16	8	2	2	1	4,5	

TRANSMITTANCE

INCIDENT PATCH	41

	Es/Ei (%)	OUTG. PATCH
MÁX	37,118	41
MÍN	0,008	3
ABS. MEAN	0,221	
SCATT. MEAN	0,060	
SUM (%)	43,127	

VERTICAL SECTION

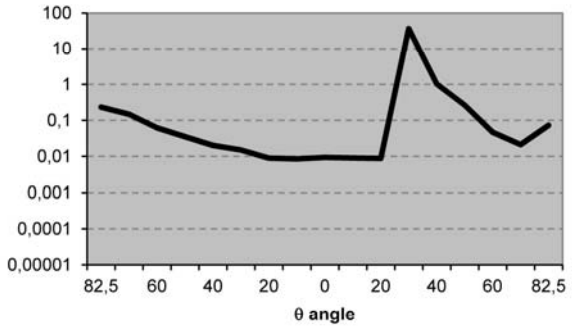

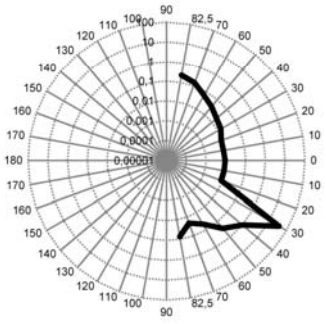

HORIZONTAL SECTION

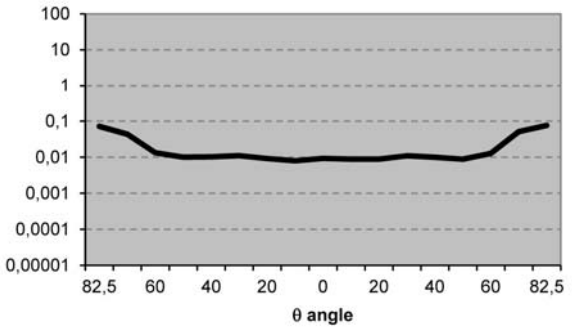

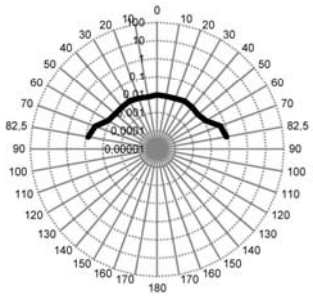

MESH SAMPLE NUMBER

02g

PARAMETERS

LW	SW	w	e	b	i	color
16	8	2	2	1	4,5	

TRANSMITTANCE

INCIDENT PATCH	41

	Es/Ei (%)	OUTG. PATCH
MÁX	36,947	41
MÍN	0,001	28
ABS. MEAN	0,183	
SCATT. MEAN	0,022	
SUM (%)	38,697	

VERTICAL SECTION

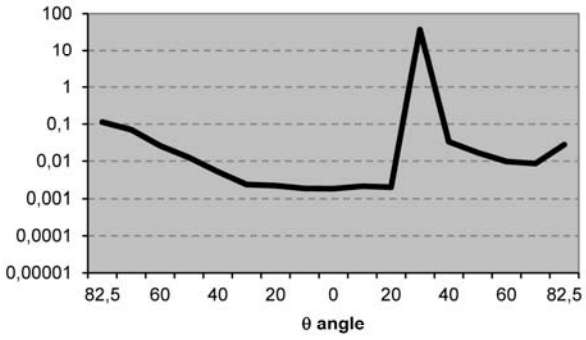

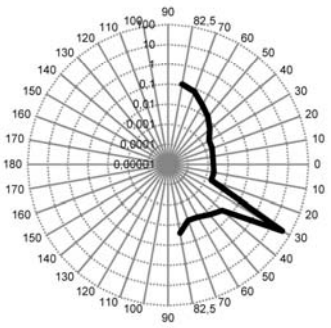

HORIZONTAL SECTION

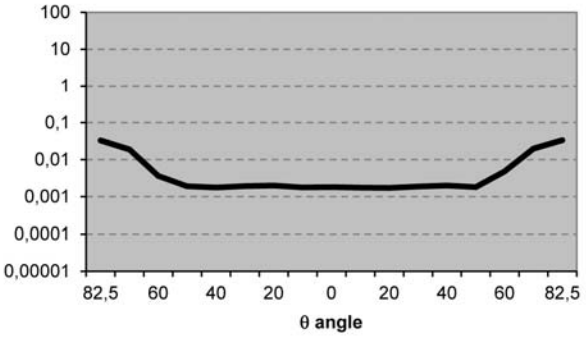

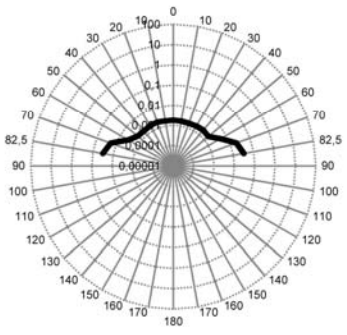

MESH SAMPLE NUMBER

02b

PARAMETERS

LW	SW	w	e	b	i	color
16	8	2	2	1	4,5	

TRANSMITTANCE

INCIDENT PATCH	41

	Es/Ei (%)	OUTG. PATCH
MÁX	36,945	41
MÍN	0,000	70
ABS. MEAN	0,163	
SCATT. MEAN	0,002	
SUM (%)	37,114	

VERTICAL SECTION

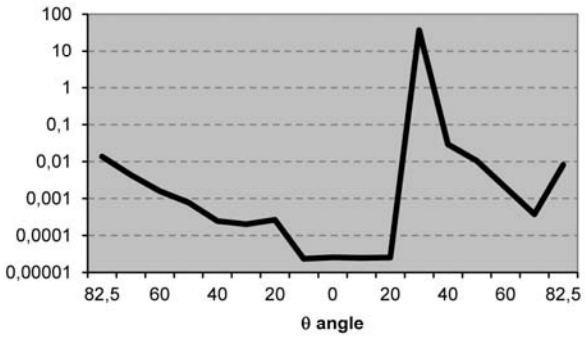

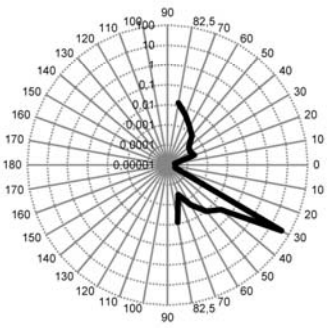

HORIZONTAL SECTION

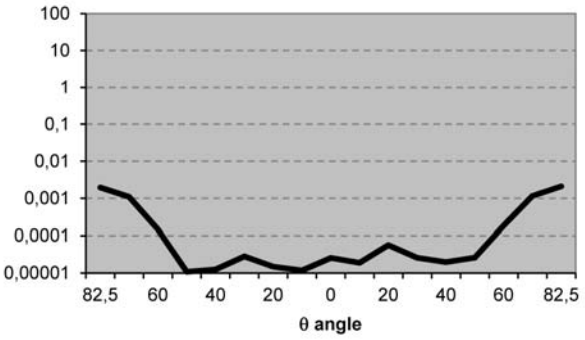

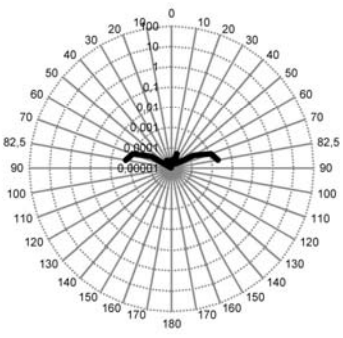

MESH SAMPLE NUMBER

03w

PARAMETERS

LW	SW	w	e	b	i	color
62,5	23	8	1	2	25	

TRANSMITTANCE

INCIDENT PATCH	41

	Es/Ei (%)	OUTG. PATCH
MÁX	13,532	41
MÍN	0,013	130
ABS. MEAN	0,115	
SCATT. MEAN	0,057	
SUM (%)	18,355	

VERTICAL SECTION

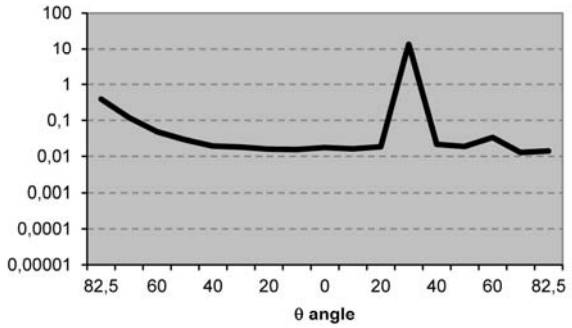

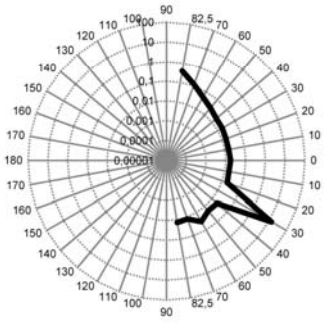

HORIZONTAL SECTION

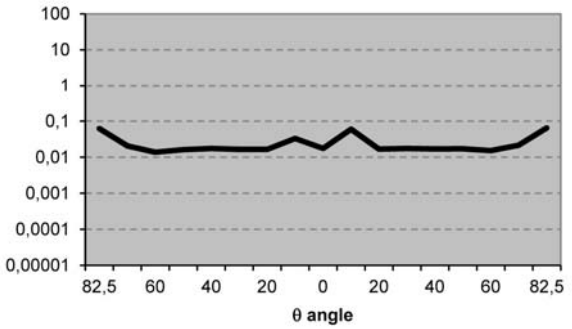

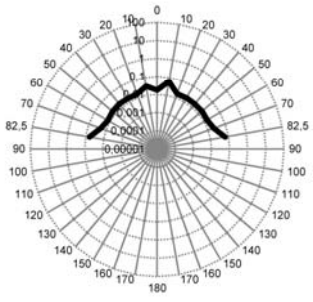

MESH SAMPLE NUMBER

03g

PARAMETERS

LW	SW	w	e	b	i	color
62,5	23	8	1	2	25	

TRANSMITTANCE

INCIDENT PATCH	41

	Es/Ei (%)	OUTG. PATCH
MÁX	13,516	41
MÍN	0,003	130
ABS. MEAN	0,081	
SCATT. MEAN	0,023	
SUM (%)	15,148	

VERTICAL SECTION

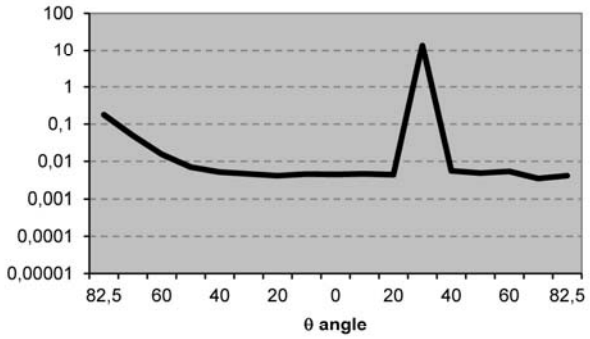

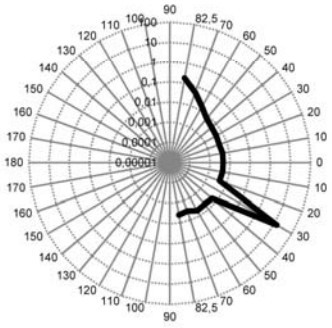

HORIZONTAL SECTION

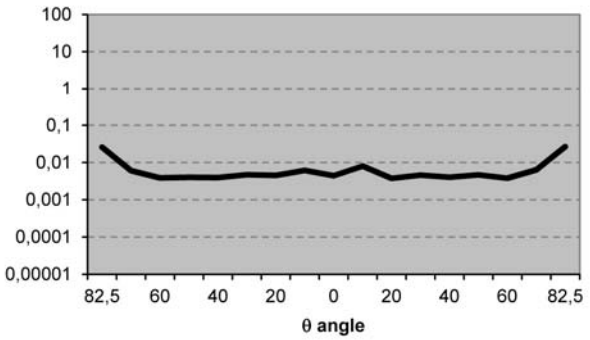

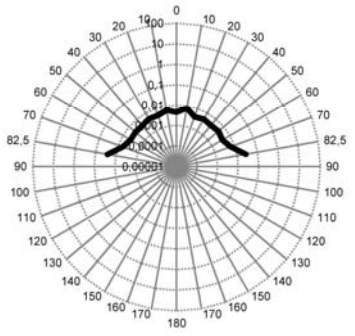

MESH SAMPLE NUMBER

03b

PARAMETERS

LW	SW	w	e	b	i	color
62,5	23	8	1	2	25	

TRANSMITTANCE

INCIDENT PATCH	41

	Es/Ei (%)	OUTG. PATCH
MÁX	13,512	41
MÍN	0,000	114
ABS. MEAN	0,060	
SCATT. MEAN	0,001	
SUM (%)	13,597	

VERTICAL SECTION

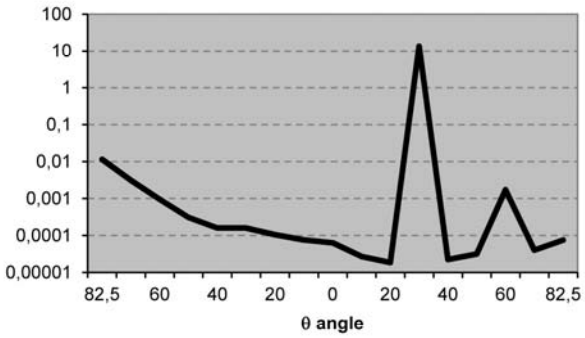

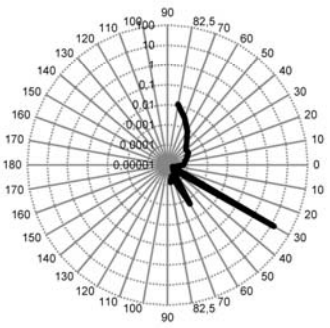

HORIZONTAL SECTION

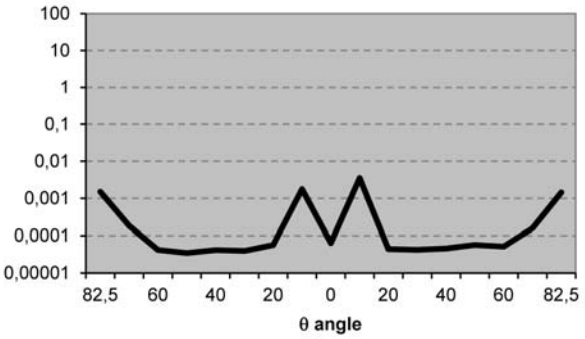

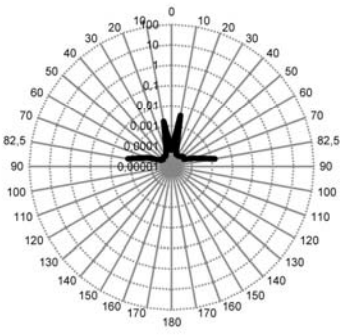

MESH SAMPLE NUMBER

04w

PARAMETERS

LW	SW	w	e	b	i	color
10	6,5	2,1	1	1	4,5	

TRANSMITTANCE

INCIDENT PATCH	41

	Es/Ei (%)	OUTG. PATCH
MÁX	21,825	41
MÍN	0,009	17
ABS. MEAN	0,149	
SCATT. MEAN	0,054	
SUM (%)	26,365	

VERTICAL SECTION

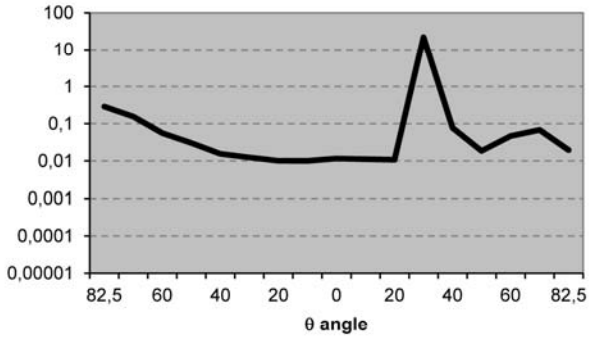

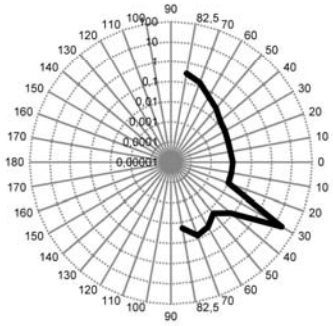

HORIZONTAL SECTION

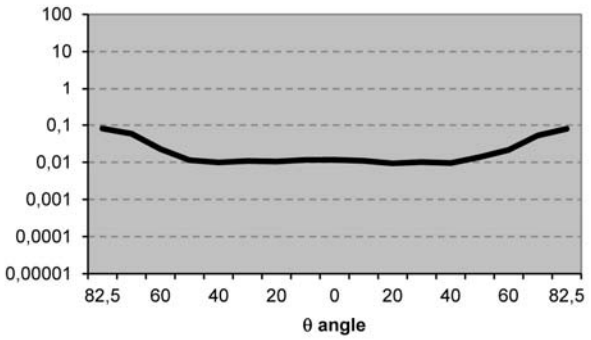

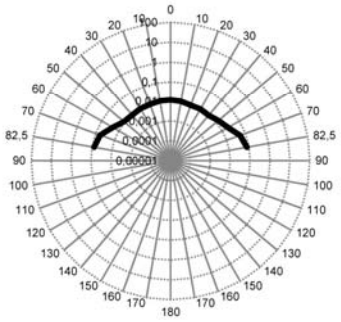

MESH SAMPLE NUMBER

04g

PARAMETERS

LW	SW	w	e	b	i	color
10	6,5	2,1	1	1	4,5	

TRANSMITTANCE

INCIDENT PATCH	41

	Es/Ei (%)	OUTG. PATCH
MÁX	21,745	41
MÍN	0,002	58
ABS. MEAN	0,117	
SCATT. MEAN	0,022	
SUM (%)	23,376	

VERTICAL SECTION

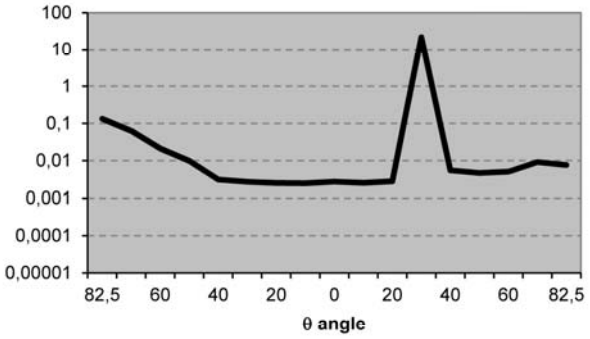

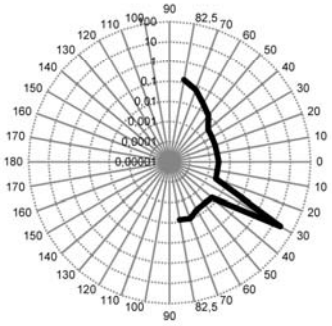

HORIZONTAL SECTION

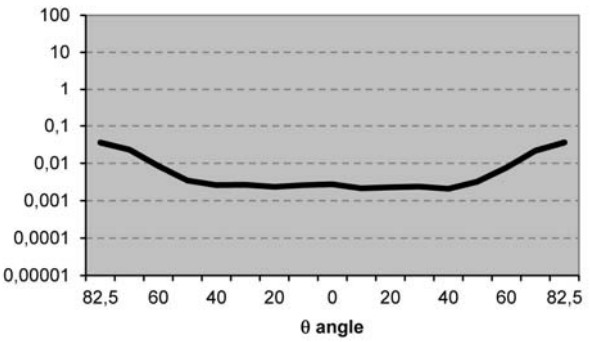

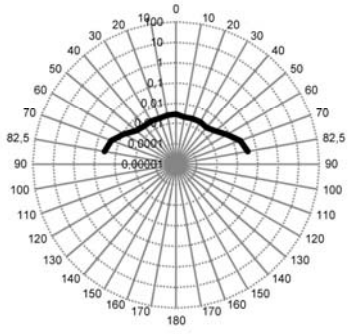

MESH SAMPLE NUMBER

04b

PARAMETERS

LW	SW	w	e	b	i	color
10	6,5	2,1	1	1	4,5	

TRANSMITTANCE

INCIDENT PATCH	41

	Es/Ei (%)	OUTG. PATCH
MÁX	21,742	41
MÍN	0,000	21
ABS. MEAN	0,096	
SCATT. MEAN	0,002	
SUM (%)	21,846	

VERTICAL SECTION

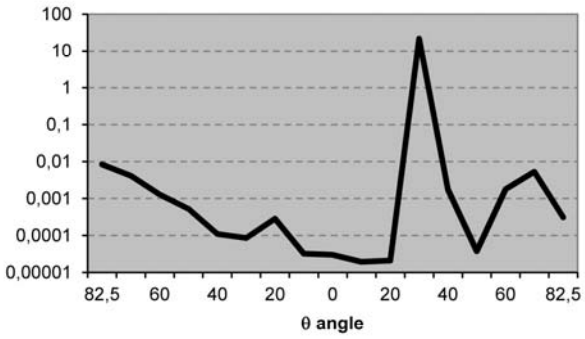

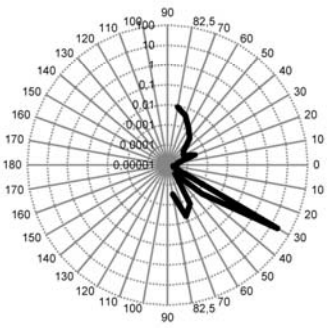

HORIZONTAL SECTION

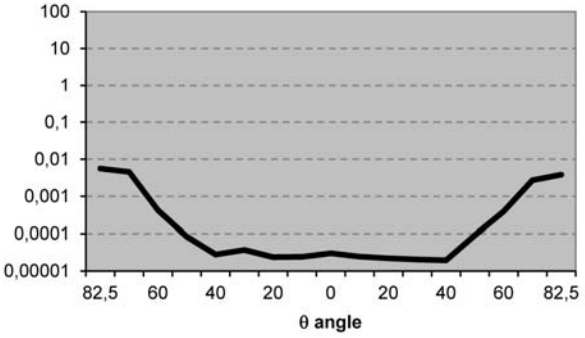

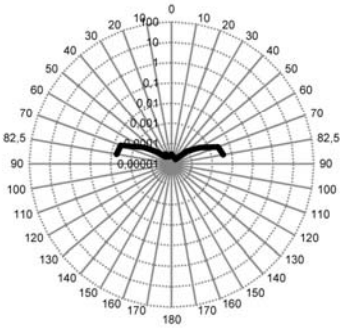

MESH SAMPLE NUMBER

05w

PARAMETERS

LW	SW	w	e	b	i	color
6	4,5	1,5	1	1	2	

TRANSMITTANCE

INCIDENT PATCH	41

	Es/Ei (%)	OUTG. PATCH
MÁX	22,121	41
MÍN	0,011	55
ABS. MEAN	0,159	
SCATT. MEAN	0,063	
SUM (%)	28,214	

VERTICAL SECTION

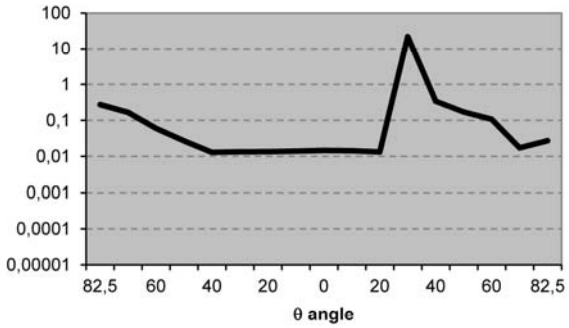

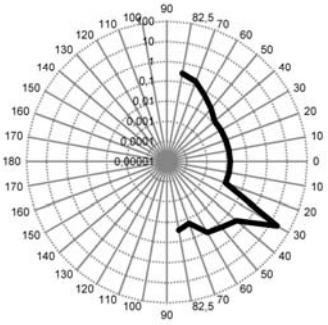

HORIZONTAL SECTION

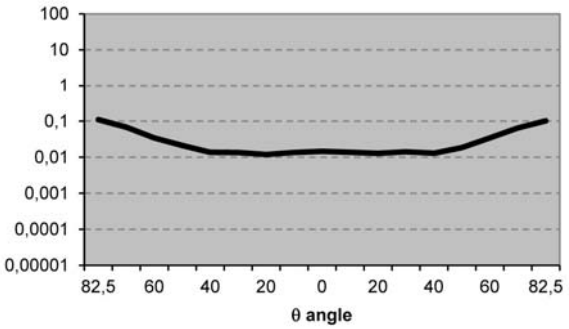

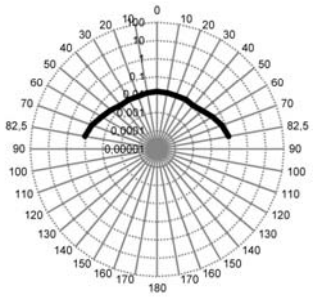

MESH SAMPLE NUMBER

05g

PARAMETERS

LW	SW	w	e	b	i	color
6	4,5	1,5	1	1	2	

TRANSMITTANCE

INCIDENT PATCH	41

	Es/Ei (%)	OUTG. PATCH
MÁX	22,109	41
MÍN	0,002	55
ABS. MEAN	0,121	
SCATT. MEAN	0,025	
SUM (%)	24,064	

VERTICAL SECTION

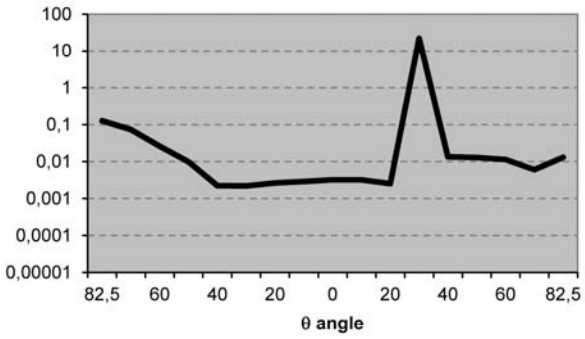

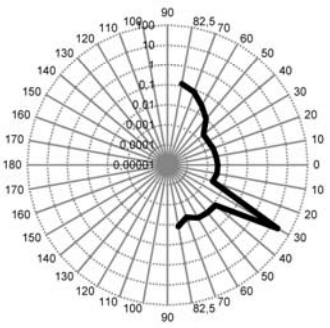

HORIZONTAL SECTION

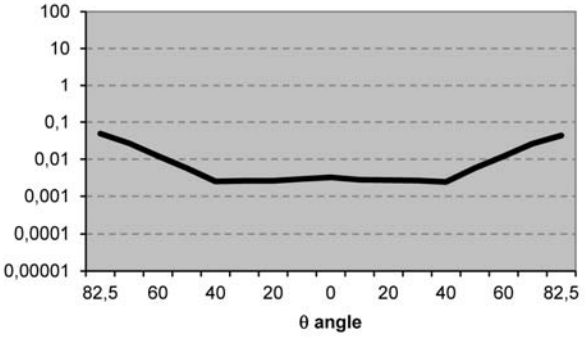

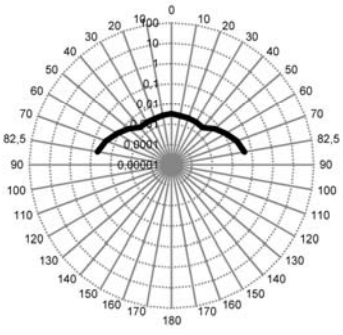

MESH SAMPLE NUMBER

05b

PARAMETERS

LW	SW	w	e	b	i	color
6	4,5	1,5	1	1	2	

TRANSMITTANCE

INCIDENT PATCH	41

	Es/Ei (%)	OUTG. PATCH
MÁX	22,106	41
MÍN	0,000	22
ABS. MEAN	0,098	
SCATT. MEAN	0,002	
SUM (%)	22,252	

VERTICAL SECTION

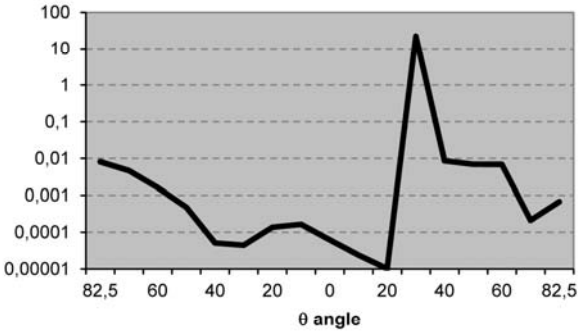

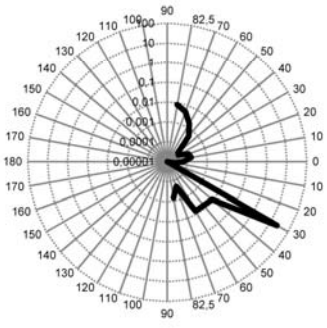

HORIZONTAL SECTION

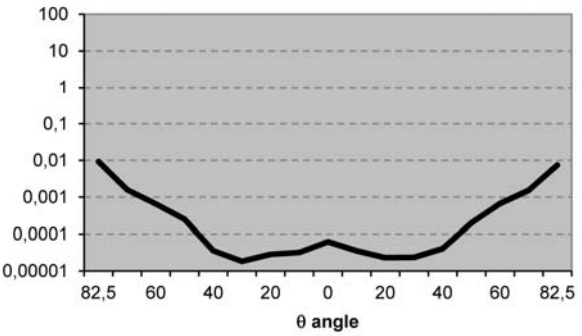

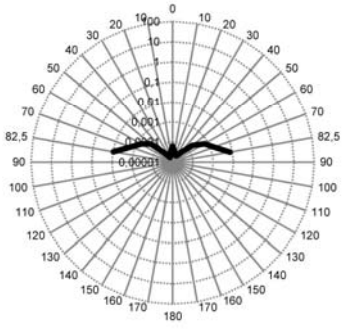

MESH SAMPLE NUMBER

06w

PARAMETERS

LW	SW	w	e	b	i	color
60	21	10	1,5	2	33	

TRANSMITTANCE

INCIDENT PATCH	41

	Es/Ei (%)	OUTG. PATCH
MÁX	1,897	41
MÍN	0,001	113
ABS. MEAN	0,019	
SCATT. MEAN	0,011	
SUM (%)	2,765	

VERTICAL SECTION

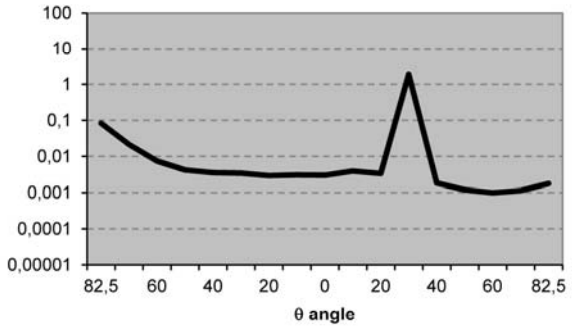

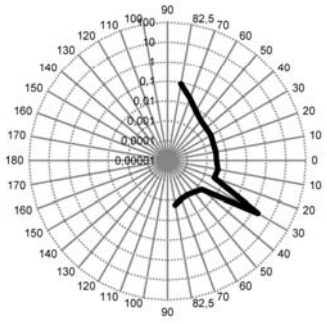

HORIZONTAL SECTION

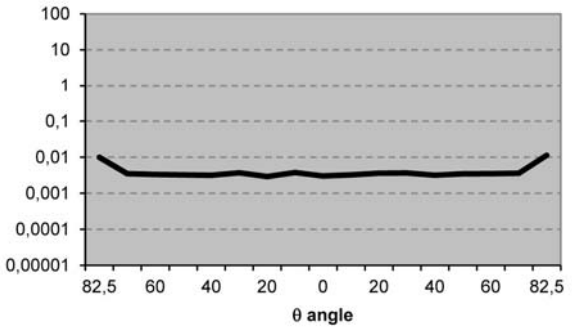

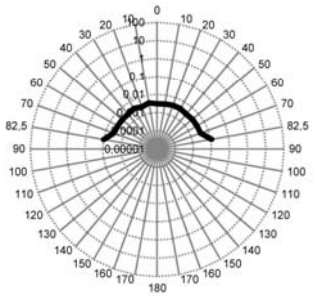

MESH SAMPLE NUMBER

06g

PARAMETERS

LW	SW	w	e	b	i	color
60	21	10	1,5	2	33	

TRANSMITTANCE

INCIDENT PATCH	41

	Es/Ei (%)	OUTG. PATCH
MÁX	1,895	41
MÍN	0,000	112
ABS. MEAN	0,012	
SCATT. MEAN	0,003	
SUM (%)	2,137	

VERTICAL SECTION

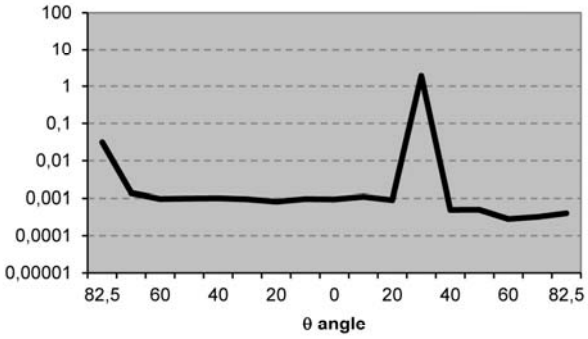

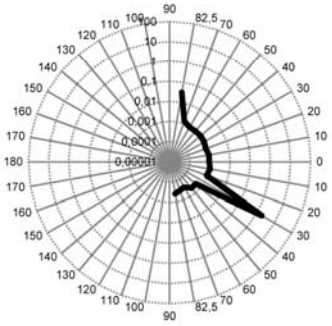

HORIZONTAL SECTION

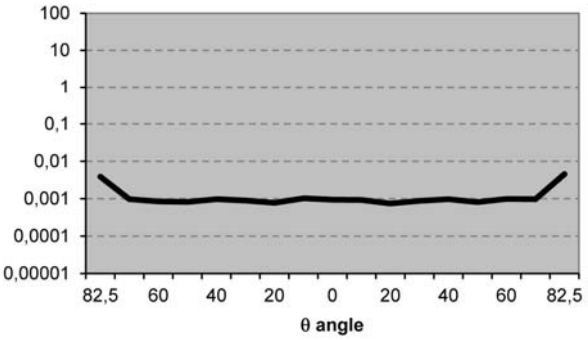

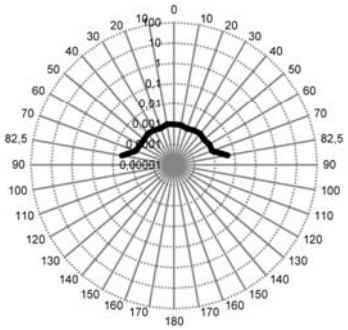

MESH SAMPLE NUMBER

06b

PARAMETERS

LW	SW	w	e	b	i	color
60	21	10	1,5	2	33	

TRANSMITTANCE

INCIDENT PATCH	41

	Es/Ei (%)	OUTG. PATCH
MÁX	1,895	41
MÍN	0,000	112
ABS. MEAN	0,012	
SCATT. MEAN	0,003	
SUM (%)	2,137	

VERTICAL SECTION

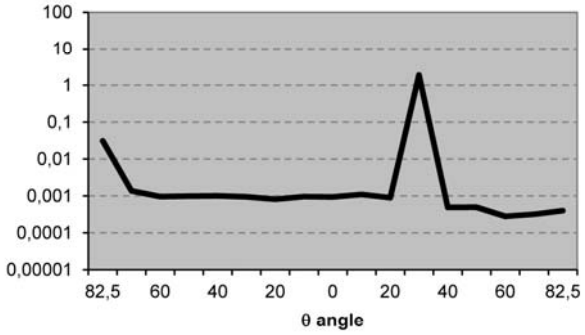

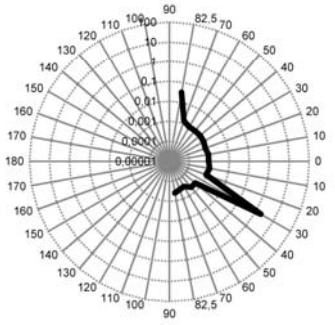

HORIZONTAL SECTION

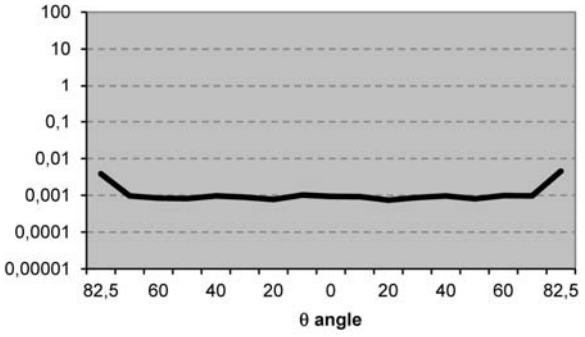

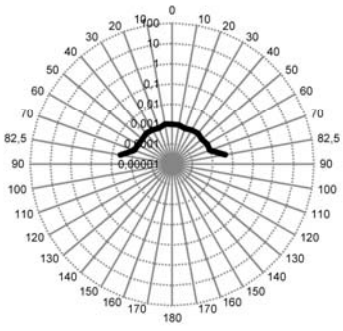

MESH SAMPLE NUMBER

07w

PARAMETERS

LW	SW	w	e	b	i	color
115	52	23	1	2	43,5	

TRANSMITTANCE

INCIDENT PATCH	41

	Es/Ei (%)	OUTG. PATCH
MÁX	1,747	41
MÍN	0,007	130
ABS. MEAN	0,048	
SCATT. MEAN	0,040	
SUM (%)	5,438	

VERTICAL SECTION

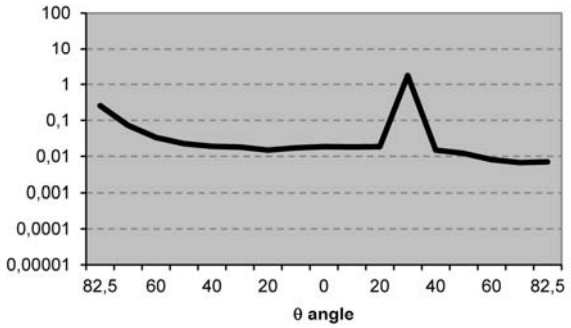

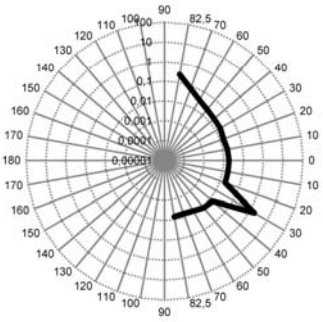

HORIZONTAL SECTION

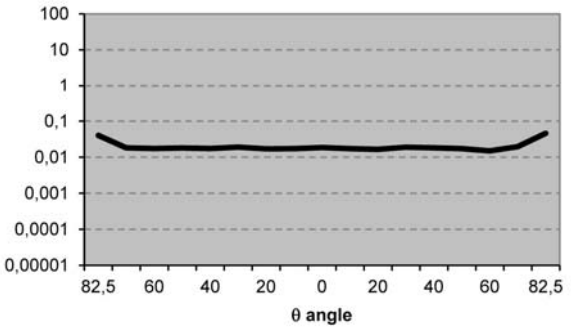

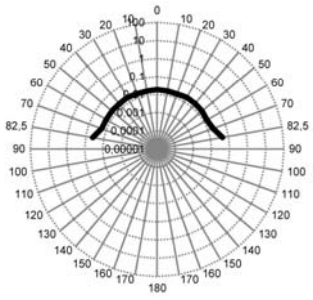

MESH SAMPLE NUMBER

07g

PARAMETERS

LW	SW	w	e	b	i	color
115	52	23	1	2	43,5	

TRANSMITTANCE

INCIDENT PATCH	41

	Es/Ei (%)	OUTG. PATCH
MÁX	1,733	41
MÍN	0,002	143
ABS. MEAN	0,022	
SCATT. MEAN	0,014	
SUM (%)	2,806	

VERTICAL SECTION

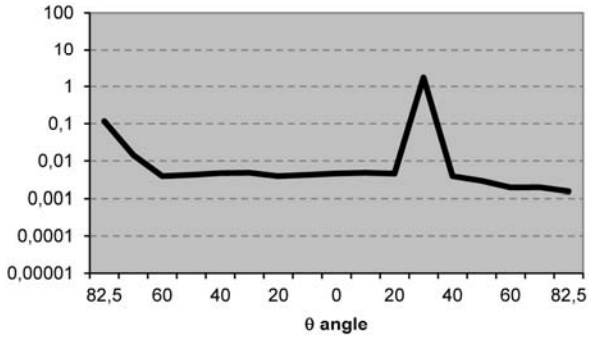

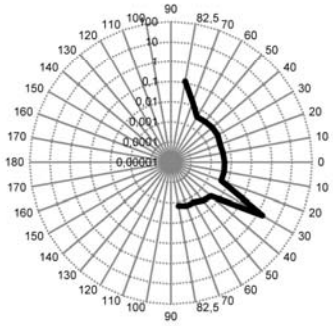

HORIZONTAL SECTION

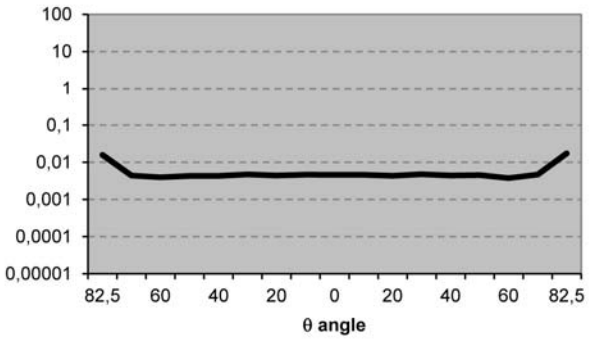

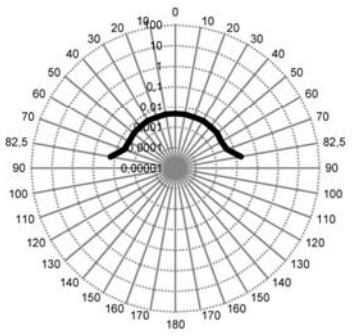

MESH SAMPLE NUMBER

07b

PARAMETERS

LW	SW	w	e	b	i	color
115	52	23	1	2	43,5	

TRANSMITTANCE

INCIDENT PATCH	41

	Es/Ei (%)	OUTG. PATCH
MÁX	1,729	41
MÍN	0,000	130
ABS. MEAN	0,008	
SCATT. MEAN	0,001	
SUM (%)	1,766	

VERTICAL SECTION

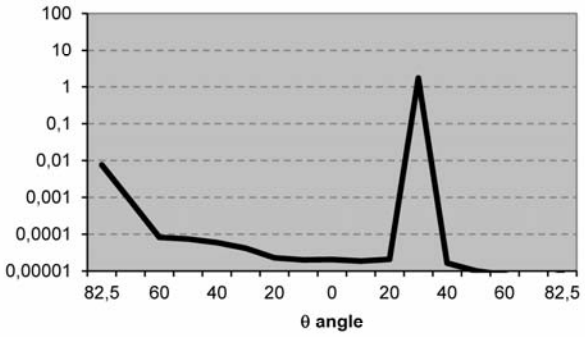

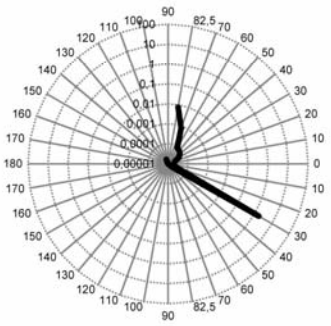

HORIZONTAL SECTION

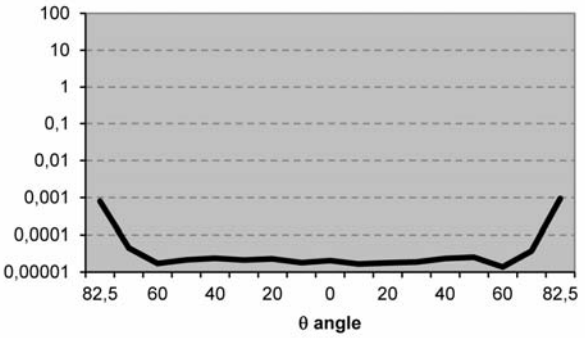

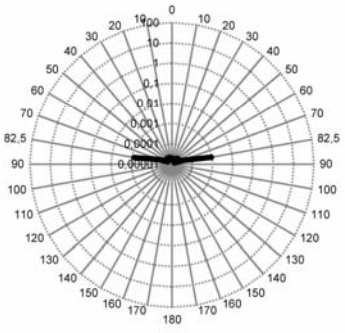

MESH SAMPLE NUMBER

08w

PARAMETERS

LW	SW	w	e	b	i	color
110	50	24	2	3,5	50	

TRANSMITTANCE

INCIDENT PATCH	41

	Es/Ei (%)	OUTG. PATCH
MÁX	2,553	41
MÍN	0,003	130
ABS. MEAN	0,038	
SCATT. MEAN	0,027	
SUM (%)	5,071	

VERTICAL SECTION

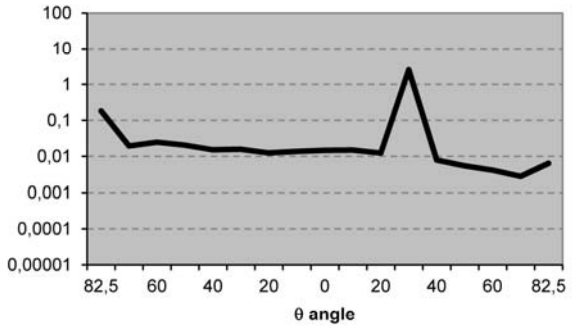

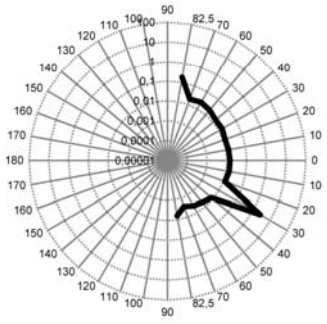

HORIZONTAL SECTION

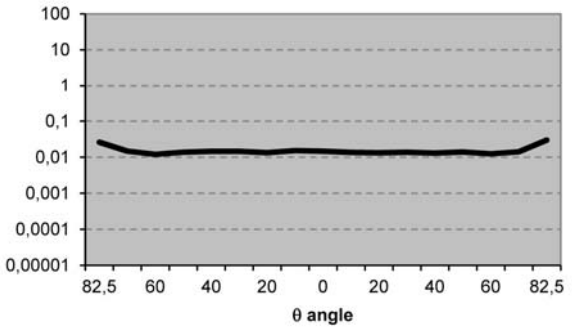

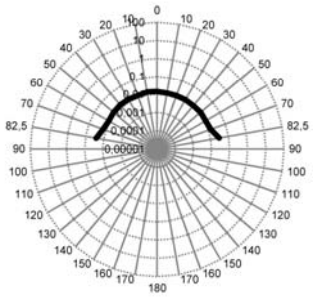

MESH SAMPLE NUMBER

08g

PARAMETERS

LW	SW	w	e	b	i	color
110	50	24	2	3,5	50	

TRANSMITTANCE

INCIDENT PATCH	41

	Es/Ei (%)	OUTG. PATCH
MÁX	2,545	41
MÍN	0,001	130
ABS. MEAN	0,020	
SCATT. MEAN	0,009	
SUM (%)	3,253	

VERTICAL SECTION

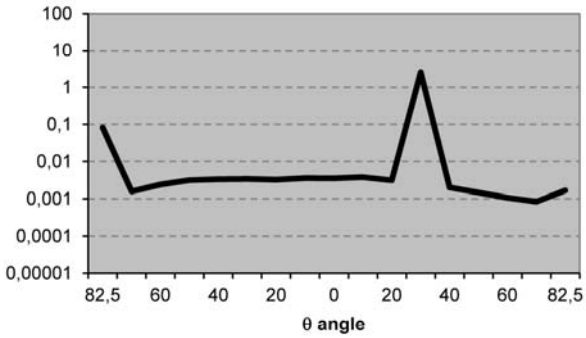

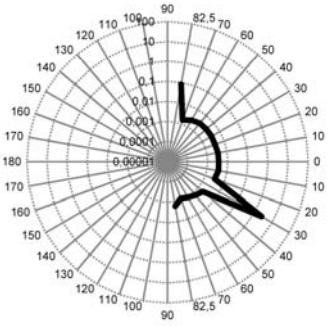

HORIZONTAL SECTION

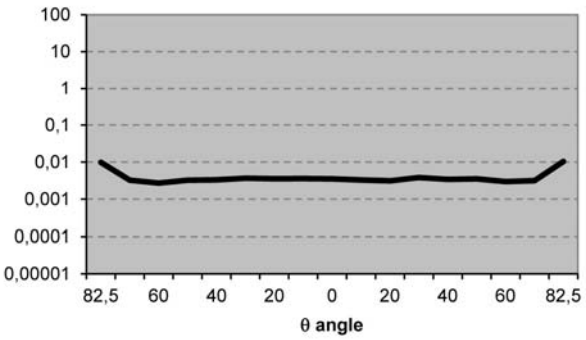

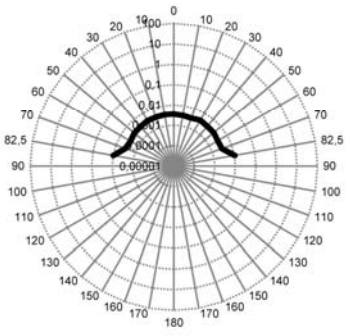

MESH SAMPLE NUMBER

08b

PARAMETERS

LW	SW	w	e	b	i	color
110	50	24	2	3,5	50	

TRANSMITTANCE

INCIDENT PATCH	41

	Es/Ei (%)	OUTG. PATCH
MÁX	2,542	41
MÍN	0,000	130
ABS. MEAN	0,012	
SCATT. MEAN	0,000	
SUM (%)	2,566	

VERTICAL SECTION

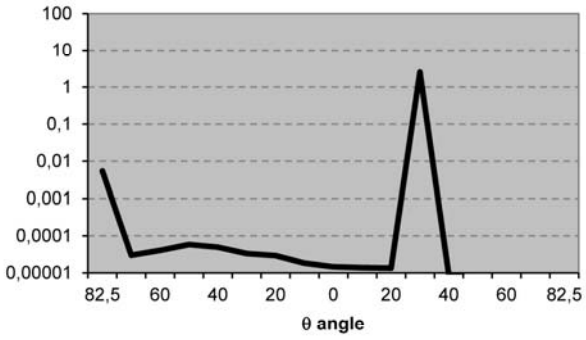

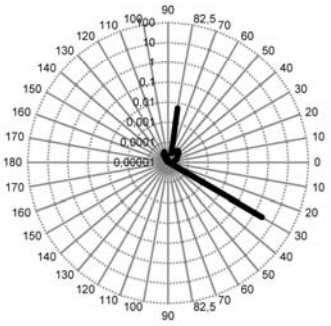

HORIZONTAL SECTION

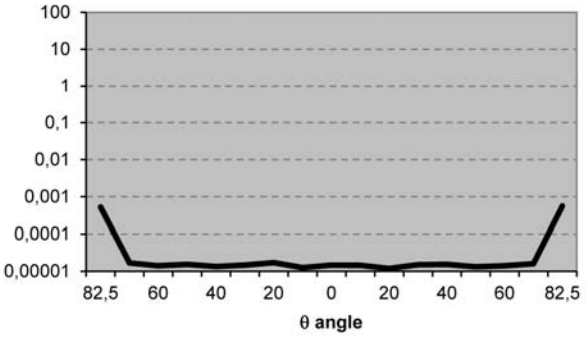

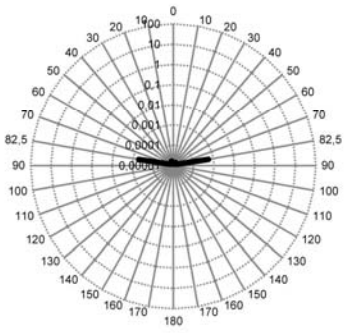

MESH SAMPLE NUMBER

09w

PARAMETERS

LW	SW	w	e	b	i	color
110	40	15	2	2	33	

TRANSMITTANCE

INCIDENT PATCH	41

	Es/Ei (%)	OUTG. PATCH
MÁX	11,916	41
MÍN	0,016	143
ABS. MEAN	0,121	
SCATT. MEAN	0,069	
SUM (%)	18,022	

VERTICAL SECTION

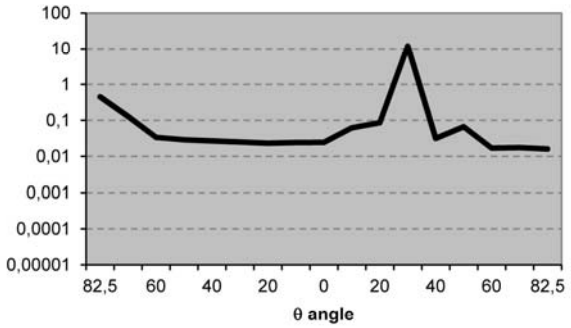

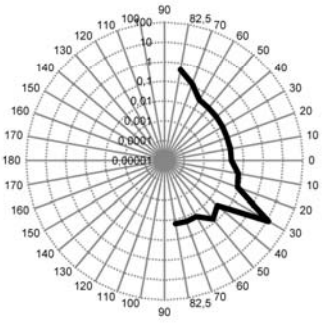

HORIZONTAL SECTION

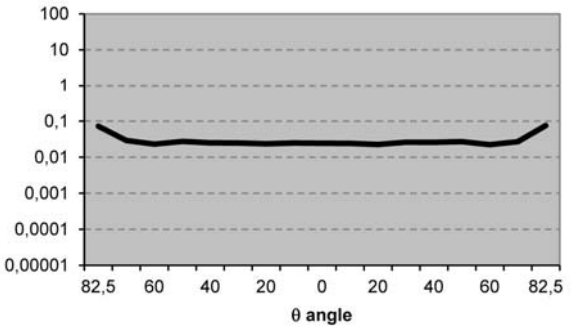

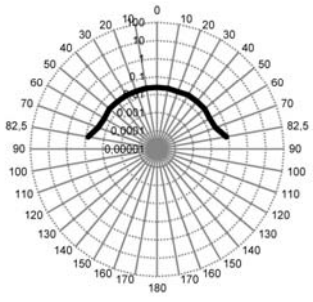

MESH SAMPLE NUMBER

09g

PARAMETERS

LW	SW	w	e	b	i	color
110	40	15	2	2	33	

TRANSMITTANCE

INCIDENT PATCH	41

	Es/Ei (%)	OUTG. PATCH
MÁX	11,894	41
MÍN	0,004	129
ABS. MEAN	0,079	
SCATT. MEAN	0,027	
SUM (%)	13,881	

VERTICAL SECTION

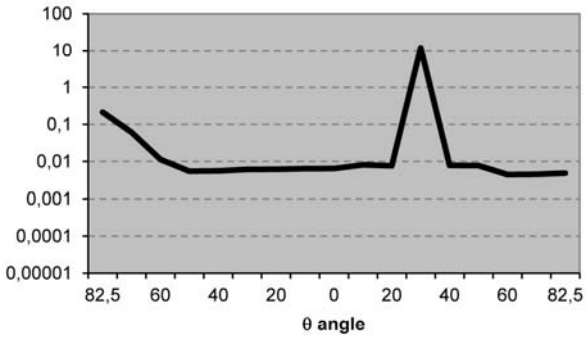

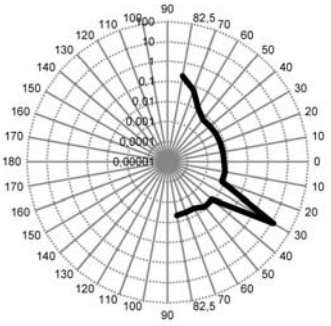

HORIZONTAL SECTION

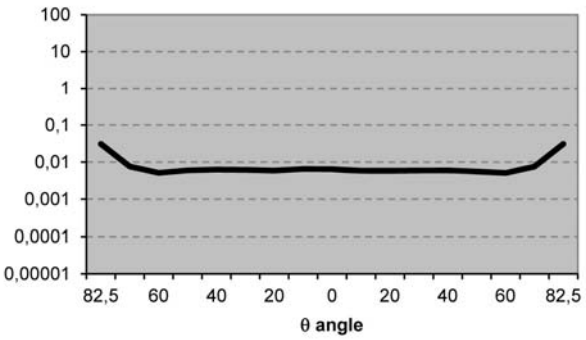

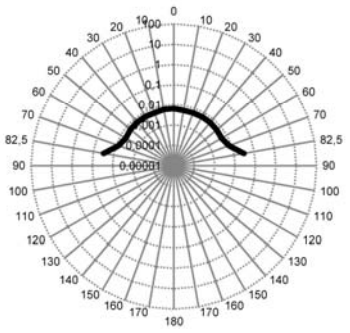

MESH SAMPLE NUMBER

09b

PARAMETERS

LW	SW	w	e	b	i	color
110	40	15	2	2	33	

TRANSMITTANCE

INCIDENT PATCH	41

	Es/Ei (%)	OUTG. PATCH
MÁX	11,886	41
MÍN	0,000	108
ABS. MEAN	0,053	
SCATT. MEAN	0,002	
SUM (%)	11,982	

VERTICAL SECTION

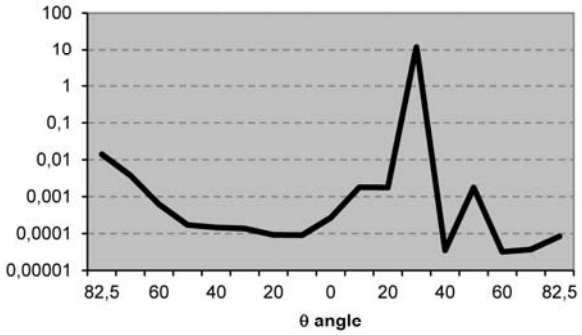

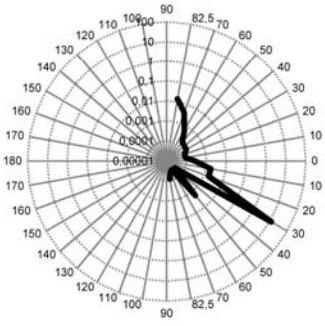

HORIZONTAL SECTION

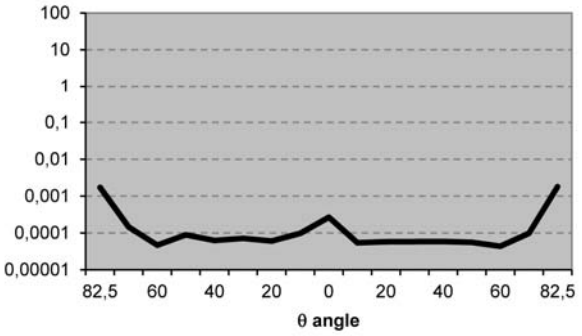

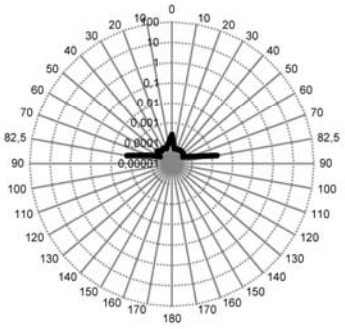

MESH SAMPLE NUMBER

10w

PARAMETERS

LW	SW	w	e	b	i	color
6	4	1,2	1	1	2,5	

TRANSMITTANCE

INCIDENT PATCH	41

	Es/Ei (%)	OUTG. PATCH
MÁX	26,033	41
MÍN	0,005	14
ABS. MEAN	0,164	
SCATT. MEAN	0,050	
SUM (%)	30,496	

VERTICAL SECTION

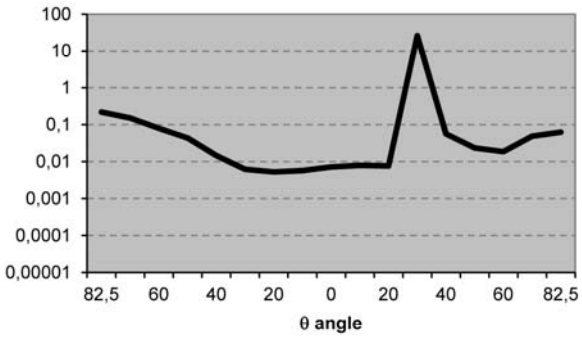

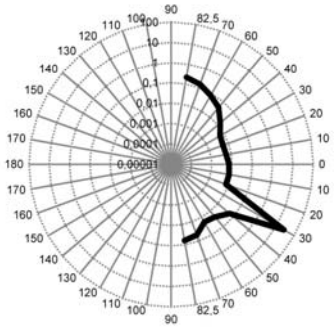

HORIZONTAL SECTION

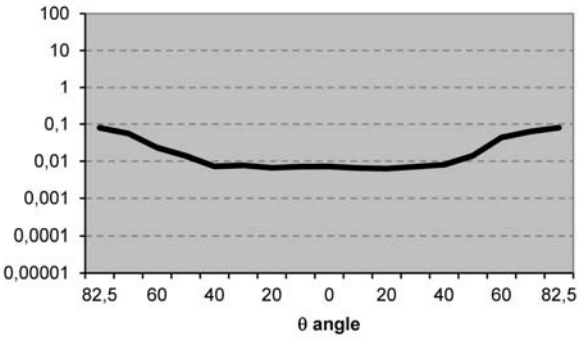

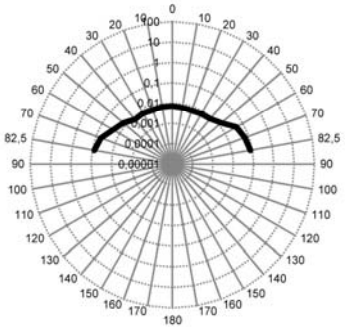

MESH SAMPLE NUMBER

10g

PARAMETERS

LW	SW	w	e	b	i	color
6	4	1,2	1	1	2,5	

TRANSMITTANCE

INCIDENT PATCH	41

	Es/Ei (%)	OUTG. PATCH
MÁX	26,025	41
MÍN	0,001	14
ABS. MEAN	0,134	
SCATT. MEAN	0,020	
SUM (%)	27,656	

VERTICAL SECTION

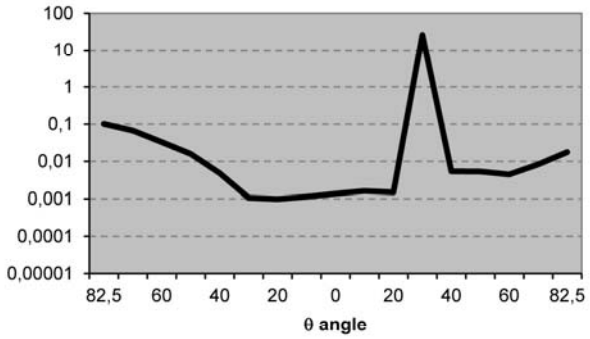

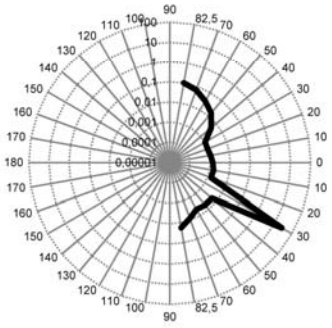

HORIZONTAL SECTION

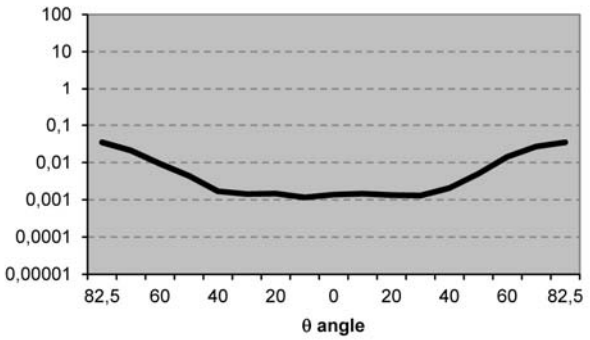

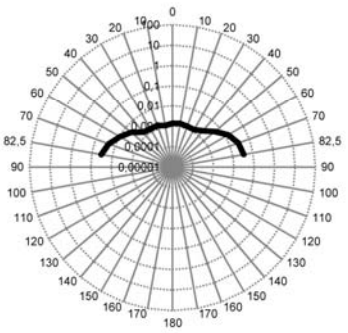

MESH SAMPLE NUMBER

10b

PARAMETERS

LW	SW	w	e	b	i	color
6	4	1,2	1	1	2,5	

TRANSMITTANCE

INCIDENT PATCH	41

	Es/Ei (%)	OUTG. PATCH
MÁX	26,022	41
MÍN	0,000	16
ABS. MEAN	0,115	
SCATT. MEAN	0,002	
SUM (%)	26,162	

VERTICAL SECTION

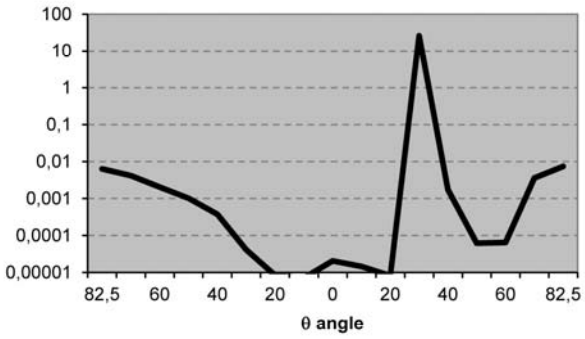

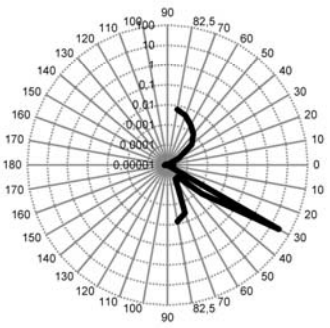

HORIZONTAL SECTION

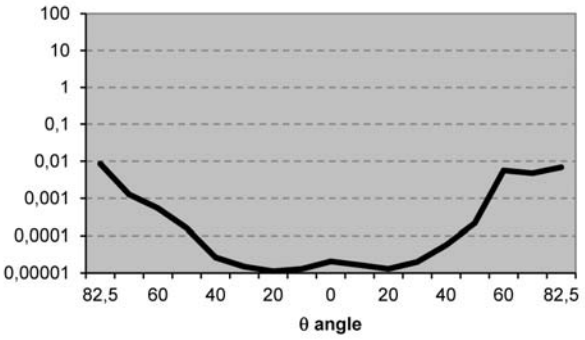

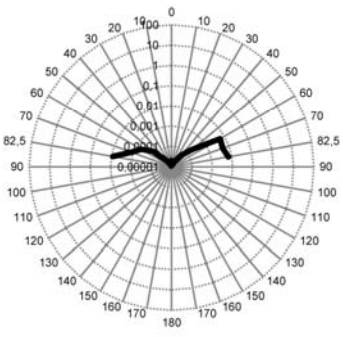

MESH SAMPLE NUMBER

11w

PARAMETERS

LW	SW	w	e	b	i	color
60	22	7	2	2	18	

TRANSMITTANCE

INCIDENT PATCH	41

	Es/Ei (%)	OUTG. PATCH
MÁX	27,120	41
MÍN	0,012	79
ABS. MEAN	0,201	
SCATT. MEAN	0,084	
SUM (%)	34,294	

VERTICAL SECTION

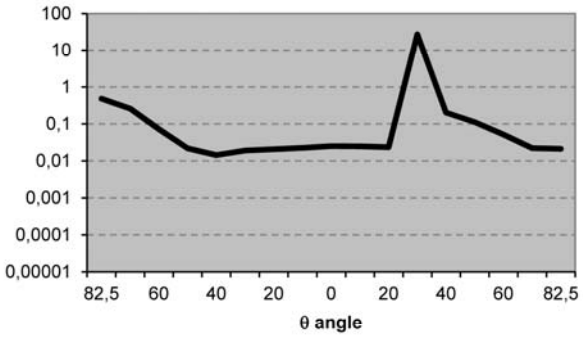

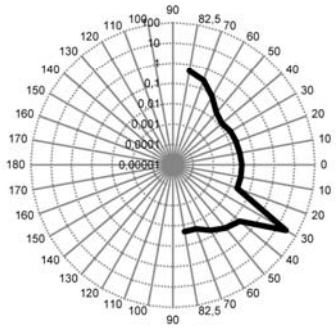

HORIZONTAL SECTION

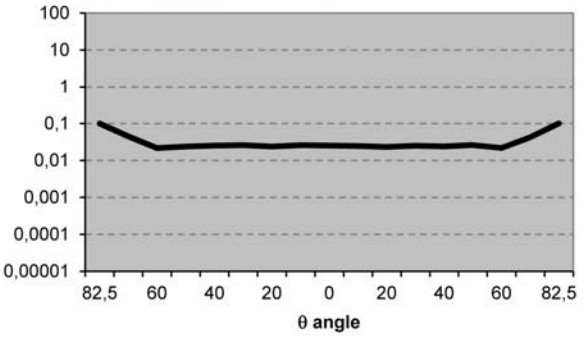

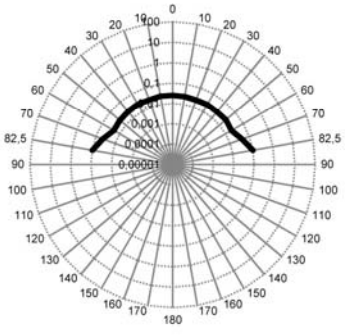

MESH SAMPLE NUMBER

11g

PARAMETERS

LW	SW	w	e	b	i	color
60	22	7	2	2	18	

TRANSMITTANCE

INCIDENT PATCH	41

	Es/Ei (%)	OUTG. PATCH
MÁX	26,931	41
MÍN	0,003	51
ABS. MEAN	0,152	
SCATT. MEAN	0,034	
SUM (%)	29,492	

VERTICAL SECTION

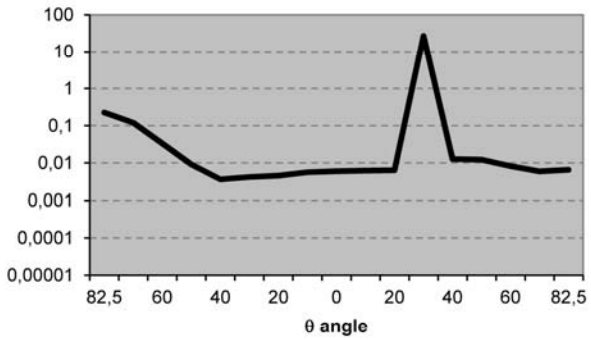

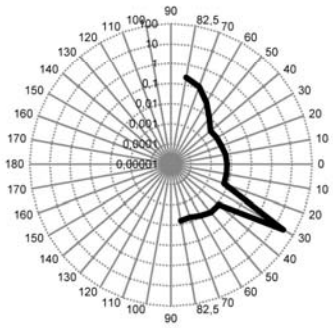

HORIZONTAL SECTION

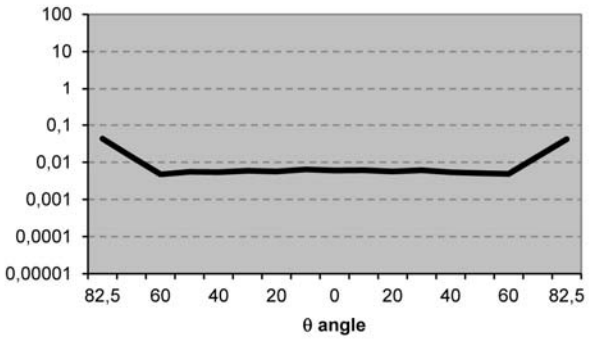

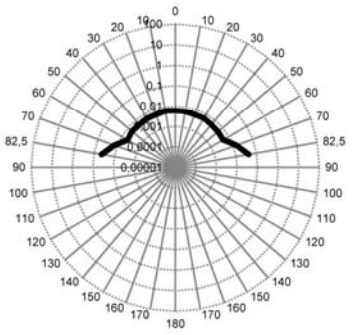

MESH SAMPLE NUMBER

11b

PARAMETERS

LW	SW	w	e	b	i	color
60	22	7	2	2	18	

TRANSMITTANCE

INCIDENT PATCH	41

	Es/Ei (%)	OUTG. PATCH
MÁX	26,923	41
MÍN	0,000	107
ABS. MEAN	0,119	
SCATT. MEAN	0,002	
SUM (%)	27,061	

VERTICAL SECTION

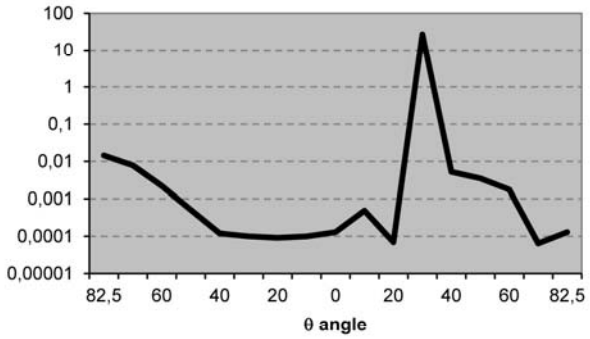

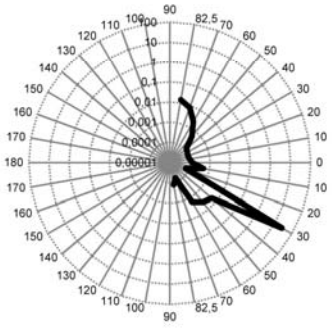

HORIZONTAL SECTION

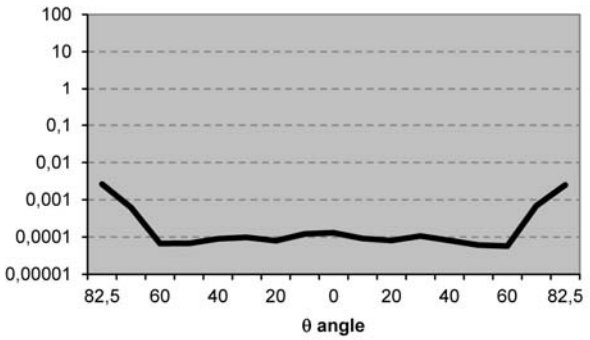

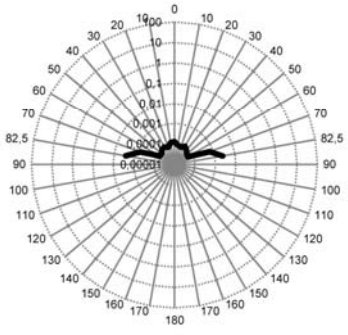

MESH SAMPLE NUMBER

12w

PARAMETERS

LW	SW	w	e	b	i	color
115	48	20	1,5	2	39	

TRANSMITTANCE

INCIDENT PATCH	41

	Es/Ei (%)	OUTG. PATCH
MÁX	5,151	41
MÍN	0,012	143
ABS. MEAN	0,079	
SCATT. MEAN	0,057	
SUM (%)	10,394	

VERTICAL SECTION

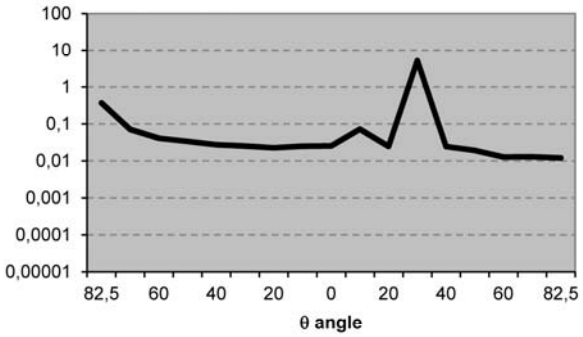

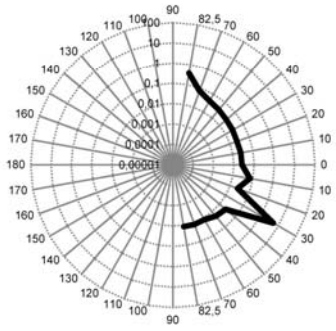

HORIZONTAL SECTION

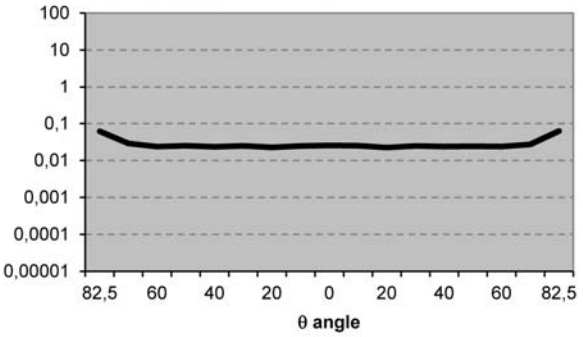

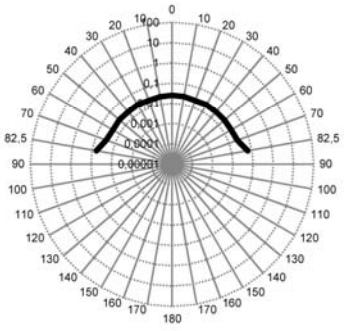

MESH SAMPLE NUMBER

12g

PARAMETERS

LW	SW	w	e	b	i	color
115	48	20	1,5	2	39	

TRANSMITTANCE

INCIDENT PATCH	41

	Es/Ei (%)	OUTG. PATCH
MÁX	5,128	41
MÍN	0,003	130
ABS. MEAN	0,044	
SCATT. MEAN	0,022	
SUM (%)	6,744	

VERTICAL SECTION

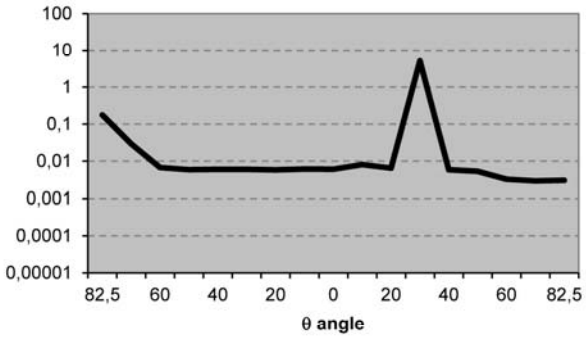

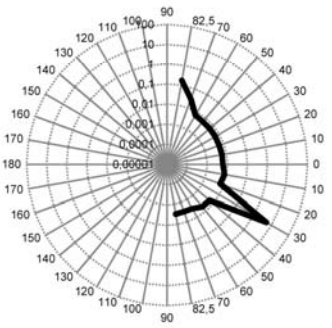

HORIZONTAL SECTION

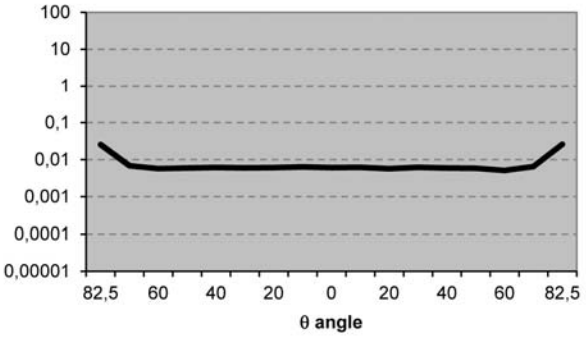

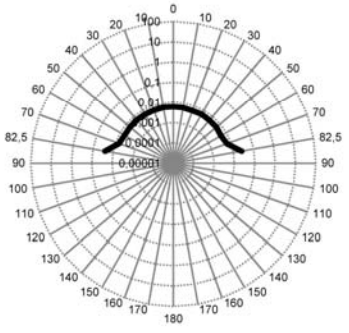

MESH SAMPLE NUMBER

12b

PARAMETERS

LW	SW	w	e	b	i	color
115	48	20	1,5	2	39	

TRANSMITTANCE

INCIDENT PATCH	41

	Es/Ei (%)	OUTG. PATCH
MÁX	5,121	41
MÍN	0,000	143
ABS. MEAN	0,023	
SCATT. MEAN	0,001	
SUM (%)	5,187	

VERTICAL SECTION

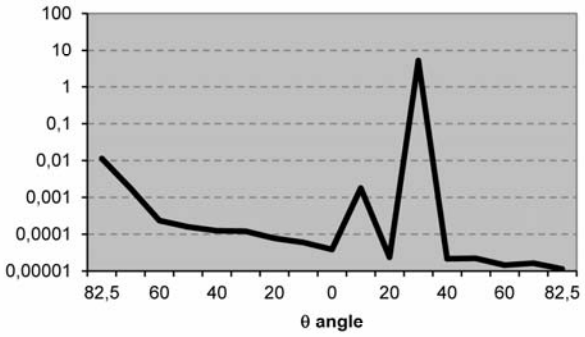

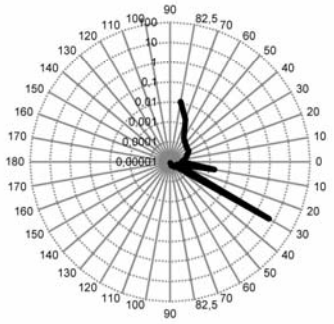

HORIZONTAL SECTION

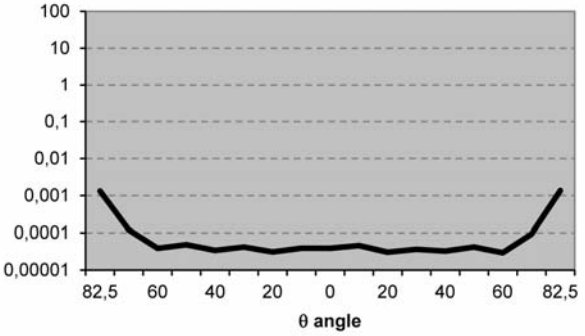

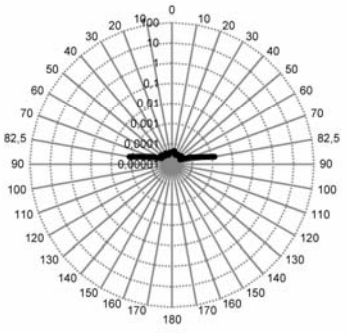

B.3 Comparative analysis with lab

The following series of tables show the comparison between computer aided and laboratory assessment results, for each analyzed mesh. Remember that, as seen in chapter 6, all measurements are referring to laboratory test angles, and therefore, to specular transmission.

Results are given in data tables with 7 rows and 13 columns (one for every fixing position in rotation of the sample-holder around *x* and *y* axis), where each box contains a number expressing the transmittance (%) for each light direction (resulting from the combination of the two mentioned rotations). There are only 7 rows for *y* axis due to the vertical symmetry of EM. The boxes related to the positions where the laboratory sample holder obstructed the radiation (voiding those registers), are empty and crossed out.

MESH SAMPLE NUMBER

01b

PARAMETERS

LW	SW	w	e	b	i	color
200	73	24	1	7	33	

SPECULAR TRANSMITTANCE (%)

COMPUTER AIDED ASSESSMENT RESULT

y \ x	0º	15º	30º	45º	60º	75º	90º	105º	120º	135º	150º	165º	180º
0º		18,60	**8,74**	11,43	**22,35**	33,12	**43,20**	52,73	**65,32**	78,18	**85,97**	50,27	
15º		18,60	8,84	8,13	25,09	**35,26**	43,94	**51,31**	62,68	81,89	84,13	50,27	
30º		18,60	8,84	**11,18**	**23,27**	38,00	**42,36**	49,17	**65,02**	**79,76**	84,13	50,27	
45º		20,63	9,86	12,50	**24,69**	34,75	43,94	54,25	**63,50**	75,09	82,10	48,17	
60º		23,67	10,67	16,87	30,78	30,78	**43,28**	58,32	58,32	70,11	70,22	42,24	
75º			27,76	27,66	40,93	40,93	40,93	40,93	40,93	47,47	44,90		
90º													

LABORATORY ASSESSMENT RESULT

y \ x	0º	15º	30º	45º	60º	75º	90º	105º	120º	135º	150º	165º	180º
0º		1,52	0,04	12,78	25,27	35,17	43,00	51,38	62,25	74,58	79,86	33,70	
15º		1,19	0,08	11,23	25,72	35,01	42,87	51,21	61,13	73,20	80,92	29,33	
30º		0,84	0,05	11,20	26,19	39,79	43,26	51,87	61,70	74,36	78,51	29,95	
45º		0,68	0,07	11,22	25,54	34,98	42,98	53,56	62,16	71,58	72,92	36,45	
60º		1,11	0,23	9,24	25,14	35,25	43,10	52,27	58,89	61,18	51,79	20,48	
75º			1,80	10,97	27,27	34,13	40,56	43,22	38,36	29,73	23,65		
90º													

ABSOLUTE DEVIATION BETWEEN BOTH METHODS

y \ x	0º	15º	30º	45º	60º	75º	90º	105º	120º	135º	150º	165º	180º
0º		17,08	**8,70**	1,35	**2,92**	2,05	**0,20**	1,35	**3,07**	3,60	**6,12**	16,57	
15º		17,41	8,76	3,10	0,63	**0,24**	1,07	**0,10**	1,56	8,69	3,22	20,95	
30º		17,76	8,79	**0,02**	**2,93**	1,80	**0,90**	2,70	**3,32**	**5,40**	5,62	20,32	
45º		19,95	9,79	1,28	**0,85**	0,24	0,96	0,70	**1,34**	3,50	9,17	11,72	
60º		22,56	10,44	7,62	5,64	4,46	**0,18**	6,05	0,57	8,93	18,43	21,76	
75º			25,96	16,69	13,66	6,80	0,37	2,30	2,57	17,74	21,25		
90º													

MAXIMUM DEVIATION (%)	25,96
MINIMUM DEVIATION (%)	0,02
AVERAGE DEVIATION (%)	7,37
AV. DEVIATION - COINCIDING MEASUREMENT ANGLES (%)	2,42

MESH SAMPLE NUMBER

01g

PARAMETERS

LW	SW	w	e	b	i	color
200	73	24	1	7	33	

SPECULAR TRANSMITTANCE (%)

COMPUTER AIDED ASSESSMENT RESULT

y \ x	0º	15º	30º	45º	60º	75º	90º	105º	120º	135º	150º	165º	180º
0º		18,60	**8,75**	11,44	**22,36**	33,13	**43,21**	52,73	**65,33**	78,18	**85,97**	50,28	
15º		18,60	8,85	8,14	25,10	**35,26**	43,95	**51,31**	62,68	81,89	84,14	50,28	
30º		18,60	8,85	**11,19**	**23,28**	38,00	**42,37**	49,17	**65,03**	**79,76**	84,14	50,28	
45º		20,63	9,86	12,51	**24,70**	34,75	43,95	54,26	**63,50**	75,09	82,10	48,19	
60º		23,68	10,68	16,87	30,79	30,79	**43,28**	58,33	58,33	70,11	70,22	42,26	
75º			27,76	27,67	40,93	40,93	40,93	40,93	40,93	47,47	44,91		
90º													

LABORATORY ASSESSMENT RESULT

y \ x	0º	15º	30º	45º	60º	75º	90º	105º	120º	135º	150º	165º	180º
0º		0,63	0,13	10,39	23,57	32,76	40,90	49,08	58,45	71,40	79,38	38,78	
15º		0,52	0,14	10,54	23,92	33,26	41,64	49,48	58,77	71,86	82,44	33,43	
30º		0,52	0,16	11,12	23,47	32,95	40,44	48,26	58,72	72,53	78,25	32,20	
45º		0,51	0,23	11,41	24,53	33,13	41,37	49,47	60,64	71,37	73,54	35,06	
60º		0,90	0,49	10,55	24,73	33,62	41,12	49,17	57,51	61,18	51,55	17,95	
75º			2,90	14,94	26,57	35,06	38,78	35,57	40,99	32,13	14,91		
90º													

ABSOLUTE DEVIATION BETWEEN BOTH METHODS

y \ x	0º	15º	30º	45º	60º	75º	90º	105º	120º	135º	150º	165º	180º
0º		17,97	**8,61**	1,05	**1,22**	0,37	**2,30**	3,65	**6,87**	6,78	**6,60**	11,50	
15º		18,09	8,71	2,40	1,18	**2,01**	2,31	**1,83**	3,91	10,03	1,69	16,86	
30º		18,08	8,69	**0,07**	**0,19**	5,06	**1,93**	0,92	**6,30**	**7,23**	5,89	18,08	
45º		20,12	9,64	1,10	**0,17**	1,63	2,57	4,79	**2,86**	3,72	8,56	13,13	
60º		22,78	10,19	6,33	6,06	2,83	**2,17**	9,15	0,82	8,93	18,67	24,31	
75º			24,86	12,73	14,36	5,88	2,15	5,36	0,06	15,34	30,00		
90º													

MAXIMUM DEVIATION (%)	30,00
MINIMUM DEVIATION (%)	0,06
AVERAGE DEVIATION (%)	7,81
AV. DEVIATION - COINCIDING MEASUREMENT ANGLES (%)	3,36

MESH SAMPLE NUMBER

01w

PARAMETERS

LW	SW	w	e	b	i	color
200	73	24	1	7	33	

SPECULAR TRANSMITTANCE (%)

COMPUTER AIDED ASSESSMENT RESULT

y \ x	0º	15º	30º	45º	60º	75º	90º	105º	120º	135º	150º	165º	180º
0º		18,62	**8,77**	11,48	**22,39**	33,15	**43,23**	52,75	**65,34**	78,19	**86,86**	50,31	
15º		18,62	8,88	8,18	25,13	**35,28**	43,96	**51,33**	62,70	82,08	84,67	50,31	
30º		18,62	8,88	**11,23**	**23,39**	38,02	**42,39**	49,19	**65,04**	**79,84**	84,67	50,31	
45º		20,64	9,89	12,58	**24,73**	34,79	43,97	54,26	**63,51**	75,33	82,24	48,31	
60º		23,69	10,70	16,91	30,82	30,82	**43,30**	58,64	58,64	70,37	70,77	42,30	
75º			27,84	27,79	41,09	41,09	41,09	41,09	41,09	47,70	45,22		
90º													

LABORATORY ASSESSMENT RESULT

y \ x	0º	15º	30º	45º	60º	75º	90º	105º	120º	135º	150º	165º	180º
0º		1,59	1,09	12,95	24,57	38,05	41,57	49,77	58,85	70,90	73,38	23,37	
15º		1,44	1,11	13,30	26,23	33,72	41,98	49,13	58,38	69,18	76,84	21,29	
30º		1,64	1,19	13,92	24,59	38,63	42,52	49,13	58,44	69,96	74,80	31,05	
45º		1,76	1,24	14,53	26,25	38,54	42,40	50,38	60,47	70,93	76,00	49,42	
60º		2,04	1,61	13,42	25,27	34,37	48,73	50,62	59,12	63,53	61,45	32,38	
75º			4,19	14,67	28,33	34,33	45,17	46,07	45,73	37,64	22,67		
90º													

ABSOLUTE DEVIATION BETWEEN BOTH METHODS

y \ x	0º	15º	30º	45º	60º	75º	90º	105º	120º	135º	150º	165º	180º
0º		17,02	**7,68**	1,47	**2,18**	4,90	**1,66**	2,98	**6,50**	7,29	**13,48**	26,94	
15º		17,18	7,76	5,12	1,10	**1,56**	1,99	**2,19**	4,32	12,91	7,82	29,02	
30º		16,97	7,69	**2,70**	**1,20**	0,61	**0,14**	0,06	**6,60**	**9,88**	9,86	19,26	
45º		18,88	8,65	1,95	**1,52**	3,75	1,57	3,89	**3,04**	4,40	6,24	1,10	
60º		21,64	9,09	3,48	5,54	3,55	**5,44**	8,02	0,48	6,84	9,32	9,92	
75º			23,65	13,12	12,76	6,77	4,08	4,97	4,64	10,06	22,54		
90º													

MAXIMUM DEVIATION (%)	29,02
MINIMUM DEVIATION (%)	0,06
AVERAGE DEVIATION (%)	7,80
AV. DEVIATION - COINCIDING MEASUREMENT ANGLES (%)	4,38

MESH SAMPLE NUMBER

02g

PARAMETERS

LW	SW	w	e	b	i	color
16	8	2	2	1	4,5	

SPECULAR TRANSMITTANCE (%)

COMPUTER AIDED ASSESSMENT RESULT

y \ x	0º	15º	30º	45º	60º	75º	90º	105º	120º	135º	150º	165º	180º
0º		26,72	**17,06**	27,56	**36,95**	37,15	**37,38**	39,03	**39,59**	39,79	**36,45**	26,01	
15º		26,72	17,46	24,57	36,74	**36,85**	36,64	**38,17**	41,31	41,92	37,46	26,01	
30º		26,72	17,46	**27,71**	**37,96**	35,83	**37,25**	37,05	**41,92**	**42,73**	37,46	26,01	
45º		30,38	19,49	27,16	**36,03**	37,76	38,47	38,27	**40,50**	38,22	34,21	28,99	
60º		36,19	21,02	27,61	33,70	33,70	**39,29**	36,65	36,65	36,54	27,01	31,61	
75º			38,13	32,28	30,89	30,89	30,89	30,89	30,89	32,72	36,29		
90º													

LABORATORY ASSESSMENT RESULT

y \ x	0º	15º	30º	45º	60º	75º	90º	105º	120º	135º	150º	165º	180º
0º		0,41	0,25	21,56	33,90	40,92	45,53	50,92	55,57	58,70	45,32	5,78	
15º		0,27	0,27	21,11	34,45	40,98	45,57	49,94	53,93	56,28	45,60	4,45	
30º		0,25	0,28	20,92	33,33	40,31	44,49	47,76	51,35	51,47	39,52	7,65	
45º		0,23	0,33	21,05	33,70	40,40	45,32	47,96	47,30	44,90	32,46	4,86	
60º		0,46	0,43	17,42	33,97	41,18	45,15	39,67	35,87	28,24	11,84	3,50	
75º			1,61	12,57	22,59	25,84	25,93	16,50	9,62	4,87	6,14		
90º													

ABSOLUTE DEVIATION BETWEEN BOTH METHODS

y \ x	0º	15º	30º	45º	60º	75º	90º	105º	120º	135º	150º	165º	180º
0º		26,32	**16,81**	6,00	**3,04**	3,77	**8,15**	11,89	**15,98**	18,90	**8,87**	20,23	
15º		26,45	17,20	3,46	2,29	**4,14**	8,93	**11,78**	12,62	14,36	8,14	21,56	
30º		26,47	17,19	**6,79**	**4,63**	4,48	**7,24**	10,72	**9,43**	**8,73**	2,06	18,36	
45º		30,16	19,17	6,11	**2,34**	2,64	6,85	9,69	**6,80**	6,68	1,75	24,13	
60º		35,72	20,59	10,19	0,27	7,47	**5,86**	3,02	0,78	8,31	15,17	28,11	
75º			36,51	19,71	8,29	5,04	4,95	14,38	21,27	27,85	30,15		
90º													

MAXIMUM DEVIATION (%)	36,51
MINIMUM DEVIATION (%)	0,27
AVERAGE DEVIATION (%)	12,61
AV. DEVIATION - COINCIDING MEASUREMENT ANGLES (%)	8,04

MESH SAMPLE NUMBER

02w

PARAMETERS

LW	SW	w	e	b	i	color
16	8	2	2	1	4,5	

SPECULAR TRANSMITTANCE (%)

COMPUTER AIDED ASSESSMENT RESULT

y \ x	0º	15º	30º	45º	60º	75º	90º	105º	120º	135º	150º	165º	180º
0º		26,73	**17,15**	27,66	**37,12**	37,16	**37,39**	39,03	**39,83**	39,88	**36,82**	26,04	
15º		26,73	17,48	24,59	36,81	**36,85**	36,65	**38,17**	41,47	42,09	37,56	26,04	
30º		26,73	17,48	**27,73**	**38,14**	35,84	**37,26**	37,06	**41,93**	**42,82**	37,56	26,04	
45º		30,39	19,51	27,20	**36,04**	37,84	38,48	38,42	**40,66**	38,33	34,45	29,06	
60º		36,20	21,03	27,62	33,84	33,84	**39,57**	36,79	36,79	36,55	27,03	31,69	
75º			38,13	32,33	30,98	30,98	30,98	30,98	30,98	32,77	36,30		
90º													

LABORATORY ASSESSMENT RESULT

y \ x	0º	15º	30º	45º	60º	75º	90º	105º	120º	135º	150º	165º	180º
0º		1,89	2,07	25,03	39,42	41,38	46,53	52,76	60,03	65,22	50,12	6,52	
15º		1,90	2,13	23,36	39,30	41,22	47,14	51,79	58,51	61,64	49,11	4,04	
30º		2,16	2,41	24,78	39,53	41,73	47,92	52,61	57,87	60,44	47,96	12,63	
45º		2,13	2,45	26,47	35,09	47,21	48,83	52,04	54,05	53,15	43,69	9,94	
60º		1,98	3,10	19,45	33,00	40,25	51,69	46,69	41,57	36,56	20,24	2,09	
75º			4,88	14,56	22,42	25,84	30,55	24,26	15,78	5,53	1,70		
90º													

ABSOLUTE DEVIATION BETWEEN BOTH METHODS

y \ x	0º	15º	30º	45º	60º	75º	90º	105º	120º	135º	150º	165º	180º
0º		24,84	**15,08**	2,63	**2,30**	4,22	**9,13**	13,72	**20,20**	25,34	**13,30**	19,52	
15º		24,83	15,35	1,23	2,49	**4,36**	10,49	**13,61**	17,04	19,55	11,55	21,99	
30º		24,57	15,07	**2,95**	**1,39**	5,89	**10,66**	15,55	**15,94**	**17,62**	10,40	13,40	
45º		28,26	17,06	0,73	**0,95**	9,37	10,35	13,62	**13,39**	14,81	9,24	19,12	
60º		34,21	17,93	8,17	0,84	6,41	**12,12**	9,90	4,78	0,01	6,79	29,60	
75º			33,25	17,77	8,56	5,14	0,43	6,72	15,20	27,24	34,61		
90º													

MAXIMUM DEVIATION (%)	34,61
MINIMUM DEVIATION (%)	0,01
AVERAGE DEVIATION (%)	13,17
AV. DEVIATION - COINCIDING MEASUREMENT ANGLES (%)	10,20

MESH SAMPLE NUMBER

03b

PARAMETERS

LW	SW	w	e	b	i	color
62,5	23	8	1	2	25	

SPECULAR TRANSMITTANCE (%)

COMPUTER AIDED ASSESSMENT RESULT

y \ x	0º	15º	30º	45º	60º	75º	90º	105º	120º	135º	150º	165º	180º
0º		17,89	**7,32**	6,86	**13,51**	20,83	**25,96**	31,39	**39,62**	49,17	**59,95**	52,79	
15º		17,89	7,32	6,50	15,24	**23,67**	26,47	**30,89**	39,93	50,70	58,72	52,79	
30º		17,89	7,32	**7,21**	**12,70**	24,79	**26,01**	30,99	**40,13**	**48,97**	58,72	52,79	
45º		19,71	7,82	8,38	**15,85**	22,96	26,87	34,04	**38,71**	48,36	56,90	50,54	
60º		22,96	9,65	10,67	19,61	19,61	**27,84**	36,27	36,27	44,30	58,73	47,15	
75º			24,59	21,99	28,72	28,72	28,72	28,72	28,72	39,50	42,87		
90º													

LABORATORY ASSESSMENT RESULT

y \ x	0º	15º	30º	45º	60º	75º	90º	105º	120º	135º	150º	165º	180º
0º		0,28	0,03	0,39	13,15	19,03	26,24	32,07	39,58	48,83	53,96	9,01	
15º		0,49	0,03	0,30	11,36	19,10	29,07	31,60	38,61	47,91	56,49	20,79	
30º		0,43	0,03	0,33	10,44	19,47	26,00	31,84	38,72	47,44	54,11	32,87	
45º		0,38	0,03	0,28	12,37	19,01	26,32	32,83	38,85	47,29	53,54	30,64	
60º		0,68	0,05	0,39	11,64	20,05	26,03	31,49	37,16	41,79	46,47	29,52	
75º			0,74	1,22	8,91	15,84	22,38	23,66	21,42	15,32	5,53		
90º													

ABSOLUTE DEVIATION BETWEEN BOTH METHODS

y \ x	0º	15º	30º	45º	60º	75º	90º	105º	120º	135º	150º	165º	180º
0º		17,61	**7,29**	6,47	**0,36**	1,79	**0,28**	0,68	**0,04**	0,34	**5,99**	43,78	
15º		17,40	7,29	6,20	3,88	**4,57**	2,60	**0,72**	1,31	2,79	2,24	32,00	
30º		17,46	7,28	**6,89**	**2,26**	5,32	**0,00**	0,86	**1,41**	**1,53**	4,61	19,92	
45º		19,33	7,80	8,10	**3,48**	3,95	0,56	1,21	**0,14**	1,07	3,36	19,90	
60º		22,28	9,60	10,27	7,96	0,44	**1,81**	4,78	0,89	2,50	12,26	17,63	
75º			23,85	20,77	19,82	12,89	6,34	5,06	7,30	24,18	37,34		
90º													

MAXIMUM DEVIATION (%)	43,78
MINIMUM DEVIATION (%)	0,00
AVERAGE DEVIATION (%)	8,59
AV. DEVIATION - COINCIDING MEASUREMENT ANGLES (%)	2,45

MESH SAMPLE NUMBER

03g

PARAMETERS

LW	SW	w	e	b	i	color
62,5	23	8	1	2	25	

SPECULAR TRANSMITTANCE (%)

COMPUTER AIDED ASSESSMENT RESULT

y \ x	0º	15º	30º	45º	60º	75º	90º	105º	120º	135º	150º	165º	180º
0º		17,89	**7,32**	6,86	**13,52**	20,83	**25,96**	31,40	**39,62**	49,18	**59,95**	52,80	
15º		17,89	7,32	6,51	15,24	**23,68**	26,47	**30,89**	39,93	50,70	58,73	52,80	
30º		17,89	7,32	**7,22**	**12,71**	24,79	**26,01**	30,99	**40,13**	**48,97**	58,73	52,80	
45º		19,71	7,83	8,39	**15,85**	22,96	26,88	34,04	**38,71**	48,36	56,90	50,55	
60º		22,96	9,66	10,67	19,61	19,61	**27,84**	36,27	36,27	44,30	58,73	47,16	
75º			24,59	22,00	28,73	28,73	28,73	28,73	28,73	39,50	42,87		
90º													

LABORATORY ASSESSMENT RESULT

y \ x	0º	15º	30º	45º	60º	75º	90º	105º	120º	135º	150º	165º	180º
0º		0,80	0,08	0,45	10,04	17,91	23,59	29,54	36,57	45,48	50,60	24,53	
15º		0,71	0,08	0,26	10,16	17,88	24,02	29,64	35,99	44,22	53,18	28,37	
30º		0,65	0,09	0,23	12,06	18,97	24,75	29,85	36,45	44,69	55,70	29,95	
45º		0,39	0,09	0,52	12,34	18,95	24,91	30,86	35,98	44,03	48,92	25,76	
60º		0,59	0,16	0,53	10,50	18,33	23,76	26,18	33,65	36,15	32,13	10,33	
75º			0,88	1,50	7,59	17,43	22,02	21,97	18,60	11,98	4,81		
90º													

ABSOLUTE DEVIATION BETWEEN BOTH METHODS

y \ x	0º	15º	30º	45º	60º	75º	90º	105º	120º	135º	150º	165º	180º
0º		17,08	**7,24**	6,41	**3,48**	2,92	**2,37**	1,86	**3,06**	3,69	**9,35**	28,26	
15º		17,17	7,24	6,25	5,08	**5,80**	2,45	**1,25**	3,93	6,48	5,55	24,42	
30º		17,24	7,23	**6,99**	**0,64**	5,83	**1,26**	1,14	**3,68**	**4,28**	3,02	22,84	
45º		19,33	7,74	7,86	**3,52**	4,02	1,96	3,18	**2,73**	4,33	7,97	24,79	
60º		22,37	9,50	10,15	9,12	1,29	**4,09**	10,10	2,62	8,15	26,61	36,83	
75º			23,72	20,49	21,14	11,30	6,70	6,76	10,12	27,52	38,07		
90º													

MAXIMUM DEVIATION (%)	38,07
MINIMUM DEVIATION (%)	0,64
AVERAGE DEVIATION (%)	9,99
AV. DEVIATION - COINCIDING MEASUREMENT ANGLES (%)	3,98

MESH SAMPLE NUMBER

03w

PARAMETERS

LW	SW	w	e	b	i	color
62,5	23	8	1	2	25	

SPECULAR TRANSMITTANCE (%)

COMPUTER AIDED ASSESSMENT RESULT

y \ x	0º	15º	30º	45º	60º	75º	90º	105º	120º	135º	150º	165º	180º
0º		17,89	**7,33**	6,88	**13,53**	20,84	**25,98**	31,40	**39,63**	49,20	**60,20**	53,45	
15º		17,89	7,33	6,52	15,26	**23,69**	26,48	**30,90**	39,94	50,74	58,83	53,45	
30º		17,89	7,33	**7,24**	**12,82**	24,80	**26,02**	31,00	**40,14**	**48,99**	58,83	53,45	
45º		19,72	7,84	8,40	**15,87**	22,98	26,93	34,05	**38,73**	48,39	57,00	51,09	
60º		22,96	9,66	10,69	19,62	19,62	**27,99**	36,32	36,32	**44,32**	59,03	47,39	
75º			24,60	22,13	29,03	29,03	29,03	29,03	29,03	39,85	43,36		
90º													

LABORATORY ASSESSMENT RESULT

y \ x	0º	15º	30º	45º	60º	75º	90º	105º	120º	135º	150º	165º	180º
0º		0,82	0,62	1,02	11,75	18,20	29,55	32,53	40,37	51,84	59,23	25,91	
15º		0,86	0,67	1,17	12,25	19,98	30,64	33,45	40,97	51,76	64,12	35,73	
30º		1,26	0,72	1,19	11,84	20,03	27,57	33,71	41,42	52,56	63,66	43,54	
45º		1,30	0,74	1,22	11,18	19,86	26,59	39,49	41,55	52,49	62,46	42,50	
60º		1,73	1,02	1,22	13,16	20,32	26,94	34,13	40,85	46,35	45,85	24,23	
75º			2,07	2,87	9,12	15,97	22,97	26,78	25,53	17,42	8,02		
90º													

ABSOLUTE DEVIATION BETWEEN BOTH METHODS

y \ x	0º	15º	30º	45º	60º	75º	90º	105º	120º	135º	150º	165º	180º
0º		17,07	**6,71**	5,86	**1,78**	2,65	**3,57**	1,12	**0,74**	2,64	**0,97**	27,54	
15º		17,03	6,66	5,36	3,01	**3,71**	4,16	**2,55**	1,03	1,02	5,30	17,72	
30º		16,63	6,61	**6,05**	**0,97**	4,78	**1,55**	2,71	**1,28**	**3,57**	4,83	9,91	
45º		18,41	7,09	7,18	**4,69**	3,12	0,33	5,44	**2,82**	4,11	5,47	8,59	
60º		21,23	8,64	9,47	6,46	0,69	**1,04**	2,19	4,54	2,03	13,19	23,16	
75º			22,52	19,26	19,91	13,05	6,05	2,25	3,50	22,43	35,34		
90º													

MAXIMUM DEVIATION (%)	35,34
MINIMUM DEVIATION (%)	0,33
AVERAGE DEVIATION (%)	7,83
AV. DEVIATION - COINCIDING MEASUREMENT ANGLES (%)	2,80

MESH SAMPLE NUMBER

04b

PARAMETERS

LW	SW	w	e	b	i	color
10	6,5	2,1	1	1	4,5	

SPECULAR TRANSMITTANCE (%)

COMPUTER AIDED ASSESSMENT RESULT

y \ x	0°	15°	30°	45°	60°	75°	90°	105°	120°	135°	150°	165°	180°
0°		22,88	**11,58**	12,39	**21,74**	25,75	**27,79**	30,68	**35,35**	42,47	**42,47**	33,10	
15°		22,88	12,40	12,19	22,25	**27,03**	28,60	**30,28**	35,05	41,35	43,38	33,10	
30°		22,88	12,40	**13,31**	**21,54**	28,04	**28,55**	31,29	**36,27**	**41,96**	43,38	33,10	
45°		25,49	13,31	14,94	**20,83**	25,20	28,55	33,02	**36,37**	40,14	45,21	35,26	
60°		29,59	17,27	17,17	21,74	21,74	**25,10**	29,87	29,87	34,75	35,06	34,90	
75°			35,82	28,85	25,52	25,52	25,52	25,52	25,52	30,72	36,43		
90°													

LABORATORY ASSESSMENT RESULT

y \ x	0°	15°	30°	45°	60°	75°	90°	105°	120°	135°	150°	165°	180°
0°		1,39	0,03	2,30	15,64	18,74	20,35	22,31	23,83	23,19	16,45	0,08	
15°		1,67	0,03	1,44	14,78	18,81	20,44	21,75	23,18	22,24	15,57	0,11	
30°		1,15	0,03	1,54	13,73	19,11	20,43	21,24	21,73	19,84	11,11	0,14	
45°		0,72	0,03	1,22	14,64	18,14	19,58	19,70	18,87	12,89	1,97	0,09	
60°		0,59	0,05	0,57	8,83	13,80	14,83	13,33	7,41	0,81	0,04	0,42	
75°			0,78	0,34	1,67	2,64	1,61	0,34	0,17	0,43	0,41		
90°													

ABSOLUTE DEVIATION BETWEEN BOTH METHODS

y \ x	0°	15°	30°	45°	60°	75°	90°	105°	120°	135°	150°	165°	180°
0°		21,49	**11,55**	10,09	**6,10**	7,02	**7,43**	8,37	**11,53**	19,27	**26,02**	33,02	
15°		21,20	12,37	10,75	7,47	**8,22**	8,16	**8,52**	11,87	19,11	27,81	32,98	
30°		21,73	12,37	**11,77**	**7,81**	8,93	**8,12**	10,05	**14,54**	**22,13**	32,27	32,95	
45°		24,76	13,28	13,72	**6,19**	7,05	8,98	13,33	**17,50**	27,25	43,24	35,17	
60°		29,00	17,22	16,60	12,92	7,94	**10,26**	16,55	22,46	33,94	35,02	34,48	
75°			35,03	28,51	23,86	22,89	23,91	25,18	25,36	30,29	36,02		
90°													

MAXIMUM DEVIATION (%)	43,24
MINIMUM DEVIATION (%)	6,10
AVERAGE DEVIATION (%)	18,92
AV. DEVIATION - COINCIDING MEASUREMENT ANGLES (%)	11,85

MESH SAMPLE NUMBER

04g

PARAMETERS

LW	SW	w	e	b	i	color
10	6,5	2,1	1	1	4,5	

SPECULAR TRANSMITTANCE (%)

COMPUTER AIDED ASSESSMENT RESULT

y \ x	0º	15º	30º	45º	60º	75º	90º	105º	120º	135º	150º	165º	180º
0º		22,88	**11,58**	12,40	**21,75**	25,76	**27,79**	30,68	**35,36**	42,47	**42,47**	33,11	
15º		22,88	12,40	12,20	22,25	**27,03**	28,60	**30,28**	35,05	41,35	43,39	33,11	
30º		22,88	12,40	**13,31**	**21,54**	28,04	**28,55**	31,29	**36,27**	**41,96**	43,39	33,11	
45º		25,49	13,31	14,94	**20,83**	25,20	28,55	33,02	**36,37**	40,14	45,21	35,27	
60º		29,59	17,27	17,17	21,75	21,75	**25,10**	29,87	29,87	34,75	35,07	34,91	
75º			35,82	28,86	25,53	25,53	25,53	25,53	25,53	30,72	36,44		
90º													

LABORATORY ASSESSMENT RESULT

y \ x	0º	15º	30º	45º	60º	75º	90º	105º	120º	135º	150º	165º	180º
0º		0,71	0,06	2,55	15,26	18,47	19,77	21,57	23,46	22,34	15,20	0,25	
15º		0,67	0,06	2,21	14,19	18,13	19,88	21,19	22,36	21,54	14,83	0,20	
30º		0,81	0,06	2,18	14,59	18,33	19,93	20,57	21,23	19,43	10,13	0,18	
45º		0,55	0,05	1,01	14,49	17,24	18,76	18,96	17,35	12,52	1,42	0,09	
60º		0,59	0,11	1,03	8,88	13,03	15,17	12,36	7,16	0,84	0,05	0,31	
75º			0,78	0,47	1,75	2,50	1,63	0,41	0,12	0,14	0,33		
90º													

ABSOLUTE DEVIATION BETWEEN BOTH METHODS

y \ x	0º	15º	30º	45º	60º	75º	90º	105º	120º	135º	150º	165º	180º
0º		22,17	**11,52**	9,85	**6,49**	7,29	**8,02**	9,11	**11,90**	20,13	**27,27**	32,86	
15º		22,21	12,34	9,98	8,07	**8,90**	8,73	**9,09**	12,69	19,81	28,55	32,90	
30º		22,07	12,34	**11,13**	**6,96**	9,71	**8,62**	10,72	**15,04**	**22,53**	33,25	32,93	
45º		24,94	13,26	13,93	**6,34**	7,95	9,80	14,07	**19,03**	27,62	43,80	35,17	
60º		29,00	17,17	16,14	12,87	8,72	**9,93**	17,52	22,71	33,91	35,01	34,60	
75º			35,03	28,39	23,78	23,02	23,89	25,12	25,41	30,58	36,10		
90º													

MAXIMUM DEVIATION (%)	43,80
MINIMUM DEVIATION (%)	6,34
AVERAGE DEVIATION (%)	19,22
AV. DEVIATION - COINCIDING MEASUREMENT ANGLES (%)	12,18

MESH SAMPLE NUMBER

04w

PARAMETERS

LW	SW	w	e	b	i	color
10	6,5	2,1	1	1	4,5	

SPECULAR TRANSMITTANCE (%)

COMPUTER AIDED ASSESSMENT RESULT

y \ x	0°	15°	30°	45°	60°	75°	90°	105°	120°	135°	150°	165°	180°
0°		22,88	**11,59**	12,42	**21,82**	25,76	**27,80**	30,69	**35,36**	42,49	**42,56**	33,28	
15°		22,88	12,41	12,21	22,26	**27,04**	28,61	**30,29**	35,06	41,40	43,47	33,28	
30°		22,88	12,41	**13,33**	**21,55**	28,05	**28,56**	31,30	**36,35**	**41,99**	43,47	33,28	
45°		25,49	13,32	15,04	**20,92**	25,21	28,73	33,17	**36,38**	40,34	45,22	35,59	
60°		29,60	17,28	17,19	21,83	21,83	**25,11**	30,05	30,05	34,86	35,47	35,01	
75°			35,82	28,96	25,68	25,68	25,68	25,68	25,68	30,90	36,59		
90°													

LABORATORY ASSESSMENT RESULT

y \ x	0°	15°	30°	45°	60°	75°	90°	105°	120°	135°	150°	165°	180°
0°		0,80	0,32	2,88	14,34	18,68	19,98	22,25	24,19	23,98	17,43	0,94	
15°		0,77	0,32	2,05	14,19	18,57	20,37	21,66	23,04	22,75	17,23	0,90	
30°		1,05	0,35	3,30	14,62	18,24	20,40	21,04	21,52	20,26	12,57	0,77	
45°		1,03	0,36	1,92	14,31	17,62	19,21	19,76	18,72	13,99	2,89	0,53	
60°		1,08	0,50	1,22	11,25	14,59	16,24	13,86	8,64	1,40	0,35	0,44	
75°			1,24	0,86	2,47	3,34	2,39	0,81	0,34	0,27	0,44		
90°													

ABSOLUTE DEVIATION BETWEEN BOTH METHODS

y \ x	0°	15°	30°	45°	60°	75°	90°	105°	120°	135°	150°	165°	180°
0°		22,08	**11,27**	9,53	**7,49**	7,09	**7,82**	8,44	**11,17**	18,51	**25,13**	32,34	
15°		22,11	12,08	10,16	8,08	**8,46**	8,24	**8,63**	12,02	18,65	26,24	32,38	
30°		21,84	12,06	**10,04**	**6,94**	9,81	**8,15**	10,25	**14,83**	**21,73**	30,90	32,52	
45°		24,46	12,96	13,12	**6,61**	7,59	9,52	13,41	**17,67**	26,35	42,33	35,06	
60°		28,51	16,78	15,97	10,58	7,24	**8,86**	16,19	21,41	33,46	35,13	34,57	
75°			34,58	28,10	23,21	22,34	23,29	24,87	25,34	30,63	36,15		
90°													

MAXIMUM DEVIATION (%)	42,33
MINIMUM DEVIATION (%)	6,61
AVERAGE DEVIATION (%)	18,64
AV. DEVIATION - COINCIDING MEASUREMENT ANGLES (%)	11,65

MESH SAMPLE NUMBER

05b

PARAMETERS

LW	SW	w	e	b	i	color
6	4,5	1,5	1	1	2	

SPECULAR TRANSMITTANCE (%)

COMPUTER AIDED ASSESSMENT RESULT

y \ x	0º	15º	30º	45º	60º	75º	90º	105º	120º	135º	150º	165º	180º
0º		23,52	**13,24**	14,54	**22,11**	24,40	**24,45**	28,18	**31,96**	38,14	**37,25**	26,86	
15º		23,52	14,14	13,34	23,60	**23,30**	24,75	**27,78**	32,46	38,54	37,05	26,86	
30º		23,52	14,14	**15,44**	**22,61**	24,99	**27,08**	28,98	**33,56**	**37,75**	37,05	26,86	
45º		27,28	14,44	17,13	**23,30**	24,70	27,29	27,88	**30,27**	30,12	33,16	30,47	
60º		33,90	19,92	19,32	23,30	23,30	**22,81**	21,71	21,71	24,20	23,61	34,80	
75º			38,31	31,21	27,07	27,07	27,07	27,07	27,07	29,72	36,11		
90º													

LABORATORY ASSESSMENT RESULT

y \ x	0º	15º	30º	45º	60º	75º	90º	105º	120º	135º	150º	165º	180º
0º		1,56	0,04	4,69	16,37	24,60	24,92	27,70	29,49	28,60	20,89	0,23	
15º		1,90	0,07	4,32	15,99	21,38	28,17	26,87	28,14	27,30	20,28	2,25	
30º		1,14	0,16	4,00	15,29	21,32	23,66	26,00	26,67	25,09	14,62	0,22	
45º		0,88	0,04	3,43	15,78	19,77	22,28	24,15	23,61	19,31	3,32	0,08	
60º		0,96	0,07	2,03	10,70	16,11	18,10	17,67	12,49	3,59	0,10	0,68	
75º			0,88	0,83	3,51	5,92	6,29	2,51	0,41	0,24	0,39		
90º													

ABSOLUTE DEVIATION BETWEEN BOTH METHODS

y \ x	0º	15º	30º	45º	60º	75º	90º	105º	120º	135º	150º	165º	180º
0º		21,95	**13,21**	9,85	**5,73**	0,20	**0,46**	0,48	**2,47**	9,55	**16,36**	26,62	
15º		21,62	14,07	9,02	7,61	**1,92**	3,42	**0,91**	4,32	11,24	16,77	24,61	
30º		22,38	13,98	**11,43**	**7,31**	3,68	**3,42**	2,98	**6,89**	**12,65**	22,43	26,63	
45º		26,40	14,40	13,70	**7,52**	4,94	5,00	3,74	**6,66**	10,82	29,84	30,38	
60º		32,94	19,85	17,29	12,60	7,20	**4,71**	4,04	9,21	20,61	23,50	34,12	
75º			37,43	30,38	23,56	21,14	20,78	24,56	26,66	29,48	35,72		
90º													

MAXIMUM DEVIATION (%)	37,43
MINIMUM DEVIATION (%)	0,20
AVERAGE DEVIATION (%)	14,77
AV. DEVIATION - COINCIDING MEASUREMENT ANGLES (%)	6,78

MESH SAMPLE NUMBER

05g

PARAMETERS

LW	SW	w	e	b	i	color
6	4,5	1,5	1	1	2	

SPECULAR TRANSMITTANCE (%)

COMPUTER AIDED ASSESSMENT RESULT

y \ x	0º	15º	30º	45º	60º	75º	90º	105º	120º	135º	150º	165º	180º
0º		23,52	**13,25**	14,54	**22,11**	24,40	**24,46**	28,18	**31,97**	38,14	**37,25**	26,86	
15º		23,52	14,14	13,35	23,60	**23,31**	24,75	**27,79**	32,46	38,54	37,05	26,86	
30º		23,52	14,14	**15,44**	**22,61**	25,00	**27,09**	28,98	**33,56**	**37,75**	37,05	26,86	
45º		27,28	14,44	17,13	**23,31**	24,71	27,29	27,89	**30,28**	30,13	33,16	30,47	
60º		33,91	19,92	19,33	23,31	23,31	**22,81**	21,71	21,71	24,20	23,61	34,81	
75º			38,31	31,22	27,07	27,07	27,07	27,07	27,07	29,72	36,11		
90º													

LABORATORY ASSESSMENT RESULT

y \ x	0º	15º	30º	45º	60º	75º	90º	105º	120º	135º	150º	165º	180º
0º		0,22	7,70	19,81	22,08	23,25	23,93	23,45	20,48	12,26	0,20	0,00	
15º		0,73	0,08	4,85	14,13	18,85	21,75	23,76	25,00	24,20	17,30	0,75	
30º		0,94	0,08	4,71	13,86	18,97	21,75	22,81	23,66	22,01	12,23	0,30	
45º		0,72	0,07	3,50	13,24	17,82	20,70	21,38	20,51	15,81	2,93	0,12	
60º		0,56	0,12	2,05	10,60	14,80	17,74	16,18	11,82	3,39	0,14	0,33	
75º			0,69	0,91	3,15	5,04	5,64	2,37	0,58	0,27	0,85		
90º													

ABSOLUTE DEVIATION BETWEEN BOTH METHODS

y \ x	0º	15º	30º	45º	60º	75º	90º	105º	120º	135º	150º	165º	180º
0º		23,30	**5,55**	5,26	**0,03**	1,15	**0,53**	4,74	**11,48**	25,89	**37,05**	26,86	
15º		22,78	14,07	8,50	9,47	**4,45**	3,00	**4,03**	7,46	14,34	19,75	26,11	
30º		22,58	14,07	**10,74**	**8,75**	6,03	**5,33**	6,17	**9,90**	**15,73**	24,82	26,57	
45º		26,56	14,37	13,64	**10,06**	6,89	6,59	6,51	**9,77**	14,31	30,23	30,35	
60º		33,35	19,80	17,27	12,71	8,51	**5,07**	5,54	9,89	20,81	23,47	34,48	
75º			37,62	30,31	23,92	22,03	21,43	24,70	26,50	29,45	35,26		
90º													

MAXIMUM DEVIATION (%)	37,62
MINIMUM DEVIATION (%)	0,03
AVERAGE DEVIATION (%)	16,22
AV. DEVIATION - COINCIDING MEASUREMENT ANGLES (%)	9,23

MESH SAMPLE NUMBER

05w

PARAMETERS

LW	SW	w	e	b	i	color
6	4,5	1,5	1	1	2	

SPECULAR TRANSMITTANCE (%)

COMPUTER AIDED ASSESSMENT RESULT

y \ x	0º	15º	30º	45º	60º	75º	90º	105º	120º	135º	150º	165º	180º
0º		23,52	**13,26**	14,56	**22,12**	24,41	**24,47**	28,20	**31,98**	38,30	**37,58**	27,02	
15º		23,52	14,15	13,37	23,61	**23,32**	24,76	**27,80**	32,47	38,64	37,21	27,02	
30º		23,52	14,15	**15,46**	**22,70**	25,01	**27,10**	28,99	**33,57**	**37,90**	37,21	27,02	
45º		27,29	14,46	17,15	**23,32**	24,97	27,31	27,92	**30,28**	30,14	33,18	30,49	
60º		33,91	20,01	19,43	23,41	23,41	**22,97**	21,73	21,73	24,22	23,78	34,83	
75º			38,38	31,38	27,31	27,31	27,31	27,31	27,31	29,89	36,19		
90º													

LABORATORY ASSESSMENT RESULT

y \ x	0º	15º	30º	45º	60º	75º	90º	105º	120º	135º	150º	165º	180º
0º		0,88	0,51	5,85	16,86	22,06	28,56	27,82	30,67	30,94	26,59	1,55	
15º		0,82	0,50	2,32	16,12	20,46	24,03	26,64	28,66	28,64	21,88	1,57	
30º		1,09	0,54	5,08	16,03	21,47	24,24	26,37	27,66	26,74	17,43	1,00	
45º		1,09	0,50	4,59	16,88	20,42	23,08	24,66	26,18	20,46	5,57	0,67	
60º		1,27	0,63	3,05	12,30	17,22	20,42	19,65	15,96	5,85	0,68	0,53	
75º			1,57	1,88	5,08	7,08	8,74	4,35	1,15	0,72	0,64		
90º													

ABSOLUTE DEVIATION BETWEEN BOTH METHODS

y \ x	0º	15º	30º	45º	60º	75º	90º	105º	120º	135º	150º	165º	180º
0º		22,64	**12,75**	8,71	**5,26**	2,35	**4,09**	0,38	**1,31**	7,36	**10,98**	25,48	
15º		22,71	13,65	11,05	7,49	**2,86**	0,73	**1,15**	3,81	10,00	15,33	25,45	
30º		22,43	13,61	**10,38**	**6,67**	3,53	**2,86**	2,62	**5,91**	**11,16**	19,79	26,02	
45º		26,19	13,96	12,56	**6,44**	4,55	4,22	3,26	**4,10**	9,68	27,61	29,82	
60º		32,64	19,38	16,38	11,11	6,19	**2,55**	2,08	5,77	18,37	23,10	34,30	
75º			36,81	29,50	22,24	20,23	18,57	22,96	26,16	29,17	35,55		
90º													

MAXIMUM DEVIATION (%)	36,81
MINIMUM DEVIATION (%)	0,38
AVERAGE DEVIATION (%)	14,00
AV. DEVIATION - COINCIDING MEASUREMENT ANGLES (%)	5,90

MESH SAMPLE NUMBER

06b

PARAMETERS

LW	SW	w	e	b	i	color
60	21	10	1,5	2	33	

SPECULAR TRANSMITTANCE (%)

COMPUTER AIDED ASSESSMENT RESULT

y \ x	0º	15º	30º	45º	60º	75º	90º	105º	120º	135º	150º	165º	180º
0º		10,25	**3,29**	2,49	**1,89**	1,99	**3,38**	5,43	**6,28**	9,67	**15,05**	27,05	
15º		10,25	2,99	2,79	1,79	**1,99**	3,64	**4,78**	6,88	9,87	13,66	27,05	
30º		10,25	2,99	**1,50**	**2,09**	2,49	**3,09**	5,58	**6,58**	**10,67**	13,66	27,05	
45º		11,57	2,69	2,89	**3,39**	2,49	4,84	5,48	**6,18**	10,17	14,75	27,52	
60º		13,72	4,49	3,39	3,29	3,29	**4,19**	6,28	6,28	9,77	17,35	30,36	
75º			13,52	10,64	9,95	9,95	9,95	9,95	9,95	17,07	24,74		
90º													

LABORATORY ASSESSMENT RESULT

y \ x	0º	15º	30º	45º	60º	75º	90º	105º	120º	135º	150º	165º	180º
0º		1,33	0,09	0,01	0,10	2,43	4,80	6,20	7,29	8,68	11,56	22,43	
15º		1,44	0,07	0,01	0,11	2,10	4,71	6,01	7,09	8,48	12,09	17,13	
30º		1,13	0,04	0,01	0,09	2,31	5,36	5,88	7,08	8,68	11,62	10,00	
45º		0,67	0,02	0,02	0,22	1,67	4,71	6,25	7,28	8,96	11,60	8,02	
60º		0,43	0,05	0,03	0,19	2,36	5,30	6,16	7,30	8,47	9,47	3,90	
75º			0,69	0,19	0,35	2,34	4,16	5,23	5,72	5,53	3,91		
90º													

ABSOLUTE DEVIATION BETWEEN BOTH METHODS

y \ x	0º	15º	30º	45º	60º	75º	90º	105º	120º	135º	150º	165º	180º
0º		8,93	**3,20**	2,48	**1,80**	0,43	**1,41**	0,76	**1,01**	0,99	**3,49**	4,62	
15º		8,81	2,92	2,78	1,68	**0,10**	1,07	**1,22**	0,22	1,39	1,57	9,92	
30º		9,12	2,95	**1,48**	**2,00**	0,18	**2,26**	0,30	**0,50**	**1,98**	2,04	17,05	
45º		10,90	2,67	2,87	**3,17**	0,82	0,13	0,77	**1,10**	1,21	3,15	19,50	
60º		13,28	4,44	3,36	3,10	0,93	**1,11**	0,12	1,02	1,30	7,88	26,46	
75º			12,83	10,45	9,60	7,61	5,80	4,72	4,24	11,55	20,83		
90º													

MAXIMUM DEVIATION (%)	26,46
MINIMUM DEVIATION (%)	0,10
AVERAGE DEVIATION (%)	4,65
AV. DEVIATION - COINCIDING MEASUREMENT ANGLES (%)	1,72

MESH SAMPLE NUMBER

06g

PARAMETERS

LW	SW	w	e	b	i	color
60	21	10	1,5	2	33	

SPECULAR TRANSMITTANCE (%)

COMPUTER AIDED ASSESSMENT RESULT

y \ x	0º	15º	30º	45º	60º	75º	90º	105º	120º	135º	150º	165º	180º
0º		10,25	**3,29**	2,49	**1,89**	2,00	**3,38**	5,43	**6,28**	9,67	**15,05**	27,06	
15º		10,25	2,99	2,79	1,80	**2,00**	3,64	**4,79**	6,88	9,87	13,66	27,06	
30º		10,25	2,99	**1,50**	**2,09**	2,49	**3,09**	5,58	**6,58**	**10,67**	13,66	27,06	
45º		11,57	2,69	2,89	**3,39**	2,49	4,84	5,48	**6,18**	10,17	14,75	27,53	
60º		13,72	4,49	3,39	3,29	3,29	**4,19**	6,28	6,28	9,77	17,35	30,37	
75º			13,52	10,64	9,95	9,95	9,95	9,95	9,95	17,07	24,74		
90º													

LABORATORY ASSESSMENT RESULT

y \ x	0º	15º	30º	45º	60º	75º	90º	105º	120º	135º	150º	165º	180º
0º		1,22	0,20	0,03	0,05	2,17	4,47	5,57	7,02	8,76	12,23	18,34	
15º		1,18	0,14	0,03	0,05	2,18	4,44	5,71	6,88	8,64	12,90	17,70	
30º		1,16	0,08	0,03	0,06	2,16	5,11	5,67	6,87	8,72	12,49	11,72	
45º		0,68	0,03	0,03	0,09	2,33	5,12	5,85	6,93	9,00	12,00	7,79	
60º		0,53	0,08	0,04	0,15	2,34	5,30	5,95	7,23	8,56	9,03	3,55	
75º			0,69	0,19	0,41	1,92	4,48	5,34	5,69	5,59	3,14		
90º													

ABSOLUTE DEVIATION BETWEEN BOTH METHODS

y \ x	0º	15º	30º	45º	60º	75º	90º	105º	120º	135º	150º	165º	180º
0º		9,04	**3,09**	2,46	**1,84**	0,18	**1,08**	0,14	**0,74**	0,91	**2,82**	8,71	
15º		9,07	2,85	2,76	1,74	**0,19**	0,80	**0,92**	0,01	1,23	0,76	9,36	
30º		9,09	2,91	**1,47**	**2,03**	0,34	**2,02**	0,09	**0,28**	**1,95**	1,16	15,33	
45º		10,90	2,66	2,86	**3,30**	0,16	0,28	0,37	**0,74**	1,17	2,75	19,74	
60º		13,19	4,41	3,35	3,14	0,95	**1,11**	0,33	0,95	1,21	8,31	26,83	
75º			12,83	10,45	9,54	8,03	5,47	4,62	4,26	11,49	21,60		
90º													

MAXIMUM DEVIATION (%)	26,83
MINIMUM DEVIATION (%)	0,01
AVERAGE DEVIATION (%)	4,60
AV. DEVIATION - COINCIDING MEASUREMENT ANGLES (%)	1,57

MESH SAMPLE NUMBER

06w

PARAMETERS

LW	SW	w	e	b	i	color
60	21	10	1,5	2	33	

SPECULAR TRANSMITTANCE (%)

COMPUTER AIDED ASSESSMENT RESULT

y \ x	0º	15º	30º	45º	60º	75º	90º	105º	120º	135º	150º	165º	180º
0º		10,30	**3,29**	2,49	**1,90**	2,05	**3,39**	5,44	**6,29**	9,68	**15,15**	27,99	
15º		10,30	2,99	2,79	1,80	**2,00**	3,73	**4,79**	6,88	9,88	13,69	27,99	
30º		10,30	2,99	**1,50**	**2,10**	2,50	**3,18**	5,59	**6,59**	**10,67**	13,69	27,99	
45º		11,60	2,69	2,89	**3,39**	2,50	4,96	5,50	**6,19**	10,18	14,77	28,62	
60º		13,72	4,49	3,39	3,29	3,29	**4,19**	6,33	6,33	9,79	17,43	31,79	
75º			13,57	10,74	10,16	10,16	10,16	10,16	10,16	17,29	25,13		
90º													

LABORATORY ASSESSMENT RESULT

y \ x	0º	15º	30º	45º	60º	75º	90º	105º	120º	135º	150º	165º	180º
0º		0,49	0,22	0,10	0,20	2,17	4,56	5,95	7,05	8,65	11,85	15,03	
15º		0,71	0,17	0,10	0,20	2,11	4,50	5,79	6,91	8,44	12,29	13,37	
30º		1,08	0,12	0,10	0,19	2,06	4,47	5,67	6,92	8,74	12,39	12,78	
45º		0,79	0,09	0,11	0,22	2,15	4,61	5,99	7,18	9,26	12,62	10,70	
60º		0,68	0,17	0,12	0,27	2,25	5,51	6,12	7,51	9,00	10,29	6,08	
75º			1,01	0,39	0,48	2,05	4,99	5,69	6,26	6,14	4,70		
90º													

ABSOLUTE DEVIATION BETWEEN BOTH METHODS

y \ x	0º	15º	30º	45º	60º	75º	90º	105º	120º	135º	150º	165º	180º
0º		9,81	**3,07**	2,39	**1,70**	0,13	**1,18**	0,52	**0,77**	1,03	**3,31**	12,96	
15º		9,59	2,82	2,69	1,60	**0,11**	0,77	**1,00**	0,03	1,43	1,40	14,62	
30º		9,22	2,87	**1,39**	**1,90**	0,44	**1,29**	0,08	**0,34**	**1,94**	1,30	15,21	
45º		10,81	2,61	2,78	**3,17**	0,35	0,36	0,49	**0,99**	0,92	2,15	17,93	
60º		13,03	4,32	3,28	3,02	1,04	**1,31**	0,21	1,18	0,79	7,15	25,71	
75º			12,55	10,34	9,68	8,11	5,17	4,47	3,90	11,16	20,43		
90º													

MAXIMUM DEVIATION (%)	25,71
MINIMUM DEVIATION (%)	0,03
AVERAGE DEVIATION (%)	4,66
AV. DEVIATION - COINCIDING MEASUREMENT ANGLES (%)	1,56

MESH SAMPLE NUMBER

07b

PARAMETERS

LW	SW	w	e	b	i	color
115	52	23	1	2	43,5	

SPECULAR TRANSMITTANCE (%)

COMPUTER AIDED ASSESSMENT RESULT

y \ x	0º	15º	30º	45º	60º	75º	90º	105º	120º	135º	150º	165º	180º
0º		11,63	**4,07**	2,19	**1,73**	6,66	**10,05**	16,68	**21,97**	30,61	**43,33**	56,50	
15º		11,63	4,78	3,25	2,14	**6,00**	10,88	**15,97**	20,95	32,34	42,72	56,50	
30º		11,63	4,78	**3,05**	**2,64**	8,14	**11,59**	15,86	**21,87**	**32,24**	42,72	56,50	
45º		13,34	4,17	3,66	**3,46**	6,10	13,07	18,10	**21,76**	31,68	39,77	54,14	
60º		16,65	6,20	4,68	5,39	5,39	**14,34**	21,36	21,36	29,09	45,16	51,86	
75º			18,90	15,96	18,67	18,67	18,67	18,67	18,67	32,11	41,40		
90º													

LABORATORY ASSESSMENT RESULT

y \ x	0º	15º	30º	45º	60º	75º	90º	105º	120º	135º	150º	165º	180º
0º		0,71	0,06	0,01	1,08	7,93	12,15	16,67	22,36	29,63	40,29	37,85	
15º		0,69	0,04	0,01	1,20	7,79	11,90	16,19	21,41	28,68	40,79	41,24	
30º		0,80	0,02	0,01	1,26	8,01	11,73	16,11	21,46	29,03	38,89	39,62	
45º		0,56	0,01	0,01	1,35	8,14	11,90	16,60	21,45	29,28	39,08	34,36	
60º		0,46	0,03	0,02	1,51	8,01	11,43	16,16	21,27	27,35	28,74	14,78	
75º			0,60	0,20	1,96	6,34	10,40	14,54	17,64	17,79	7,81		
90º													

ABSOLUTE DEVIATION BETWEEN BOTH METHODS

y \ x	0º	15º	30º	45º	60º	75º	90º	105º	120º	135º	150º	165º	180º
0º		10,92	**4,01**	2,18	**0,65**	1,27	**2,10**	0,01	**0,39**	0,98	**3,04**	18,66	
15º		10,94	4,74	3,25	0,93	**1,79**	1,01	**0,23**	0,46	3,66	1,93	15,27	
30º		10,83	4,76	**3,04**	**1,39**	0,13	**0,13**	0,24	**0,40**	**3,21**	3,83	16,89	
45º		12,78	4,16	3,65	**2,10**	2,04	1,17	1,51	**0,31**	2,40	0,69	19,78	
60º		16,18	6,17	4,66	3,88	2,62	**2,91**	5,20	0,09	1,73	16,41	37,08	
75º			18,30	15,76	16,71	12,33	8,27	4,13	1,03	14,32	33,58		
90º													

MAXIMUM DEVIATION (%)	37,08
MINIMUM DEVIATION (%)	0,01
AVERAGE DEVIATION (%)	6,33
AV. DEVIATION - COINCIDING MEASUREMENT ANGLES (%)	1,71

MESH SAMPLE NUMBER

07g

PARAMETERS

LW	SW	w	e	b	i	color
115	52	23	1	2	43,5	

SPECULAR TRANSMITTANCE (%)

COMPUTER AIDED ASSESSMENT RESULT

y \ x	0°	15°	30°	45°	60°	75°	90°	105°	120°	135°	150°	165°	180°
0°		11,63	**4,07**	2,19	**1,73**	6,67	**10,05**	16,68	**21,97**	30,62	**43,33**	56,51	
15°		11,63	4,78	3,26	2,14	**6,01**	10,89	**15,97**	20,95	32,34	42,72	56,51	
30°		11,63	4,78	**3,05**	**2,65**	8,14	**11,60**	15,87	**21,87**	**32,24**	42,72	56,51	
45°		13,34	4,17	3,66	**3,46**	6,11	13,07	18,11	**21,77**	31,68	39,77	54,15	
60°		16,65	6,21	4,68	5,39	5,39	**14,34**	21,36	21,36	29,09	45,16	51,87	
75°			18,90	15,96	18,67	18,67	18,67	18,67	18,67	32,11	41,40		
90°													

LABORATORY ASSESSMENT RESULT

y \ x	0°	15°	30°	45°	60°	75°	90°	105°	120°	135°	150°	165°	180°
0°		0,38	0,15	0,04	1,07	6,95	11,81	16,30	21,61	29,06	39,40	43,54	
15°		0,36	0,12	0,04	1,16	6,81	11,52	15,64	20,97	28,46	38,35	41,69	
30°		0,36	0,08	0,04	1,11	6,79	11,56	15,53	20,57	28,35	37,72	37,37	
45°		0,26	0,06	0,06	1,19	6,76	11,51	15,57	20,79	28,44	36,80	31,63	
60°		0,56	0,12	0,08	1,42	8,17	11,98	15,97	20,74	25,71	27,10	10,90	
75°			0,88	0,34	1,90	6,44	13,26	13,88	16,36	15,87	7,02		
90°													

ABSOLUTE DEVIATION BETWEEN BOTH METHODS

y \ x	0°	15°	30°	45°	60°	75°	90°	105°	120°	135°	150°	165°	180°
0°		11,26	**3,92**	2,15	**0,66**	0,29	**1,75**	0,38	**0,36**	1,55	**3,93**	12,97	
15°		11,28	4,66	3,21	0,98	**0,81**	0,63	**0,33**	0,02	3,89	4,37	14,83	
30°		11,28	4,70	**3,01**	**1,54**	1,35	**0,04**	0,33	**1,30**	**3,89**	5,00	19,14	
45°		13,08	4,11	3,60	**2,27**	0,66	1,57	2,54	**0,97**	3,24	2,97	22,52	
60°		16,09	6,09	4,61	3,97	2,77	**2,36**	5,39	0,62	3,38	18,06	40,97	
75°			18,02	15,62	16,77	12,23	5,41	4,79	2,32	16,24	34,38		
90°													

MAXIMUM DEVIATION (%)	40,97
MINIMUM DEVIATION (%)	0,02
AVERAGE DEVIATION (%)	6,62
AV. DEVIATION - COINCIDING MEASUREMENT ANGLES (%)	1,81

MESH SAMPLE NUMBER

07w

PARAMETERS

LW	SW	w	e	b	i	color
115	52	23	1	2	43,5	

SPECULAR TRANSMITTANCE (%)

COMPUTER AIDED ASSESSMENT RESULT

y \ x	0º	15º	30º	45º	60º	75º	90º	105º	120º	135º	150º	165º	180º
0º		11,63	**4,07**	2,20	**1,75**	6,68	**10,07**	16,69	**21,98**	30,64	**43,36**	58,75	
15º		11,63	4,78	3,26	2,16	**6,02**	10,90	**15,98**	20,97	32,36	42,76	58,75	
30º		11,63	4,78	**3,06**	**2,66**	8,15	**11,61**	15,88	**21,88**	**32,26**	42,76	58,75	
45º		13,34	4,18	3,67	**3,48**	6,20	13,13	18,13	**21,79**	31,70	39,80	56,47	
60º		16,65	6,21	4,69	5,41	5,41	**14,35**	21,40	21,40	29,14	45,37	54,88	
75º			18,90	16,07	19,02	19,02	19,02	19,02	19,02	32,59	42,47		
90º													

LABORATORY ASSESSMENT RESULT

y \ x	0º	15º	30º	45º	60º	75º	90º	105º	120º	135º	150º	165º	180º
0º		0,78	0,50	0,45	2,40	8,23	11,71	15,89	20,62	27,01	36,04	35,19	
15º		0,77	0,47	0,45	1,86	8,21	12,05	16,12	20,13	26,63	38,47	48,71	
30º		0,85	0,48	0,46	2,30	8,32	12,05	15,83	20,72	27,82	38,28	38,18	
45º		0,75	0,47	0,50	1,49	8,42	12,46	16,57	20,49	28,94	38,34	37,27	
60º		1,18	0,63	0,52	2,74	7,78	11,10	16,74	21,52	27,32	29,32	17,62	
75º			1,61	1,10	3,12	7,38	14,80	14,97	17,83	17,72	8,33		
90º													

ABSOLUTE DEVIATION BETWEEN BOTH METHODS

y \ x	0º	15º	30º	45º	60º	75º	90º	105º	120º	135º	150º	165º	180º
0º		10,85	**3,57**	1,74	**0,66**	1,55	**1,64**	0,81	**1,37**	3,63	**7,32**	23,55	
15º		10,87	4,31	2,82	0,30	**2,19**	1,16	**0,14**	0,84	5,73	4,28	10,04	
30º		10,78	4,31	**2,60**	**0,36**	0,17	**0,44**	0,05	**1,16**	**4,44**	4,48	20,56	
45º		12,59	3,71	3,17	**1,98**	2,22	0,68	1,57	**1,30**	2,76	1,47	19,21	
60º		15,47	5,58	4,17	2,67	2,37	**3,26**	4,66	0,12	1,82	16,04	37,26	
75º			17,29	14,97	15,90	11,64	4,22	4,05	1,19	14,88	34,14		
90º													

MAXIMUM DEVIATION (%)	37,26
MINIMUM DEVIATION (%)	0,05
AVERAGE DEVIATION (%)	6,42
AV. DEVIATION - COINCIDING MEASUREMENT ANGLES (%)	2,16

MESH SAMPLE NUMBER

08b

PARAMETERS

LW	SW	w	e	b	i	color
110	50	24	2	3,5	50	

SPECULAR TRANSMITTANCE (%)

COMPUTER AIDED ASSESSMENT RESULT

y \ x	0°	15°	30°	45°	60°	75°	90°	105°	120°	135°	150°	165°	180°
0°		14,03	**6,20**	3,81	**2,54**	2,64	**5,18**	10,22	**14,54**	22,83	**37,73**	50,66	
15°		14,03	6,71	4,58	2,44	**1,83**	5,44	**9,76**	13,73	25,12	36,21	50,66	
30°		14,03	6,71	**4,68**	**3,36**	3,56	**6,31**	9,05	**15,97**	**25,93**	36,21	50,66	
45°		16,47	6,10	4,88	**4,27**	4,07	7,58	12,41	**16,27**	24,36	32,85	49,24	
60°		20,12	8,54	5,70	4,47	4,47	**8,75**	15,26	15,26	22,78	39,06	49,04	
75°			23,08	19,06	18,37	18,37	18,37	18,37	18,37	31,60	42,30		
90°													

LABORATORY ASSESSMENT RESULT

y \ x	0°	15°	30°	45°	60°	75°	90°	105°	120°	135°	150°	165°	180°
0°		0,49	0,09	0,03	0,02	2,87	7,52	11,61	16,40	22,74	33,33	48,29	
15°		0,60	0,09	0,03	0,01	3,37	7,47	11,52	16,11	22,45	34,55	47,30	
30°		0,56	0,04	0,01	0,01	2,86	7,35	11,34	16,03	22,53	33,24	43,01	
45°		0,61	0,03	0,02	0,01	2,65	8,03	11,69	16,49	23,15	33,29	37,21	
60°		0,99	0,05	0,02	0,03	3,38	8,80	11,78	16,17	21,71	27,20	14,54	
75°			0,69	0,14	0,17	2,60	7,30	10,55	14,24	13,79	10,49		
90°													

ABSOLUTE DEVIATION BETWEEN BOTH METHODS

y \ x	0°	15°	30°	45°	60°	75°	90°	105°	120°	135°	150°	165°	180°
0°		13,53	**6,12**	3,78	**2,52**	0,23	**2,34**	1,39	**1,85**	0,09	**4,40**	2,38	
15°		13,43	6,62	4,55	2,43	**1,54**	2,03	**1,76**	2,38	2,68	1,65	3,36	
30°		13,47	6,68	**4,67**	**3,35**	0,70	**1,05**	2,29	**0,06**	**3,41**	2,97	7,65	
45°		15,86	6,08	4,86	**4,26**	1,42	0,45	0,71	**0,21**	1,21	0,44	12,03	
60°		19,13	8,49	5,67	4,44	1,10	**0,05**	3,48	0,91	1,08	11,86	34,50	
75°			22,39	18,92	18,21	15,77	11,07	7,82	4,13	17,81	31,82		
90°													

MAXIMUM DEVIATION (%)	34,50
MINIMUM DEVIATION (%)	0,05
AVERAGE DEVIATION (%)	6,46
AV. DEVIATION - COINCIDING MEASUREMENT ANGLES (%)	2,51

MESH SAMPLE NUMBER

08w

PARAMETERS

LW	SW	w	e	b	i	color
110	50	24	2	3,5	50	

SPECULAR TRANSMITTANCE (%)

COMPUTER AIDED ASSESSMENT RESULT

y \ x	0º	15º	30º	45º	60º	75º	90º	105º	120º	135º	150º	165º	180º
0º		14,03	**6,21**	3,82	**2,55**	2,66	**5,20**	10,24	**14,56**	22,89	**38,25**	51,35	
15º		14,03	6,71	4,58	2,45	**1,85**	5,46	**9,78**	13,75	25,20	36,58	51,35	
30º		14,03	6,71	**4,68**	**3,37**	3,58	**6,32**	9,07	**15,99**	**25,98**	36,58	51,35	
45º		16,49	6,10	4,89	**4,28**	4,17	7,62	12,43	**16,31**	24,42	33,11	49,80	
60º		20,19	8,55	5,70	4,49	4,49	**9,00**	15,30	15,30	22,85	39,32	49,44	
75º			23,09	19,31	18,82	18,82	18,82	18,82	18,82	32,14	43,00		
90º													

LABORATORY ASSESSMENT RESULT

y \ x	0º	15º	30º	45º	60º	75º	90º	105º	120º	135º	150º	165º	180º
0º		0,80	0,28	0,29	0,39	3,43	7,65	11,52	16,47	22,98	34,29	38,29	
15º		0,83	0,28	0,28	0,37	1,19	7,93	11,81	16,11	22,73	35,98	33,43	
30º		0,98	0,28	0,29	0,39	4,01	7,79	11,60	15,97	23,10	35,15	45,17	
45º		0,93	0,28	0,34	0,41	3,48	7,85	11,85	16,28	23,47	34,86	37,21	
60º		0,96	0,43	0,36	0,45	3,83	8,44	12,38	17,00	23,18	32,37	17,18	
75º			1,43	0,75	0,82	3,57	8,46	10,95	13,73	14,41	9,51		
90º													

ABSOLUTE DEVIATION BETWEEN BOTH METHODS

y \ x	0º	15º	30º	45º	60º	75º	90º	105º	120º	135º	150º	165º	180º
0º		13,22	**5,92**	3,53	**2,16**	0,76	**2,46**	1,28	**1,91**	0,09	**3,96**	13,06	
15º		13,20	6,44	4,30	2,08	**0,66**	2,47	**2,03**	2,36	2,47	0,60	17,92	
30º		13,05	6,44	**4,39**	**2,97**	0,43	**1,47**	2,53	**0,01**	**2,89**	1,44	6,18	
45º		15,56	5,82	4,55	**3,87**	0,69	0,23	0,58	**0,02**	0,95	1,75	12,59	
60º		19,23	8,11	5,34	4,04	0,66	**0,56**	2,92	1,70	0,33	6,96	32,25	
75º			21,66	18,56	18,00	15,25	10,36	7,87	5,09	17,72	33,49		
90º													

MAXIMUM DEVIATION (%)	33,49
MINIMUM DEVIATION (%)	0,01
AVERAGE DEVIATION (%)	6,58
AV. DEVIATION - COINCIDING MEASUREMENT ANGLES (%)	2,35

MESH SAMPLE NUMBER

09b

PARAMETERS

LW	SW	w	e	b	i	color
110	40	15	2	2	33	

SPECULAR TRANSMITTANCE (%)

COMPUTER AIDED ASSESSMENT RESULT

y \ x	0°	15°	30°	45°	60°	75°	90°	105°	120°	135°	150°	165°	180°
0°		23,70	**9,55**	7,11	**11,89**	20,12	**26,06**	33,48	**42,87**	54,71	**69,50**	56,14	
15°		23,70	10,06	8,23	13,82	**22,15**	27,13	**34,24**	42,97	56,29	66,96	56,14	
30°		23,70	10,06	**8,13**	**13,11**	24,38	**25,70**	31,80	**44,40**	**55,37**	66,96	56,14	
45°		26,31	10,97	9,50	**15,04**	22,66	27,43	35,97	**43,08**	55,78	64,72	52,77	
60°		31,22	12,70	10,87	19,81	19,81	**29,36**	39,52	39,52	50,70	63,70	47,67	
75°			31,84	26,65	32,34	32,34	32,34	32,34	32,34	43,30	46,84		
90°													

LABORATORY ASSESSMENT RESULT

y \ x	0°	15°	30°	45°	60°	75°	90°	105°	120°	135°	150°	165°	180°
0°		0,58	0,07	1,26	13,47	21,68	32,97	35,63	44,17	54,85	65,71	38,90	
15°		0,64	0,06	0,94	13,27	21,11	32,21	35,18	43,32	54,44	69,97	45,51	
30°		0,56	0,03	0,82	13,67	22,26	29,04	35,07	43,12	55,13	68,17	38,04	
45°		0,48	0,03	1,04	13,79	21,08	28,98	41,00	43,24	55,10	64,31	38,95	
60°		0,59	0,07	1,41	14,54	20,66	28,80	35,83	43,28	49,97	47,15	19,76	
75°			0,83	2,62	13,25	20,61	29,54	32,30	31,05	22,82	8,41		
90°													

ABSOLUTE DEVIATION BETWEEN BOTH METHODS

y \ x	0°	15°	30°	45°	60°	75°	90°	105°	120°	135°	150°	165°	180°
0°		23,12	**9,48**	5,85	**1,58**	1,56	**6,90**	2,16	**1,30**	0,14	**3,79**	17,24	
15°		23,06	9,99	7,29	0,55	**1,04**	5,08	**0,94**	0,35	1,85	3,02	10,63	
30°		23,14	10,03	**7,31**	**0,57**	2,12	**3,34**	3,28	**1,28**	**0,24**	1,21	18,10	
45°		25,83	10,94	8,46	**1,25**	1,57	1,54	5,03	**0,17**	0,68	0,41	13,82	
60°		30,64	12,63	9,47	5,27	0,84	**0,56**	3,70	3,76	0,73	16,55	27,91	
75°			31,01	24,03	19,09	11,73	2,80	0,05	1,29	20,48	38,43		
90°													

MAXIMUM DEVIATION (%)	38,43
MINIMUM DEVIATION (%)	0,05
AVERAGE DEVIATION (%)	8,41
AV. DEVIATION - COINCIDING MEASUREMENT ANGLES (%)	2,65

MESH SAMPLE NUMBER

09w

PARAMETERS

LW	SW	w	e	b	i	color
110	40	15	2	2	33	

SPECULAR TRANSMITTANCE (%)

COMPUTER AIDED ASSESSMENT RESULT

y \ x	0º	15º	30º	45º	60º	75º	90º	105º	120º	135º	150º	165º	180º
0º		23,70	**9,56**	7,14	**11,92**	20,14	**26,08**	33,49	**42,89**	54,84	**69,82**	56,63	
15º		23,70	10,07	8,25	13,85	**22,17**	27,14	**34,26**	42,99	56,34	67,09	56,63	
30º		23,70	10,07	**8,15**	**13,14**	24,41	**25,72**	31,82	**44,42**	**55,41**	67,09	56,63	
45º		26,31	10,99	9,52	**15,15**	22,68	27,47	36,02	**43,09**	55,80	64,92	53,09	
60º		31,23	12,71	10,90	19,92	19,92	**29,39**	39,56	39,56	50,80	63,71	48,28	
75º			31,85	26,79	32,72	32,72	32,72	32,72	32,72	43,55	46,91		
90º													

LABORATORY ASSESSMENT RESULT

y \ x	0º	15º	30º	45º	60º	75º	90º	105º	120º	135º	150º	165º	180º
0º		1,13	0,74	2,06	13,21	21,89	32,52	35,40	42,99	53,34	65,47	36,74	
15º		1,19	0,75	2,00	13,19	21,56	32,55	34,60	41,36	52,09	67,18	42,75	
30º		1,51	0,79	2,15	12,91	21,30	32,23	33,96	40,99	51,83	66,58	42,25	
45º		1,63	0,84	2,64	13,21	21,18	27,88	39,33	41,89	53,80	65,85	52,85	
60º		1,76	1,10	2,84	15,33	21,88	28,99	35,95	43,83	50,26	53,09	27,97	
75º			2,40	4,67	13,39	23,66	31,68	31,53	33,87	27,93	14,29		
90º													

ABSOLUTE DEVIATION BETWEEN BOTH METHODS

y \ x	0º	15º	30º	45º	60º	75º	90º	105º	120º	135º	150º	165º	180º
0º		22,57	**8,82**	5,08	**1,29**	1,75	**6,44**	1,91	**0,10**	1,50	**4,35**	19,89	
15º		22,51	9,32	6,25	0,66	**0,61**	5,40	**0,35**	1,63	4,25	0,08	13,88	
30º		22,20	9,28	**6,01**	**0,23**	3,11	**6,51**	2,14	**3,43**	**3,58**	0,51	14,38	
45º		24,68	10,15	6,89	**1,94**	1,50	0,41	3,32	**1,20**	2,01	0,93	0,24	
60º		29,46	11,62	8,05	4,59	1,96	**0,40**	3,61	4,28	0,54	10,62	20,31	
75º			29,45	22,12	19,33	9,07	1,05	1,19	1,14	15,63	32,62		
90º													

MAXIMUM DEVIATION (%)	32,62
MINIMUM DEVIATION (%)	0,08
AVERAGE DEVIATION (%)	7,66
AV. DEVIATION - COINCIDING MEASUREMENT ANGLES (%)	3,02

MESH SAMPLE NUMBER

10b

PARAMETERS

LW	SW	w	e	b	i	color
6	4	1,2	1	1	2,5	

SPECULAR TRANSMITTANCE (%)

COMPUTER AIDED ASSESSMENT RESULT

y \ x	0º	15º	30º	45º	60º	75º	90º	105º	120º	135º	150º	165º	180º
0º		22,57	**12,26**	16,98	**26,02**	29,14	**30,29**	30,90	**32,85**	33,51	**28,54**	25,50	
15º		22,57	12,86	15,27	27,43	**28,54**	29,49	**30,25**	32,05	34,27	30,25	25,50	
30º		22,57	12,86	**18,39**	**25,82**	30,64	**30,64**	29,34	**34,77**	**32,45**	30,25	25,50	
45º		25,51	14,77	18,89	**26,33**	28,03	29,89	29,64	**30,65**	30,55	30,95	29,30	
60º		29,97	17,58	20,40	22,51	22,51	**23,82**	25,62	25,62	27,43	23,01	34,32	
75º			34,92	27,96	24,38	24,38	24,38	24,38	24,38	27,19	33,11		
90º													

LABORATORY ASSESSMENT RESULT

y \ x	0º	15º	30º	45º	60º	75º	90º	105º	120º	135º	150º	165º	180º
0º		0,32	0,02	5,57	14,98	19,84	22,82	25,40	27,92	28,06	18,49	0,27	
15º		1,03	0,02	5,24	14,56	19,18	22,30	24,45	26,31	26,11	18,07	0,34	
30º		0,89	0,02	5,02	14,53	19,77	22,83	24,04	25,26	23,94	14,14	0,22	
45º		0,49	0,02	3,87	13,46	18,28	20,79	22,25	21,13	17,31	4,51	0,13	
60º		0,37	0,04	1,76	9,79	14,55	16,48	15,48	11,62	3,02	0,10	0,31	
75º			0,60	0,41	2,05	3,27	2,02	0,61	0,22	0,16	0,33		
90º													

ABSOLUTE DEVIATION BETWEEN BOTH METHODS

y \ x	0º	15º	30º	45º	60º	75º	90º	105º	120º	135º	150º	165º	180º
0º		22,26	**12,24**	11,41	**11,04**	9,30	**7,47**	5,49	**4,94**	5,45	**10,05**	25,23	
15º		21,54	12,85	10,04	12,87	**9,36**	7,19	**5,79**	5,74	8,15	12,18	25,16	
30º		21,68	12,84	**13,37**	**11,30**	10,88	**7,81**	5,30	**9,51**	**8,52**	16,11	25,28	
45º		25,01	14,75	15,02	**12,87**	9,75	9,10	7,39	**9,51**	13,24	26,43	29,17	
60º		29,60	17,55	18,63	12,72	7,96	**7,34**	10,15	14,01	24,41	22,91	34,01	
75º			34,32	27,55	22,33	21,11	22,36	23,78	24,16	27,03	32,77		
90º													

MAXIMUM DEVIATION (%)	34,32
MINIMUM DEVIATION (%)	4,94
AVERAGE DEVIATION (%)	15,71
AV. DEVIATION - COINCIDING MEASUREMENT ANGLES (%)	9,41

MESH SAMPLE NUMBER

10w

PARAMETERS

LW	SW	w	e	b	i	color
6	4	1,2	1	1	2,5	

SPECULAR TRANSMITTANCE (%)

COMPUTER AIDED ASSESSMENT RESULT

y \ x	0º	15º	30º	45º	60º	75º	90º	105º	120º	135º	150º	165º	180º
0º		22,58	**12,28**	17,04	**26,03**	29,18	**30,30**	30,90	**32,86**	33,52	**28,56**	25,92	
15º		22,58	12,88	15,30	27,44	**28,54**	29,50	**30,25**	32,06	34,35	30,35	25,92	
30º		22,58	12,88	**18,41**	**25,84**	30,65	**30,65**	29,35	**34,84**	**32,47**	30,35	25,92	
45º		25,51	14,79	18,95	**26,34**	28,04	29,90	29,66	**30,66**	30,64	30,97	29,52	
60º		29,98	17,60	20,50	22,52	22,52	**23,89**	25,64	25,64	27,45	23,04	34,53	
75º			34,92	28,02	24,43	24,43	24,43	24,43	24,43	27,31	33,35		
90º													

LABORATORY ASSESSMENT RESULT

y \ x	0º	15º	30º	45º	60º	75º	90º	105º	120º	135º	150º	165º	180º
0º		0,90	0,59	2,28	15,06	20,53	27,56	27,70	30,80	32,44	23,69	1,27	
15º		0,99	0,55	5,73	15,57	20,62	24,07	26,99	29,71	30,65	23,99	1,46	
30º		1,33	0,60	4,84	15,12	20,54	24,19	25,87	27,94	27,60	19,28	1,25	
45º		1,32	0,62	4,84	15,87	19,67	22,88	24,72	24,38	21,50	8,74	0,75	
60º		1,11	0,74	3,16	10,81	16,52	19,45	18,49	14,92	5,91	0,70	0,64	
75º			1,61	1,11	2,77	4,01	3,59	1,45	0,77	0,52	1,26		
90º													

ABSOLUTE DEVIATION BETWEEN BOTH METHODS

y \ x	0º	15º	30º	45º	60º	75º	90º	105º	120º	135º	150º	165º	180º
0º		21,68	**11,69**	14,76	**10,97**	8,65	**2,74**	3,20	**2,06**	1,08	**4,87**	24,65	
15º		21,58	12,33	9,57	11,87	**7,92**	5,42	**3,26**	2,35	3,69	6,36	24,47	
30º		21,25	12,28	**13,57**	**10,72**	10,11	**6,46**	3,48	**6,90**	**4,87**	11,07	24,67	
45º		24,19	14,17	14,10	**10,47**	8,37	7,02	4,94	**6,28**	9,14	22,23	28,77	
60º		28,86	16,86	17,34	11,71	6,01	**4,44**	7,14	10,72	21,53	22,35	33,89	
75º			33,31	26,91	21,66	20,42	20,84	22,98	23,66	26,79	32,09		
90º													

MAXIMUM DEVIATION (%)	33,89
MINIMUM DEVIATION (%)	1,08
AVERAGE DEVIATION (%)	14,06
AV. DEVIATION - COINCIDING MEASUREMENT ANGLES (%)	7,15

MESH SAMPLE NUMBER

11b

PARAMETERS

LW	SW	w	e	b	i	color
60	22	7	2	2	18	

SPECULAR TRANSMITTANCE (%)

COMPUTER AIDED ASSESSMENT RESULT

y \ x	0º	15º	30º	45º	60º	75º	90º	105º	120º	135º	150º	165º	180º
0º		25,01	**12,40**	16,16	**26,92**	34,09	**39,35**	47,55	**56,48**	65,94	**64,83**	36,80	
15º		25,01	13,11	12,30	28,14	**35,56**	41,66	**45,92**	56,08	68,89	63,91	36,80	
30º		25,01	13,11	**14,53**	**26,42**	36,98	**39,11**	43,18	**56,29**	**67,36**	63,91	36,80	
45º		26,88	13,72	16,82	**26,72**	35,36	41,30	47,45	**55,17**	64,72	65,34	38,27	
60º		30,41	16,76	21,03	33,43	33,43	**40,44**	51,31	51,31	59,24	51,11	36,84	
75º			34,18	30,76	37,17	37,17	37,17	37,17	37,17	40,79	40,00		
90º													

LABORATORY ASSESSMENT RESULT

y \ x	0º	15º	30º	45º	60º	75º	90º	105º	120º	135º	150º	165º	180º
0º		1,05	0,02	9,70	24,60	39,31	41,79	50,11	59,24	68,90	59,95	10,83	
15º		1,03	0,02	10,26	24,75	39,34	40,40	49,02	57,59	67,17	68,45	5,46	
30º		0,70	0,02	9,96	23,48	34,24	41,67	49,25	57,87	67,77	58,62	11,29	
45º		0,77	0,03	1,68	23,88	28,28	41,37	50,08	57,60	64,43	59,08	19,94	
60º		0,46	0,10	7,30	24,88	33,10	42,32	47,31	50,81	50,29	37,87	5,09	
75º			0,97	8,39	19,51	28,43	31,68	31,91	25,85	13,21	3,75		
90º													

ABSOLUTE DEVIATION BETWEEN BOTH METHODS

y \ x	0º	15º	30º	45º	60º	75º	90º	105º	120º	135º	150º	165º	180º
0º		23,96	**12,38**	6,45	**2,32**	5,22	**2,44**	2,57	**2,76**	2,95	**4,88**	25,97	
15º		23,99	13,09	2,03	3,39	**3,78**	1,25	**3,10**	1,51	1,72	4,53	31,34	
30º		24,32	13,08	**4,57**	**2,93**	2,74	**2,55**	6,08	**1,59**	**0,40**	5,29	25,51	
45º		26,11	13,68	15,14	**2,85**	7,08	0,07	2,63	**2,43**	0,30	6,26	18,33	
60º		29,94	16,67	13,73	8,55	0,33	**1,88**	4,00	0,50	8,94	13,23	31,75	
75º			33,22	22,37	17,67	8,74	5,50	5,26	11,32	27,57	36,25		
90º													

MAXIMUM DEVIATION (%)	36,25
MINIMUM DEVIATION (%)	0,07
AVERAGE DEVIATION (%)	10,36
AV. DEVIATION - COINCIDING MEASUREMENT ANGLES (%)	3,39

MESH SAMPLE NUMBER

11w

PARAMETERS

LW	SW	w	e	b	i	color
60	22	7	2	2	18	

SPECULAR TRANSMITTANCE (%)

COMPUTER AIDED ASSESSMENT RESULT

y \ x	0º	15º	30º	45º	60º	75º	90º	105º	120º	135º	150º	165º	180º
0º		25,03	**12,42**	16,23	**27,12**	34,11	**39,37**	47,57	**56,49**	66,22	**65,29**	36,84	
15º		25,03	13,13	12,42	28,24	**35,58**	41,67	**45,94**	56,09	69,36	64,24	36,84	
30º		25,03	13,13	**14,57**	**26,45**	37,01	**39,14**	43,19	**56,38**	**67,47**	64,24	36,84	
45º		26,89	13,75	17,01	**26,99**	35,59	41,32	47,46	**55,25**	64,92	65,74	38,37	
60º		30,42	16,79	21,13	33,53	33,53	**40,45**	51,63	51,63	59,40	51,21	36,96	
75º			34,29	31,02	37,62	37,62	37,62	37,62	37,62	40,99	40,02		
90º													

LABORATORY ASSESSMENT RESULT

y \ x	0º	15º	30º	45º	60º	75º	90º	105º	120º	135º	150º	165º	180º
0º		1,16	1,21	10,46	24,48	37,24	40,46	47,93	57,27	68,23	63,07	16,35	
15º		1,27	1,21	9,26	23,50	36,77	39,84	47,64	55,89	66,00	66,67	8,76	
30º		1,80	1,27	9,16	23,33	36,56	40,07	47,01	56,17	67,22	62,33	18,18	
45º		2,23	1,32	10,53	22,59	32,45	39,47	47,81	55,41	64,64	59,69	25,87	
60º		2,23	1,62	8,00	23,47	32,60	36,73	52,69	52,66	53,24	42,66	9,05	
75º			2,81	8,35	11,17	22,93	30,20	34,37	30,60	18,62	4,06		
90º													

ABSOLUTE DEVIATION BETWEEN BOTH METHODS

y \ x	0º	15º	30º	45º	60º	75º	90º	105º	120º	135º	150º	165º	180º
0º		23,87	**11,21**	5,77	**2,64**	3,13	**1,10**	0,37	**0,78**	2,01	**2,22**	20,49	
15º		23,76	11,93	3,16	4,74	**1,19**	1,83	**1,70**	0,20	3,37	2,43	28,08	
30º		23,23	11,86	**5,42**	**3,11**	0,44	**0,93**	3,82	**0,21**	**0,25**	1,91	18,66	
45º		24,66	12,43	6,48	**4,40**	3,14	1,85	0,35	**0,16**	0,28	6,05	12,49	
60º		28,19	15,17	13,13	10,06	0,93	**3,72**	1,05	1,02	6,16	8,55	27,91	
75º			31,47	22,67	26,44	14,69	7,42	3,25	7,02	22,37	35,96		
90º													

MAXIMUM DEVIATION (%)	35,96
MINIMUM DEVIATION (%)	0,16
AVERAGE DEVIATION (%)	9,15
AV. DEVIATION - COINCIDING MEASUREMENT ANGLES (%)	2,60

MESH SAMPLE NUMBER

12b

PARAMETERS

LW	SW	w	e	b	i	color
115	48	20	1,5	2	39	

SPECULAR TRANSMITTANCE (%)

COMPUTER AIDED ASSESSMENT RESULT

y \ x	0º	15º	30º	45º	60º	75º	90º	105º	120º	135º	150º	165º	180º
0º		15,77	**7,17**	4,56	**5,12**	10,91	**17,28**	23,97	**31,03**	42,30	**59,31**	57,87	
15º		15,77	6,45	5,22	6,04	**13,42**	17,11	**21,72**	31,55	45,79	57,77	57,87	
30º		15,77	6,45	**5,02**	**6,45**	13,42	**17,51**	23,56	**33,60**	**43,53**	57,77	57,87	
45º		18,19	7,68	5,89	**6,66**	12,70	19,61	27,25	**33,39**	43,23	54,91	54,98	
60º		23,04	9,63	6,66	9,73	9,73	**20,08**	30,22	30,22	40,56	58,19	50,32	
75º			24,28	20,63	24,50	24,50	24,50	24,50	24,50	39,29	46,73		
90º													

LABORATORY ASSESSMENT RESULT

y \ x	0º	15º	30º	45º	60º	75º	90º	105º	120º	135º	150º	165º	180º
0º		0,32	0,07	0,09	8,04	16,31	21,78	29,43	38,14	50,33	64,99	54,70	
15º		0,34	0,07	0,08	9,00	13,19	21,90	32,41	37,30	49,25	66,67	56,18	
30º		0,25	0,03	0,07	7,85	15,78	21,24	33,33	37,45	49,27	62,60	51,20	
45º		0,19	0,02	0,25	7,84	16,44	22,94	29,24	41,72	47,07	54,46	39,24	
60º		0,84	0,05	0,27	9,06	15,29	22,28	28,33	34,78	39,53	37,29	13,08	
75º			0,74	0,99	7,80	15,37	19,42	24,37	23,80	18,42	6,48		
90º													

ABSOLUTE DEVIATION BETWEEN BOTH METHODS

y \ x	0º	15º	30º	45º	60º	75º	90º	105º	120º	135º	150º	165º	180º
0º		15,45	**7,10**	4,47	**2,92**	5,40	**4,50**	5,46	**7,11**	8,03	**5,68**	3,18	
15º		15,44	6,39	5,15	2,96	**0,24**	4,79	**10,70**	5,76	3,46	8,89	1,69	
30º		15,52	6,42	**4,95**	**1,39**	2,36	**3,72**	9,78	**3,85**	**5,74**	4,83	6,68	
45º		18,00	7,66	5,64	**1,19**	3,74	3,32	2,00	**8,33**	3,85	0,45	15,74	
60º		22,21	9,58	6,39	0,67	5,56	**2,20**	1,89	4,56	1,03	20,89	37,23	
75º			23,54	19,65	16,70	9,13	5,08	0,13	0,70	20,87	40,25		
90º													

MAXIMUM DEVIATION (%)	40,25
MINIMUM DEVIATION (%)	0,13
AVERAGE DEVIATION (%)	8,10
AV. DEVIATION - COINCIDING MEASUREMENT ANGLES (%)	4,64

MESH SAMPLE NUMBER

12w

PARAMETERS

LW	SW	w	e	b	i	color
115	48	20	1,5	2	39	

SPECULAR TRANSMITTANCE (%)

COMPUTER AIDED ASSESSMENT RESULT

y \ x	0º	15º	30º	45º	60º	75º	90º	105º	120º	135º	150º	165º	180º
0º		15,77	**7,18**	4,57	**5,15**	10,93	**17,30**	23,98	**31,05**	42,33	**59,79**	58,41	
15º		15,77	6,46	5,24	6,16	**13,53**	17,12	**21,73**	31,57	45,82	58,11	58,41	
30º		15,77	6,46	**5,04**	**6,48**	13,44	**17,53**	23,57	**33,61**	**43,56**	58,11	58,41	
45º		18,20	7,69	5,91	**6,68**	12,80	19,63	27,32	**33,43**	43,28	55,25	55,63	
60º		23,05	9,64	6,68	9,82	9,82	**20,10**	30,26	30,26	40,57	58,64	50,91	
75º			24,37	20,85	24,98	24,98	24,98	24,98	24,98	40,11	47,87		
90º													

LABORATORY ASSESSMENT RESULT

y \ x	0º	15º	30º	45º	60º	75º	90º	105º	120º	135º	150º	165º	180º
0º		1,39	0,66	0,94	9,07	16,91	23,63	30,69	39,06	51,17	62,59	29,83	
15º		1,33	0,67	0,86	9,66	15,97	23,79	30,10	38,22	50,25	67,43	42,92	
30º		1,47	0,68	0,87	9,91	16,65	23,80	34,08	38,01	50,18	64,19	54,40	
45º		1,40	0,68	0,97	10,51	16,42	24,04	30,88	39,36	51,19	63,38	56,05	
60º		1,55	0,90	1,13	10,16	16,70	24,75	30,83	39,31	47,68	49,57	24,45	
75º			2,07	1,96	7,78	16,30	24,04	27,98	31,11	27,83	14,11		
90º													

ABSOLUTE DEVIATION BETWEEN BOTH METHODS

y \ x	0º	15º	30º	45º	60º	75º	90º	105º	120º	135º	150º	165º	180º
0º		14,39	**6,51**	3,63	**3,92**	5,98	**6,33**	6,71	**8,00**	8,84	**2,80**	28,58	
15º		14,45	5,79	4,38	3,50	**2,44**	6,67	**8,37**	6,65	4,43	9,32	15,49	
30º		14,30	5,78	**4,16**	**3,43**	3,21	**6,26**	10,51	**4,40**	**6,63**	6,08	4,01	
45º		16,80	7,02	4,94	**3,82**	3,63	4,40	3,56	**5,92**	7,91	8,14	0,42	
60º		21,50	8,74	5,55	0,34	6,88	**4,65**	0,57	9,05	7,10	9,08	26,46	
75º			22,29	18,89	17,19	8,68	0,94	3,00	6,13	12,28	33,76		
90º													

MAXIMUM DEVIATION (%)	33,76
MINIMUM DEVIATION (%)	0,34
AVERAGE DEVIATION (%)	8,37
AV. DEVIATION - COINCIDING MEASUREMENT ANGLES (%)	5,18

APPENDIX C

TRANSFER OF RESULTS TO REAL CASES

MATRIX FOR THE COORDINATE SYSTEM CONVERSION

The results obtained in laboratory and computer aided assessments are all geometrically referred to an EM mesh plane. That is to say, the radiation directions expressed during the assessment process are based on a reference coordinate system placed on the mesh plane itself. On the contrary, when we want to analyze the transmittance of facades in real cases, the reference system used to define solar radiation direction is based on the geographic coordinate system.

In order to transfer the registers obtained in the achieved assessments to real cases, it will be necessary to carry out an operation that allows us to define the radiation direction according to the mesh plane coordinate system, in order to get the data from the assessment methods. Besides the geographic position of the sun we must also know the position of the mesh in the building and the orientation and inclination of the façade.

C.1 Definition of the base or reference coordinate system of the mesh plane (used in assessments)

Assuming that an EM mesh has a front face and a back face, as well as a head and a tail we needed to establish a valid reference for any mesh and the easiest way was to refer to the manufacturing process. As the mesh comes out from the shear while in manufacture, an observer situated in front of the machine will have the mesh showing its front face and the head at the top (as shown in the following image and already defined in section 2.3.1).

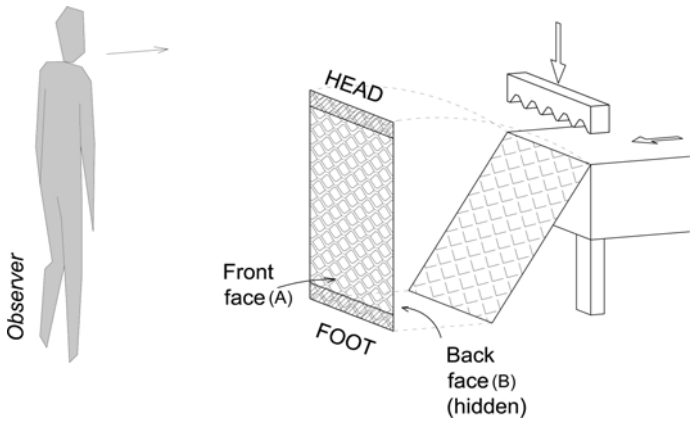

Fig. C.1. Mesh orientation when coming out from manufacture

Let us take an ordinary EM mesh, usually named rhombus shaped EM, diamond shaped EM or regular EM. If we analyze the perimeter defined by the hollows of that mesh, we will observe that this hollow perimeter is formed by a continuous curve from one side and by a sequence of three straight lines from the other. These three straight lines are originated at the manufacturing process, being this the side where the blade applies the pressure. In fact this uneven line is the *carbon copy* of the blade's profile. Having as reference these hollows of the EM meshes, the head of the mesh will be located in the direction of the curve while the foot of the mesh will be located in the direction of the uneven line.

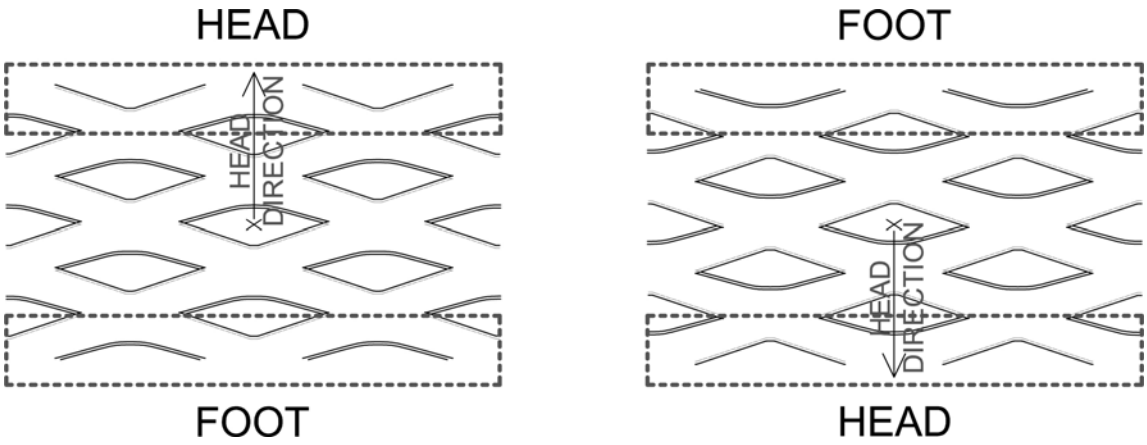

Fig. C.2. EM meshes head and foot identification from the hollows perimeter form

The front face of the mesh will be the one where the blade impacts on during the manufacturing process to cut the original metal sheet. It can be distinguished because it shows some marks created by the blade perpendicular to the cut. On this face the curved side of the hollow perimeter is situated outer than the uneven side of the perimeter, that folds backwards. In the reverse face, the uneven line remains in the front while the curve is on the bottom.

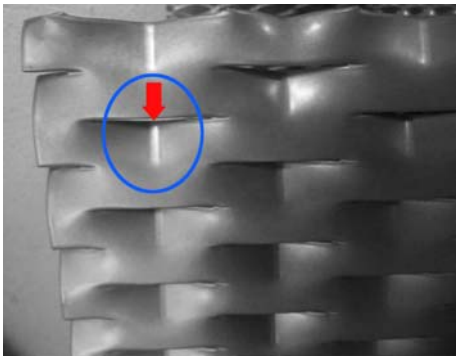

Fig. C.3. Marks made by the blade in the front face of the EM mesh

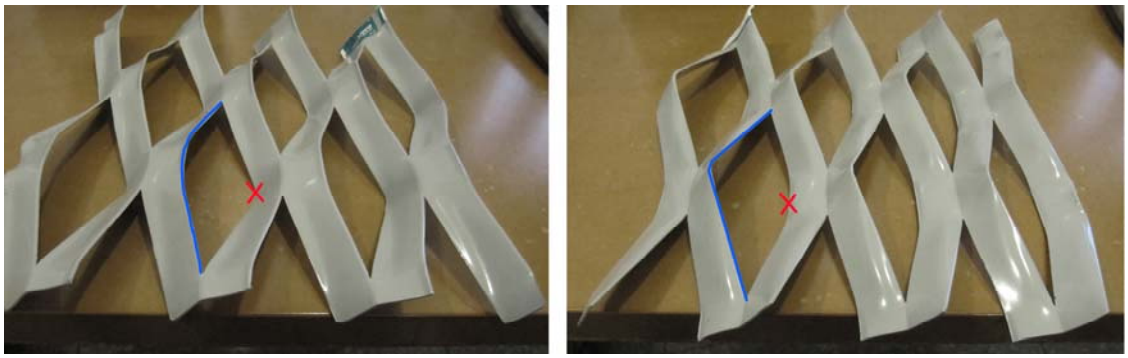

Fig. C.4. On the left, an EM mesh on a table with its front face upwards. On the right, an EM mesh on a table with its reverse face upwards. The most external part of the mesh in each position is painted blue. The point where the mesh leans on the table is marked with a red cross

As aforementioned, the base or coordinate reference system used in our assessment is situated on the plane of the EM mesh. The axes of the reference system are situated taking the mesh as it comes out from the shear machine in manufacture, that is, showing its front face and with the head above. These axes are defined by three perpendicular unit vectors.

- *x* axis: this is the horizontal axis of the plane and it is positive from left to right when we are looking to the mesh plane from the front
- *y* axis: it's the vertical axis of the plane, positive in the direction from foot to head
- *z* axis: is the normal axis to the mesh plane and it is positive in the direction that gets away from the mesh plane from its front face

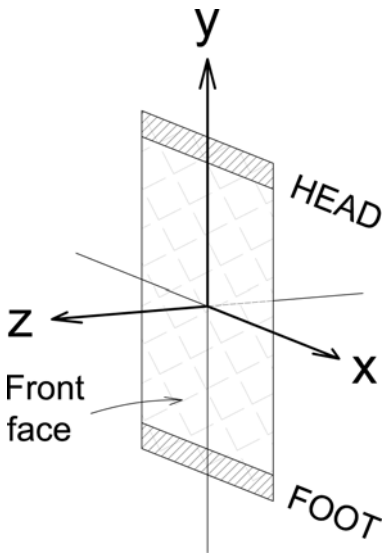

Fig.C.5. Reference Coordinate System used in assessment

So, we can define a vector relative to this base or reference system expressing the radiation direction:

$$\begin{pmatrix} a \\ b \\ c \end{pmatrix}$$

C.2 Geographic coordinate system to define sun's position

To predict the direction and amount of radiation arriving to the outside of a building in a precise location and position, we can use solar carts, analytic methods or empirical data.

To define the position of the sun a coordinate system based on the celestial sphere is used. This celestial sphere is defined by the vertical direction, the direction joining the centre of the earth with our position in it, and the horizon plane, the perpendicular plane to the vertical direction.

In this celestial sphere we define a reference system made up of three axes based on the cardinal points or cardinal directions (North, East, South and West) contained in the horizon plane and the vertical direction. This system allows defining the position of the sun in the celestial sphere and therefore the direction of its radiation. One axis will be going from

North to South, the second one will be on the direction East-West (both of them in the horizon plane) and the third one on the direction Zenith-Nadir (vertical direction).

To define the suns position relative to this reference system the polar coordinates azimuth angle (ψ_s) and sun altitude (γ_s) are used. The azimuth angle measures the displacement of the sun from the South on the horizon plane. The sun altitude measures the altitude of the sun from the horizon plane.

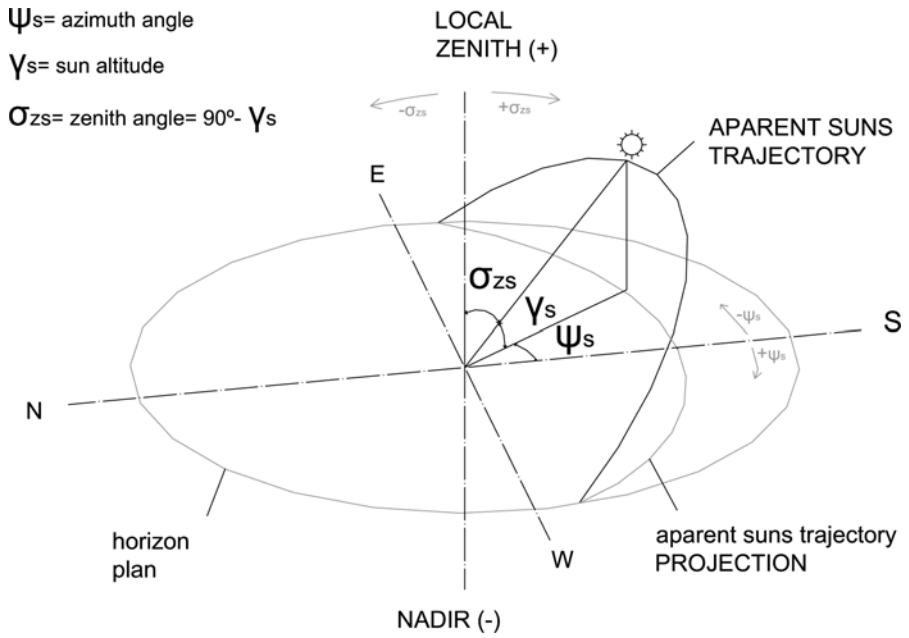

Fig. C.6. Geographic Coordinate System, azimuth angle and sun altitude

With this reference system and defined polar coordinates, we can express the direction of sun radiation relative to this geographic coordinate system with a vector:

$$\begin{pmatrix} a' \\ b' \\ c' \end{pmatrix} = \begin{pmatrix} \cos\gamma_s \sin -\psi_s \\ \sin\gamma_s \\ \cos\gamma_s \cos -\psi_s \end{pmatrix}$$

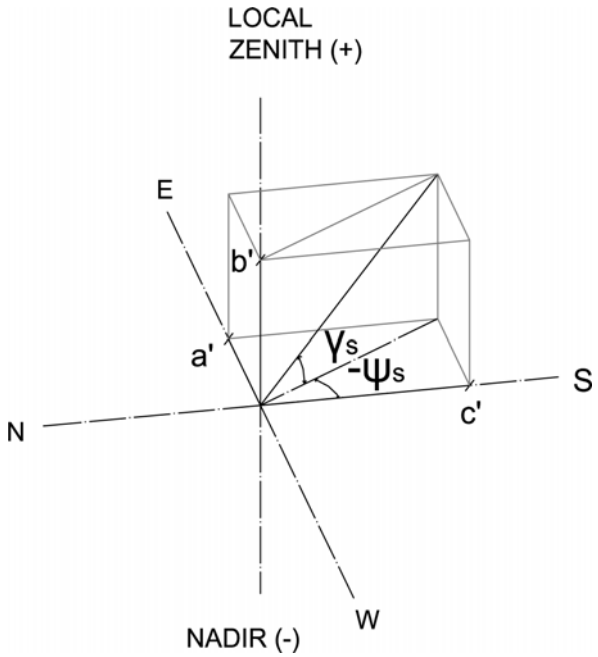

Fig. C.7. Vector defining sun radiation direction on the geographic coordinate system

C.3 Position, orientation and inclination of the EM mesh on a facade

In order to relate the mesh reference system with the sun's reference system, it is necessary to know the relative location of each other. Therefore, the ***position***, ***inclination*** and ***orientation*** that the EM mesh will have in the façade must be expressed in the geographic coordinate system.

The ***position*** refers to the way the EM mesh is placed in the façade. In other words, it will define if the mesh is placed with the head above, with the head bellow or in any other halfway position between them. This variable will be measured by an angle named as α, the spin made by the mesh around the *z* axis of its own reference system, departing from its original position with its head above and showing its front face (measured counterclockwise direction).

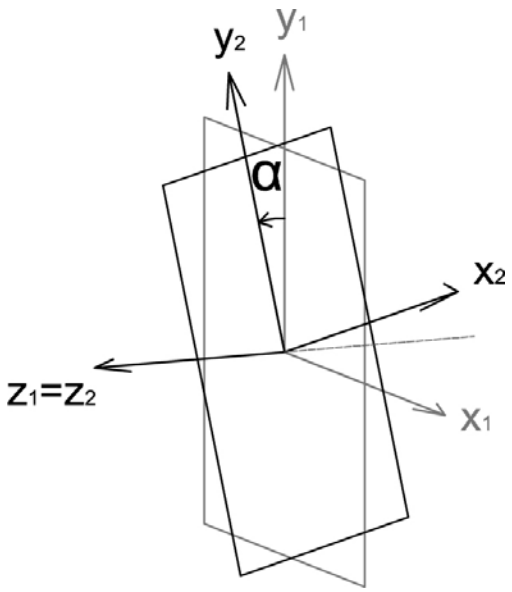

Fig. C.8. Spin around the normal to the EM mesh plane and α angle

Secondly, we must define the façade ***inclination***, that is to say, if the EM mesh will be installed vertically or if it will lean in any one direction. It will be measured by the angle named as β. This β angle will indicate the spin of the mesh around the East-West axis to arrive to have the façade *inclination*, departing from a vertical position (measured clockwise). This angle will be the one between the line of maximum slope of the façade and the Zenith-Nadir axis (verticals direction).

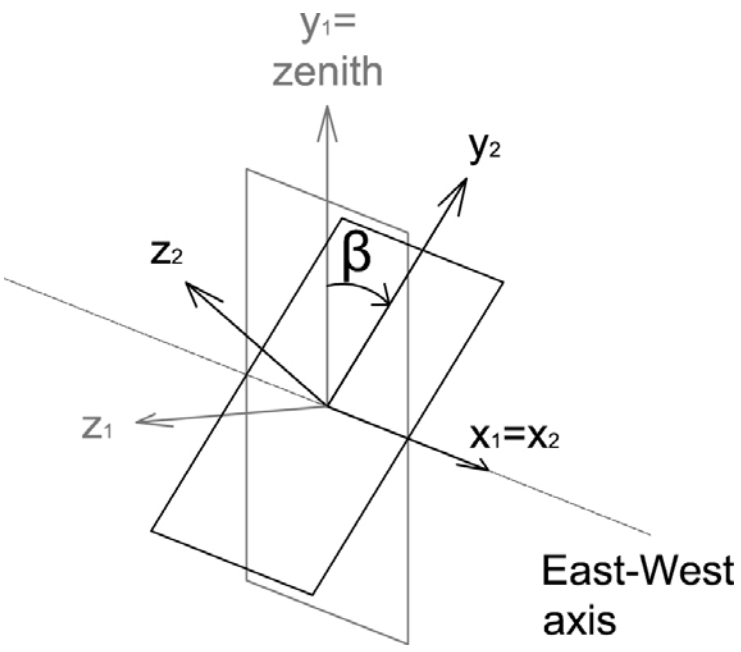

Fig. C.9. Spin around the East-West axis and β angle

Finally, it will be necessary to define the façade ***orientation***. Departing from a South orientated façade, the *orientation* will be the spin made around the Zenith-Nadir axis. The *orientation* will be measured by the angle named *δ*. This angle will be the one formed by the perpendicular to the cut line between the façade plane and the horizon plane and the South direction (measured counterclockwise). So the *orientation* will measure the deviation of the façade from the South.

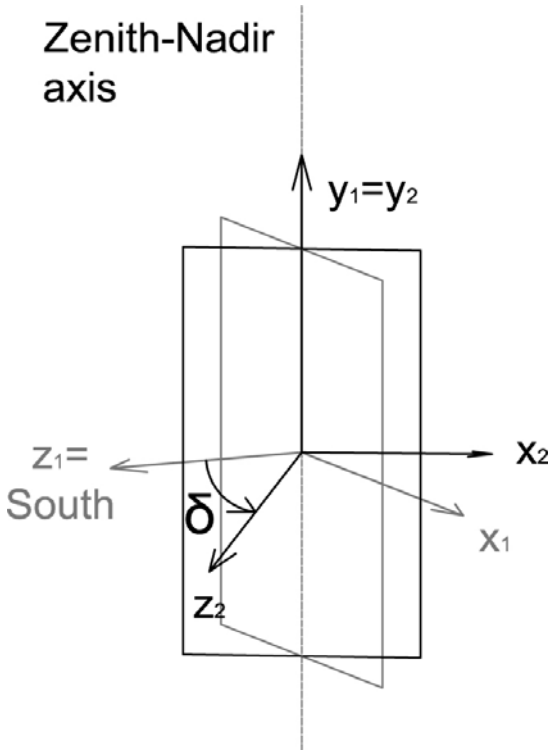

Fig. C.10. Spin around the Zenith-Nadir axis and δ angle

In architecture, the best tools to measure these angles that define the position of EM meshes are the architectural plans themselves. By means of the following pictures we explain how to measure them for a case study.

In this text, we often talk about *facades* but a more appropriate term would be *building envelopes*, as a more general concept which can include roofs, ceilings or any surface enclosing or covering the inner spaces.

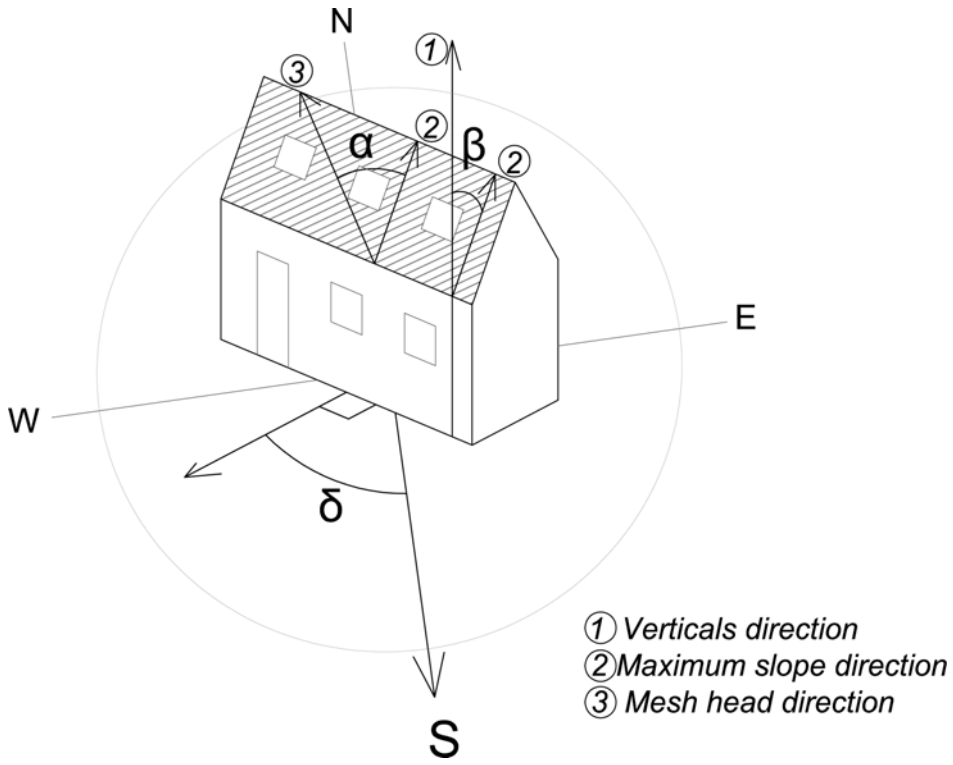

Fig. C.11. Axonometric view of a case study. The striped façade is the one we are going to use to take out the position, inclination and orientation. The direction of the stripes indicates the direction of the horizontal axis of the EM mesh

The *position* of the mesh, defined by the angle named α, can be measured in the elevation of the building envelope (not the front elevation of the building if the envelope is not vertical). We must know where the head and the foot of the EM mesh are placed to get the *head direction* (direction from foot to head of the mesh, see section C.1). The α angle will be the one between this head direction and the façades maximum slope direction.

With the aim of measuring the façade *inclination* we need a side elevation of the façade or a section cutting this façade. In that elevation or section we will have the direction of the maximum slope of the façade. The β angle measuring this inclination will be the one between the vertical direction and the direction of the maximum slope.

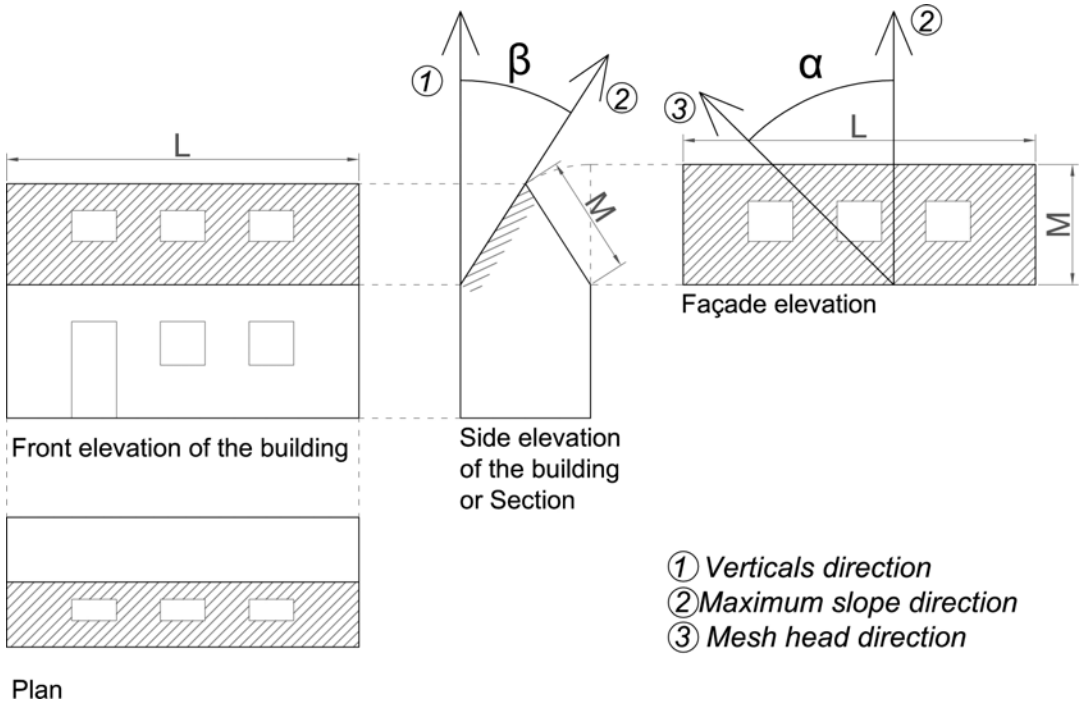

Fig. C.12. Architectural plans of the case study. Measuring α angle in the elevation of the envelope and β angle in the side elevation of the building (or section)

To measure the *orientation* of the building envelope, we need a location map where the building is oriented relative to the geographic coordinates system. In that map (called *oriented plan*), we will measure the δ angle from the perpendicular line to a horizontal line of the envelope to the South direction. If the mesh is showing its back face outwards, we should add 180º to this δ angle.

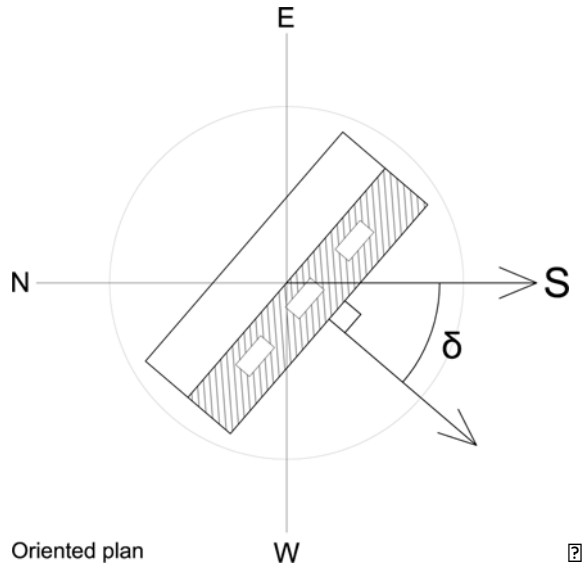

Fig. C.13. Measuring δ angle in the *oriented plan* of the building

C.4 System conversion matrix

A vector can be represented in different coordinate systems. In linear algebra, a vector represented in a known system or basis can be represented on another different basis, so it is possible to achieve an equivalent representation of the vector in this second basis. This transformation is called change of basis and is made by means of a conversion matrix. A coordinate system or basis is defined by a set of unitary vectors. The conversion matrix defines in each column this set of vectors of a coordinate system. Multiplying a vector by a conversion matrix gives as result the equivalent representation of that vector in a second coordinate system (Change of Basis 2014).

Once we have defined the *position*, *inclination* and *orientation* of the EM mesh in the façade, both reference coordinate systems (mesh-system and geographic system) can be easily related. This way, by means of a simple operation, we will be able to express the vector defining the sun radiation direction based in the mesh reference system. We must multiply the vector defining the sun radiation direction in the geographic coordinates system by a conversion matrix that depends on the *position*, *inclination* and *orientation* data of the mesh. This operation gives as result another vector that will express the direction of the same radiation in the reference system of the mesh:

$$\begin{pmatrix} a \\ b \\ c \end{pmatrix} = \begin{pmatrix} \cos\alpha\cos\delta + \sin\alpha\sin\beta\sin\delta & \cos\beta\sin\alpha & \sin\delta\cos\alpha - \sin\alpha\sin\beta\cos\delta \\ -\sin\alpha\cos\delta + \cos\alpha\sin\beta\sin\delta & \cos\alpha\cos\beta & -\sin\alpha\sin\delta - \cos\delta\sin\beta\cos\alpha \\ -\sin\delta\cos\beta & \sin\beta & \cos\beta\cos\delta \end{pmatrix} \begin{pmatrix} a' \\ b' \\ c' \end{pmatrix}$$

Remember that the vector defined on the geographic coordinates system can be expressed by the azimuth angle and the sun altitude, so the operation will be the following:

$$\begin{pmatrix} a \\ b \\ c \end{pmatrix} = \begin{pmatrix} \cos\alpha\cos\delta + \sin\alpha\sin\beta\sin\delta & \cos\beta\sin\alpha & \sin\delta\cos\alpha - \sin\alpha\sin\beta\cos\delta \\ -\sin\alpha\cos\delta + \cos\alpha\sin\beta\sin\delta & \cos\alpha\cos\beta & -\sin\alpha\sin\delta - \cos\delta\sin\beta\cos\alpha \\ -\sin\delta\cos\beta & \sin\beta & \cos\beta\cos\delta \end{pmatrix} \begin{pmatrix} \cos\gamma_s \sin -\psi_s \\ \sin\gamma_s \\ \cos\gamma_s \cos -\psi_s \end{pmatrix}$$

C.5 Description of the process to transfer the assessments results to real cases

The process to transfer the assessments results to real cases can be summed up in the following way:

- Decide the place, day of the year and hour of that day for which we want to obtain the data. This fact brings us to a specific geographic position of the sun and its solar coordinates: azimuth angle=ψ_s and sun altitude=γ_s.
- Define the position, inclination and orientation in which the mesh will be placed in the building (position=α; inclination=β and orientation=δ)
- Make the following operation to obtain the vector that defines the incident radiation direction in the mesh reference system:

$$\begin{pmatrix} a \\ b \\ c \end{pmatrix} = \begin{pmatrix} \cos\alpha\cos\delta + \sin\alpha\sin\beta\sin\delta & \cos\beta\sin\alpha & \sin\delta\cos\alpha - \sin\alpha\sin\beta\cos\delta \\ -\sin\alpha\cos\delta + \cos\alpha\sin\beta\sin\delta & \cos\alpha\cos\beta & -\sin\alpha\sin\delta - \cos\delta\sin\beta\cos\alpha \\ -\sin\delta\cos\beta & \sin\beta & \cos\beta\cos\delta \end{pmatrix} \begin{pmatrix} \cos\gamma_s \sin -\psi_s \\ \sin\gamma_s \\ \cos\gamma_s \cos -\psi_s \end{pmatrix}$$

- Conversion of this resultant vector in polar coordinates or rotation angles used in laboratory assessment. We will name as λ the rotation around *x* axis of the lab-device and the rotation around *y* axis will be named as φ. Both angles are represented in the following picture:

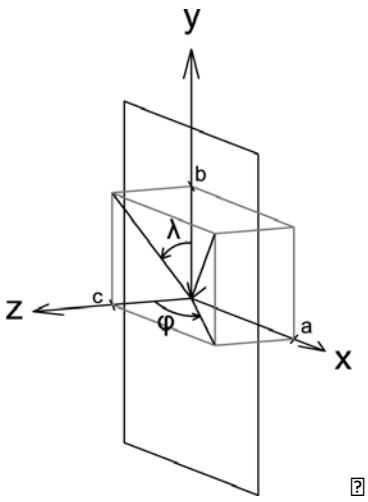

Fig. C.14. Incident radiation direction vector; *x*, *y* and *z* coordinates of it and λ and φ angles defining the same vector

Be aware of the direction of the measurements of the angles and remember the fact that *z* axis of the EM mesh reference system is projected from its front face, so it is positive from this face.

So we can define these λ and φ angles in the following way:

$$\lambda = \arctan\frac{c}{b} \qquad\qquad \varphi = \arctan\frac{a}{c}$$

If *b* value of the vector equals 0, λ angle will be 90º. In the same way, if *c* value of the vector equals 0, φ angle will be 90º also.

In the data tables search for the values corresponding to those angles. The value of λ angle, being the rotation around *y* axis, corresponds to a row of the data tables shown in appendix A, while the value of φ angle corresponds to a column of those tables.

As in our assessment we have chosen some specific directions for the incident radiation, it is very likely that the angles obtained for real cases do not agree exactly with those analyzed and represented in the tables. In that case, we should take the closest angles from the tables and interpolate their corresponding values.

A further task could be to automate all these process and operations and include them in a computer aided assessment tool to obtain a complete automatic assessment process.

References

Change of Basis
2014 Wikipedia, the Free Encyclopedia.
http://en.wikipedia.org/w/index.php?title=Change_of_basis&oldid=627831564, accessed November 28, 2014.